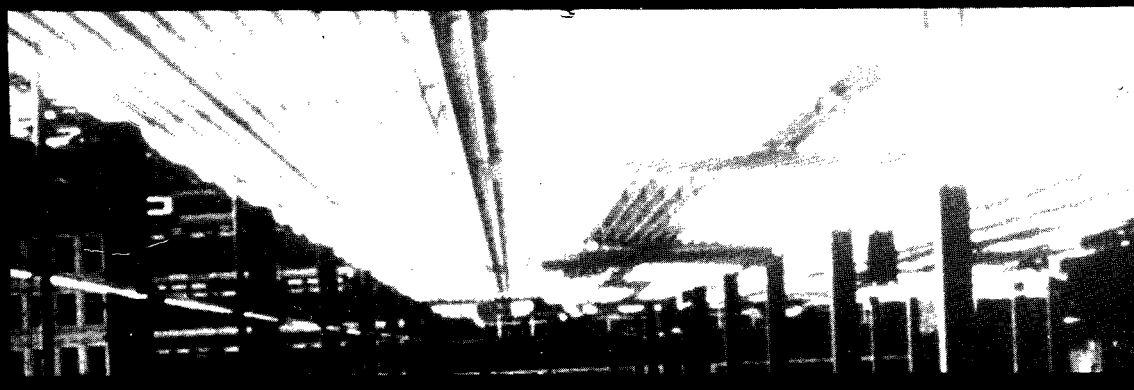

COMPOSITE STRUCTURES OF STEEL AND CONCRETE

VOLUME 1

BEAMS, SLABS, COLUMNS, AND FRAMES FOR BUILDINGS

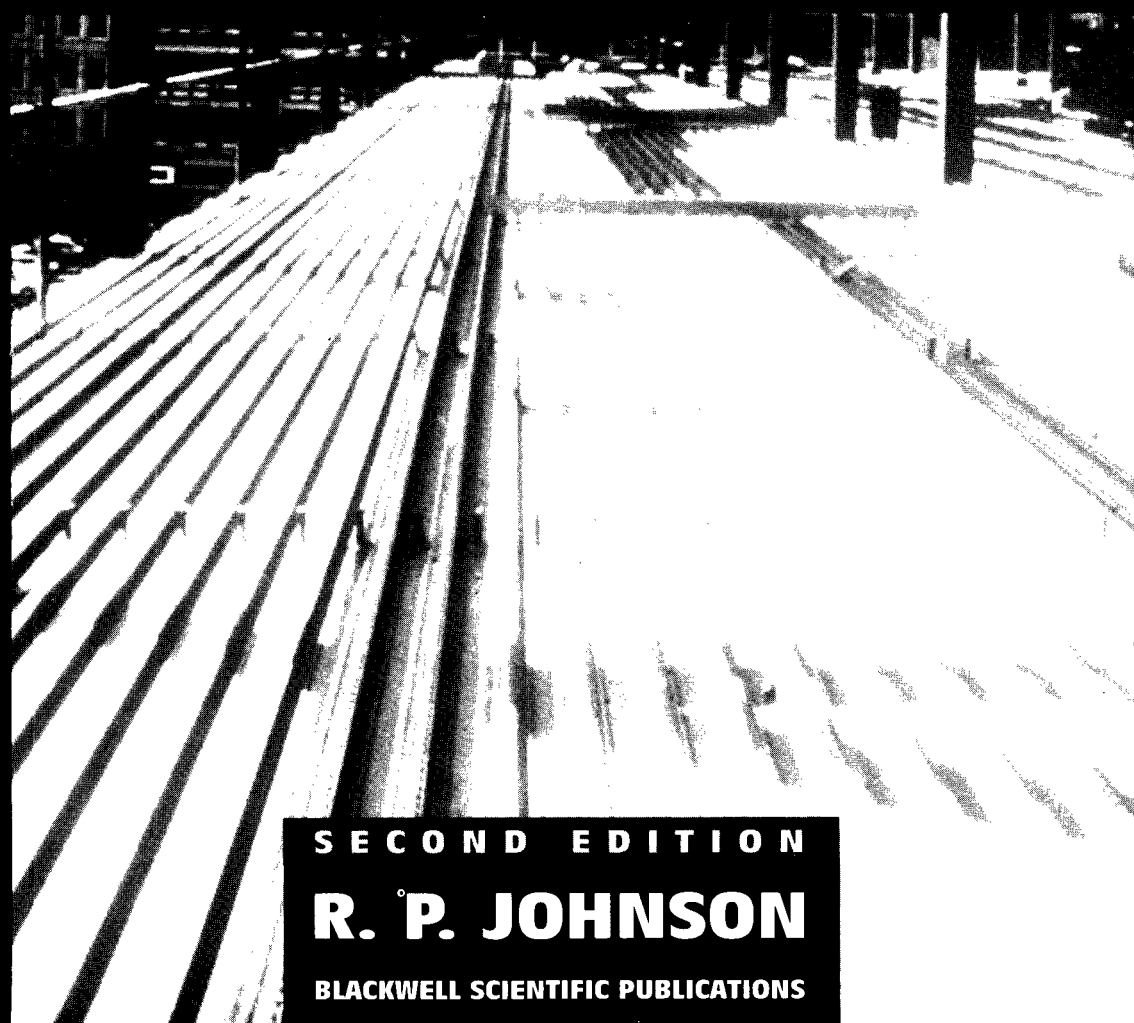

SECOND EDITION

R. P. JOHNSON

BLACKWELL SCIENTIFIC PUBLICATIONS

COMPOSITE STRUCTURES OF STEEL AND CONCRETE

VOLUME 1

BEAMS, SLABS, COLUMNS, AND FRAMES FOR BUILDINGS

Also available

COMPOSITE STRUCTURES OF STEEL AND CONCRETE

VOLUME 2: BRIDGES

Second Edition

R.P.Johnson and R.J. Buckby

COMPOSITE STRUCTURES OF STEEL AND CONCRETE

VOLUME 1

BEAMS, SLABS, COLUMNS, AND FRAMES FOR BUILDINGS

Second Edition

R.P. JOHNSON
MA, FEng, FICE, FIStructE
Professor of Civil Engineering
University of Warwick

OXFORD
BLACKWELL SCIENTIFIC PUBLICATIONS
LONDON EDINBURGH BOSTON
MELBOURNE PARIS BERLIN VIENNA

First edition © 1975 by the Constructional Steel Research and Development Organisation

Blackwell Scientific Publications
Editorial Offices:
Osney Mead, Oxford OX2 0EL
25 John Street, London WC1N 2BL
23 Ainslie Place, Edinburgh EH3 6AJ
238 Main Street, Cambridge,
Massachusetts 02142, USA
54 University Street, Carlton,
Victoria 3053, Australia

Other Editorial Offices:
Librairie Arnette SA
1, rue de Lille
75007 Paris
France

Blackwell Wissenschafts-Verlag GmbH
Düsseldorfer Str. 38
D-10707 Berlin
Germany

Blackwell MZV
Feldgasse 13
A-1238 Wien
Austria

First published by Crosby Lockwood Staples 1975
Paperback edition published by Granada Publishing 1982
Reprinted 1984
Second Edition published by Blackwell Scientific Publications 1994

Typeset by Florencetype Ltd, Kewstoke, Avon
Printed and bound in Great Britain at the Alden Press Limited, Oxford and Northampton

DISTRIBUTORS

Marston Book Services Ltd
PO Box 87
Oxford OX2 0DT
(*Orders*: Tel: 0865 791155
Fax: 0865 791927
Telex: 837515)

USA
Blackwell Scientific Publications, Inc.
238 Main Street
Cambridge, MA 02142
(*Orders*: Tel: 800 759-6102
617 876 7000)

Canada
Oxford University Press
70 Wynford Drive
Don Mills
Ontario M3C 1J9
(*Orders*: Tel: 416 441-2941)

Australia
Blackwell Scientific Publications Pty Ltd
54 University Street
Carlton, Victoria 3053
(*Orders*: Tel: 03 347-5552)

British Library
Cataloguing in Publication Data

A catalogue record for this book is available from the British Library

ISBN 0-632-02507-7

Library of Congress
Cataloging in Publication Data

Johnson, R. P. (Roger Paul)
Composite structures of steel and concrete / R.P. Johnson.—2nd ed.
p. cm.
Includes bibliographical references and index. Contents: v. 1. Beams, slabs, columns, and frames for building
ISBN 0–632–02507–7 (v. 1)
1. Composite construction. I. Title.
TA664.J63 1994
624.1'821—dc20 94–4646
CIP

Contents

Preface

This volume provides an introduction to the theory and design of composite structures of steel and concrete. Readers are assumed to be familiar with the elastic and plastic theories for the analysis for bending and shear of cross-sections of beams and columns of a single material, such as structural steel, and to have some knowledge of reinforced concrete. No previous knowledge is assumed of the concept of shear connection within a member composed of concrete and structural steel, nor of the use of profiled steel sheeting in composite slabs. Shear connection is covered in depth in Chapter 2 and Appendix A, and the principal types of composite member in Chapters 3, 4 and 5.

All material of a fundamental nature that is applicable to both buildings and bridges is included, plus more detailed information and a worked example relating to buildings. Subjects mainly relevant to bridges are covered in Volume 2. These include composite plate and box girders and design for repeated loading.

The design methods are illustrated by sample calculations. For this purpose a simple problem, or variations of it, has been used throughout the volume. The reader will find that the strengths of materials, loadings, and dimensions for this structure soon remain in the memory. The design should not be assumed to be an optimum solution to the problem, because one object here has been to encounter a wide range of design problems, whereas in practice one seeks to avoid them.

This volume is intended for undergraduate and graduate students, for university teachers, and for engineers in professional practice who seek familiarity with composite structures. Most readers will wish to develop the skills needed both to design new structures and to predict the behaviour of existing ones. This is now always done using guidance from a code of practice. The most comprehensive and broadly-based code available is Eurocode 4, which is introduced in Chapter 1. It makes use of recent research and of current practice, particularly that of western Europe and Australasia. It has much in common with the latest national codes in these regions, but its scope is wider. It is fully consistent with the latest codes for the design of concrete and steel structures, Eurocodes 2 and 3 respectively.

All the design methods explained in this volume are those of the

Eurocodes. The worked example, a multi-storey framed structure for a building, includes design to draft Eurocode 4: Part 1.2 for resistance to fire.

At the time of writing, the relevant Parts of Eurocodes 2, 3, and 4 have been issued throughout western Europe for trial use for a period of three years. In each country, each code is accompanied by its National Application Document (NAD), to enable it to be used before other European standards to which it refers (e.g. for actions (loadings)) are complete.

These documents may not yet be widely available, so this volume is self-contained. Readers do not need access to any Eurocodes, international standards, or NADs; but they should not assume that the worked examples here are fully in accordance with the Eurocodes as implemented in their own country. It is quite likely that some of the values used for γ and ψ factors will be different.

Engineers who need to use a Eurocode in professional practice should also consult the relevant Designers' Handbook. These are available in English for Parts 1.1 of Eurocodes 2, 3, and 4. They can only be read in conjunction with the relevant code. They are essentially commentaries, starting from a higher level of existing knowledge than that assumed here.

The use of the Eurocodes as the basis for this volume has led to the re-writing of over 80% of the first edition, and the provision of a new set of worked examples.

The author has since 1959 shared the excitements of research on composite structures with many colleagues and research students, and has since 1972 shared the challenge of drafting Eurocode 4: Part 1.1 with other members of multi-national committees, particularly Henri Mathieu, Karlheinz Roik, Jan Stark, and David Anderson. The substantial contributions made by these friends and colleagues to the author's understanding of this subject are gratefully acknowledged. However, responsibility for what is presented here rests with the writer, who would be glad to be informed of any errors that may be found.

Thanks are due also to Joan Carrington, for secretarial assistance with Eurocode 4, as well as this volume, to Jill Linfoot, for the diagrams, and to the Engineering Department, the University of Warwick, for other facilities provided.

R.P. Johnson
March 1994

Symbols

The symbols used in the Eurocodes are based on ISO 3898: 1987, 'Bases for design of structures – Notation – General symbols'. They are more consistent than in current British codes, and have generally been used in this volume.

A accidental action; area
a distance; geometrical data
b width; breadth
C factor; critical perimeter; secant stiffness
c distance
d diameter; depth; distance
E effect of actions; modulus of elasticity
e eccentricity; distance
F action; force
f strength (of a material); natural frequency; factor
f_{ck} characteristic compressive strength of concrete
f_{sk} characteristic yield strength of reinforcement
f_y nominal tensile yield strength of structural steel
G permanent action; shear modulus
g permanent action
H horizontal force
h height; thickness
I second moment of area
K coefficient
k coefficient; factor; connector modulus; stiffness
L length; span
l length; span
M bending moment; mass
M_{Rd} design value of the resisting bending moment
M_{Sd} design value of the applied internal bending moment
m bending moment per unit width; mass per unit length or area; factor for composite slab
N axial force; number of shear connectors
n modular ratio; number

P_R shear resistance of a shear connector
p pitch (spacing)
Q variable action
q variable action
R resistance; response factor; reaction
r radius of gyration
S internal forces and moments; width of slab
s spacing; slip
t thickness; time
u perimeter; distance
V shear force; vertical force or load
v shear force per unit length
W section modulus
w crack width; load per unit length
X value of a property of a material
x distance; axis
y distance; axis
Z shape factor
z distance; axis; lever arm
α angle; ratio; factor
β angle; ratio; factor
γ partial safety factor (always with subscript: e.g. A, F, G, M, Q, a, c, s, v)
Δ difference in . . . (precedes main symbol)
δ steel contribution ratio; deflection
ϵ strain; coefficient
ζ critical damping ratio
η coefficient; resistance ratio
θ temperature
λ load factor; slenderness ratio (or $\bar{\lambda}$)
μ coefficient of friction; moment ratio
ν Poisson's ratio
ρ unit mass; reinforcement ratio
σ normal stress
τ shear stress
ϕ diameter of a reinforcing bar; rotation; curvature
χ reduction factor (for buckling); ratio
ψ factors defining representative values of variable actions; stress ratio

Subscripts

A accidental
a structural steel

b buckling; beam
c compression; concrete; cylinder
cr critical
cu cube
d design
e elastic (or el); effective (or eff)
f flange; full; finishes; fire; Fourier
G permanent
g centre of area
h hogging
i index (replacing a numeral)
k characteristic
l longitudinal
LT lateral-torsional
M material
m mean
min minimum
n neutral axis
p (possibly supplementing a) profiled steel sheeting; perimeter; plastic
pl plastic
Q variable
R resistance
r reduced; rib
rms root mean square
S internal force; internal moment
s reinforcing steel; shear span; slab
t tension; total (overall); transverse
u ultimate
v related to shear connection
w web
x axis along a member
y major axis of cross-section; yield
z minor axis of cross-section
ϕ diameter

0,1,2, etc. particular values

Chapter 1
Introduction

1.1 Composite beams and slabs

The design of structures for buildings and bridges is mainly concerned with the provision and support of load-bearing horizontal surfaces. Except in long-span bridges, these floors or decks are usually made of reinforced concrete, for no other material has a better combination of low cost, high strength, and resistance to corrosion, abrasion, and fire.

The economical span for a reinforced concrete slab is little more than that at which its thickness becomes just sufficient to resist the point loads to which it may be subjected or, in buildings, to provide the sound insulation required. For spans of more than a few metres it is cheaper to support the slab on beams or walls than to thicken it. When the beams are also of concrete, the monolithic nature of the construction makes it possible for a substantial breadth of slab to act as the top flange of the beam that supports it.

At spans of more than about 10 m, and particularly where the susceptibility of steel to damage by fire is not a problem, as for example in bridges and multi-storey car parks, steel beams become cheaper than concrete beams. It used to be customary to design the steelwork to carry the whole weight of the concrete slab and its loading; but by about 1950 the development of shear connectors had made it practicable to connect the slab to the beam, and so to obtain the T-beam action that had long been used in concrete construction. The term 'composite beam' as used in this book refers to this type of structure.

The same term is used for beams in which prestressed and *in-situ* concrete act together, and there are many other examples of composite action in structures, such as between brick walls and beams supporting them, or between a steel-framed shed and its cladding; but these are outside the scope of this book.

No income is received from money invested in the construction of a multi-storey building such as a large office block until the building is occupied. For a construction time of two years, this loss of income from capital may be 10% of the total cost of the building; that is, about one-third of the cost of the structure. The construction time is strongly influenced by

the time taken to construct a typical floor of the building, and here structural steel has an advantage over *in-situ* concrete.

Even more time can be saved if the floor slabs are cast on permanent steel formwork that acts first as a working platform, and then as bottom reinforcement for the slab. This formwork, known as *profiled steel sheeting*, has long been used in tall buildings in North America.[1] Its use is now standard practice in most regions where the sheeting is readily available, such as Europe, Australasia and Japan. These floors span in one direction only, and are known as *composite slabs*. Where the steel sheet is flat, so that two-way spanning occurs, the structure is known as a *composite plate*. These occur in box-girder bridges, and are covered in Chapter 9 (Volume 2).

Profiled sheeting and partial-thickness precast concrete slabs are known as *structurally participating* formwork. Fibre-reinforced plastic or cement sheeting, sometimes used in bridges, is referred to as *structurally non-participating*, because once the concrete slab has hardened, the strength of the sheeting is ignored in design.

The degree of fire protection that must be provided is another factor that influences the choice between concrete, composite and steel structures, and here concrete has an advantage. Little or no fire protection is required for open multi-storey car parks, a moderate amount for office blocks, and most of all for warehouses and public buildings. Many methods have been developed for providing steelwork with fire protection.[2] Design against fire and the prediction of resistance to fire is known as fire engineering. There are relevant codes of practice, including a draft European code for composite structures.[3] Full or partial encasement in concrete is an economical method for steel columns, since the casing makes the columns much stronger. Full encasement of steel beams, once common, is now more expensive than the use of lightweight non-structural materials. It is used for some bridge beams (Volume 2). Concrete encasement of the web only, cast before the beam is erected, is more common in continental Europe than in the UK. It enhances the buckling resistance of the member (Section 3.5.2), as well as providing fire protection.

The choice between steel, concrete, and composite construction for a particular structure thus depends on many factors that are outside the scope of this book. Composite construction is particularly competitive for medium or long span structures where a concrete slab or deck is needed for other reasons, where there is a premium on rapid construction, and where a low or medium level of fire protection to steelwork is sufficient.

1.2 Composite columns and frames

When the stanchions in steel frames were first encased in concrete to protect them from fire, they were still designed for the applied load as if uncased. It was then realised that encasement reduced the effective slenderness of the column, and so increased its buckling load. Empirical methods for calculating the reduced slenderness still survive in some design codes for structural steelwork (Section 5.2).

This simple approach is not rational, for the concrete encasement also carries its share of both the axial load and the bending moments. More economical design methods, validated by tests, are now available (Section 5.6).

Where fire protection for the steel is not required, a composite column can be constructed without the use of formwork by filling a steel tube with concrete. A notable early use of filled tubes (1966) was in a four-level motorway interchange.[4] Design methods are now available for their use in buildings (Section 5.6.7).

In framed structures, there may be composite beams, composite columns, or both. Design methods have to take account of the interaction between beams and columns, so that many types of beam-to-column connection must be considered. Their behaviour can range from 'nominally pinned' to 'rigid', and influences bending moments throughout the frame. Two buildings with rigid-jointed composite frames were built in Great Britain in the early 1960s, in Cambridge[5] and London[6]. Current practice is mainly to use nominally pinned connections. In buildings, it is expensive to make connections so stiff that they can be modelled as 'rigid'. Even the simplest connections have sufficient stiffness to reduce deflexions of beams to an extent that is useful, so there is much current interest in testing connections and developing design methods for frames with 'semi-rigid' connections. No such method is yet widely accepted (Section 5.3).

1.3 Design philosophy and the Eurocodes

1.3.1 Background

In design, account must be taken of the random nature of loading, the variability of materials, and the defects that occur in construction, to reduce the probability of unserviceability or failure of the structure during its design life to an acceptably low level. Extensive study of this subject since about 1950 has led to the incorporation of the older 'safety factor' and 'load factor' design methods into a comprehensive 'limit state' design philosophy. Its first important application in Great Britain was in 1972, in CP 110, *The structural use of concrete.* All recent British and most international codes of practice for the design of structures now use it.

Work on international codes began after the Second World War, first on concrete structures and then on steel structures. A committee for composite structures, set up in 1971, prepared the Model Code of 1981.[7] Soon after January 1993 had been set as the target date for the completion of the Common Market in Europe, the Commission of the European Communities began (in 1982) to support work on documents now known as Eurocodes. It acts for the twelve countries of the European Union (formerly the EEC). In 1990, the seven countries of the European Free Trade Area (EFTA) joined in, and responsibility for managing the work was transferred to the Comité Européen Normalisation (CEN). This is an association of the national standards institutions of the 19 countries, which extend from Iceland and Finland in the north to Portugal and Greece in the south.

It is now planned to prepare nine Eurocodes with a total of over 50 Parts. Each is published first as a preliminary standard (ENV), accompanied in each country by a National Application Document. All of the Eurocodes relevant to this volume are or soon will be at this stage. They are as follows:

Eurocode 1: Part 1, Basis of design;[8]
Eurocode 1: Basis of design, and actions. Part 2, General rules and gravity and impressed loads, snow, wind, and fire;[9]
Eurocode 2: Part 1.1, Design of concrete structures; General rules and rules for buildings;[10]
Eurocode 3: Part 1.1, Design of steel structures; General rules and rules for buildings;[11]
Eurocode 4: Part 1.1, Design of composite steel and concrete structures; General rules and rules for buildings;[12]
Eurocode 4: Part 1.2, Structural fire design.[13]

At the end of its ENV period of three years, each Part of a Eurocode is revised, and will then be published as an EN (European standard), so the EN versions of the Parts listed above should appear from 1998 onwards. It is the intention that a few years later all relevant national codes in the 19 countries will be withdrawn from use.

The current British code that is most relevant to this volume is BS 5950: Part 3: Section 3.1: 1990.[14] It has much in common with Eurocode 4: Part 1.1, because the two were developed in parallel. The design philosophy, terminology, and notations of the Eurocodes have been harmonised to a greater extent than those of the current British codes, so it is convenient generally to follow the Eurocodes in this volume. Eurocode 4: Part 1.1 will be cited simply as 'Eurocode 4' or 'EC4', and reference will be made to significant differences from BS 5950.

This volume is intended to be self-contained, and to provide an introduction to its subject. Those who use Eurocode 4 in professional practice may need to refer to the relevant Handbook.[15]

1.3.2 Limit state design philosophy

1.3.2.1 Actions

Parts 1.1 of Eurocodes 2, 3 and 4 each have a Chapter 2, 'Basis of design', in which the definitions, classifications, and principles of limit state design are set out in detail, with emphasis on design of structures for buildings. Much of these chapters will eventually be superseded by Eurocode 1: Part 1, where the scope is being extended to include bridges, towers, masts, silos and tanks, foundations, etc.

The word 'actions' in the title of Eurocode 1: Part 2 does not appear in British codes. Actions are classified as

- direct actions (forces or loads applied to the structure), or
- indirect actions (deformations imposed on the structure, for example by settlement of foundations, change of temperature, or shrinkage of concrete).

'Actions' thus has a wider meaning than 'loads'. Similarly, the Eurocode term 'effects of actions' has a wider meaning than 'stress resultant', because it includes stresses, strains, deformations, crack widths, etc., as well as bending moments, shear forces, etc. The Eurocode term for 'stress resultant' is 'internal force or moment'.

The scope of the following introduction to limit state design is limited to that of the design examples in this volume. There are two classes of *limit states*:

- ultimate, which are associated with structural failure; and
- serviceability, such as excessive deformation, vibration, or width of cracks in concrete.

There are three types of *design situation*:

- persistent, corresponding to normal use;
- transient, for example, during construction; and
- accidental, such as fire or earthquake.

There are three main types of *action*:

- permanent (G), such as self-weight of a structure, sometimes called 'dead load';
- variable (Q), such as imposed, wind or snow load, sometimes called 'live load'; and
- accidental (A), such as impact from a vehicle.

The spatial variation of an action is either:

- fixed (typical of permanent actions); or
- free (typical of other actions), and meaning that the action may occur over only a part of the area or length concerned.

Permanent actions are represented (and specified) by a *characteristic value*, G_k. 'Characteristic' implies a defined fractile of an assumed statistical distribution of the action, modelled as a random variable. For permanent loads it is usually the mean value (50% fractile).

Variable loads have four *representative values*:

- characteristic (Q_k), normally the lower 5% fractile;
- combination ($\psi_0 Q_k$), for use where the action is assumed to accompany the design value of another variable action;
- frequent ($\psi_1 Q_k$); and
- quasi-permanent ($\psi_2 Q_k$).

Values of the combination factors ψ_0, ψ_1, and ψ_2 (all less than 1.0) are given in the relevant Part of Eurocode 1. For example, for imposed loads on the floors of offices, category B, they are 0.7, 0.5 and 0.3, respectively.

Design values of actions are, in general, $F_d = \gamma_F F_k$, and in particular:

$$G_d = \gamma_G G_k \tag{1.1}$$

$$Q_d = \gamma_Q Q_k \quad \text{or} \quad Q_d = \gamma_Q \psi_i Q_k \tag{1.2}$$

where γ_G and γ_Q are partial safety factors for actions, given in Eurocode 1. They depend on the limit state considered, and on whether the action is unfavourable or favourable for (i.e. tends to increase or decrease) the action effect considered. The values used in this volume are given in Table 1.1.

Table 1.1 Values of γ_G and γ_Q for persistent design situations.

Type of action	*Permanent*		*Variable*	
	unfavourable	*favourable*	*unfavourable*	*favourable*
Ultimate limit states	1.35*	1.35*	1.5	0
Serviceability limit states	1.0	1.0	1.0	0

*Except for checking loss of equilibrium, or where the coefficient of variation is large.

The *effects of actions* are the responses of the structure to the actions:

$$E_d = E(F_d) \tag{1.3}$$

where the function E represents the process of structural analysis. Where the effect is an internal force or moment, it is sometimes denoted S_d (from the French word sollicitation), and *verification for an ultimate limit state* consists of checking that

$$S_d \leq R_d \quad \text{or} \quad E_d \leq R_d \tag{1.4}$$

where R_d is the relevant design resistance of the system or member or cross-section considered.

1.3.2.2 Resistances

Resistances, R_d, are calculated using design values of properties of materials, X_d, given by

$$X_d = \frac{X_k}{\gamma_M} \tag{1.5}$$

where X_k is a characteristic value of the property, and γ_M is the partial safety factor for that property.

The characteristic value is typically a 5% lower fractile (e.g. for compressive strength of concrete). Where the statistical distribution is not well established, it is replaced by a *nominal* value (e.g. the yield strength of structural steel) that is so chosen that it can be used in design in place of X_k.

Table 1.2 Values of γ_M for resistances and properties of materials.

Material	*Structural steel*	*Reinforcing steel*	*Profiled sheeting*	*Concrete*	*Shear connection*
Property	f_y	f_{sk}	f_{yp}	f_{ck} or f_{cu}	P_{Rk}
Symbol for γ_M	γ_a	γ_s	γ_{ap}	γ_c	γ_v
Ultimate limit states	1.10	1.15	1.10	1.5	1.25
Serviceability limit states	1.0	1.0	1.0	1.0 or 1.3	1.0

Notation: f_y and f_{yp} are nominal yield strengths, f_{sk} is a characteristic yield strength, and f_{ck} and f_{cu} are respectively characteristic cylinder and cube strengths.

In Eurocode 4, the subscript M in γ_M is replaced by a letter that indicates the material concerned, as shown in Table 1.2, which gives the values of γ_M used in this volume. A welded stud shear connector is treated like a single material, even though its resistance to shear, P_R, is influenced by the properties of both steel and concrete.

1.3.2.3 'Boxed values' of γ_F, γ_M, and ψ

In the Eurocodes, numerical values given for these factors (and for certain other data) are enclosed in boxes. These indicate that the Members of CEN (the national standards organisations) are allowed to specify other values in their National Application Documents. This may be necessary where characteristic actions are being taken from national codes, or where

a country wishes to use a different margin of safety from that given by the boxed values.

The value of γ_a, for structural steel, at ultimate limit states has been particularly controversial, and several countries (including the UK) are expected to adopt values lower than the 1.10 given in the Eurocodes and used in this volume.

1.3.2.4 Combinations of actions

The Eurocodes treat systematically a subject for which many empirical procedures have been used in the past. For ultimate limit states, the principles are:

- permanent actions are present in all combinations;
- each variable action is chosen in turn to be the 'leading' action (i.e. to have its full design value), and is combined with lower 'combination' values of other relevant variable actions;
- the design action effect is the most unfavourable of those calculated by this process.

The use of combination values allows for the lack of correlation between time-dependent variable actions.

As an example, it is assumed that a bending moment M_d in a member is influenced by its own weight (G), by an imposed vertical load (Q_1) and by wind loading (Q_2). The fundamental combinations for verification for persistent design situations are:

$$\gamma_G G_k + \gamma_{Q1} Q_{k,1} + \gamma_{Q2} \psi_{0,2} Q_{k,2} \tag{1.6}$$

and

$$\gamma_G G_k + \gamma_{Q1} \psi_{0,1} Q_{k,1} + \gamma_{Q2} Q_{k,2} \,. \tag{1.7}$$

In practice, it is usually obvious which combination will govern. For low-rise buildings, wind is rarely critical for floors, so expression (1.6), with imposed load leading, would be used; but for a long-span lightweight roof, expression (1.7) could govern, and both positive and negative wind pressures would be considered.

The combination for accidental design situations is given in Section 3.3.7.

For serviceability limit states, three combinations are defined. The most onerous of these, the 'rare' combination, is recommended in Eurocode 4 for checking deformations of beams and columns. For the example given above, it is:

$$G_k + Q_{k,1} + \psi_{0,2} Q_{k,2} \tag{1.8}$$

or

$$G_k + \psi_{0,1} Q_{k,1} + Q_{k,2} \,. \tag{1.9}$$

Assuming that Q_1 is the leading variable action, the others are:

- frequent combination:

$$G_k + \psi_{1,1} Q_{k,1} + \psi_{2,2} Q_{k,2} \tag{1.10}$$

- quasi-permanent combination:

$$G_k + \psi_{2,1} Q_{k,1} + \psi_{2,2} Q_{k,2} \,. \tag{1.11}$$

The quasi-permanent combination is recommended in Eurocode 4 for checking widths of cracks in concrete. The frequent combination is not at present used in Eurocode 4: Part 1.1.

The values of the combination factors to be used in this volume, taken from draft Eurocode 1, are given in Table 1.3.

Table 1.3 Combination factors.

Factor	ψ_0	ψ_1	ψ_2
Imposed floor loading in office building, category C	0.7	0.7	0.6
Wind loading	0.6	0.5	0

1.3.2.5 Simplified combinations of actions

Eurocode 4 allows the use of simplified combinations for the design of building structures. For the example above, and assuming that Q_1 is more adverse than Q_2, they are as follows:

- for ultimate limit states, the more adverse of

$$\gamma_G G_k + \gamma_{Q1} Q_{k,1} \tag{1.12}$$

and

$$\gamma_G G_k + 0.9\,(\gamma_{Q1} Q_{k,1} + \gamma_{Q2} Q_{k,2}) \tag{1.13}$$

- for the rare combination at serviceability limit states, the more adverse of

$$G_k + Q_{k,1} \tag{1.14}$$

and

$$G_k + 0.9\,(Q_{k,1} + Q_{k,2}) \,. \tag{1.15}$$

1.3.2.6 Comments on limit state design philosophy

'Working stress' or 'permissible stress' design has been replaced by limit states design partly because limit states provide identifiable criteria for satisfactory performance. Stresses cannot be calculated with the same confidence as resistances of members, and high values may or may not be significant.

One apparent disadvantage of limit states design is that as limit states occur at various load levels, several sets of design calculations are needed, whereas with some older methods, one was sufficient. This is only partly true, for it has been found possible when drafting codes of practice to identify many situations in which design for, say, ultimate limit states will automatically ensure that certain types of serviceability will not occur; and vice versa. In Eurocode 4: Part 1.1 it has generally been possible to avoid specifying limiting stresses for serviceability limit states, by using the methods described in Sections 3.4.5, 3.7, 4.2.5 and 4.4.

1.4 Properties of materials

Information on the properties of structural steel, concrete, and reinforcement is readily available. Only that which has particular relevance to composite structures will be given here.

For the determination of the bending moments and shear forces in a beam or framed structure (known as 'global analysis') all three materials can be assumed to behave in a linear-elastic manner, though an effective modulus has to be used for the concrete, to allow for its creep under sustained compressive stress. The effects of cracking of concrete in tension, and of shrinkage, can be allowed for, but are rarely significant in buildings.

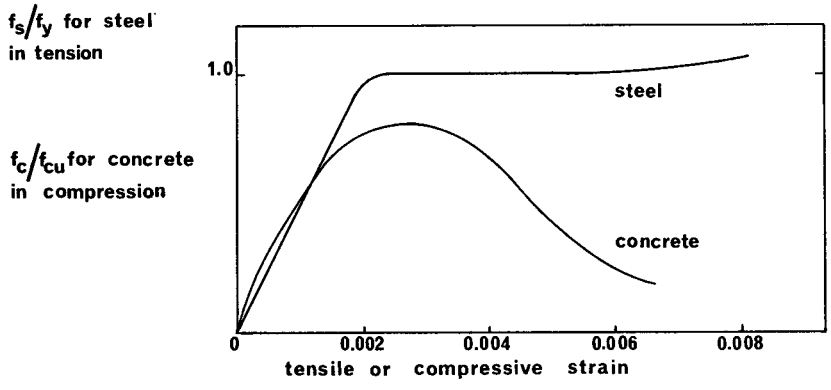

Fig. 1.1 Stress–strain curves for concrete and structural steel.

Rigid-plastic global analysis can sometimes be used (Section 4.3.3), despite the profound difference between a typical stress-strain curve for concrete in compression, and those for structural steel or reinforcement, in tension or compression, that is illustrated in Fig. 1.1. Concrete reaches its maximum compressive stress at a strain of between 0.002 and 0.003, and at higher strains it crushes, losing almost all its compressive strength. It is very brittle in tension, having a strain capacity of only about 0.0001 (i.e. 0.1 mm per metre) before it cracks. The figure also shows that the maximum stress reached by concrete in a beam or column is little more than 80% of its cube strength. Steel yields at a strain similar to that given for crushing of concrete, but on further straining the stress in steel continues to increase slowly, until the total strain is at least 40 times the yield strain. The subsequent necking and fracture is of significance for composite members only above internal supports of continuous beams, for the useful resistance of a cross-section is reached when all of the steel yields, when steel in compression buckles, or when concrete crushes.

Resistances of cross-sections are determined ('local analysis') using plastic analysis wherever possible, because results of elastic analyses are unreliable, unless careful account is taken of cracking, shrinkage, and creep of concrete, and also because plastic analysis is simpler and leads to more economical design.

The higher value of γ_M that is used for concrete, in comparison with steel (Table 1.2) reflects not only the higher variability of the strength of test specimens, but also the variation in the strength of concrete over the depth of a member, due to migration of water before setting, and the larger errors in the dimensions of cross-sections, particularly in the positions of reinforcing bars.

Brief comments are now given on individual materials.

Concrete

A typical strength class for concrete in Eurocodes 2 and 4 is denoted C25/30, where the characteristic compressive strengths at 28 days are $f_{ck} = 25$ N/mm^2 (cylinder) and $f_{cu} = 30$ N/mm^2 (cube). All design formulae use f_{ck}, not f_{cu}, so in worked examples here, 'Grade 30' concrete (in British terminology) will be used, with f_{ck} taken as 25 N/mm^2. Other properties for this concrete, given in Eurocode 4, are as follows:

- mean tensile strength, $f_{ctm} = 2.6$ N/mm^2
- with upper and lower 5% fractiles: $f_{ctk\ 0.95} = 3.3$ N/mm^2
  $f_{ctk\ 0.05} = 1.8$ N/mm^2
- basic shear strength, $\tau_{Rd} = 0.25\, f_{ctk\ 0.05}/\gamma_c = 0.30$ N/mm^2
- coefficient of linear thermal expansion, 10×10^{-6} per °C.

'Normal-density' concrete typically has a density, ρ, of 2400 kg/m^3. It is used for composite columns and web encasement in worked examples

here, but the floor slabs are constructed in lightweight-aggregate concrete with density $\rho = 1900$ kg/m^3. The mean secant modulus of elasticity is given in Eurocode 4 for grade C25/30 concrete as

$$E_{cm} = 30.5\ (\rho/2400)^2\ \text{kN/mm}^2,$$

with ρ in kg/m^3 units.

Reinforcing steel

Standard strength grades for reinforcing steel will be specified in EN 10 080[16] in terms of a characteristic yield strength f_{sk}. Values of f_{sk} used in worked examples here are 460 N/mm^2, for ribbed bars, and 500 N/mm^2, for welded steel fabric or mesh. It is assumed here that both types of reinforcement satisfy the specifications for 'high bond action' and 'high ductility' to be given in EN 10 080.

The modulus of elasticity for reinforcement, E_s, is normally taken as 200 kN/mm^2; but in a composite section it may be assumed to have the value for structural steel, $E_a = 210$ kN/mm^2, as the error is negligible.

Structural steel

Standard strength grades for structural steel are given in EN 10 025[17] in terms of a nominal yield strength f_y and ultimate tensile strength f_u. These values may be adopted as characteristic values in calculations. The grade used in worked examples here is S 355, for which

$$f_y = 355\ \text{N/mm}^2, \quad f_u = 510\ \text{N/mm}^2$$

for elements of all thicknesses up to 40 mm.

The density of structural steel is assumed to be 7850 kg/m^3. Its coefficient of linear thermal expansion is given in Eurocode 3 as 12×10^{-6} per °C, but for simplicity the value 10×10^{-6} per °C (as for reinforcement and normal-density concrete) may be used in the design of composite structures for buildings.

Profiled steel sheeting

This material is available with yield strengths (f_{yp}) ranging from 235 N/mm^2 to at least 460 N/mm^2, in profiles with depths ranging from 45 mm to over 200 mm, and with a wide range of shapes. These include both re-entrant and open troughs, as in Fig. 3.9. There are various methods for achieving composite action with a concrete slab, discussed in Section 2.4.3.

Sheets are normally between 0.8 mm and 1.5 mm thick, and are protected from corrosion by a zinc coating about 0.02 mm thick on each face. Elastic properties of the material may be assumed to be as for structural steel.

Shear connectors

Details of these and the measurement of their resistance to shear are given in Chapter 2.

1.5 Direct actions (loading)

The characteristic loadings to be used in worked examples are now given. They are taken from draft Eurocode 1.

The *permanent loads* (dead load) are the weights of the structure and its finishes. In composite members, the structural steel component is usually built first, so a distinction must be made between load resisted by the steel component only, and load applied to the member after the concrete has developed sufficient strength for composite action to be effective. The division of the dead load between these categories depends on the method of construction. Composite beams and slabs are classified as *propped* or *unpropped*. In propped construction, the steel member is supported at intervals along its length until the concrete has reached a certain proportion, usually three-quarters, of its design strength. The whole of the dead load is then assumed to be resisted by the composite member. Where no props are used, it is assumed in elastic analysis that the steel member alone resists its own weight and that of the formwork and the concrete slab. Other dead loads such as floor finishes and internal walls are added later, and so are assumed to be carried by the composite member. In ultimate-strength methods of analysis (Section 3.5.3) it can be assumed that the effect of the method of construction of the resistance of a member is negligible.

The principal vertical *variable load* in a building is a uniformly-distributed load on each floor. For offices, Eurocode 1: Part 2.4 gives 'for areas subject to overcrowding and access areas' its characteristic value as

$$q_k = 5.0 \text{ kN/m}^2. \tag{1.16}$$

For checking resistance to point loads a concentrated load

$$Q_k = 7.0 \text{ kN} \tag{1.17}$$

is specified, acting on any area 50 mm square. These rather high loads are chosen to allow for a possible change of use of the building. A more typical loading q_k for an office floor is 3.0 kN/m^2.

Where a member such as a column is carrying loads q_k from n storeys ($n > 2$), the total of these loads may be multiplied by a factor

$$\alpha_n = \frac{2 + (n - 2)\psi_0}{n} \tag{1.18}$$

where ψ_0 is given in Table 1.3. This allows for the low probability that all n floors will be fully loaded at once.

The principal horizontal variable load for a building is wind. Wind loads are given in Eurocode 1: Part 2.7.They usually consist of pressure or suction on each external surface, though frictional drag may be significant on large flat areas. Wind loads rarely influence the design of composite

beams, but can be important in framed structures not braced against sidesway (Section 5.4.2) and in all tall buildings.

Methods of calculation that consider distributed and point loads are sufficient for all types of direct action. Indirect actions such as differential changes of temperature and shrinkage of concrete can cause stresses and deflections in composite structures, but rarely influence the structural design of buildings. Their effects in composite bridge beams are explained in Volume 2.

1.6 Methods of analysis and design

The purpose of this section is to provide a preview of the principal methods of analysis used in this volume, and to show that most of them are straightforward applications of methods in common use for steel or for concrete structures.

The steel designer will be familiar with the elementary elastic theory of bending, and the simple plastic theory in which the whole cross-section of a member is assumed to be at yield, in either tension or compression. Both theories are used for composite members, the differences being as follows:

- concrete in tension is usually neglected in elastic theory, and always neglected in plastic theory;
- in the elastic theory, concrete in compression is 'transformed' to steel by dividing its breadth by the modular ratio E_a/E_c;
- in the plastic theory, the equivalent 'yield stress' of concrete in compression is assumed in Eurocodes 2 and 4 to be $0.85\,f_{ck}$, where f_{ck} is the characteristic cylinder strength of the concrete. Examples of this method will be found in Sections 3.5.3 and 5.6.4.

In the UK, the compressive strength of concrete is specified as a cube strength, f_{cu}. In the strength classes defined in the Eurocodes (C20/25 to C50/60) the ratios f_{ck}/f_{cu} range from 0.78 to 0.83, so the stress $0.85\,f_{ck}$ corresponds to a value between $0.66\,f_{cu}$ and $0.70\,f_{cu}$. It is thus consistent with BS 5950[14] which uses $0.67\,f_{cu}$ for the unfactored plastic resistance of cross-sections.

The factor 0.85 takes account of several differences between a standard cylinder test and what concrete experiences in a structural member. These include the longer duration of loading in the structure, the presence of a stress gradient across the section considered, and differences in the boundary conditions for the concrete.

The concrete designer will be familiar with the method of transformed sections, and with the rectangular-stress-block theory outlined above. The basic difference from the elastic behaviour of reinforced concrete beams is that the steel section in a composite beam is more than

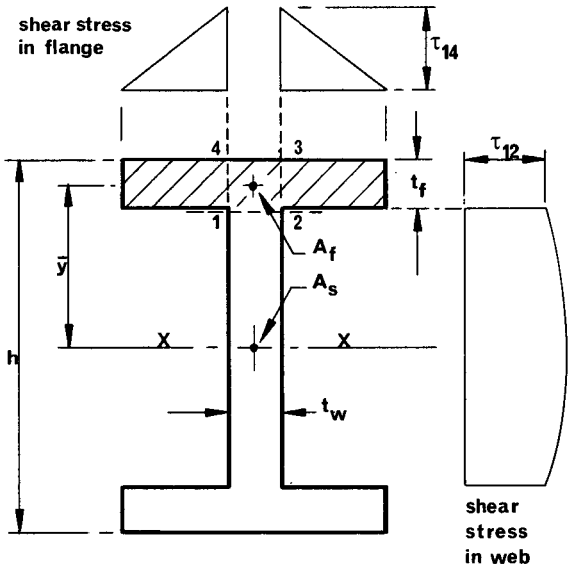

Fig. 1.2 Shear stresses in elastic I-section.

tension reinforcement, because it has a significant bending stiffness of its own. It also resists most of the vertical shear.

The formulae for the elastic properties of composite sections are more complex that those for steel or reinforced concrete sections. The chief reason is that the neutral axis for bending may lie in the web, the steel flange, or the concrete flange of the member. The theory is not in principle any more complex than that used for a steel I-beam.

Longitudinal shear

Students usually find this subject troublesome even though the formula

$$\tau = \frac{VA\bar{y}}{Ib} \tag{1.19}$$

is familiar from their study of vertical shear stress in elastic beams, so a note on the use of this formula may be helpful. Its proof can be found in any undergraduate-level textbook on strength of materials.

We consider first the shear stresses in the elastic I-beam shown in Fig. 1.2 due to a vertical shear force V. For the cross-section 1–2 through the web, the 'excluded area' is the flange, of area A_f, and the distance $\bar{y}$ of its centroid from the neutral axis is $\frac{1}{2}(h - t_f)$. The longitudinal shear stress τ_{12} on plane 1–2, of breadth t_w, is therefore

$$\tau_{12} = \frac{\frac{1}{2} VA_f(h - t_f)}{It_w}$$

where I is the second moment of area of the section about the axis XX.

Consideration of the longitudinal equilibrium of the small element 1234 shows that if its area $t_w t_f$ is much less than A_f, then the mean shear stress on planes 1–4 and 2–3 is given approximately by

$$\tau_{14} t_f = \tfrac{1}{2} \tau_{12} t_w$$

Repeated use of (1.19) for various cross-sections shows that the variation of longitudinal shear stress is parabolic in the web and linear in the flanges, as shown in Fig. 1.2.

The second example is the elastic beam shown in section in Fig. 1.3. This represents a composite beam in sagging bending, with the neutral axis at depth x, a concrete slab of thickness h_c, and the interface between the slab and the structural steel (which is assumed to have no top flange) at level 6–5. The concrete has been transformed to steel, so the cross-hatched area is the equivalent steel section. The concrete in area ABCD is assumed to be cracked, to resist no longitudinal stress, but to be capable of transferring shear stress.

Equation (1.19) is based on rate of change of bending stress, so in applying it here, area ABCD is omitted when the 'excluded area' is calculated. Let the cross-hatched area of flange be A_f, as before. The longitudinal shear stress on plane 6–5 is given by

$$\tau_{65} = \frac{V A_f \bar{y}}{I t_w} \tag{1.20}$$

where $\bar{y}$ is the distance from the centroid of the excluded area to the

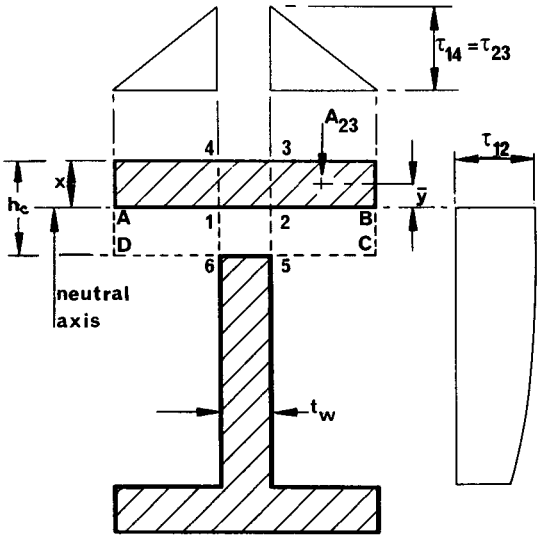

Fig. 1.3 Shear stresses in a composite section with the neutral axis in the concrete slab.

neutral axis, *not to plane 6–5*. If A and $\bar{y}$ are calculated for the cross-hatched area below plane 6–5, the same value τ_{65} is obtained, because it is the equality of these two $A\bar{y}$s that determines the value x.

For plane 6–5, the shear force per unit length of beam (symbol v), equal to $\tau_{65}t_w$, is more meaningful than τ_{65} because this is the force resisted by the shear connectors, according to elastic theory. This theory is used for the design of shear connection in bridge decks, but not in buildings, as there is a simpler ultimate-strength method (Section 3.6).

For a plane such as 2–3, the longitudinal shear force per unit length is given by equation (1.19) as

$$v = \tau_{23}x = \frac{VA_{23}\bar{y}}{I}. \tag{1.21}$$

The shear stress in the concrete on this plane, τ_c, is

$$\tau_c = \frac{v}{h_c}. \tag{1.22}$$

It is not equal to τ_{23} because the cracked concrete can resist shear; and it does not have to be divided by the modular ratio, even though the transformed section is of steel, because the transformation is of widths, not depths. This is a stress on an area that has not been reduced by transformation. An alternative explanation is that shear forces v from equation (1.21) are independent of the material considered, because transformation does not alter the ratio A_{23}/I.

The variation of τ_c across the width of the concrete flange is 'triangular' as shown at the top of Fig. 1.3.

Longitudinal slip

Shear connectors are not rigid, so that a small longitudinal slip occurs between the steel and concrete components of a composite beam. The problem does not arise in other types of structure, and relevant analyses are quite complex (Section 2.6 and Appendix A). They are not needed in design, for which simplified methods have been developed.

Deflections

The effects of creep and shrinkage make the calculation of deflections in reinforced concrete beams more complex than for steel beams, but the limiting span/depth ratios given in codes such as BS 8110[18] provide a simple means of checking for excessive deflection. These are unreliable for composite beams, especially where unpropped construction is used, so deflections are normally checked by calculations similar to those used for reinforced concrete, as shown in Section 3.7.

Vertical shear

The methods used for steel beams are applicable also to composite beams. In beams with slender webs, some advantage can be taken of the connec-

tion of the steel beam to a concrete slab; but the resistance of a concrete flange to vertical shear is normally neglected, as it is much less than that of the steel member.

Buckling of flanges and webs of beams
This will be a new problem to many designers of reinforced concrete. In continuous beams it leads to restrictions on the slenderness of unstiffened flanges and webs (Section 3.5.2). In Eurocode 4, these are identical to those given for steel beams in Eurocode 3; and in the British code,[14] the values for webs are slightly more restrictive than those for steel beams.

Crack-width control
The maximum spacings for reinforcing bars recommended in codes for reinforced concrete are intended to limit the widths of cracks in concrete, for reasons of appearance and to avoid corrosion of reinforcement. In composite structures for buildings, cracking is likely to be a problem only in encased beams, or where the top surfaces of continuous beams are exposed to corrosion. The principles of crack-width control are as for reinforced concrete, but calculations may be more complicated (Section 4.2.5). They can normally be avoided by using the bar-spacing rules given in Eurocode 4.

Continuous beams
In developing a simple design method for continuous beams in buildings (Chapter 4), use has been made of the simple plastic theory (as used for steel structures) and of redistribution of moments (as used for concrete structures).

Columns
The only British code that gives a design method for composite columns is BS 5400: Part 5, 'Composite bridges', and that method (described in Chapter 14, Volume 2) is rather complex for use in buildings. Eurocode 4 given a new and simpler method, developed in Germany, which is described in Section 5.6.

Framed structures for buildings
Composite members normally form part of a frame that is essentially steel, rather than concrete, so the design methods given in Eurocode 4 (Section 5.4) are based on those of Eurocode 3, for steel structures. Beam-to-column connections are classified in the same way, and the same criteria are used for classifying frames as 'braced' or 'unbraced' and as 'sway' or 'non-sway'. No design method for composite frames has yet been developed that is both simple and rational, and much research is in progress, particularly on design using semi-rigid connections.

Structural fire design

The high thermal conductivity of structural steel and profiled steel sheeting causes them to lose strength in fire more quickly than concrete does. Structures for buildings are required to have fire resistance of minimum duration (typically, 30 minutes to 2 hours) to enable occupants to escape, and to protect fire fighters. This leads to the provision either of minimum thicknesses of concrete and areas of reinforcement, or of thermal insulation for steelwork. Fire testing combined with parametric studies by finite-element analysis have led to reliable design methods. Fire engineering is an extensive subject, so only a few of these methods are explained here, in Sections 3.3.7, 3.10, and 5.6.2, with worked examples in Sections 3.4.6
and 3.11.4.

Chapter 2

Shear Connection

2.1 Introduction

The established design methods for reinforced concrete and for structural steel give no help with the basic problem of connecting steel to the concrete. The force applied to this connection is mainly, but not entirely, longitudinal shear. As with bolted and welded joints, the connection is a region of severe and complex stress that defies accurate analysis, and so methods of connection have been developed empirically and verified by tests. They are described in Section 2.4.

The simplest type of composite member used in practice occurs in floor structures of the type shown in Fig. 3.1. The concrete floor slab is continuous over the steel I-sections, and is supported by them. It is designed to span in the y-direction in the same way as when supported by walls or the ribs of reinforced concrete T-beams. When shear connection is provided between the steel member and the concrete slab, the two together span in the x-direction as a composite beam. The steel member has not been described as a 'beam', because its main function at midspan is to resist tension, as does the reinforcement in a T-beam. The compression is assumed to be resisted by an 'effective' breadth of slab, as explained in Section 3.4.

In buildings, but not in bridges, these concrete slabs are often composite with profiled steel sheeting (Fig. 2.8), which rests on the top flange of the steel beam. Other types of cross-section that can occur in composite beams are shown in Fig. 2.1.

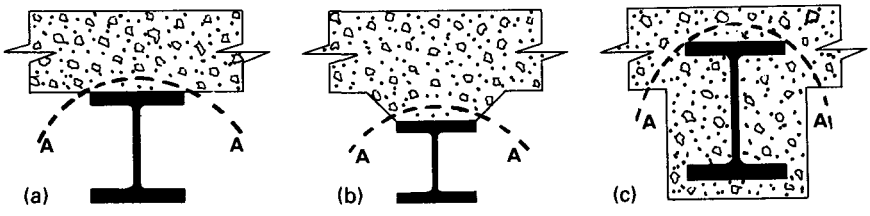

Fig. 2.1 Typical cross-sections of composite beams.

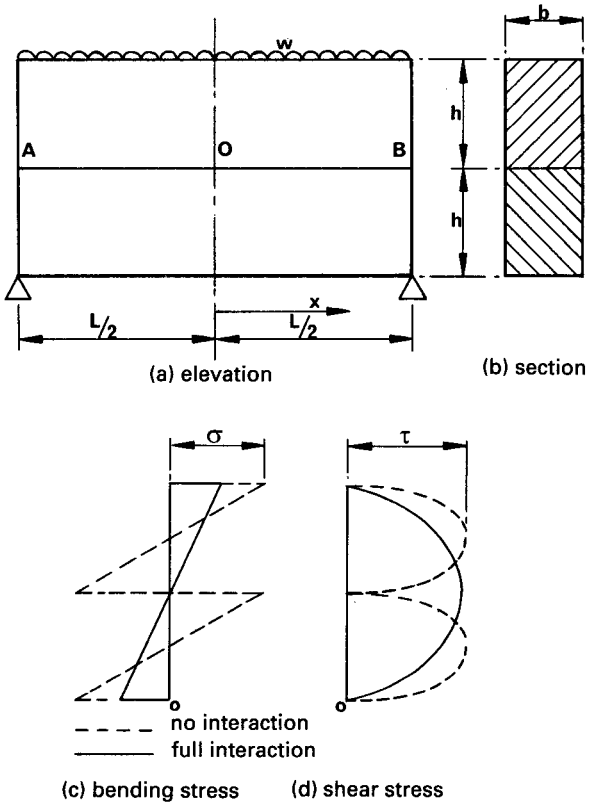

Fig. 2.2 Effect of shear connection on bending and shear stresses.

The ultimate-strength design methods used for shear connection in beams and columns in buildings are described in Sections 3.6 and 5.6.6, respectively. The elasticity-based methods used in bridges are explained in Section 8.5 and Chapter 10 in Volume 2.

The subjects of the present chapter are: the effects of shear connection on the behaviour of very simple beams, current methods of shear connection, standard tests on shear connectors, and shear connection in composite slabs.

2.2 Simply-supported beam of rectangular cross-section

Flitched beams, whose strength depended on shear connection between parallel timbers, were used in mediaeval times, and survive today in the form of glued-laminated construction. Such a beam, made from two members of equal size (Fig. 2.2), will now be studied. It carries a load w per unit length over a span L, and its components are made of an elastic material with Young's modulus E. The weight of the beam is neglected.

2.2.1 No shear connection

We assume first that there is no shear connection or friction on the interface AB. The upper beam cannot deflect more than the lower one, so each carries load $w/2$ per unit length as if it were an isolated beam of second moment of area $bh^3/12$, and the vertical compressive stress across the interface is $w/2b$. The midspan bending moment in each beam is $wL^2/16$. By elementary beam theory, the stress distribution at midspan is as in Fig. 2.2.(c), and the maximum bending stress in each component, σ, is given by

$$\sigma = \frac{My_{\max}}{I} = \frac{wL^2}{16}\frac{12}{bh^3}\frac{h}{2} = \frac{3wL^2}{8bh^2}. \tag{2.1}$$

The maximum shear stress, τ, occurs near a support. The parabolic distribution given by simple elastic theory is shown in Fig. 2.2(d); and at the centre-line of each member,

$$\tau = \frac{3}{2}\frac{wL}{4}\frac{1}{bh} = \frac{3wL}{8bh}. \tag{2.2}$$

The maximum deflection , δ, is given by the usual formula

$$\delta = \frac{5(w/2)L^4}{384EI} = \frac{5}{384}\frac{w}{2}\frac{12L^4}{Ebh^3} = \frac{5wL^4}{64Ebh^3}. \tag{2.3}$$

The bending moment in each beam at a section distant x from midspan is $M_x = w(L^2 - 4x^2)/16$, so that the longitudinal strain ϵ_x at the bottom fibre of the upper beam is

$$\epsilon_x = \frac{My_{\max}}{EI} = \frac{3w}{8Ebh^2}(L^2 - 4x^2). \tag{2.4}$$

There is an equal and opposite strain in the top fibre of the lower beam, so that the difference between the strains in these adjacent fibres, known as the *slip strain*, is $2\epsilon_x$.

It is easy to show by experiment with two or more flexible wooden laths or rulers that under load, the end faces of the two-component beam have the shape shown in Fig. 2.3(a). The slip at the interface, s, is zero at $x = 0$ (from symmetry) and a maximum at $x = \pm L/2$. The cross-section at $x = 0$ is the only one where plane sections remain plane. The slip strain, defined above, is not the same as slip. In the same way that strain is rate of change of displacement, slip strain is the rate of change of slip along the beam. Thus from (2.4),

$$\frac{ds}{dx} = 2\epsilon_x = \frac{3w}{4EBh^2}(L^2 - 4x^2). \tag{2.5}$$

Integration gives

$$s = \frac{w}{4Ebh^2}(3L^2x - 4x^3). \tag{2.6}$$

The constant of integration is zero, since $s = 0$ when $x = 0$, so that (2.6) gives the distribution of slip along the beam.

Results (2.5) and (2.6) for the beam studied in Section 2.7 are plotted in Fig. 2.3. This shows that at midspan, slip strain is a maximum and slip is zero, and at the ends of the beam, slip is a maximum and slip strain is zero. From (2.6), the maximum slip (when $x = L/2$) is $wL^3/4Ebh^2$. Some idea of the magnitude of this slip is given by relating it to the maximum deflection of the two beams. From (2.3), the ratio of slip to deflection is $3.2h/L$. The ratio $L/2h$ for a beam is typically about 20, so that the end slip is less than a tenth of the deflection. We conclude that *shear connection must be very stiff if it is to be effective.*

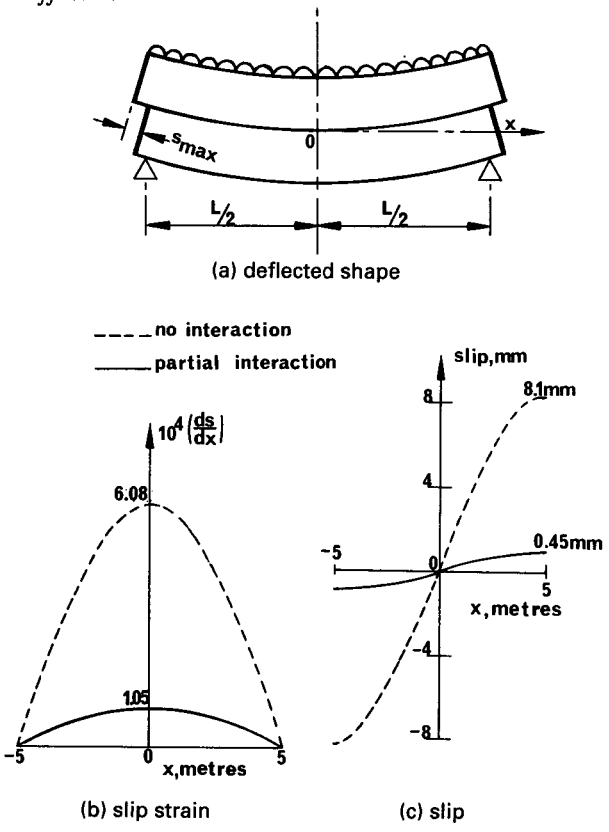

Fig. 2.3 Deflections, slip strain and slip.

2.2.2 Full interaction

It is now assumed that the two halves of the beam shown in Fig. 2.2 are joined together by an infinitely stiff shear connection. The two members then behave as one. Slip and slip strain are everywhere zero, and it can be assumed that plane sections remain plane. This situation is known as *full*

interaction. With one exception (Section 3.5.3), all design of composite beams and columns in practice is based on the assumption that full interaction is achieved.

For the composite beam of breadth b and depth $2h$, $I = 2bh^3/3$, and elementary theory gives the midspan bending moment as $wL^2/8$. The extreme fibre bending stress is

$$\sigma = \frac{My_{max}}{I} = \frac{wL^2}{8}\frac{3}{2bh^3}h = \frac{3wL^2}{16bh^2}. \tag{2.7}$$

The vertical shear at section x is

$$V_x = wx \tag{2.8}$$

so the shear stress at the neutral axis is

$$\tau_x = \frac{3}{2}wx\frac{1}{2bh} = \frac{3wx}{4bh} \tag{2.9}$$

and the maximum shear stress is

$$\tau = \frac{3wL}{8bh}. \tag{2.10}$$

The stresses are compared in Figs. 2.2(c) and (d) with those for the non-composite beam. Owing to the provision of the shear connection, the maximum shear stress is unchanged, but the maximum bending stress is halved.

The midspan deflection is

$$\delta = \frac{5wL^4}{384EI} = \frac{5wL^4}{256Ebh^3} \tag{2.11}$$

which is one-quarter of the previous deflection (equation (2.3)). Thus the provision of shear connection increases both the strength and the stiffness of a beam of given size, and in practice leads to a reduction in the size of the beam required for a given loading, and usually to a reduction in its cost.

In this example – but not always – the interface AOB coincides with the neutral axis of the composite member, so that the maximum longitudinal shear stress at the interface is equal to the maximum vertical shear stress, which occurs at $x = \pm L/2$ and is $3wL/8bh$, from (2.10).

The shear connection must be designed for the longitudinal shear per unit length, v, which is known as the *shear flow*. In this example it is given by

$$v_x = \tau_x b = \frac{3wx}{4h}. \tag{2.12}$$

The total shear flow in a half span is found, by integration of equation

(2.12), to be $3wL^2/(32h)$. Typically, $L/2h \simeq 20$, so the shear connection in the whole span has to resist a total shear force

$$2 \times \frac{3}{32}\frac{L}{h} wl \simeq 8wL.$$

Thus, this shear force is eight times the total load carried by the beam. A useful rule of thumb is that the strength of the shear connection for a beam is an order of magnitude greater than the load to be carried; it shows that shear connection has to be very strong.

In elastic design, the shear connectors are spaced in accordance with the shear flow. Thus, if the design shear resistance of a connector is P_{Rd}, the pitch or spacing at which they should be provided, p, is given by $pv_x \not> P_{Rd}$. From equation (2.12) this is

$$p \not> \frac{4P_{Rd}h}{3wx} \quad . \tag{2.13}$$

This is known as 'triangular' spacing, from the shape of the graph of v against x (Fig. 2.4).

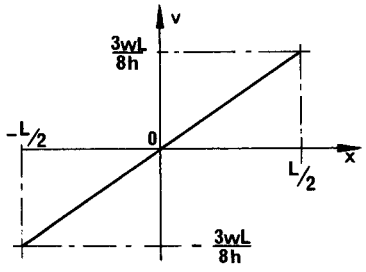

Fig. 2.4 Shear flow for 'triangular' spacing of connectors.

2.3 Uplift

In the preceding example, the stress normal to the interface AOB (Fig. 2.2) was everywhere compressive, and equal to $w/2b$ except at the ends of the beam. The stress would have been tensile if the load w had been applied to the lower member. Such loading is unlikely, except when travelling cranes are suspended from the steelwork of a composite floor above; but there are other situations in which stresses tending to cause uplift can occur at the interface. These arise from complex effects such as the torsional stiffness of reinforced concrete slabs forming flanges of composite beams, the triaxial stresses in the vicinity of shear connectors and, in box-girder bridges, the torsional stiffness of the steel box.

Tension across the interface can also occur in beams of non-uniform section or with partially completed flanges. Two members without shear connection, as shown in Fig. 2.5, provide a simple example. AB is supported on CD and carries distributed loading. It can easily be shown by elastic theory that if the flexural rigidity of AB exceeds about one-tenth of that of CD, then the whole of the load on AB is transferred to CD at points A and B, with separation of the beams between these points. If AB was connected to CD, there would be uplift forces at midspan.

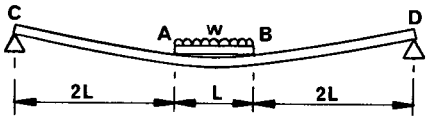

Fig. 2.5 Uplift forces.

Almost all connectors used in practice are therefore so shaped that they provide resistance to uplift as well as to slip. Uplift forces are so much less than shear forces that it is not normally necessary to calculate or estimate them for design purposes, provided that connectors with some uplift resistance are used.

2.4 Methods of shear connection

2.4.1 Bond

Until the use of deformed bars became common, most of the reinforcement for concrete consisted of smooth mild-steel bars. The transfer of shear from steel to concrete was assumed to occur by bond or adhesion at the concrete–steel interface. Where the steel component of a composite member is surrounded by reinforced concrete, as in an encased beam, Fig. 2.1(c), or an encased stanchion, Fig. 5.15, the analogy with reinforced concrete suggests that no shear connectors need be provided. Tests have shown that this is usually true for cased stanchions and filled tubes, where bond stresses are low, and also for cased beams in the elastic range. But in design it is necessary to restrict bond stress to a low value, to provide a margin for the incalculable effects of shrinkage of concrete, poor adhesion to the underside of steel surfaces, and stresses due to variations of temperature.

Research on the ultimate strength of cased beams[19] has shown that at high loads, calculated bond stresses have little meaning, due to the development of cracking and local bond failures. If longitudinal shear failure occurs, it is invariably on a surface such as AA in Fig. 2.1(c), and not around the perimeter of the steel section. For these reasons, British codes

of practice do not allow ultimate-strength design methods to be used for composite beams without shear connectors.

Most composite beams have cross-sections of types (a) or (b) in Fig. 2.1. Tests on such beams show that at low loads, most of the longitudinal shear is transferred by bond at the interface, that bond breaks down at higher loads, and that once broken it cannot be restored. So in design calculations, bond strength is taken as zero, and in research, bond is deliberately destroyed by greasing the steel flange before the concrete is cast. For uncased beams, the most practicable form of shear connection is some form of dowel welded to the top flange of the steel member and subsequently surrounded by *in-situ* concrete when the floor or deck slab is cast.

2.4.2 Shear connectors

The most widely used type of connector is the headed stud (Fig. 2.6). These range in diameter from 13 to 25 mm, and in length (h) from 65 to 100 mm, though longer studs are sometimes used. The current British code of practice[14] requires the steel from which the studs are manufactured to have an ultimate tensile strength of at least 450 N/mm^2 and an elongation of at least 15%. The advantages of stud connectors are that the welding process is rapid, they provide little obstruction to reinforcement in the concrete slab, and they are equally strong and stiff in shear in all directions normal to the axis of the stud.

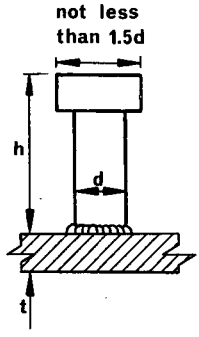

Fig. 2.6 Headed stud shear connector.

There are two factors that influence the diameter of studs. One is the welding process, which becomes increasingly difficult and expensive at diameters exceeding 20 mm, and the other is the thickness t (Fig. 2.6) of the plate or flange to which the stud is welded. A study made in the USA[20] found that the full static strength of the stud can be developed if d/t is less than about 2.7, and a limit of 2.5 is given in Eurocode 4. Tests using repeated loading[21] led to the rule in the British bridge code[22] that where the flange plate is subjected to fluctuating tensile stress, d/t may not

exceed 1.5. These rules prevent the use of welded studs as shear connection in composite slabs.

The maximum shear force that can be resisted by a stud is relatively low, about 150 kN. Other types of connector with higher strength have been developed, primarily for use in bridges. These are bars with hoops (Fig. 2.7(a)), tees with hoops, horseshoes, and channels (Fig. 2.7(b)). Bars with hoops are the strongest of these, with ultimate shear strengths up to 1000 kN. Eurocode 4 also gives design rules for block connectors, anchors made from reinforcing bars, angle connectors and friction-grip bolts. Epoxy adhesives have been tried, but it is not clear how resistance to uplift can reliably be provided where the slab is attached to the steel member only at its lower surface.

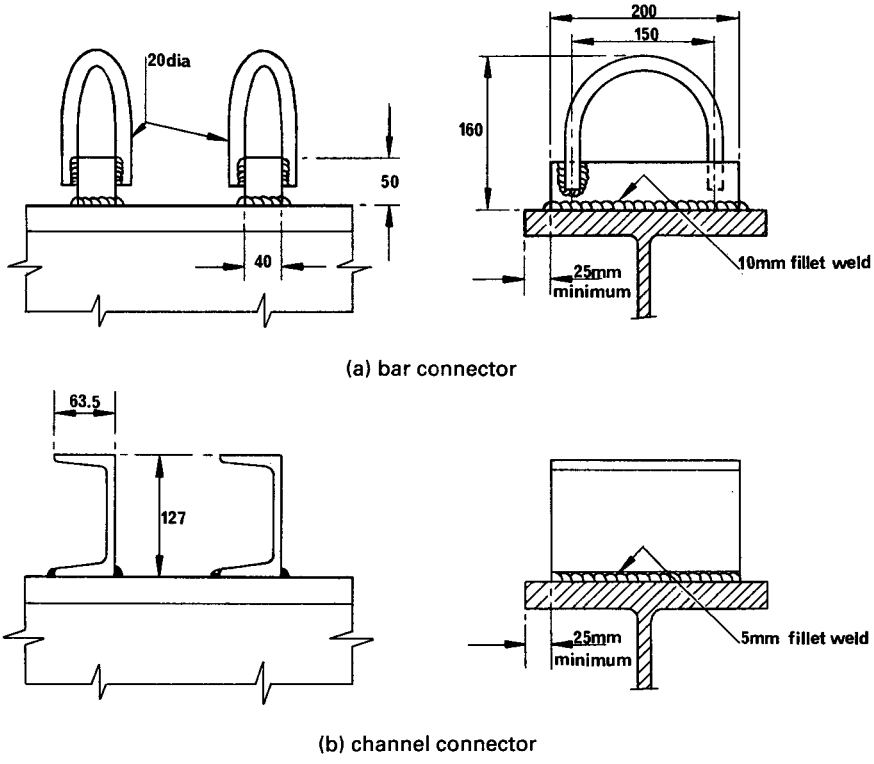

Fig. 2.7 Other types of shear connector.

2.4.3 Shear connection for profiled steel sheeting

This material is commonly used as permanent formwork for floor slabs in buildings, then known as *composite slabs*. Typical cross-sections are shown

in Figs 2.8, 2.14, 2.20, and 3.12. As it is impracticable to weld shear connectors to material that may be less than 1 mm thick, shear connection is provided either by pressed or rolled dimples that project into the concrete, or by giving the steel profile a re-entrant shape that prevents separation of the steel from the concrete.

The resistance of composite slabs to longitudinal shear is covered in Section 2.8, and their design in Section 3.3.

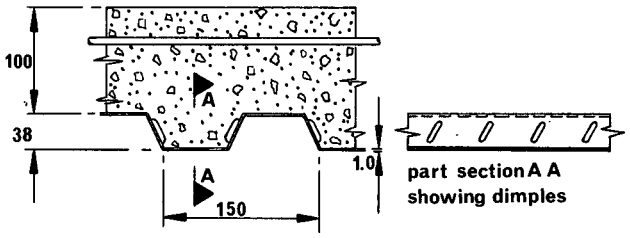

Fig. 2.8 Composite slab.

2.5 Properties of shear connectors

The property of a shear connector most relevant to design is the relationship between the shear force transmitted, P, and the slip at the interface, s. This load–slip curve should ideally be found from tests on composite beams, but in practice a simpler specimen is necessary. Most of the data on connectors have been obtained from various types of 'push-out' or 'push' test. The flanges of a short length of steel I-section are connected to two small concrete slabs. The details of the 'standard push test' of Eurocode 4 are shown in Fig. 2.9. The slabs are bedded onto the lower platen of a compression-testing machine or frame, and load is applied to the upper end of the steel section. Slip between the steel member and the two slabs is measured at several points, and the average slip is plotted against the load per connector. A typical load–slip curve is shown in Fig. 2.10, from a test using composite slabs.[23]

In practice, designers normally specify shear connectors for which strengths have already been established, for it is an expensive matter to carry out sufficient tests to determine design strengths for a new type of connector. If reliable results are to be obtained, the test must be specified in detail, for the load-slip relationship is influenced by many variables, including:

(1) number of connectors in the test specimen,

(2) mean longitudinal stress in the concrete slab surrounding the connectors,
(3) size, arrangement, and strength of slab reinforcement in the vicinity of the connectors,
(4) thickness of concrete surrounding the connectors,
(5) freedom of the base of each slab to move laterally, and so to impose uplift forces on the connectors,
(6) bond at the steel–concrete interface,
(7) strength of the concrete slab, and
(8) degree of compaction of the concrete surrounding the base of each connector.

The details shown in Fig. 2.9 include requirements relevant to items 1 to 6. The amount of reinforcement specified and the size of the slabs are greater than for the British standard test,[22] which has barely changed since it was introduced in 1965. The Eurocode test gives results that are less influenced by splitting of the slabs, and so give better predictions of the behaviour of connectors in beams.[15]

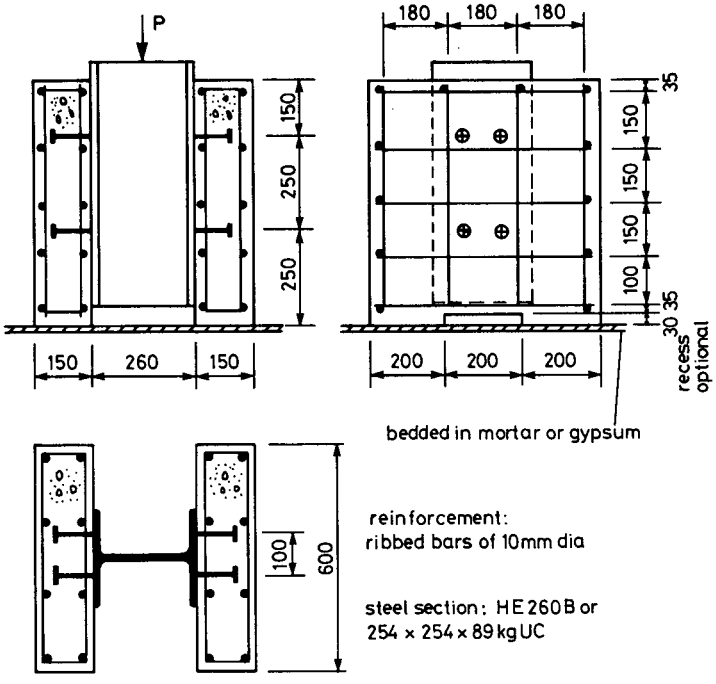

Fig. 2.9 Standard push test.

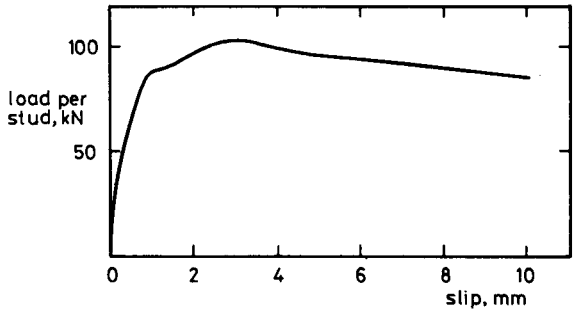

Fig. 2.10 Typical load–slip curve for 19-mm stud connectors in a composite slab.

Tests have to be done for a range of concrete strengths, because the strength of the concrete influences the mode of failure, as well as the failure load. Studs may reach their maximum load when the concrete surrounding them fails, but in stronger concrete, they shear off. This is why the design shear resistance of studs with $h/d \geqslant 4$ is given in Eurocode 4 as the lesser of two values:

$$P_{Rd} = \frac{0.8 f_u (\pi d^2/4)}{\gamma_v} \tag{2.14}$$

and

$$P_{Rd} = \frac{0.29 d^2 (f_{ck} E_{cm})^{1/2}}{\gamma_v} \tag{2.15}$$

where f_u is the ultimate tensile strength of the steel ($\leqslant$ 500 N/mm^2), and f_{ck} and E_{cm} are the cylinder strength and mean secant (elastic) modulus of the concrete, respectively. Dimensions h and d are shown in Fig. 2.6. The value recommended for the partial safety factor γ_v is 1.25, based on statistical calibration studies. When f_u = 450 N/mm^2, equation (2.14) governs when f_{ck} exceeds about 30 N/mm^2.

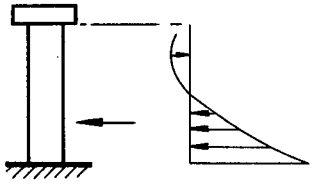

Fig. 2.11 Bearing stress on the shank of a stud connector.

Ignoring γ_v, it is evident that equation (2.14) represents shear failure in the shank of the stud at a mean stress of $0.8 f_u$. To explain equation (2.15),

let us assume that the force P_R is distributed over a length of connector equal to twice the shank diameter, because research has shown that the bearing stress on a shank is concentrated near the base, as sketched in Fig. 2.11. An approximate mean stress is then $0.145(f_{ck}E_{cm})^{1/2}$. Its value, as given by Eurocode 4, ranges from 110 N/mm^2 for class C20/25 concrete to 171 N/mm^2 for class C40/50 concrete, so for these concretes the mean bearing stress at concrete failure ranges from $5.5f_{ck}$ to $4.3f_{ck}$. This estimate ignores the enlarged diameter at the weld collar at the base of the stud, shown in Fig. 2.6; but it is clear that the effective compressive strength is several times the cylinder strength of the concrete.

This very high strength is possible only because the concrete bearing on the connector is restrained laterally by the surrounding concrete, its reinforcement, and the steel flange. The results of push tests are likely to be influenced by the degree of compaction of the concrete, and even by the arrangement of particles of aggregate, in this small but critical region. This is thought to be the main reason for the scatter of the results obtained.

The usual way of allowing for this scatter is to specify that the characteristic resistance P_{Rk} be taken as 10% below the lowest of the results from three tests, and then corrected for any excess of the measured strength of the connector material above the minimum specified value.

The load–slip curve for a connector in a beam is influenced by the difference between the longitudinal stress in a concrete flange and that in the slabs in a push test. Where the flange is in compression the load/slip ratio (the stiffness) in the elastic range exceeds the push-test value, but the ultimate strength is about the same. For slabs in tension (e.g. in a region of hogging moment), the connection is significantly less stiff[24] but the ultimate shear resistance is only slightly lower. This is one reason why partial shear connection (Section 3.6) is allowed in Eurocode 4 only in regions of sagging bending moment.

There are two situations in which the resistance of a connector found from push tests may be too high for use in design. One is repeated loading, such as that due to the passage of traffic over a bridge. This subject is covered in Chapter 10 (Volume 2). The other is where the lateral restraint to the concrete in contact with the connector is less than that provided in a push test, as in a haunched beam with connectors too close to a free surface (Fig. 2.12). For this reason, the use of the standard equations for resistance

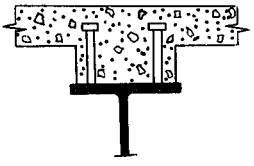

Fig. 2.12 Haunch with connectors too close to a free surface.

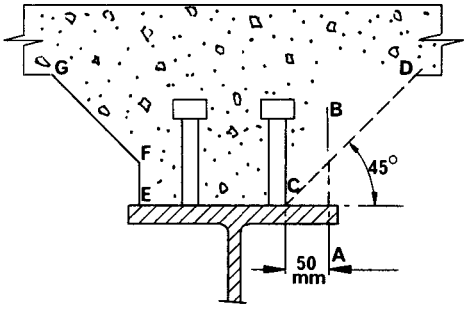

Fig. 2.13 Detailing rules for haunches.

of connectors is allowed in haunched beams only where the cross-section of the haunch satisfies certain conditions. In Eurocode 4, these are that the concrete cover to the side of the connectors may not be less than 50 mm (line AB in Fig. 2.13), and that the free concrete surface may not lie within the line CD, which runs from the base of the connector at an angle of 45° with the steel flange. A haunch that just satisfies these rules is shown as EFG.

There are also rules for the detailing of reinforcement for haunches, which apply also at the free edge of an L-beam.

Tests show that the ability of lightweight-aggregate concrete to resist the high local stresses at shear connectors is slightly less than that of normal-density concrete of the same cube strength. This is allowed for in Eurocode 4 by the lower value of E_{cm} that is specified for lightweight concrete. For concrete of density 1750 kg/m^3, the resistance given by equation (2.15) is only 73% of that for normal-density concrete. This is considered in the UK to be too low; the corresponding ratio in BS 5950[14] is 90%.

2.5.1 Stud connectors used with profiled steel sheeting

Where profiled sheeting is used, stud connectors are located within concrete ribs that have the shape of a haunch, which may run in any direction relative to the direction of span of the composite beam. Tests show that the shear resistance of connectors is sometimes lower than it is in a solid slab, for materials of the same strength, because of local failure of the concrete rib.

For this reason, Eurocode 4 specifies reduction factors, applied to the resistance P_{Rd} found from equation (2.14) or (2.15). For sheeting with ribs parallel to the beam, the factor is

$$k_l = 0.6 \frac{b_o}{h_p}\left(\frac{h}{h_p} - 1\right) \leq 1.0 \qquad (2.16)$$

where the dimensions b_o, h_p, and h are illustrated in Fig. 2.14, and h is taken as not greater than $h_p + 75$ mm.

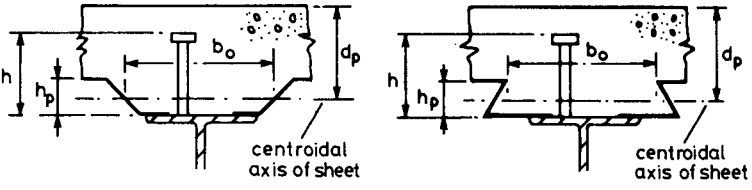

Fig. 2.14 Composite beam and composite slab spanning in the same direction.

For sheeting with ribs transverse to the beam the factor is

$$k_t = \frac{0.7}{\sqrt{N_r}} \frac{b_o}{h_p} \left(\frac{h}{h_p} - 1 \right) \leqslant 1.0 \qquad (2.17)$$

where N_r is the number of connectors in one rib where it crosses a beam, not to be taken as greater than 2 in calculations.

These factors are based on formulae developed in North America[25] modified to allow for the results of more recent tests[15, 23] on European profiles. It is known that they do not provide a uniform margin of safety. More test data are needed to enable them to be improved, and as a basis for reduction factors for connectors other than studs. Also, a distinction should perhaps be made between studs welded to the steel flange through a hole in the sheeting (the usual practice in some countries) and the British (and North American) practice of 'through-deck welding'.

2.6 Partial interaction

In studying the simple composite beam with full interaction (Section 2.2.2), it was assumed that slip was everywhere zero. However, the results of push tests show (e.g. Fig. 2.10) that even at the smallest loads, slip is not zero. It is therefore necessary to know how the behaviour of a beam is modified by the presence of slip. This is best illustrated by an analysis based on elastic theory. It leads to a differential equation that has to be solved afresh for each type of loading, and is therefore too complex for use in design offices. Even so, partial-interaction theory is useful, for it provides a starting point for the development of simpler methods for predicting the behaviour of beams at working load, and finds application in the calculation of interface shear forces due to shrinkage and differential thermal expansion.

The problem to be studied and the relevant variables are defined below. The details of the theory, and of its application to a composite beam, are given in Appendix A.The results and comments on them are given below and in Section 2.7.

Elastic analysis is relevant to situations in which the loads on connectors do not exceed about half their ultimate strength. The relevant part OB of the load–slip curve (Fig. 2.10) can be replaced with little error by the straight line OB. The ratio of load to slip given by this line is known as the *connector modulus*, k.

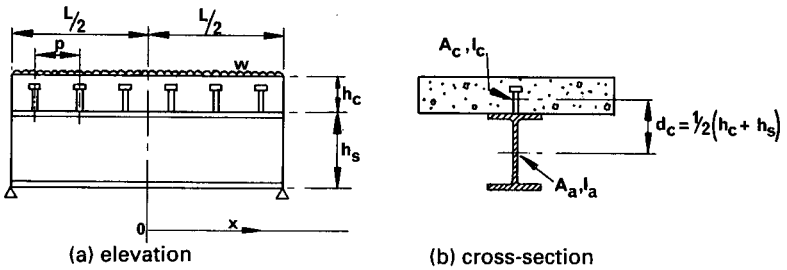

Fig. 2.15 Simply-supported composite beam.

For simplicity, the scope of the analysis is restricted to a simply supported composite beam of span L (Fig. 2.15), carrying a distributed load w per unit length. The cross-section consists of a concrete slab of thickness h_c, cross-sectional area A_c, and second moment of area I_c, and a symmetrical steel section with corresponding properties h_s, A_a, and I_a. The distance between the centroids of the concrete and steel cross-sections, d_c, is given by

$$d_c = \frac{h_c + h_s}{2}. \tag{2.18}$$

Shear connectors of modulus k are provided at uniform spacing p along the length of the beam.

The elastic modulus of the steel is E_a, and that of the concrete for short-term loading is E_c. Allowance is made for creep of concrete by using an effective modulus E_c' in the analysis, where

$$E_c' = k_c E_c,$$

and k_c is a reduction coefficient, calculated from the ratio of creep strain to elastic strain. The modular ratio n is defined by $n = E_a/E_c$, so that

$$E_c' = \frac{k_c E_a}{n}. \tag{2.19}$$

The concrete is assumed to be as stiff in tension as in compression, for it is found that tensile stresses in concrete are low enough for little error to result in this analysis, except when the degree of shear connection is very low.

The results of the analysis are expressed in terms of two functions of the cross-section of the member and the stiffness of its shear connection, α and β. These are defined by the following equations, in which notation established in CP117: Part 2[26] has been used.

$$\frac{1}{A_0} = \frac{n}{k_c A_c} + \frac{1}{A_a} \tag{2.20}$$

$$\frac{1}{A'} = d_c^2 + \frac{I_0}{A_0} \tag{2.21}$$

$$I_0 = \frac{k_c I_c}{n} + I_a \tag{2.22}$$

$$\alpha^2 = \frac{k}{pE_a I_0 A'} \tag{2.23}$$

$$\beta = \frac{A' p d_c}{k}. \tag{2.24}$$

In a composite beam, the steel section is thinner than the concrete section, and the steel has a much higher coefficient of thermal conductivity. Thus the steel responds more rapidly than the concrete to changes of temperature. If the two components were free, their lengths would change at different rates; but the shear connection prevents this, and the resulting stresses in both materials can be large enough to influence design. The shrinkage of the concrete slab has a similar effect. A simple way of allowing for such differential strains in this analysis is to assume that after connection to the steel, the concrete slab shortens uniformly, by an amount ϵ_c per unit length, relative to the steel.

It is shown in Appendix A that the governing equation relating slip s to distance along the beam from midspan, x, is

$$\frac{d^2 s}{dx^2} - \alpha^2 s = -\alpha^2 \beta w x \tag{2.25}$$

and that the boundary conditions for the present problem are:

$$\left.\begin{aligned} s &= 0 && \text{when } x = 0 \\ \frac{ds}{dx} &= -\epsilon_c && \text{when } x = \pm L/2 \end{aligned}\right\} \tag{2.26}$$

The solution of (2.25) is then

$$s = \beta w x - \left(\frac{\beta w + \epsilon_c}{\alpha}\right) \operatorname{sech}\left(\frac{\alpha L}{2}\right) \sinh \alpha x. \tag{2.27}$$

Expressions for the slip strain and the stresses throughout the beam can be obtained from this result. The stresses at a cross-section are found to depend on the loading, boundary conditions and shear connection for the whole beam. They cannot be calculated from the bending moment and shear force at the section considered. This is the main reason why design methods simple enough for use in practice have to be based on full-interaction theory.

2.7 Effect of slip on stresses and deflections

Full-interaction and no-interaction elastic analyses are given in Section 2.2 for a composite beam made from two elements of equal size and stiffness. Its cross-section (Fig. 2.2(b)) can be considered as the transformed section for the steel and concrete beam shown in Fig. 2.16. Partial-interaction analysis of this beam (Appendix A) illustrates well the effect of connector flexibility on interface slip and hence on stresses and deflections, even though the cross-section is not one that would be used in practice.

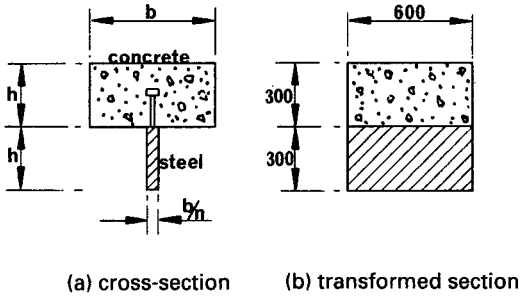

Fig. 2.16 Transformed section of steel and concrete beam.

The numerical values, chosen to be typical of a composite beam, are given in Section A.2. Substitution in (2.27) gives the relation between s and x for a beam of depth 0.6 m and span 10 m as

$$10^4 s = 1.05x - 0.0017 \sinh (1.36x). \tag{2.28}$$

The maximum slip occurs at the ends of the span, where $x = \pm 5$ m. From equation (2.28), it is ± 0.45 mm.

The results obtained in Sections 2.2.1 and 2.2.2 are also applicable to this beam. From equation (2.6), the maximum slip if there were no shear connection would be $\pm$ 8.1 mm. Thus the shear connectors reduce end slip substantially, but do not eliminate it. The variations of slip strain and slip along the span for no interaction and partial interaction are shown in Fig. 2.3.

The connector modulus k was taken as 150 kN/mm (Appendix A). The maximum load per connector is k times the maximum slip, so the partial-interaction theory gives this load as 67 kN, which is sufficiently far below the ultimate strength of 100 kN per connector for the assumption of a linear load–slip relationship to be reasonable. Longitudinal strains at midspan given by full-interaction and partial-interaction theories are shown in Fig. 2.17. The increase in extreme-fibre strain due to slip, 28×10^{-6}, is much less than the slip strain at the interface, 104×10^{-6}. The maximum compressive stress in the concrete is increased by slip from 12.2 to 12.8 N/mm^2, a change of 5%. This higher stress is 43% of the cube strength, so the assumption of elastic behaviour is reasonable.

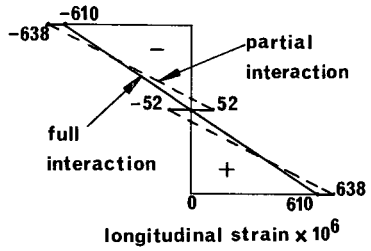

Fig. 2.17 Longitudinal strains at midspan.

The ratio of the partial-interaction curvature to the full-interaction curvature is 690/610, or 1.13. Integration of curvatures along the beam shows that the increase in deflection, due to slip, is also about 13%. The effects of slip on deflection are found in practice to be less than is implied by this example, because here a rather low value of connector modulus has been used, and the effect of bond has been neglected.

The longitudinal compressive force in the concrete at midspan is proportional to the mean compressive strain. From Fig. 2.17, this is 305×10^{-6} for full interaction and 293×10^{-6} for partial interaction, a reduction of 4%.

The influence of slip on the flexural behaviour of the member may be summarised as follows. The bending moment at midspan, $wL^2/8$, can be considered to be the sum of a 'concrete' moment M_c, a 'steel' moment M_a, and a 'composite' moment Fd_c (Fig. A.1):

$$M_c + M_a + Fd_c = \frac{wL^2}{8}.$$

In the full-interaction analysis, Fd_c contributes 75% of the total moment, and M_c and M_a 12.5% each. The partial-interaction analysis shows that slip reduces the contribution from Fd_c to 72% of the total, so that the contributions from M_c and M_a rise to 14%, corresponding to an increase in curvature of (14 − 12.5)/12.5, or about 13%.

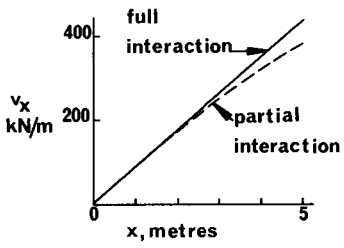

Fig. 2.18 Longitudinal shear force per unit length.

The interface shear force per unit length, v_x, is given by equation (2.12) for full interaction and by equations (A.1) and (2.28) for partial interaction. The expressions for v_x over a half span are plotted in Fig. 2.18, and show that in the elastic range, the distribution of loading on the connectors is similar to that given by full-interaction theory. The reasons for using uniform rather than 'triangular' spacing of connectors are discussed in Section 3.6.

2.8 Longitudinal shear in composite slabs

There are three types of shear connection between a profiled steel sheet and a concrete slab. At first, reliance was placed on the natural bond between the two. This is unreliable unless separation at the interface ('uplift') is prevented, so sheets with re-entrant profiles, such as Holorib, were developed. This type of shear connection is known as 'frictional interlock'. The second type is 'mechanical interlock', provided by pressing dimples or ribs (Fig. 2.8) into the sheet. The effectiveness of these embossments depends entirely on their depth, which must be accurately controlled during manufacture. The third type of shear connection is 'end anchorage'. This can be provided where the end of a sheet rests on a steel beam, by means of shot-fired pins, or by welding studs through the sheeting to the steel flange.

2.8.1 The *m-k* or shear-bond test

The effectiveness of shear connection is studied by means of loading tests on simply-supported composite slabs, as sketched in Fig. 2.19. Specifications for such tests are given in Section 10.3 of Eurocode 4 and in BS 5950: Part 4.[27] The length of each shear span, L_s, is usually $L/4$, where L is the span, which is typically about 3.0 m. There are three possible modes of failure:

- in flexure, at a cross-section such as 1–1 in Fig. 2.19;
- in longitudinal shear, along a length such as 2–2; and
- in vertical shear, at a cross-section such as 3–3.

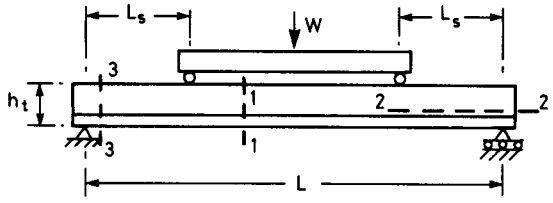

Fig. 2.19 Critical sections for a composite slab.

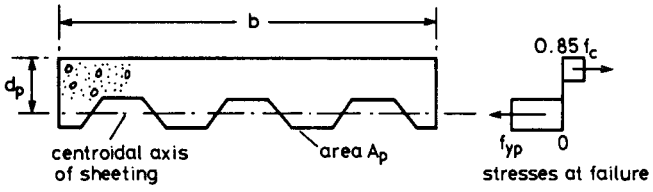

Fig. 2.20 Bending resistance of a composite slab.

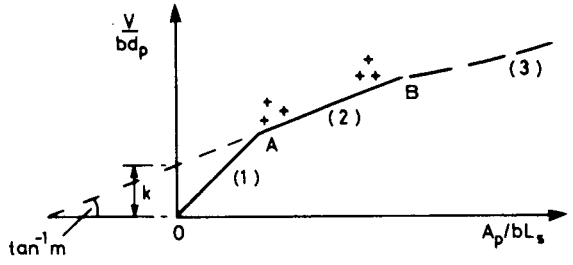

Fig. 2.21 Definition of m and k.

The expected mode of failure in a test depends on the ratio of L_s to the effective depth d_p of the slab, shown in Fig. 2.20. In tests to Eurocode 4, the results are plotted on a diagram with axes V/bd_p and A_p/bL_s (Fig. 2.21), for reasons that are now explained.

At high L_s/d_p, flexural failure occurs. The maximum bending moment, M_u, is given by

$$M_u = VL_s \tag{2.29}$$

where V is the maximum vertical shear, assumed to be much greater than the self-weight of the slab. A test specimen, of breadth b, should include a number of complete wavelengths of sheeting, of total cross-sectional area A_p. Flexural failure is modelled by simple plastic theory, with all the steel at its yield stress, f_{yp} (Fig. 2.20), and sufficient concrete at $0.85f_c$, where f_c is the cylinder strength, for longitudinal equilibrium. The lever arm is a little less than d_p, but approximately,

$$M_u \propto A_p f_{yp} d_p . \tag{2.30}$$

From equation (2.29)

$$\frac{V}{bd_p} = \frac{M_u}{bd_p L_s} \propto \frac{A_p f_{yp}}{bL_s}. \tag{2.31}$$

The strength f_{yp} is not varied during a series of tests, and has no influence on longitudinal shear failure. It is therefore omitted from the axes on Fig. 2.21, and equation (2.31) shows that flexural failure should plot as a straight line through the origin.

At low L_s/d_p, vertical shear failure occurs. The mean vertical shear stress on the concrete is roughly equal to V/bd_p. It is assumed in current codes that the ratio A_p/bL_s has little influence on its ultimate value, so vertical shear failures are represented by a horizontal line on Fig. 2.21. However, Patrick and Bridge[28] have shown that this should be a rising curve.

Longitudinal shear failures occur at intermediate values of L_s/d_p, and lie near the line

$$\frac{V}{bd_p} = m\left(\frac{A_p}{bL_s}\right) + k \tag{2.32}$$

as shown by AB on Fig. 2.21, where m and k are constants to be determined by testing. Design based on equation (2.32) is one of the two methods given in Eurocode 4. (The other is treated in Section 3.3.2.) The present method is similar to one that has been widely used for several decades,[27,29] known as the 'm-k method'. In that method, m and k are usually defined by the equation

$$V = bd_p(f_c)^{1/2}\left[m\frac{A_p}{bL_s(f_c)^{1/2}} + k\right] \tag{2.33}$$

where f_c is the measured cylinder or cube strength of the concrete. This equation can give unsatisfactory results for m and k when f_c varies widely within a series of tests, so f_c has been omitted from equation (2.32). A comparison of the two methods[15] has shown that this has little effect on m; but the two equations give different values for k, in different units. A value found by, for example, the method of BS 5950: Part 4 cannot be used in design to Eurocode 4; but a new value can be determined from the original test data.

A typical set of tests consists of a group of three, with L_s/d_p such that the results lie near point A on Fig. 2.21, and a second group with lower L_s/d_p, such that the results lie near point B. Values of m and k are found for a line drawn below the lowest result in each group, at a distance that allows for the scatter of the test data.

All six failures have to be in longitudinal shear. These failures typically commence when a crack occurs in the concrete under one of the load points, associated with loss of bond along the shear span and measurable slip at the end of the span. If this leads to failure of the slab, the shear

connection is classified as 'brittle'. Such failures occur suddenly, and are penalised in design to Eurocode 4 by a 20% reduction in design resistance.

Where the eventual failure load exceeds the load causing the first end slip by more than 10%, the failure is classified as 'ductile'. Recently-developed profiles for sheeting have better mechanical interlock than earlier shapes, which relied more on frictional interlock and were more susceptible to 'brittle' failure. The influence of bond is minimised in the standard test, by the application of several thousand cycles of repeated loading up to 1.5 times the expected loading in service, before loading to failure.

When a new profile is developed, values of m and k have to be determined, in principle, for each thickness of sheeting, each overall depth of slab to be used, and for a range of concrete strengths. Codes allow some simplification, but the testing remains a long and costly process. The m-k test is also unsatisfactory in other ways.[15, 30] A test using much smaller specimens, that may in time replace it, is now described.

2.8.2 The slip-block test

This test has been developed in Australia since 1989,[30, 31] for profiles that provide ductile shear connection. A piece of sheeting one wavelength wide and about 300 mm long is attached by spot welding to a baseplate (Fig. 2.22). A cover slab of similar thickness to the composite slab is cast on it. A vertical load V is applied through rollers, and a horizontal force H as shown in the figure. Longitudinal slip, s, is measured.

The procedure is illustrated in Fig. 2.23. Bond is broken in a preliminary test. A load V is applied (point A), and kept constant while H is increased until slip begins (point B). The load V is then slowly reduced, so that slipping occurs and H falls off slightly. This is continued until the block is

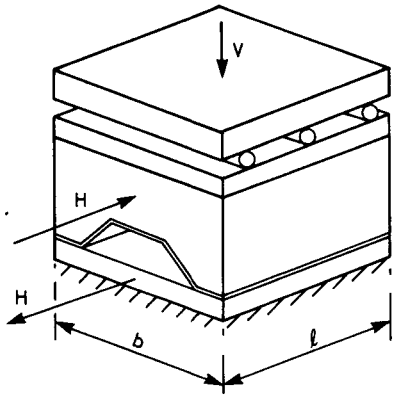

Fig. 2.22 Slip-block test.

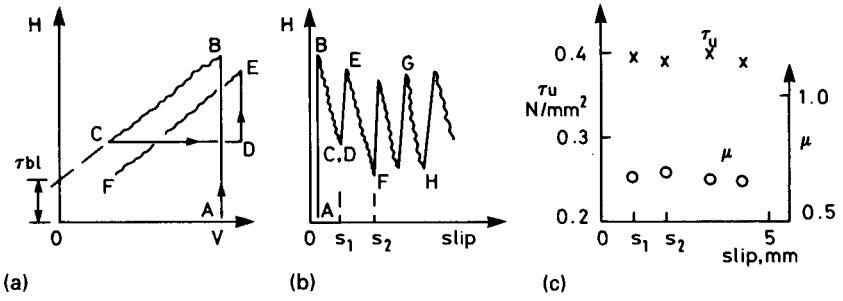

Fig. 2.23 Results of a slip-block test.

about to lift at one end (point C). Load V is again increased (to point D), and the cycle is repeated, this time at slightly greater slip. Further cycles follow, as shown by slip lines GH, etc., on Fig. 2.23(b). The slope of each slip line gives a value for the coefficient of friction, μ, and its intercept on the H-axis in Fig. 2.23(a) gives a value for $\tau_u bl$, where τ_u is the mean shear stress per unit horizontal area, because

$$H = \tau_u bl + \mu V.$$

The values of τ_u and μ so found are plotted against the slips at points C, F, H, etc., as shown in Fig. 2.23(c). This shows clearly how ductile the connection is. For design, single values of τ_u and μ can be used. It has been found[30] that accurate predictions of the behaviour of composite slabs are obtained when the values used correspond to between 2 mm and 3 mm of slip in the slip-block test.

The design procedure for a composite slab using this method is explained in Section 3.4.3.

Chapter 3
Simply-supported Composite Slabs and Beams

3.1 Introduction

The subjects of this and subsequent chapters are treated in the sequence in which they developed. Relevant structural behaviour is discovered by experience or research, and is then represented by mathematical models. These make use of standardised properties of materials, such as the yield strength of steel, and enable the behaviour of a member under load to be predicted. The models are developed into design rules, as found in codes of practice, by simplifying them wherever possible, defining their scope and introducing partial safety factors.

Research workers often propose alternative models, and language barriers are such that the model preferred in one country may be little known elsewhere. The writers of codes try to select the most rational and widely-applicable of the available models, but must also consider existing design practices and the need for simplicity. The design rules used in this volume are taken from the Eurocodes, which differ slightly from the corresponding British codes; but the underlying models are usually the same, and significant differences will be explained.

There will inevitably be minor differences between the methods used here and those of any code which the reader may consult. Only the preliminary (ENV) versions of the Eurocodes are yet available, and each country can choose 'national' values for the partial safety factors, that may differ from those given in the codes.

The methods to be described are illustrated by the design calculations for part of a framed structure for a building. To avoid repetition, the results obtained at each stage are used in subsequent work. Much of the material on beams finds application also in bridge structures, which are treated in Volume 2.

The notation used is that of the Eurocodes. It is more consistent than that used in current British codes, less ambiguous, but sometimes more complex. It is listed at the start of the book. The following comments on it may be useful.

(1) The following subscripts are widely used:

a	structural steel (French: acier)
ap (or p)	profiled steel sheeting
c	concrete
d	design (implying that γ factors are included)
k	characteristic (implying that γ factors are not included)
s	reinforcing steel
v	related to shear connection.

(2) The notation f_y for yield strength of stuctural steel is used because it is so well established; but f_{ak} would be more consistent.

(3) Design checks for ultimate limit states consist typically of verifying that a bending moment (for example) calculated from actions does not exceed a bending resistance. The notation for this is

$$M_{Sd} \leq M_{Rd} \tag{3.1}$$

where S refers to actions (French: sollicitation) and R to resistance. It is useful to make this clear distinction between action effect and resistance.

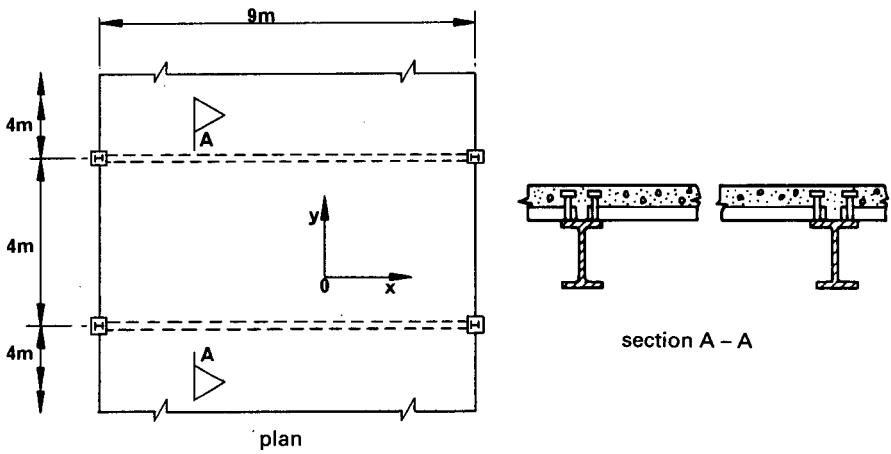

Fig. 3.1 Design example – structure for a typical floor.

3.2 The design example

In a framed structure for a wing of a building, the columns are arranged at 4 m centres in two rows 9 m apart. A design is required for a typical floor, which consists of a composite floor slab continuous over and composite with steel beams that span between the columns as shown in Fig. 3.1. The characteristic strengths and the partial safety factors at the ultimate limit state for materials (γ_M) are assumed to be as follows:

structural steel; yield strength	$f_y = 355$ N/mm^2,	$\gamma_a = 1.10$
reinforcement; yield strength	$f_{sk} = 460$ N/mm^2,	$\gamma_s = 1.15$
concrete; cube strength	$f_{cu} = 30$ N/mm^2,	$\gamma_c = 1.5$
welded steel fabric; yield strength	$f_{sk} = 500$ N/mm^2,	$\gamma_s = 1.15$
shear connectors; 19-mm headed studs		
100 mm high; ultimate strength	$f_u = 450$ N/mm^2,	$\gamma_v = 1.25$.

Other properties of the concrete

Lightweight-aggregate concrete is used, with unit mass $\rho = 1900$ kg/m^3. The Eurocodes give the following values for other properties of this concrete:

characteristic cylinder strength:	f_{ck}	= 25 N/mm^2
secant modulus of elasticity:	E_{cm}	= 19.1 kN/mm^2
modular ratio for short-term loading:	n	= 210/19.1 = 11.0
characteristic tensile strengths:		
mean value	f_{ctm}	= 2.6 N/mm^2
5% lower fractile	$f_{ctk\,0.05}$	= 1.8 N/mm^2.

Creep of concrete is allowed for by using an effective modulus $E'_{cm} = E_{cm}/3$.

Resistance of the shear connectors

The design shear resistance is given by equation (2.15) and is

$$P_{Rd} = \frac{0.29 \times 19^2(25 \times 19\,100)^{0.5}}{1.25 \times 1000} = 57.9 \text{ kN}. \qquad (3.2)$$

Permanent actions

The unit weight of the concrete is increased from 19 to 20 kN/m^3 to allow for reinforcement, and the unit weight of structural steel is taken as 77 kN/m^3.

The characteristic weight of floor and ceiling finishes is taken as 1.3 kN/m^2, plus an allowance of 1.2 kN/m^2 for non-structural partition walls.

Variable actions

The floors to be designed are assumed to be in category C of Eurocode 1: Part 2,[9] 'areas susceptible to overcrowding, including access areas'. The characteristic variable loadings are as given in Chapter 1:

$$q_k = 5.0 \text{ kN/m}^2 \qquad (1.16)\text{bis}$$

or

$$Q_k = 7.0 \text{ kN on a 50-mm square area}. \qquad (1.17)\text{bis}$$

3.3 Composite floor slabs

Composite slabs have for several decades been the most widely used method of suspended floor construction for steel-framed buildings in North

America. Within the last twenty years there have been many advances in design procedures, and a wide range of profiled sheetings has become available in Europe. The British Standard for the design of composite floors[27] first appeared in 1982, and there are preliminary Eurocodes for design of both the sheeting alone[32] and the composite slab[12].

The steel sheeting has to support not only the wet concrete for the floor slab, but other loads that are imposed during concreting. These may include the heaping of concrete and pipeline or pumping loads. The minimum characteristic value given for these in Eurocode 4 is 1.5 kN/m^2 on any area 3 m by 3 m, plus 0.75 kN/m^2 on the remaining area.

Profiled steel sheeting

The sheeting is very thin, for economic reasons; usually between 0.8 mm and 1.2 mm. It has to be galvanised to resist corrosion, and this adds about 0.04 mm to the overall thickness. It is specified in Eurocode 3:Part 1.3 that where design is based on the nominal thickness of the steel, the sheet must have at least 95% of that thickness – but it is not a simple matter for the user to check this! The sheets are pressed or cold rolled, and are typically about 1 m wide and up to 6 m long. They are designed to span in the longitudinal direction only. For many years, sheets were typically 50 mm deep, and the limiting span was about 3 m. The cost of propping the sheets during concreting led to the development of deeper profiles; but design of composite slabs is still often governed by a limit on deflection. There is then no advantage in using a high-yield steel, so most sheeting in the UK is of mild steel.

The local buckling stress of a flat panel within sheeting should ideally exceed its yield strength; but this requires breadth/thickness ratios of less than about 35. Modern profiles have local stiffening ribs, but it is difficult to achieve slendernesses less than about 50, so that for flexure, the sections are in Class 4 (i.e. the buckling stress is below the yield stress). Calculation of the resistance to bending then becomes complex, and involves trial and error.

The specified or nominal yield strength is that of the flat sheet from which the sheeting is made. In the finished product, the yield strength is higher at every bend and corner, because of work hardening.

To enable it to fulfil its second role, as reinforcement for the concrete slab, dimples are pressed into the surface of the sheeting, to act as shear connectors. These dimpled areas may not be fully effective in resisting longitudinal stress, so both they and the local buckling reduce the second moment of area (I) of the sheeting to below the value calculated for the gross steel section.

For these reasons, manufacturers commission tests on prototype sheets, and provide designers either with test-based values of resistance and stiffness, or with 'safe-load' tables calculated from those values.

Design of composite slab

The cross-sectional area of steel sheeting that is needed for the construction phase often provides more than enough bottom reinforcement for the composite slab. It is then usual to design the slabs as simply-supported. The concrete is of course continuous over the supporting beams, and alternate sheets may be as well (e.g. if 6-m sheets are used for a succession of 3-m spans).

These 'simply-supported' slabs require top longitudinal reinforcement at their supports, to control the widths of cracks. The amount is specified in Eurocode 4 as 0.2% of the cross-sectional area of concrete above the steel ribs for unpropped construction, and 0.4% for propped construction.

Long-span slabs are sometimes designed as continuous over their supports.They are analysed as described in Section 4.7. Several action effects that have to be considered in the design of composite slabs are now considered. The methods are illustrated by the worked example in Section 3.4.

3.3.1 Resistance of composite slabs to sagging bending

The width of slab considered in calculations, b, is usually taken as one metre, but for clarity only a width of one wavelength is shown in Fig. 3.2. The overall thickness h_t is required by Eurocode 4 to be not less than 80 mm; and the thickness of concrete above the 'main flat surface' of the top of the ribs of the sheeting, to be not less than 40 mm. Normally, this thickness is 60 mm or more, to provide sufficient sound or fire insulation, and resistance to concentrated loads.

Except where the sheeting is unusually deep, the neutral axis for bending lies in the concrete, where there is full shear connection; but in regions with partial shear connection, there is always a neutral axis within the steel section. Local buckling of compressed sheeting then has to be considered. This is done by using effective widths of flat regions of sheeting. These widths are allowed (in Eurocode 4) to be up to twice the limits given for

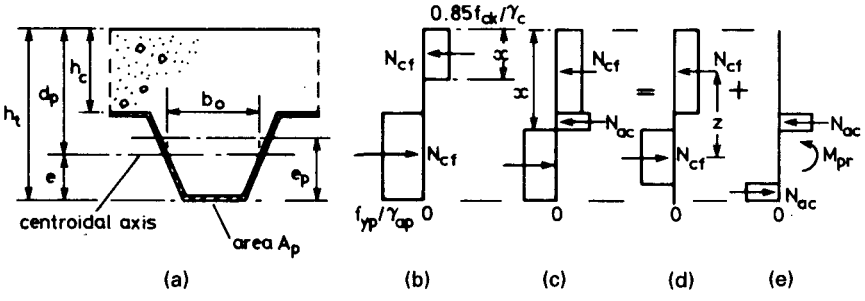

Fig. 3.2 Resistance of composite slab to sagging bending.

Class 1 steel web plates in beams, because the concrete prevents the sheeting from buckling upwards, which shortens the wavelength of the buckles.

For sheeting in tension, the width of embossments should be neglected in calculating the effective area, unless tests have shown that a larger area is effective.

For these reasons, the effective area per metre width, A_p, and the height of the centre of area above the bottom of the sheet, e, are usually based on tests. These usually show that e_p, the height of the plastic neutral axis of the sheeting, is different from e.

Because local buckling is allowed for in this way, the bending resistance can be calculated by simple plastic theory. There are three situations, as follows.

(1) Neutral axis above the sheeting

The assumed distribution of longitudinal bending stresses is shown in Fig. 3.2(b). There must be full shear connection, so that the compressive force in the concrete, N_{cf}, is equal to the yield force for the steel:

$$N_{cf} = N_{pa} = \frac{A_p f_{yp}}{\gamma_{ap}} \tag{3.3}$$

where γ_{ap} is the partial safety factor for the nominal yield strength f_{yp} of the sheeting. The depth of the stress block in the concrete is given by

$$x = \frac{N_{cf}}{b(0.85 f_{ck}/\gamma_c)}. \tag{3.4}$$

For simplicity, and consistency with the method for composite beams, the depth to the neutral axis is assumed to be x, even though this is not in accordance with Eurocode 2. This method is therefore valid when

$$x \leqslant h_c \tag{3.5}$$

and gives

$$M_{p.Rd} = N_{cf}(d_p - 0.5x) \tag{3.6}$$

where $M_{p.Rd}$ is the design resistance to sagging bending.

(2) Neutral axis within the sheeting, and full shear connection

The stress distribution is shown in Fig. 3.2(c). The force N_{cf} is now less than N_{pa}, and is given by

$$N_{cf} = bh_c \frac{0.85 f_{ck}}{\gamma_c} \tag{3.7}$$

because compression within ribs is neglected, for simplicity. There is no simple method of calculating x, because of the complex properties of

profiled sheeting, so the following approximate method is used. The tensile force in the sheeting is decomposed, as shown in Figs 3.2(d) and (e), into a force at the bottom equal to N_{ac} (the compressive force) and a force N_a, where

$$N_a = N_{cf}. \tag{3.8}$$

The equal and opposite forces N_{ac} provide a resistance moment M_{pr}, equal to the resistance moment for the sheeting, M_{pa}, reduced by the effect of the axial force N_a. It should be noted that in Eurocode 4: Part 1.1, the value of the symbol N_{cf} depends on the ratio x/h_c. It is the lesser of the two values given by equations (3.3) and (3.7). This can be confusing; so for clarity here, a further symbol N_{pa} is introduced. It always has the value

$$N_{pa} = \frac{A_p f_{yp}}{\gamma_{ap}}. \tag{3.9}$$

The subscript f in N_{cf} denotes full shear connection. Where there is partial shear connection, the compressive force in the concrete slab is N_c, which cannot exceed N_{cf}.

The relationship between M_{pr}/M_{pa} and N_{cf}/N_{pa} depends on the profile, but is typically as shown by the dashed line ABC in Fig. 3.3(a). This is approximated in Eurocode 4 by the equation

$$M_{pr} = 1.25 M_{pa}\left[1 - \frac{N_{cf}}{N_{pa}}\right] \leqslant M_{pa}, \tag{3.10}$$

which is shown as ADC. The resistance moment is then given by

$$M_{p.Rd} = N_{cf} z + M_{pr} \tag{3.11}$$

as shown in Fig. 3.2(d) and (e). The lever arm z is found by the approximation shown by line EF in Fig. 3.3(b). This is clearly correct when $N_{cf} = N_{pa}$, because N_{ac} is then zero, so M_{pr} is zero. Equation (3.6) with $x = h_c$ then gives $M_{p.Rd}$. The lever arm is

$$z = d_p - 0.5h_c = h_t - e - 0.5h_c, \tag{3.12}$$

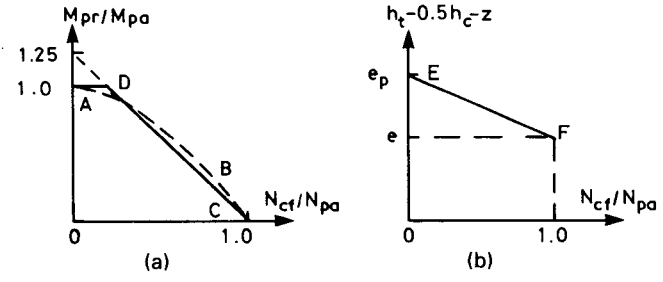

Fig. 3.3 Equations (3.10) and (3.14).

as given by point F.

To check point E, we assume that N_{cf} is nearly zero (e.g. if the concrete is very weak), so that $N_a \simeq 0$ and $M_{pr} \simeq M_{pa}$. The neutral axis for M_{pa} alone is at height e_p above the bottom of the sheet, and the lever arm for the force N_{cf} is

$$z = h_t - e_p - 0.5h_c, \tag{3.13}$$

as given by point E. This method has been validated by tests.

The line EF is given by

$$z = h_t - 0.5h_c - e_p + \frac{(e_p - e)N_{cf}}{N_{pa}}. \tag{3.14}$$

(3) Partial shear connection

The compressive force in the slab, N_c, is now less than N_{cf} and is determined by the strength of the shear connection. The depth x of the stress block is given by

$$x = \frac{N_c}{b(0.85f_{ck}/\gamma_c)} \leqslant h_c\,. \tag{3.15}$$

There is a second neutral axis within the steel sheeting, and the stress blocks are as shown in Fig. 3.2(b), for the slab (with force N_c, not N_{cf}), and Fig. 3.2(c) for the sheeting. The calculation of $M_{p.Rd}$ is as for method (2), except that N_{cf} is replaced by N_c, N_{pa} by N_{cf}, and h_c by x, so that:

$$z = h_t - 0.5x - e_p + \frac{(e_p - e)N_c}{N_{cf}}, \tag{3.16}$$

$$M_{pr} = 1.25M_{pa}\left[1 - \frac{N_c}{N_{cf}}\right] \not> M_{pa}\ , \tag{3.17}$$

$$M_{p.Rd} = N_c z + M_{pr}. \tag{3.18}$$

3.3.2 Resistance of composite slabs to longitudinal shear

For profiled sheeting that relies on frictional interlock to transmit longitudinal shear, there is no satisfactory conceptual model. This led to the development of the shear-bond test, described in Section 2.8.1, and the empirical '*m-k*' method of design, where the shear resistance is given by an equation based on (2.33), in the British code[27] or on equation (2.32), in Eurocode 4. With the safety factor added, the Eurocode equation is

$$V_{l.Rd} = \frac{bd_p\left[\dfrac{mA_p}{bL_s} + k\right]}{\gamma_{vs}} \tag{3.19}$$

where m and k are constants with dimensions of stress, determined from shear-bond tests, and $V_{l.Rd}$ is the design *vertical* shear resistance for a width of slab b. It is based on the vertical shear at an end support at which longitudinal shear failure occurs in a shear span of length L_s, shown by line 2–2 in Fig. 2.19.

For uniformly-distributed load on a span L, the length L_s is taken as $L/4$. The principle that is used when calculating L_s for other loadings is now illustrated by an example.

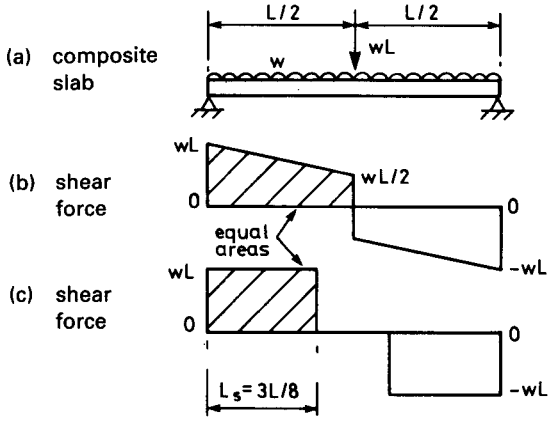

Fig. 3.4 Calculation of L_s for composite slab.

Calculation of L_s

The composite slab shown in Fig. 3.4(a) has a distributed load w per unit length and a centre point load wL, so the shear force diagram is as shown in Fig. 3.4(b). A new shear force diagram is constructed for a span with two point loads only, and the same two end reactions, such that the areas of the positive and negative parts of the diagram equal those of the original diagram. This is shown in Fig. 3.4(c), in which each shaded area is $3wL^2/8$. The positions of the point loads define the lengths of the shear spans. Here, each one is $3L/8$.

Defects of the m-k method

The method has proved to be an adequate design tool for profiles with short spans and rather brittle behaviour, that have been widely used in North America. But to exploit fully the ductile behaviour of profiles now available, with good mechanical interlock and longer spans, it is necessary to use a partial-interaction method, as explained below.

The defects of the *m-k* method and of profiles with brittle behaviour are

given in papers that set out the new methods, by Bode and Sauerborn in Germany[33] and by Patrick and Bridge in Australia[34]. They are as follows.

(1) The *m-k* method is not based on a mechanical model, so that conservative assumptions have to be made in design when the dimensions, materials, or loading differ from those used in the tests. The calculation of L_s, above, is an example of this.
(2) Many additional tests are needed before the range of application can be extended; for example, to include end anchorage or the use of longitudinal reinforcing bars.
(3) The method of evaluation of test data is the same, whether the failure is brittle or ductile. The use in Eurocode 4 of a penalty factor of 0.8 for brittle behaviour does not adequately represent the advantage of using sheeting with good mechanical interlock, because this increases with span.

Partial-interaction design

The method based on shear-bond tests[33] is described first. The method based on slip-block tests,[30] described later, takes more specific account of the effects of friction near supports and can be more economical for short spans.

For composite slabs of given cross-section and materials, the result of each shear-bond test on a profile with ductile behaviour enables the degree of partial shear connection in that test to be calculated. This gives the compressive force N_c transferred from the sheeting to the slab within the shear span of known length L_s. It is assumed that before maximum load is reached, there is complete redistribution of longitudinal shear stress at the interface, so a value for the mean ultimate shear stress τ_u can be calculated. This is done for a range of shear spans, and the lowest τ_u thus found is the basis for a design value, $\tau_{u.Rd}$. (This is where the greater effect of friction in short spans is neglected.)

At an end support, the bending resistance of the slab is that of the sheeting alone (unless it is enhanced by the use of end anchorage, as described later). At any section at distance x from the support, the force in the slab can be calculated from $\tau_{u.Rd}$, and the method of Section 3.3.1(3) enables the bending resistance $M_{p.Rd}$ at that section to be calculated. There is usually a midspan region where full shear connection is achieved, and $M_{p.Rd}$ is independent of x.

For safe design, this curve of $M_{p.Rd}$ as a function of x (the resistance diagram) must at all points lie above the bending-moment diagram for the applied loading. If the loading is increased until the curves touch, the position of the point of contact gives the location of the cross-section of flexural failure and, if the interaction is partial, the length of the shear span.

The resistance diagram can easily be modified to take advantage of any end anchorage or slab reinforcement, and the loading diagram can be of any shape.

The method based on data from slip-block tests is similar, except that the resistance is increased near end supports, by an allowance for the effects of friction.

A worked example using data from shear-bond tests is given in Section 3.4.3.

The only type of end anchorage for which design rules are given in British or European codes is the headed stud, welded through the sheeting to the top flange of a steel beam. The resistance of the anchorage is based on local failure of the sheeting, as explained in commentaries on Eurocode 4: Part 1.1[15] and BS 5950: Part 3.1.[35]

3.3.3 Resistance of composite slabs to vertical shear

Tests show that resistance to vertical shear is provided mainly by the concrete ribs. For open profiles, their effective width b_o should be taken as the mean width, though the width at the centroidal axis (Fig. 3.2(a)) is accurate enough. For re-entrant profiles, the minimum width should be used.

Design methods are based on those for shear in reinforced concrete T-beams. In Eurocode 4, the resistance of a composite slab with ribs of effective width b_o at spacing b is given as

$$V_{v.Rd} = \frac{b_o}{b} d_p \tau_{Rd} k_v (1.2 + 40\rho) \text{ per unit width} \qquad (3.20)$$

where d_p is the depth to the centroidal axis (Fig. 3.2(a)),
τ_{Rd} is the basic shear strength of the concrete (Section 1.4),
k_v allows for the higher shear strength of shallow members, given by

$$k_v = (1.6 - d_p) \geqslant 1, \text{ with } d_p \text{ in m},$$

ρ allows for a small contribution from the profiled sheeting. It is given by

$$\rho = \frac{A_p}{b_o d_p} < 0.02 \qquad (3.21)$$

where A_p is the effective area of sheeting in tension within the width b_o, which can usually be taken as the total area within that width.

In reality, the shear stress in the side walls of the steel troughs may be quite high during the construction phase. This can be ignored when checking the composite slab, and V_{Sd} should be taken as the whole of the vertical shear, including that initially resisted by the sheeting.

Resistance to vertical shear is most likely to be critical in design where span/depth ratios are low, as is the case for beams.

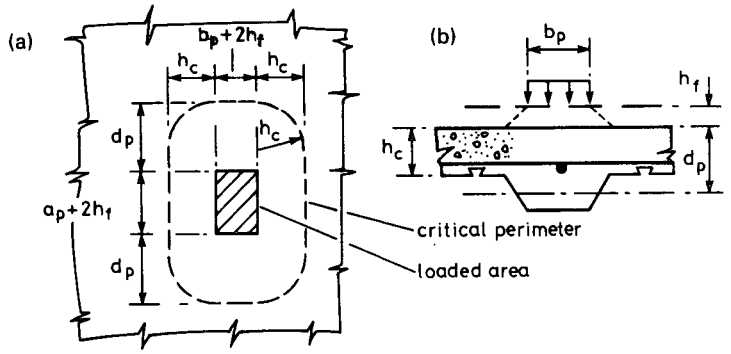

Fig. 3.5 Critical perimeter for punching shear.

3.3.4 Punching shear

Where a thin composite slab has to be designed to resist point loads (e.g. from a steel wheel of a loaded trolley), resistance to punching shear may be critical. Failure is assumed to occur on a 'critical perimeter', of length C_p, which is defined as for reinforced concrete slabs. For a loaded area a_p by b_p, remote from a free edge, and 45° spread through a screed of thickness h_f, it is as shown in Fig. 3.5(a):

$$C_p = 2\pi h_c + 2(2d_p + a_p - 2h_c) + 2b_p + 8h_f. \tag{3.22}$$

By analogy with equation (3.20), the design resistance is

$$V_{p.Rd} = C_p h_c \tau_{Rd} k_v (1.2 + 40\rho) \tag{3.23}$$

where h_c is the thickness of the slab above the sheeting. Small ribs of the type shown in Fig. 3.5(b) can be neglected when h_c is determined.

3.3.5 Concentrated point and line loads

Since composite slabs span in one direction only, their ability to carry masonry partition walls or other heavy local loads is limited. Rules are given in Eurocode 4 (and in the British code) for widths of composite slabs effective for bending and vertical shear resistance, for point and line loads, as functions of the shape and size of the loaded area. These are based on a mixture of simplified analyses, test data, and experience.

They are illustrated here for a rectangular loaded area a_p by b_p, with its centre distance L_p from the nearer support of a slab of span L, as shown in Fig. 3.6(a). The load may be assumed to be distributed over a width b_m, defined by lines at 45° (Fig. 3.6(b)), where

$$b_m = b_p + 2(h_f + h_c) \tag{3.24}$$

where h_f is the thickness of finishes, if any. The codes do not refer to distribution in the spanwise direction, but it would be reasonable to use the same rule, and take the loaded length as

$$a_m = a_p + 2(h_f + h_c). \tag{3.25}$$

The width of slab assumed to be effective for global analysis (for continuous slabs only) and for resistance is given by

$$b_e = b_m + kL_p\left[1 - \frac{L_p}{L}\right] \leqslant \text{width of slab} \tag{3.26}$$

where k is taken as 2 for bending and longitudinal shear (except for interior spans of continuous slabs, where $k = 1.33$) and as 1 for vertical shear.

For a simply-supported slab and point load Q_d, the sagging moment per unit width of slab on line AD in Fig. 3.6(a) is thus

$$m_{Sd} = Q_d L_p \frac{1 - \dfrac{L_p}{L}}{b_e}, \tag{3.27}$$

which is a maximum when $L_p = L/2$.

The variation of b_e with L_p is shown in Fig. 3.6(a). The load is assumed to be uniformly distributed along line BC, whereas the resistance is distributed along line AD, so there is sagging transverse bending under the load. The maximum sagging bending moment is at E, and is given by

$$M_{Sd} = Q_d \frac{b_e - b_m}{8}. \tag{3.28}$$

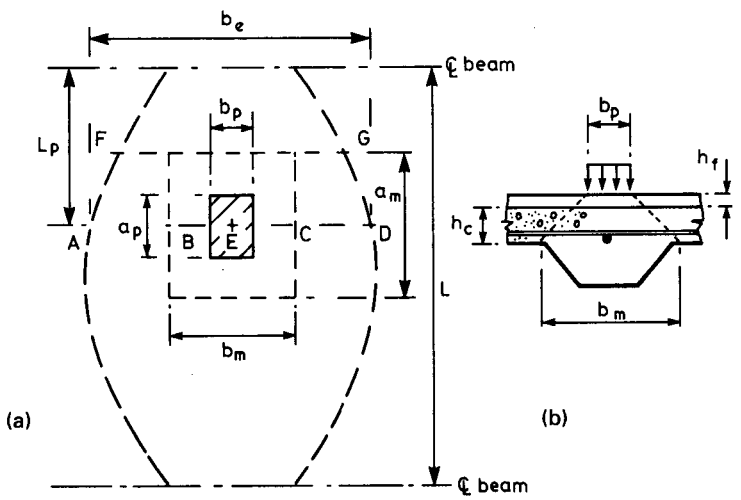

Fig. 3.6 Effective width of composite slab, for point load.

The sheeting has no tensile strength in this direction, because the corrugations can open out, so bottom reinforcement (Fig. 3.6(b)) must be provided. It is suggested that this reinforcement should be spread over the length a_m given by equation (3.25).

It is stated in Eurocode 4 that where transverse reinforcement is provided with a cross-sectional area of at least 0.2% of the area of concrete above the ribs of the sheeting, no calculations are needed for characteristic concentrated loads not exceeding 7.5 kN. Calculations in Section 3.4 show that for the slab considered there, more than 0.2% appears to be necessary, so in that case the preceding rules are more conservative than the concession.

Vertical shear should be checked along a line such as FG, when L_p is such that FG is above the edge of the flange of the steel beam. It rarely governs design.

3.3.6 Serviceability limit states for composite slabs

Cracking of concrete

The lower surface of the slab is protected by the sheeting. Cracking will occur in the top surface where the slab is continuous over a supporting beam, and will be wider if each span of the slab is designed as simply-supported, rather than continuous, and if the spans are propped during construction.

For these reasons, longitudinal reinforcement should be provided above internal supports. The minimum amounts are given by Eurocode 4 as 0.2% of the area of concrete above the sheeting, for unpropped construction, and 0.4% if propping is used. These amounts exceed that specified in the British code,[14] but even they may not ensure that crack widths do not exceed 0.3 mm. If the environment is corrosive (e.g. de-icing salt on the floor of a parking area), the slabs should be designed as continuous, with cracking controlled in accordance with Eurocode 2 (or an equivalent national code).

Deflection

Where composite slabs are designed as simply-supported and are not hidden by false ceilings, deflection may govern design. The maximum acceptable deflection is more a matter for the client than the designer; but if predicted deflections are large, the designer may have to allow for the extra weight of concrete in floors that are cast with a horizontal top surface, and provide clearance above non-structural partitions.

Eurocode 4 gives the following guidance. The deflection of sheeting due to its own weight and the wet concrete slab should not exceed $L/180$ or 20 mm, where L is the effective span. This span can be reduced to any desired level by using propped construction – but this increases cost.

For the 'in-service' situation, the rare loading combination is normally used. The maximum deflection below the level of the supports should not exceed span/250, and the increase of deflection after construction (due to creep and to variable load) should not exceed span/300, or span/350 if the floor supports brittle finishes or partitions. The Eurocode states that when verifying the composite slab, the deflection defined in the previous paragraph, above, need not be included. For a 4-m span, this suggests that the total deflection could be

$$20 + 4000/250 = 36 \text{ mm},$$

which would certainly be noticeable in practice.

It is known from experience that deflections are not excessive when span-to-depth ratios are kept within certain limits. These are given in Eurocode 4 as 25 for simply-supported slabs, 32 for spans with one end continuous, and 35 for internal spans. 'Depth' is not defined in Eurocode 4, but in Eurocode 2 these limits relate to effective depths, so for composite slabs the depth should be taken as d_p in Fig. 3.2 rather than h_t.

These limits are most likely to be exceeded in an external span, designed as simply-supported. Where possible, reference should then be made to the result of a test. Eurocode 4 advises that no account need be taken of the additional deflection due to end slip, provided that the load at which end slip reached 0.5 mm exceeded the design service load by more than 20%. Otherwise, slip should be allowed for (using test data) or end anchors should be provided. Where no test data are available, use of the tied arch model (which is usually conservative) is recommended.

Even for an end span, the provision of anti-crack reinforcement, as specified above, should reduce deflection by a useful amount. For internal spans, the Eurocode recommends that the second moment of area of the slab should be taken as the mean of values calculated for the cracked and uncracked sections. Some of these points are illustrated in the worked example in Section 3.4.

3.3.7 Fire resistance

All buildings are vulnerable to damage from fire, which is usually the first accidental design situation to be considered in design, and is the only one treated in this volume.

In the worked example, design is in accordance with the 1993 draft of Eurocode 4: Part 1.2, 'Structural fire design'.[13] The concepts and methods used are now introduced. Italic print is used for terms that are defined in Eurocode 4: Part 1.2, or in Part 2.2 of Eurocode 1, 'Actions on structures exposed to fire'.[36]

Buildings are divided by *separating members* into *fire compartments*. A fire is assumed to be confined to one compartment only, which must be

designed to contain it for a specified *failure time* (or *fire resistance* time) when subjected to a given temperature–time environment or fire exposure. A *standard fire exposure* is given in Eurocode 1: Part 2.2, and other curves are available that depend on the *fire load density* (calorific energy per unit area, for complete combustion of all combustible materials) within the compartment considered. These temperature–time curves are reproduced in furnaces for fire testing, and are simplified models of the effects of real fires.

The walls, floor, and ceiling that enclose a compartment must have a *separating function*. This is defined using two criteria:

- *thermal insulation criterion*, denoted I, concerned with limiting the transmission of heat by conduction, and
- *integrity criterion*, denoted E, concerned with preventing the passage of flames and hot gases into an adjacent compartment.

The structure of a compartment must have a *loadbearing function*, denoted R (resistance), to ensure that it can resist the design effects of actions specified for the fire situation including the effects of thermal expansion, for a period not less than the specified failure time. The *fire resistance class* of a member or compartment is denoted (for example) R60, which means that its failure time is not less than 60 minutes.

Criterion I is met mainly by specifying minimum thicknesses of incombustible insulating materials. These also contribute to meeting criterion E, which has structural implications as well. For example, excessive thermal hogging of a beam heated from below can create a gap between it and a separating wall below.

Codes give limits to the temperature rise of non-exposed surfaces, relevant to criterion I, and detailing rules relevant to criteria I and E. Design calculations relate mainly to criterion R, and only these are discussed further, in this volume.

It will be seen that, for practicable design, it is necessary to simplify the predictions of both the action effects and the resistances, to a greater extent than for 'cold' design. This last term refers to the normal design for persistent situations and ultimate limit states.

3.3.7.1 Partial safety factors for fire

It is recommended in Eurocode 1: Part 1 that all factors γ_F for accidental actions should be 1.0; i.e. that these actions should be so defined that $\gamma_{F,f} = 1.0$ is the appropriate factor. Subscript f means 'fire'.

For materials, design is based essentially on characteristic or nominal properties; so for most materials, and for shear connection, $\gamma_{M,f} = 1.0$; but the reduction below γ_M for persistent design situations is then much greater for concrete ($1.5 \rightarrow 1.0$) than for structural steel (1.1 or $1.05 \rightarrow 1.0$). The yield strength is also a conservative measure of the stress in steel at

large deformations, because of strain hardening, so it is likely that the boxed value of $\gamma_{M,f}$ for structural steel (i.e. $\gamma_{a,f}$) will be 0.9 in Eurocodes 3 and 4. This value will be used in the worked example.

3.3.7.2 Design action effects for fire

For a structural member with one type only of permanent loading and no prestress, the combination for accidental design situations given in Eurocode 1: Part 1[8] simplifies to

$$G_k + A_d + \psi_{11} Q_{k,1} + \sum_{i>1} \psi_{2,i} Q_{k,i} \tag{3.29}$$

where A_d is the design value of the accidental action, and other symbols are as in Section 1.3.2.

A floor structure for a building is usually designed for distributed loads g_k and q_k; and for fire, A_d can be taken as zero. For beams and slabs, the 'simply-supported' moments and shears are proportional to the total load per unit area. To avoid additional global analyses for fire, the action effects $E_{f,d}$ are often assumed to be given by

$$E_{f,d} = \eta_f E_d = 0.6 E_d \tag{3.30}$$

where E_d are the effects for cold design for ultimate limit states.

The value $\eta_f = 0.6$ is based on the boxed γ_F values in Eurocode 1: Part 1, as follows. From equations (3.29) and (3.30), and expression (1.6) with $Q_{k,2} = 0$, and $\psi_1 = 0.7$ (Table 1.3):

$$\eta_f = \frac{\gamma_{GA} g_k + \psi_1 q_k}{\gamma_G g_k + \gamma_Q q_k} = \frac{1.0 + 0.7 \dfrac{q_k}{g_k}}{1.35 + 1.5 \dfrac{q_k}{g_k}}. \tag{3.31}$$

The value of η_f falls from 0.64 to 0.55 as the ratio q_k/g_k rises from 0.5 to 2.0, so $\eta_f = 0.6$ is a typical value, accurate to within 10%.

It often occurs in cold design that the resistance provided, R_d, exceeds the relevant action effect, E_d. This is allowed for in fire design as follows. A resistance ratio η^* is calculated from

$$\eta^* = \eta_f \frac{E_d}{R_d}. \tag{3.32}$$

The verification condition ($R_{f,d} \geqslant E_{f,d}$) then becomes

$$R_{f,d} \geqslant \eta^* R_d. \tag{3.33}$$

This enables tabulated design data to be presented in terms of η^*, which lies between 0.3 and 0.7.

3.3.7.3 Thermal properties of materials

Stress–strain curves for steel and concrete are given as functions of temperature (θ) in draft Eurocode 4: Part 1.2. (They may later be replaced by

cross-references to Parts 1.2 of Eurocodes 3 and 2, respectively.) These are used as necessary in the worked example.

3.3.7.4 Design for load bearing function

The three methods given in Eurocode 4: Part 1.2 are outlined below. The first (given last in the Code) has the widest scope, but is the most complex. It is primarily a research tool, used to validate simpler methods.

(1) Advanced calculation models

These methods rely mainly on finite-element computations, which are done in three stages, starting with a given structure, materials, and fire exposure.

(a) The theory of heat transfer is used to obtain distributions of temperature (θ) throughout the structure as functions of the time (t) since the start of the fire.

(b) From the temperatures, distributions of thermal strains and of the stiffness and strength of the materials throughout the structure are computed, for various times, t.

(c) The design resistances of the structure are computed at various times, t, using data from stage (b). These resistances diminish as t increases, and eventually one of them falls below the corresponding design action effect. The structure satisfies criterion R if the time when this occurs exceeds the specified failure time.

(2) Simple calculation models

These methods enable the three preceding stages to be applied, in simplified form, in checks on the resistances of cross-sections. These are normally done only for the temperature distribution at the specified failure time, assuming that beams and slabs are simply-supported and columns are pin-ended at each floor level. The model for a composite slab is explained in Section 3.3.7.5.

(3) Tabulated data

For cross-sections of beams and columns that are often used in practice, results of calculations by methods (1) or (2) are presented in Eurocode 4: Part 1.2 as tabulated values of minimum dimensions, areas of reinforcement, etc., for each fire resistance class. Methods of this type are used for the beams and columns of the worked example in this volume.

3.3.7.5 Simple calculation model for unprotected composite slab

It is assumed that the dimensions and properties of materials for the slab are known, that its cold design was for distributed loading on simply-supported spans, for which the bending moments R_d and E_d are known, so that η^* (equation (3.32)) is known.

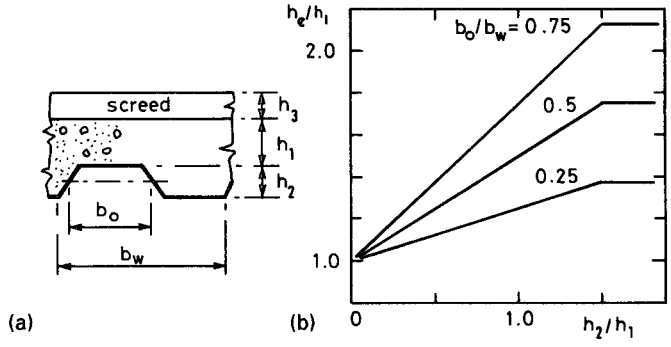

Fig. 3.7 Effective thickness of composite slab.

It is assumed that the required fire resistance period ($t_{f,r}$) is 60 minutes, and that the profiled sheeting, not protected by insulation, is heated from below by the standard fire.

The thermal insulation provided by the slab is assumed to depend only on its effective thickness. For class I60, the minimum effective thickness of lightweight concrete is given in Eurocode 4: Part 1.2 as

$$h_e \geqslant 0.9(90 - h_3) \text{ mm} \tag{3.34}$$

where h_3 is the thickness of the screed layer above the slab (but $h_3 \leqslant 20$ mm). The thickness h_e depends on the geometry of the profile:

$$\left.\begin{aligned} &\frac{h_e}{h_1} = 1 + \frac{b_o}{b_w}\frac{h_{2ef}}{h_1} \quad \text{and} \quad h_1 > 50 \text{ mm} \\ &h_{2ef} = h_2 \quad \text{but} \quad \leqslant 1.5h_1 \end{aligned}\right\} \tag{3.35}$$

where the symbols are defined in Fig. 3.7(a). Some ratios, h_e/h_1, plotted in Fig. 3.7(b), shown how h_e increases as the rib size (represented by b_o/b_w and h_2/h_1) increases.

For the bending resistance of the slab, the strength of the steel sheeting and the tensile strength of the concrete are ignored, so reinforcing bars have to be provided within the ribs. Their temperature, and hence their yield strength, depends on their effective distance from the hot surfaces, represented by u, defined by

$$\frac{1}{u} = \frac{1}{\sqrt{u_1}} + \frac{1}{\sqrt{u_2}} + \frac{1}{\sqrt{u_3}} \tag{3.36}$$

where u_1 to u_3 are distances (mm) shown in Fig. 3.8(a).

For $t_{f,r} = 60$ minutes, the design temperature θ_s of this reinforcement is given in Eurocode 4: Part 1.2 in degrees C as

$$\theta_s = 1175 - 350u \leqslant 810°C, \quad (u \leqslant 3.3). \tag{3.37}$$

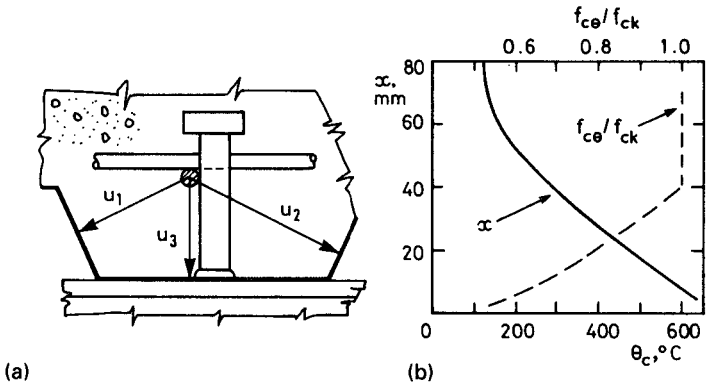

Fig. 3.8 Design data for temperatures in composite slab.

The concrete near the top of the slab is well protected from fire, so its compressive strength is assumed not to be reduced.

These assumptions enable the sagging moment of resistance to be calculated. If this does not exceed $\eta^* R_d$ (equation (3.33)), the difference can often be made up by using hogging resistance at the end of each span. The top reinforcement, provided initially to control cracking, can be assumed not to be weakened by fire. The concrete is modelled as a uniform slab of thickness h_e, defined above. The design temperature profile for lightweight concrete and class R60, as given in Eurocode 4: Part 1.2, is shown in Fig. 3.8(b), in which x is the distance above the lower surface of the effective slab, of thickness h_e. The curve $f_{c\theta}/f_{ck}$ is explained on page 73.

3.4 Example: composite slab

The strengths of materials and characteristic actions for this structure are given in Section 3.2, and a typical floor is shown in Fig. 3.1. The following calculations illustrate the methods described in Section 3.3. In practice, the calculations may be done by the company that provides the sheeting, and presented as 'safe load tables'; but here it is assumed that only raw test data are available.

For unpropped construction, the sheeting for a span of 4 m would need to be over 100 mm deep. Few such products are available, so it is assumed that the sheets will be propped at midspan during construction. The profile chosen is CF 70, manufactured by Precision Metal Forming, Ltd of Cheltenham, Gloucestershire, UK. Its overall depth is 70 mm, but the cross-section (Fig. 3.9) is such that the span/depth ratio based on this depth (28.6) is misleading. A more realistic value is 2000/55, which is 36.4. This should be adequate, as there is continuity over the prop between the two 2-m spans.

The next step is to choose a thickness for the composite slab, which will be designed as simply-supported over each 4-m span. The characteristic point load is fairly high (7.0 kN, equation (1.17)), so an overall thickness of 150 mm is assumed for the slab. The centroid of the sheeting is 30 mm above its lower surface, so the effective depth (d_p) is 120 mm and the span/depth ratio is 4000/120, or 33.3. It is normal for these ratios to be higher than typical values used for beams. Preliminary calculations then show that CF 70 sheeting of nominal thickness 0.9 mm should be sufficient.

Structural properties of profiled sheetings, determined in accordance with Eurocode 4: Part 1.1, are not available, as that code is not yet in force; but the test data on CF 70/09 sheeting are sufficient to enable them to be approximated. This has been done in the Designers' Handbook to Eurocode 4: Part 1.1,[15] and the results for sagging bending are given here and in Fig. 3.9.

Guaranteed minimum yield strength,	f_{yp}	= 280 N/mm^2.
Design thickness, allowing for zinc,	t_p	= 0.86 mm.
Effective area of cross-section,	A_p	= 1185 mm^2/m.
Second moment of area,	I_p	= 0.57 × 10^6 mm^4/m.
Characteristic plastic moment of resistance,	M_{pa}	= 4.92 kN m/m.
Distance of centroid above base,	e	= 30 mm.
Distance of plastic neutral axis above base,	e_p	= 33 mm.
Characteristic resistance to vertical shear,	V_{pa}	= 49.2 kN/m.
For resistance to longitudinal shear,	m	= 184 N/mm^2
	k	= 0.0530 N/mm^2.
For partial-interaction design,	$\tau_{u.Rd}$	= 0.23 N/mm^2.
Weight of composite slab (ρ = 1900 kg/m^3),	g_k	= 2.41 kN/m^2.

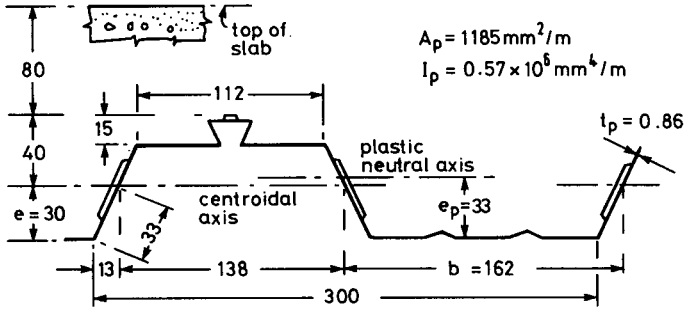

Fig. 3.9 Typical cross-section of CF 70/0.9 profiled steel sheeting.

These data are illustrative only, and should not be used in engineering practice.

3.4.1 Profiled steel sheeting as shuttering

The construction load is 1.5 kN/m^2 on any area 3 m square (Section 3.3), so the design loads are:

- permanent: $g_d = 2.41 \times 1.35 = 3.25$ kN/m^2,
- variable: $q_d = 1.5 \times 1.5 = 2.25$ kN/m^2.

The top flanges of the supporting steel beams are assumed to be at least 0.15 m wide, and the width of the prop is neglected, so the effective length of each of the two spans is

$$L_e = \frac{4000 - 150 + 70}{2} = 1960 \text{ mm}.$$

The 70 is the depth of the sheeting. This rule is taken from BS 5950: Part 4,[27] as none is given in Eurocode 4.

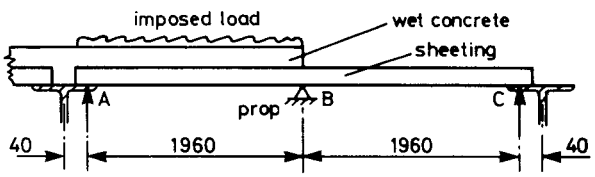

Fig. 3.10 Profiled sheeting during construction.

Flexure and vertical shear

The most adverse loading for sagging bending is shown in Fig. 3.10, in which the weight of the sheeting alone in span BC is neglected. The maximum design bending moments are:

- sagging $M_{Sd} = 0.0959 \times 5.5 \times 1.96^2 =$ **2.03 kN m/m**,
- hogging $M_{Sd} = 0.0625 \times 5.5 \times 1.96^2 = 1.32$ kN m/m.

With $\gamma_{ap} = 1.1$, the design resistance is $M_{Rd} = 4.92/1.1 =$ **4.47 kN m/m**, which is ample.

Vertical shear rarely governs design of profiled sheeting. Here, the maximum value, to the left of point B in Fig. 3.10, is

$$V_{Sd} = 0.56 \times 5.5 \times 1.96 = 6.0 \text{ kN/m},$$

far below the design resistance (49.2/1.1 = 44.7 kN/m).

Deflection

The design serviceability load is 2.41 + 1.5 = 3.91 kN/m^2. It is assumed that the prop does not deflect. The maximum deflection in span AB, if BC is unloaded, is

$$\delta_{max} = \frac{wL_e^4}{185E_aI_p} = \frac{3.91 \times 1.96^4}{185 \times 0.21 \times 0.57} = 2.6 \text{ mm}. \tag{3.38}$$

This is span/754, which is very low.

3.4.2 Composite slab – flexure and vertical shear

This continuous slab is designed as a series of simply-supported spans. The effective span is the lesser of the distance between centres of supports (4.0 m), and the clear span (assumed to be 3.85 m) plus the effective depth of the slab (0.12 m), so L_e = 3.97 m.

For vertical shear, the span is taken as 4.0 m, so that the design loading for the beams includes the whole area of slab.

The design ultimate loadings are:

- permanent: $g_d = (2.41 + 2.5) \times 1.35 = 6.63$ kN/m^2,
- variable: $q_d = 5 \times 1.5 = 7.5$ kN/m^2.

The midspan bending moment is:

$$M_{Sd} = 14.13 \times \frac{3.97^2}{8} = \mathbf{27.8\ kN\ m/m}.$$

For the bending resistance, from equation (3.3),

$$N_{cf} = 1185 \times \frac{0.28}{1.1} = 302 \text{ kN/m}. \tag{3.39}$$

The design compressive strength of the concrete is 0.85 × 25/1.5 = 14.2 N/mm^2, so from equation (3.4), the depth of the stress block is

$$x = \frac{302}{14.2} = 21.3 \text{ mm}. \tag{3.40}$$

This is less than h_c (which can be taken as 95 mm for this profile (Fig. 3.9)), so from equation (3.6),

$$M_{p.Rd} = 302\ (0.12 - 0.011) = \mathbf{32.9\ kN\ m/m}. \tag{3.41}$$

The bending resistance is sufficient.

The design vertical shear for a span of 4 m is

$$V_{Sd} = 2(6.63 + 7.5) = \mathbf{28.3\ kN/m}.$$

The resistance is given by equation (3.20). From Fig. 3.9:

$$b_o = 162 \text{ mm}, \quad b = 300 \text{ mm}, \quad d_p = 120 \text{ mm}.$$

The area A_p is

$$A_p = 0.86\,(162 - 26 + 66) = 174 \text{ mm}^2,$$

so from equation (3.21)

$$\rho = \frac{174}{162 \times 120} = 0.009$$

and

$$k_v = 1.6 - 0.12 = 1.48 \text{ m}.$$

The basic shear strength (Section 1.4) is $\tau_{Rd} = 0.30$ N/mm^2, so from equation (3.20),

$$V_{v.Rd} = \frac{162}{300} \times 120 \times 0.3 \times 1.48(1.2 + 0.36) = \mathbf{45\ kN/m}, \quad (3.42)$$

which is ample.

3.4.3 Composite slab – longitudinal shear

Longitudinal shear is checked by both the '*m-k*' and 'partial-interaction' methods, which are explained in Section 3.3.2. From equation (3.19), the *m-k* method gives the vertical shear resistance as

$$V_{l.Rd} = bd_p \frac{\left[\dfrac{mA_p}{bL_s} + k\right]}{\gamma_{vs}} = \mathbf{26.2\ kN/m}. \quad (3.43)$$

The values used are:

b	= 1.0 m,	m	= 184 N/mm^2,
d_p	= 120 mm,	k	= 0.0530 N/mm^2,
A_p	= 1185 mm^2/m,	γ_{vs}	= 1.25,
L_s	= $L/4$ = 993 mm,		

where γ_{vs} is taken as equal to γ_v in Table 1.2, and the other values are given above.

The design vertical shear is **28.3 kN/m** (Section 3.4.2), so the slab is not strong enough, using this method.

Partial-interaction method

The mean design resistance to longitudinal shear, $\tau_{u.Rd}$, is taken as 0.23 N/mm^2 for this slab (page 64). Account is taken of the shape of the profile when this value is determined from test data, so the shear resistance per metre width of sheeting is 0.23 kN per mm length. From equation (3.39), the compressive force in the slab for full shear connection, N_{cf}, is

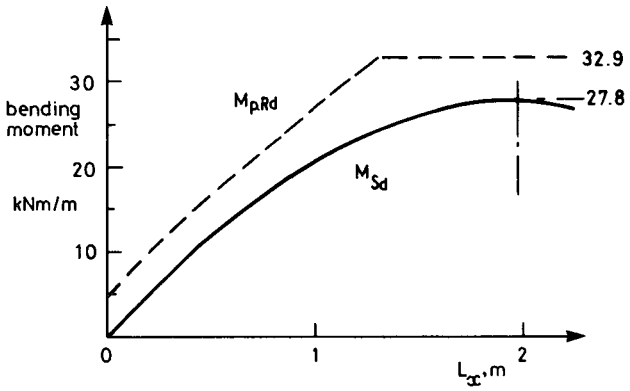

Fig. 3.11 Partial-interaction method, for longitudinal shear.

equal to N_{pa}, and is 302 kN/m. The required length of shear span to develop this force (in absence of any end anchorage) is

$$L_{sf} = \frac{N_{cf}}{b\tau_{u.Rd}} = \frac{302}{0.23} = 1313 \text{ mm}. \tag{3.44}$$

(This equation is given in clause E.3(2) of Eurocode 4: Part 1.1.) The depth of the stress block in the concrete, now denoted x_f, is then 21.3 mm, from equation (3.40). At a distance L_x ($<L_{sf}$) from an end support, the degree of shear connection is given by

$$\nu = \frac{L_x}{L_{sf}} = \frac{N_c}{N_{cf}} = \frac{x}{x_f} \tag{3.45}$$

where N_c is the force in the slab and x the depth of the stress block.

Equations (3.16) to (3.18) then become:

$$\left.\begin{aligned} z &= 150 - 0.5\nu x_f - 33 + 3\nu = 117 - 7.6\nu \\ M_{pr} &= 1.25 \times 4.47(1 - \nu) = 5.59(1 - \nu) \not> 4.47 \\ M_{p.Rd} &= \nu N_f z + M_{pr} \end{aligned}\right\} \tag{3.46}$$

These enable $M_{p.Rd}$ to be calculated for any value of L_x between zero and L_{sf}. The curve so obtained is given in Fig. 3.11. The bending-moment diagram for the loading, also shown, is a parabola with maximum value 27.8 kNm/m at midspan (from Section 3.4.2).

It is evident that the resistance is sufficient at all cross-sections, so in this example the partial-interaction method is less conservative than the *m-k* method. This is because more advantage can be taken of the ductile load-slip behaviour of these slabs, established by testing.

3.4.4 Local effects of point load

The design point load is $Q_{Sd} = 7.0 \times 1.5 =$ **10.5 kN** on any area 50 mm square, from equation (1.17) in Section 3.2. The slab has to be checked for

punching shear and local bending. It is assumed that the thickness h_f of floor finish is at least 50 mm, so the data are:

$$b_p = a_p = 50 \text{ mm}, \quad h_f = 50 \text{ mm}, \quad h_c = 95 \text{ mm}, \quad d_p = 120 \text{ mm}.$$

The small ribs at the top of the sheeting (Fig. 3.9) are neglected, so the thickness of slab above the sheeting is taken as 95 mm. Other data are as used in calculations for vertical shear (Section 3.4.2):

$$\tau_{Rd} = 0.3 \text{ N/mm}^2, \quad k_v = 1.48 \text{ m}, \quad \rho = 0.009.$$

Punching shear
From equation (3.22) in Section 3.3.4:

$$C_p = 2\pi h_c + 2(2d_p + a_p - 2h_c) + 2b_p + 8h_f = 1297 \text{ mm}.$$

From equation (3.23):

$$V_{p.Rd} = C_p h_c \tau_{Rd} k_v (1.2 + 40\rho) = \mathbf{85 \text{ kN}},$$

so the resistance is eight times the action. But local bending is not so simple.

Local bending
From equations (3.24) and (3.25) in Section 3.3.5,

$$a_m = b_m = a_p + 2(h_f + h_c) = 340 \text{ mm}.$$

The most adverse situation for local sagging bending is when the load is at midspan, so L_p (Fig. 3.6) is 1.99 m. From equation (3.26), the effective width of slab is

$$b_e = b_m + 2L_p\left[1 - \frac{L_p}{L}\right] = 2.33 \text{ m}.$$

From equation (3.27), the sagging moment per unit width is

$$m_{Sd} = Q_d L_p \frac{1 - \dfrac{L_p}{L}}{b_e} = \mathbf{4.48 \text{ kN m/m}},$$

which is well below the resistance of the slab, **32.9 kNm/m**.

The transverse sagging moment under the load is given by equation (3.28):

$$M_{Sd} = Q_d \frac{b_e - b_m}{8} = 2.61 \text{ kN m}.$$

This is resisted by a breadth a_m of reinforced concrete slab (Fig. 3.6), so the moment per unit width is

$$m_{Sd} = \frac{2.61}{0.34} = \mathbf{7.68\ kN\ m/m}.$$

If the bottom reinforcement consists of 7-mm bars resting on the ribs of the sheeting, the effective depth of the slab is $80 - 7/2 \simeq 76$ mm. If the reinforcement is fabric with $f_{sk} = 500$ N/mm^2 and bars at 200 mm pitch, the area per metre width is 193 mm^2, and the force at yield is

$$193 \times 0.500/1.15 = 83.9\ \text{kN/m}.$$

The depth of the concrete stress block is

$$x = 83.9/(0.85 \times 25/1.5) = 5.92\ \text{mm}$$

so the lever arm is $76 - 2.96 \simeq 73$ mm and

$$m_{Rd} = 83.9 \times 0.073 = \mathbf{6.12\ kNm/m}.$$

Using this method, the spacing of the 7-mm bars would have to be reduced to about 150 mm to provide a resistance exceeding 7.68 kN m/m. These calculations are approximate, and conservative in comparison with experience. It will be found later that for this slab, other limit states govern much of the slab reinforcement; but in regions where they do not, fabric of area 193 mm^2/m would probably be provided, as it satisfies the empirical rule given in clause 7.4.2.2(5) of Eurocode 4: Part 1.1 (Section 3.3.5).

3.4.5 Composite slab – serviceability

Cracking of concrete above supporting beams

Following Section 3.3.6, continuity across the steel beams should be provided by reinforcement of area 0.4% of the area of concrete. Hence,

$$A_s = 0.004 \times 1000 \times 80 = 320\ \text{mm}^2/\text{m}. \qquad (3.47)$$

The detailing is best left until longitudinal shear in the beam and fire resistance have been considered.

Deflection

Realistic calculations would have to allow not only for the use of propped construction, but also for the presence of the reinforcement of area A_s, calculated above. Both effects reduce deflections. The most adverse situation probably occurs at an end of the building, where the last 4-m span has continuity at one end only. Deflections should not be excessive there if the span-to-depth ratio is less than 32 (Section 3.3.6). The actual value is $3970/120 = 33.1$, so some calculations are now given. For simplicity, the mean of the short-term and long-term modular ratios is used. From Section 3.2, this is:

$$n = \frac{11 + 33}{2} = 22.$$

Second moments of area of the unreinforced composite slab, calculated in 'steel' units by the transformed section method are:

- if uncracked $I_1 = 12.1 \times 10^6$ mm^4/m
- cracked, sagging bending $I_2 = 8.1 \times 10^6$ mm^4/m.

The mean value, used here, is:

$$I_m = 10.1 \times 10^6 \text{ mm}^4/\text{m}. \tag{3.48}$$

The self-weight of the slab is 2.41 kN/m^2, so the load on the prop (Fig. 3.10), treated as the central support of a two-span beam, is

$$F = 2 \times 0.625 \times 2.41 \times 1.96 = 5.9 \text{ kN/m}.$$

This is assumed to act as a line load on the composite slab, when the props are removed. There is in addition a load of 2.5 kN/m^2 from finishes and partitions (g), and an imposed load q of 5.0 kN/m^2.

The midspan deflection (for a simply-supported slab) is

$$\delta = \frac{L^3}{48EI}\left[F + \frac{5(g+q)L}{8}\right] = 3.6 + 11.4 = 15.0 \text{ mm}, \tag{3.49}$$

with $L = 3.97$ m and $E = 210$ kN/mm^2. Hence,

$$\frac{\delta}{L} = \frac{15}{3970} = \frac{1}{265}.$$

This is less than the limit of 1/250 recommended in Eurocodes 3 and 4, and would be reduced by the crack-control reinforcement above one support. It would, however, be increased by any settlement of the props during construction.

3.4.6 Composite slab – fire design

The slab is designed for a standard fire duration of 60 minutes, using methods that are explained in Section 3.3.7.

The characteristic loads are:

$$g_k = 4.9 \text{ kN/m}^2$$

$$q_k = 5.0 \text{ kN/m}^2$$

so from equation (3.31),

$$\eta_f = 0.595.$$

For cold design, the midspan bending moments are:

$$E_d = 27.8 \text{ kN m/m}$$

$$R_d = 32.9 \text{ kN m/m}$$

so from equation (3.32),

$$\eta^* = 0.50,$$

and from equation (3.33),

$$\boldsymbol{M_{Rd.f} = R_{f.d} \geqslant 16.45 \text{ kN m/m}}. \tag{3.50}$$

For calculating the effective thickness, the dimensions in Fig. 3.7(a) are:

$h_1 = 95$ mm, $h_2 = 55$ mm, $h_3 = 20$ mm,
$b_o = 136$ mm, $b_w = 300$ mm

so from equation (3.35), $h_{2ef} = 55$ mm and

$$\boldsymbol{h_e} = 95\left[1 + \frac{136}{300}\frac{55}{95}\right] = \mathbf{120 \text{ mm}}. \tag{3.51}$$

From equation (3.34), the required thickness is

$$\boldsymbol{h_e} \geqslant 0.9(90 - 70) = \mathbf{63 \text{ mm}},$$

so criterion I60 is easily satisfied.

For bending resistance at midspan, it is assumed that 8-mm reinforcing bars are located above each rib in the position shown to scale in Fig. 3.8, and also in Fig. 3.12(a). This enables them to be fixed to transverse bars or fabric that rests on the small top ribs shown in Fig. 3.9. The dimensions to the hot steel surfaces are then:

$$u_1 = 72 \text{ mm}, u_2 = 102 \text{ mm}, u_3 = 60 \text{ mm}.$$

From equation (3.36),

$$u = 2.9.$$

From equation (3.37),

$$\theta_s = 160°\text{C}.$$

At this temperature, the proportional limit for cold-worked reinforcing steel is given in Eurocode 4: Part 1.2 as 0.94 f_{sk}, but the stress reaches $1.0f_{sk}$ at strains well below 2%, and this stress may be used as the design value.

The area of reinforcement per metre width is 168 mm^2, and $f_{sk} = 460$ N/mm^2, so the tensile force is 77.3 kN/m. The depth of the concrete stress block (with $\gamma_c = 1.0$) is

$$x = \frac{77.3}{0.85 \times 25} = 3.6 \text{ mm}.$$

The lever arm is

$$z = 150 - 60 - 1.8 = 88.2 \text{ mm},$$

so that

$$M_{\text{Rd.f}} = 77.3 \times 0.088 = \mathbf{6.8\ kN\ m/m}. \tag{3.52}$$

This is less than half the required value (equation (3.50)), so the contribution from crack-control reinforcement at the supports is now considered, using data from Eurocode 4: Part 1.2.

From Section 3.4.5, $A_s \geqslant 320$ mm^2/m, so 8-mm bars at 150 mm spacing (336 mm^2/m) are provided with 20 mm of top cover, as shown in Fig. 3.12(a). The force per unit width, double the previous value, is 154 kN/m. The effective thickness of the slab is 120 mm. The variation of its design temperature θ_c with distance x above its notional lower surface is shown in Fig. 3.8(b). From this curve, the variation of the compressive strength of the concrete with x is determined, and is shown, as $f_{c\theta}/f_{ck}$, in Fig. 3.8(b).

The mean compressive strength over the bottom 13 mm of the effective slab is $0.61 \times 25 = 15.2$ N/mm^2. This provides a compressive force

$$F_c = 0.85 \times 15.2 \times 13 = 168 \text{ kN/m} \tag{3.53}$$

which exceeds the force in the top reinforcement. The lever arm (Fig. 3.12) is 89 mm, so the hogging moment of resistance is

$$M_{\text{Rd.f}} = 154 \times 0.089 = \mathbf{13.7\ kN\ m/m} \tag{3.54}$$

Rigid-plastic global analysis (plastic hinge analysis) may be used for checking the resistance of continuous slabs in fire. The sum of the sagging and hogging resistances here, from results (3.52) and (3.54) is 20.5 kN m/m, which exceeds the '$wL^2/8$' moment given in equation (3.50). A separate calculation would be required for an end span.

The top reinforcement used here (T8 bars at 150 mm) also serves as transverse reinforcement for the concrete flange of each composite beam (Section 3.6.3.2) as well as crack-control reinforcement. This design could

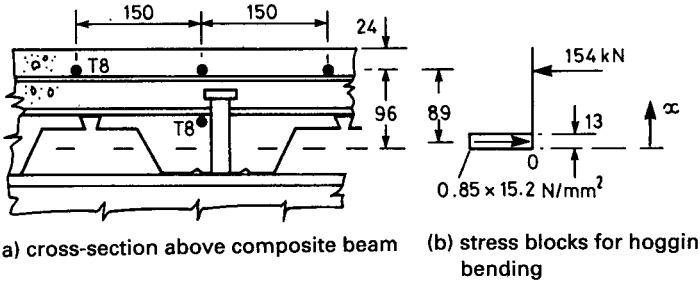

Fig. 3.12 Composite slab – design for fire.

thus be cheaper overall than the provision of thermal insulation below the sheeting.

3.5 Composite beams – sagging bending and vertical shear

Composite beams in buildings are usually supported by connections to steel or composite columns. The cheapest connections have little flexural strength, so it is convenient to design the beams as simply-supported. Such beams have the following advantages over beams designed as continuous at supports:

- very little of the steel web is in compression, and the steel top flange is restrained by the slab, so the resistance of the beam is not limited by buckling of steel;
- webs are less highly stressed, so it is easier to provide holes in them for the passage of services;
- bending moments and vertical shear forces are statically determinate, and are not influenced by cracking, creep, or shrinkage of concrete;
- there is no interaction between the behaviour of adjacent spans;
- bending moments in columns are lower, provided that the frame is braced against sidesway;
- no concrete at the top of the slab is in tension, except over supports;
- global analyses are simpler, and design is quicker.

The behaviour and design of midspan regions of continuous beams are similar to those of simply-supported beams, considered in this chapter. The other aspects of continuous beams are treated in Chapter 4.

3.5.1 Effective cross-section

The presence of profiled steel sheeting in a slab is normally ignored when the slab is considered as part of the top flange of a composite beam. Longitudinal shear in the slab (explained in Section 1.6) causes shear strain in its plane, with the result that vertical cross-sections through the composite T-beam do not remain plane, when it is loaded. At a cross-section, the mean longitudinal bending stress through the thickness of the slab varies as sketched in Fig. 3.13.

Simple bending theory can still give the correct value of the maximum stress (at point D) if the true flange breadth B is replaced by an effective breadth, b, such that the area GHJK equals the area ACDEF. Research based on elastic theory has shown that the ratio b/B depends in a complex way on the ratio of B to the span L, the type of loading, the boundary conditions at the supports, and other variables.

For beams in buildings, it is usually accurate enough to assume that the

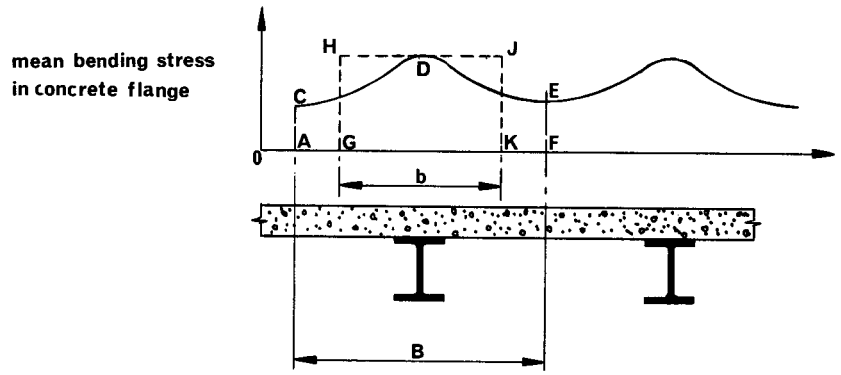

Fig. 3.13 Use of effective width to allow for shear lag.

effective width is $l_o/8$ on each side of the steel web, where l_o is the distance between points of zero bending moment. For a simply-supported beam, this is equal to the span, L, so that

$$b_{\text{eff}} = \frac{L}{4} \tag{3.55}$$

provided that a width of slab $L/8$ is present on each side of the web.

Where profiled sheeting spans at right angles to the span of the beam (as in the worked example here), only the concrete above its ribs can resist longitudinal compression (e.g. its effective thickness in Fig. 3.9 is 80 mm). Where ribs run parallel to the span of the beam, the concrete within ribs can be included, though it is rarely necessary to do so.

Longitudinal reinforcement within the slab is usually neglected in regions of sagging bending.

3.5.2 Classification of steel elements in compression

Because of local buckling, the ability of a steel flange or web to resist compression depends on its slenderness, represented by its breadth/thickness ratio. In design to Eurocode 4, as in Eurocode 3, each flange or web in compression is placed in one of four classes. The highest (least slender) class is Class 1 (plastic). The class of a cross-section of a composite beam is the lower of the classes of its web and compression flange, and this class determines the design procedures that are available.

This well-established system is summarised in Table 3.1. The Eurocodes allow several methods of plastic global analysis, of which rigid-plastic analysis (plastic hinge analysis) is the simplest. This is considered further in Section 4.3.3.

The Eurocodes give several idealised stress–strain curves for use in plastic section analysis, of which only the simplest (rectangular stress blocks) are used in this volume.

Table 3.1 Classification of sections, and methods of analysis.

Slenderness class and name	*1 plastic*	*2 compact*	*3 semi-compact*	*4 slender*
Method of global analysis	*plastic*[4]	*elastic*	*elastic*	*elastic*
Analysis of cross-sections	*plastic*[4]	*plastic*[4]	*elastic*[1]	*elastic*[2]
Maximum ratio c/t for flanges of rolled I-sections:[3]				
uncased web	8.14	8.95	12.2	no limit
encased web	8.14	12.2	17.1	no limit

Notes: (1) hole-in-the-web method enables plastic analysis to be used;
(2) with reduced effective width or yield strength;
(3) for Grade 50 steel (f_y = 355 N/mm^2); c is half the width of a flange of thickness t;
(4) elastic analysis may be used, but is more conservative.

The class boundaries are defined by limiting slenderness ratios that are proportional to $(f_y)^{-0.5}$, where f_y is the nominal yield strength of the steel. This allows for the influence of yielding on loss of resistance during buckling. The ratios in Eurocode 4: Part 1.1 for steel with f_y = 355 N/mm^2 are given in Table 3.1 for uniformly compressed flanges of rolled I-sections, of overall width $2c$.

Encasement of webs in concrete, illlustrated in Fig. 3.31, is done primarily to improve resistance to fire (Section 3.10). It also prevents rotation of a flange towards the web, which occurs during local buckling, and so enables higher c/t ratios to be used at the class 2/3 and 3/4 boundaries, as shown. At the higher compressive strains that are relied on in plastic hinge analysis, the encasement is weakened by crushing of concrete, so the c/t ratio at the class 1/2 boundary is unchanged.

The class of a steel web is strongly influenced by the proportion of its clear depth, d, that is in compression, as shown in Fig. 3.14. For the class 1/2 and 2/3 boundaries, plastic stress blocks are used, and the limiting d/t ratios are given in Eurocodes 3 and 4 as functions of α, defined in Fig. 3.14. The curves show, for example, that a web with $d/t = 40$ moves from Class 1 to Class 3 when α increases from 0.7 to 0.8. This high rate of change is significant in the design of continuous beams (Section 4.2.1).

For the class 3/4 boundary, elastic stress distributions are used, defined by the ratio ψ. Pure bending (no net axial force) corresponds to $\alpha = 0.5$, but to $\psi = -1$. The elastic neutral axis is normally higher, in a composite T-beam, than the plastic neutral axis, and its positions for propped and unpropped construction are different, so the curve for the class 3/4 boundary is not comparable with the others in Fig.3.14.

For simply-supported composite beams, the steel compression flange is restrained from local buckling (and also from lateral buckling) by its

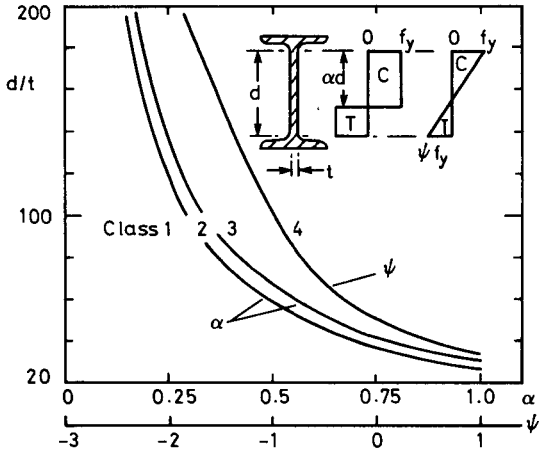

Fig. 3.14 Classification of webs, for $f_y = 355$ N/mm^2.

connection to the concrete slab, and so is in Class 1. The plastic neutral axis for full interaction is usually within the slab or steel top flange, so the web is not in compression, when flexural failure occurs, unless partial shear connection (Section 3.5.3.1) is used. Even then, α is sufficiently small for the web to be in Class 1 or 2. (This may not be so for the much deeper plate or box girders used in bridges.)

During construction of a composite beam, the steel beam alone may be in a lower slenderness class than the completed composite beam, and may be susceptible to lateral buckling. Design for this situation is governed by a code for steel structures (e.g. Eurocode 3).

3.5.3 Resistance to sagging bending

3.5.3.1 Cross-sections in Class 1 or 2

The methods of calculation for sections in Class 1 or 2 are in principle the same as those for composite slabs, explained in Section 3.3.1, to which reference should be made. The main assumptions are as follows:

- the tensile strength of concrete is neglected;
- plane cross-sections of the structural steel and reinforced concrete parts of a composite section each remain plane;

and, for plastic analysis of sections only:

- the effective area of the structural steel member is stressed to its design yield strength f_y/γ_a in tension or compression;
- the effective area of concrete in compression resists a stress of $0.85f_{ck}/\gamma_c$

constant over the whole depth between the plastic neutral axis and the most compressed fibre of the concrete.

In deriving the formulae below, it is assumed that the steel member is a rolled I-section, of cross-sectional area A_a, and the slab is composite, with profiled sheeting that spans between adjacent steel members. The composite section is in Class 1 or 2, so that the whole of the design load can be assumed to be resisted by the composite member, whether the construction was propped or unpropped. This is because the inelastic behaviour that precedes flexural failure allows internal redistribution of stresses to occur.

The effective section is shown in Fig. 3.15(a). As for composite slabs, there are three common situations, as follows. The first two occur only where full shear connection is provided.

(1) Neutral axis within the concrete slab

The stress blocks are shown in Fig. 3.15(b). The depth x, assumed to be the position of the plastic neutral axis, is found by resolving longitudinally:

$$N_{cf} = \frac{A_a f_y}{\gamma_a} = b_{eff} x \frac{0.85 f_{ck}}{\gamma_c}. \tag{3.56}$$

This method is valid when

$$x \leqslant h_c.$$

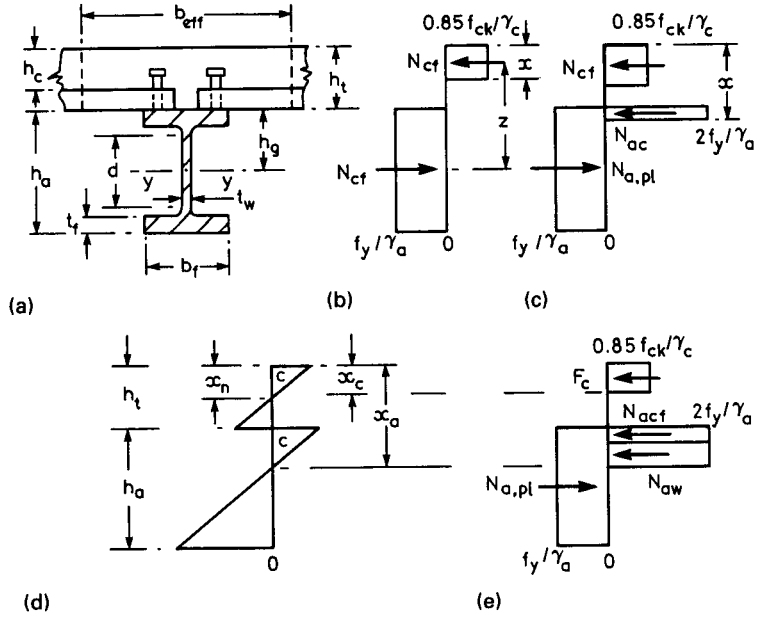

Fig. 3.15 Resistance to sagging bending of composite section in Class 1 or 2.

Taking moments about the line of action of the force in the slab,

$$M_{\text{pl.Rd}} = \frac{A_a f_y}{\gamma_a}\left(h_g + h_t - \frac{x}{2}\right) \tag{3.57}$$

where h_g defines the position of the centre of area of the steel section, which need not be symmetrical about its major (y–y) axis.

(2) Neutral axis within the steel top flange
The force N_{cf}, given by

$$N_{cf} = b_{\text{eff}} h_c \frac{0.85 f_{ck}}{\gamma_c} \tag{3.58}$$

is now less than the yield force for the steel section, denoted by

$$N_{a.pl} = \frac{A_a f_y}{\gamma_a}, \tag{3.59}$$

so the neutral axis is at a depth $x > h_t$, and is assumed to lie within the steel top flange (Fig. 3.15(c)). The condition for this is

$$N_{a.pl} - N_{cf} \leqslant 2 b_f t_f \frac{f_y}{\gamma_a}. \tag{3.60}$$

The distance x is most easily calculated by assuming that the strength of the steel in compression is $2f_y/\gamma_a$, so that the force $N_{a.pl}$ and its line of action can be left unchanged. Resolving longitudinally to determine x:

$$N_{a.pl} = N_{cf} + N_{ac} = N_{cf} + 2 b_f (x - h_t) \frac{f_y}{\gamma_a}. \tag{3.61}$$

Taking moments about the line of action of the force in the slab,

$$M_{\text{pl.Rd}} = N_{a.pl}\left(h_g + h_t - \frac{h_c}{2}\right) - N_{ac} \frac{x - h_c + h_t}{2}. \tag{3.62}$$

If x is found to exceed $h_t + t_f$, the plastic neutral axis lies within the steel web, and $M_{\text{pl.Rd}}$ can be found by a similar method.

(3) Partial shear connection
The symbol N_{cf} was used in paragraphs (1) and (2) above for consistency with the treatment of composite slabs in Eurocode 4 and in Section 3.3.1. In design, its value is always the lesser of the two values given by equations (3.56) and (3.58). It is the force which the shear connectors between the section of maximum sagging moment and each free end of the beam (a 'shear span') must be designed to resist, if full shear connection is to be provided. In draft Eurocode 4: Part 1.1 [12] the symbol used in the clause on partial shear connection in beams is F_{cf}, so in this explanation it is used in place of N_{cf}.

Let us suppose that the shear connection is designed to resist a force F_c, smaller than F_{cf}. If each connector has the same resistance to shear, and the number in each shear span is N, then the degree of shear connection is defined by:

$$\textit{degree of shear connection} = \frac{N}{N_f} = \frac{F_c}{F_{cf}} \tag{3.63}$$

where N_f is the number of connectors required for full shear connection.

The plastic moment of resistance of a composite slab with partial shear connection had to be derived in Section 3.3.1(3) by an empirical method, because the flexural properties of profiled sheeting are so complex. For composite beams, simple plastic theory can be used.

The depth of the compressive stress block in the slab, x_c, is given by

$$x_c = \frac{F_c}{0.85 b_{eff} \dfrac{f_{ck}}{\gamma_c}} \tag{3.64}$$

and is always less than h_c. The distribution of longitudinal strain in the cross-section is intermediate between the two distributions shown (for stress) in Fig. 2.2(c), and is shown in Fig. 3.15(d), in which C means compressive strain. The neutral axis in the slab is at a depth x_n greater than x_c, as shown.

In design of reinforced concrete beams and slabs it is generally assumed that x_c/x_n is between 0.8 and 0.9. The less accurate assumption $x_c = x_n$ is made for composite beams and slabs to avoid the complexity that otherwise occurs in design when $x_c \approx h_c$ or, for beams with non-composite slabs, $x_c \approx h_t$. This introduces an error in M_{pl} that is on the unsafe side, but is negligible for composite beams. It is not negligible for composite columns, where it is allowed for (Section 5.6.5.1).

There is a second neutral axis within the steel I-section. If it lies within the steel top flange, the stress blocks are as shown in Fig. 3.15(c), except that the block for the force N_{cf} is replaced by a shallower one, for force F_c. By analogy with equation (3.62) the resistance moment is

$$M_{Rd} = N_{a.pl}\left(h_g + h_t - \frac{x_c}{2}\right) - F_c \frac{x_a - x_c + h_t}{2}. \tag{3.65}$$

If the second neutral axis lies within the steel web, the stress blocks are as shown in Fig. 3.15(e). Taking moments about the top surface of the slab, the resistance moment is

$$M_{Rd} = N_{a.pl}(h_g + h_t) - \frac{F_c x_c}{2} - N_{acf}\left(h_t + \frac{t_f}{2}\right) - N_{aw}\frac{x_a + h_t + t_f}{2}, \tag{3.66}$$

where

$$N_{acf} = 2b_f t_f \frac{f_y}{\gamma_a},$$

and

$$N_{aw} = N_{a.pl} - F_c - N_{acf}.$$

Use of partial shear connection in design

The curve ABC in Fig. 3.16 shows a typical relationship between $M_{Rd}/M_{pl.Rd}$ and degree of shear connection F_c/F_{cf}, found by using the preceding equations for assumed values of F_c/F_{cf}. When F_c is taken as zero, then

$$M_{Rd} = M_{apl.Rd}$$

where $M_{apl.Rd}$ is the resistance of the steel section alone.

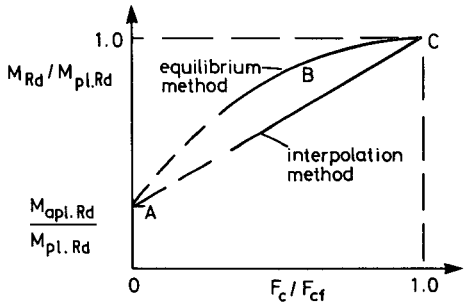

Fig. 3.16 Design methods for partial shear connection.

The curve is not valid for very low degrees of shear connection, for reasons explained in Section 3.6.2. Where it is valid, it is evident that a substantial saving in the cost of shear connectors can be obtained (e.g. by using $N/N_f = F_c/F_{cf} = 0.7$) when the required bending resistance M_{Sd} is only slightly below $M_{pl.Rd}$.

Where profiled sheeting is used, there is sometimes too little space in the troughs for N_f connectors to be provided within a shear span, and then partial-connection design becomes essential.

Unfortunately, curve ABC in Fig. 3.16 cannot be represented by a simple algebraic expression. In practice, it is therefore sometimes replaced (conservatively) by the line AC, given by

$$F_c = \left(\frac{M_{Sd} - M_{apl.Rd}}{M_{pl.Rd} - M_{apl.Rd}}\right) F_{cf}. \tag{3.67}$$

In design, M_{Sd} is known, and $M_{pl.Rd}$, $M_{apl.Rd}$ and F_{cf} are easily calculated, so this equation gives directly the design force F_c, and hence the number of connectors required in each shear span:

$$N = N_f \frac{F_c}{F_{cf}} = \frac{F_c}{P_{Rd}} \tag{3.68}$$

where P_{Rd} is the design resistance of one connector.

The design of shear connection is considered in greater depth in Section 3.6.

Variation in bending resistance along a span

In design, the bending resistance of a simply-supported beam is checked first at the section of maximum sagging moment, which is usually at midspan. For a steel beam of uniform section, the bending resistance is then obviously sufficient, elsewhere within the span; but this may not be so for a composite beam. Its bending resistance depends on the number of shear connectors between the nearer end support and the cross-section considered. This is shown by curve ABC in Fig. 3.16, because the x-coordinate is proportional to the number of connectors.

Suppose, for example, that a beam of span L is designed with partial shear connection and $N/N_f = 0.5$ at midspan. Curve ABC is redrawn in Fig. 3.17(a), with the bending resistance at midspan, $M_{Rd,max}$, denoted by B. If the connectors are uniformly spaced along the span, as is usual in buildings, then the axis N/N_f is also an axis x/L, where x is the distance from the nearer support, and N is the number of connectors effective in transferring the compression to the concrete slab over a length x from a free end. Only these connectors can contribute to the bending resistance $M_{Rd,x}$ at that section, denoted E in Fig. 3.17(b). In other words, bending failure at section E would be caused (in the design model) by longitudinal shear failure along length DE of the interface between the steel flange and the concrete slab.

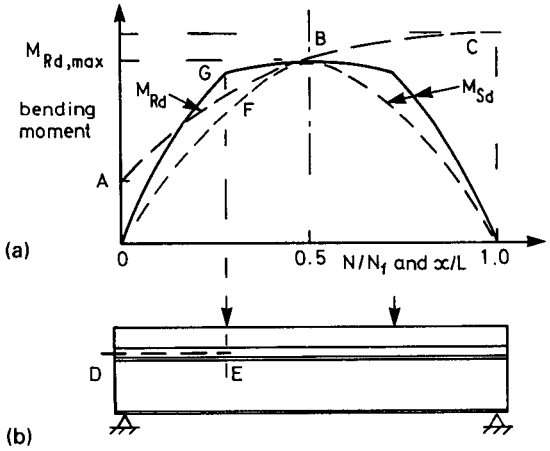

Fig. 3.17 Variation of bending resistance along a span.

Which section would in fact fail first depends on the shape of the bending-moment diagram for the loading. For uniformly-distributed loading, the curve for $M_{Sd,x}$ is parabolic, and curve 0FB in Fig. 3.17(a) shows that failure would occur at or near midspan. The addition of significant point loads (e.g. from small columns) at the quarter-span points changes the curve from 0FB to 0GB. Failure would occur near section E. A design in which M_{Sd} at midspan was equated to $M_{Rd,max}$ would be unsafe.

This is why design codes would not allow the $0.5N_f$ connectors to be spaced uniformly along the half span, for this loading. The number required for section E would be calculated first, and spaced uniformly along DE. The remainder would be located between E and midspan, at wider spacing. Spacing of connectors is further discussed in Section 3.6.1.

3.5.3.2 Cross-sections in Class 3 or 4

The resistance to bending of a beam of semi-compact or slender section is governed usually by the maximum stress in the steel section, calculated by elastic theory. Account has to be taken of the method of construction (propped or unpropped) and of the creep of concrete. The resistance may be as low as $0.7M_{pl.Rd}$, so it is fortunate that in design, it is almost always possible to ensure that sections in sagging bending are in Class 1 or 2. This is more difficult for hogging bending, as explained in Section 4.2.1.

3.5.4 Resistance to vertical shear

In a simply-supported steel beam, bending stresses near a support are within the elastic range even when the design ultimate load is applied; but in a composite beam, maximum slip occurs at end supports, so bending stresses found by simple elastic theory, based on plane sections remaining plane, may be unreliable.

Vertical shear stresses are calculated from rates of change ($d\sigma/dx$) of bending stresses σ, and so cannot easily be found near an end of a composite beam. It has been shown in tests[37] that some of the vertical shear is resisted by the concrete slab, but there is no simple design model for this, as the contribution from the slab is influenced by whether it is continuous across the end support, by how much it is cracked, and by local details of the shear connection.

It is therefore assumed in practice that vertical shear is resisted by the steel beam alone, exactly as if it were not composite. The web thickness of most rolled steel I-sections is sufficient to avoid buckling in shear, and then design is simple. The shear area A_v for such a section is given in Eurocode 3[11] as

$$A_v = 1.04\, h_a t_w, \tag{3.69}$$

with notation as in Fig. 3.15(a). The shear resistance is calculated by

assuming that the yield strength in shear is $f_y/\sqrt{3}$ (von Mises yield criterion), and that the whole of area A_v can reach this stress:

$$V_{pl.Rd} = A_v \frac{f_y/\sqrt{3}}{\gamma_a}. \tag{3.70}$$

This is thus a 'rectangular stress block' plastic model, based essentially on test data.

The maximum slenderness of an unstiffened web for which shear buckling can be neglected is given in Eurocode 4 as

$$\frac{d}{t_w} \leqslant 69\epsilon$$

if the web is not encased in concrete, and

$$\frac{d}{t_w} \leqslant 124\epsilon \tag{3.71}$$

if it is encased, with appropriate reinforcement. The dimensions d and t_w are shown in Fig 3.15(a), and

$$\epsilon = \left(\frac{235}{f_y}\right)^{1/2} \tag{3.72}$$

with f_y in N/mm^2 units. This allows for the influence of yielding on shear buckling.

Design based on shear buckling is more common in bridges than in buildings, so it is treated in Volume 2.

Interaction between bending and shear can influence the design of continuous beams, and is treated in Section 4.2.2.

3.6 Composite beams – longitudinal shear

3.6.1 Critical lengths and cross-sections

It will be shown in Section 3.7 that the bending moment at which yielding of steel first occurs in a simply-supported composite beam can be below 70% of the ultimate moment. If the bending-moment diagram is parabolic, then at ultimate load partial yielding of the steel beam can extend over more than half of the span.

At the interface between steel and concrete, the distribution of longitudinal shear is influenced by yielding, and also by the spacing of the connectors, their load/slip properties, and shrinkage and creep of the concrete slab. For these reasons, no attempt is made in design to calculate this distribution. Wherever possible, connectors are uniformly spaced along the span.

It was shown in Section 3.5.3 that this cannot always be done. For beams with all critical sections in Class 1 or 2, uniform spacing is allowed by Eurocode 4 along each *critical length*, which is a length of the interface between two adjacent *critical cross-sections*. These are defined as

- sections of maximum bending moment,
- supports,
- sections subjected to heavy concentrated loads,
- places where there is a sudden change of cross-section of the beam, and
- free ends of cantilevers.

There is also a definition for tapering members.

Where the loading is uniformly-distributed, a typical design procedure, for half the span of a beam, whether simply-supported or continuous, would be as follows.

(1) Determine the compressive force required in the concrete slab at the section of maximum sagging moment, as explained in Section 3.5.3. Let this be F_c.
(2) Determine the tensile force in the concrete slab at the support that is assumed to contribute to the bending resistance at that section (i.e. zero for a simple support, even if crack-control reinforcement is present; and the yield force in the longitudinal reinforcement, if the span is designed as continuous). Let this force be F_t.
(3) If there is a critical cross-section between these two sections, determine the force in the slab at that section. The bending moment will usually be below the yield moment, so elastic analysis of the section can be used.
(4) Choose the type of connector to be used, and determine its design resistance to shear, P_{Rd}, as explained in Section 2.5.
(5) The number of connectors required for the half span is

$$N = \frac{F_c + F_t}{P_{Rd}} . \tag{3.73}$$

The number required within a critical length where the change in longitudinal force is ΔF is $\Delta F/P_{Rd}$.

An alternative to the method of step (3) would be to use the shear force diagram for the half span considered. Such a diagram is shown in Fig. 3.18 for the length ABC of a span AD, which is continuous at A and has a heavy point load at B. The critical sections are A, B, and C. The total number of connectors is shared between lengths AB and BC in proportion to the areas of the shear force diagram, OEFH and GJH.

In practice it might be necessary to provide a few extra connectors along BC, because codes limit the maximum spacing of connectors, to prevent

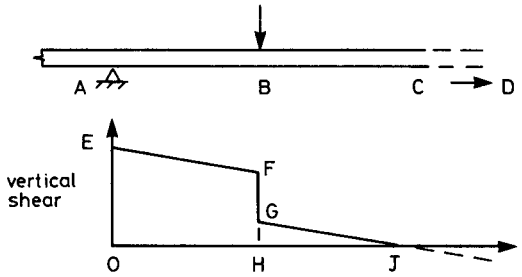

Fig. 3.18 Vertical shear in beam with off-centre point load.

uplift of the slab relative to the steel beam, and to ensure that the steel top flange is sufficiently restrained from local and lateral buckling.

3.6.2 Ductile and non-ductile connectors

The use of uniform spacing is possible because all connectors have some ductility, or *slip capacity*. This term has no standard definition, but is typically assumed to be the maximum slip at which a connector can resist 90% of its characteristic shear resistance, as defined by the falling branch of a load-slip curve obtained in a standard push test.

The slip capacity of headed stud connectors increases with the diameter of the shank, and has been found to be about 6 mm for 19-mm studs in solid concrete slabs.[38] Higher values are found in tests with single studs placed centrally within the troughs of profiled steel sheeting.

Slip enables longitudinal shear to be redistributed between the connectors in a critical length, before any of them fail. The slip required for this purpose increases at low degrees of shear connection, and as the critical length increases (a scale effect). A connector that is 'ductile' (has sufficient slip capacity) for a short span becomes 'non-ductile' in a long span, for which a more conservative design method must be used.

The definitions of 'ductile' connectors given in Eurocode 4 for headed studs welded to a steel beam with equal flanges are shown in Fig. 3.19. The more liberal definition, for use where the slab is composite, is subject to several restrictions, based on the limited scope of current research data on slip capacity.

Most other types of connector are treated in Eurocode 4 as 'non-ductile' for all spans, because until recently few push tests were continued beyond maximum load, which was usually reached at a slip of less than 3 mm, so that slip capacity was not determined. The push test specified in British codes since 1965 is, in any case, unsuitable for this purpose, because the reinforcement in the slabs is insufficient to prevent longitudinal splitting (Section 2.5).

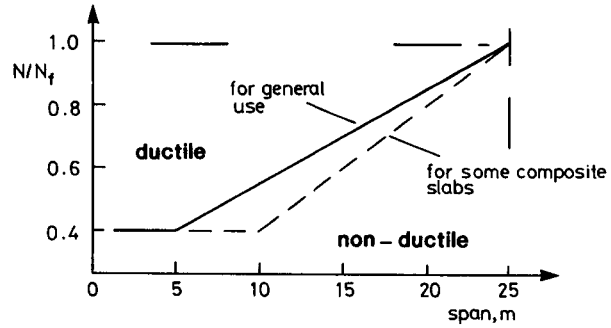

Fig. 3.19 Definition of 'ductile' for welded studs and some other connectors, for steel sections with equal flanges.

Where non-ductile connectors are used, design for full shear connection is the same (in Eurocode 4) as for ductile connectors, but for $N/N_f < 1$, the two methods shown in Fig. 3.16 are replaced by methods that require higher ratios N/N_f for a given value of $M_{Sd}/M_{pl.Rd}$. These are approximations to elastic behaviour, and so rely less on slip capacity. They are explained in Reference 15. There is also a rule in Eurocode 4 that limits the use of uniform spacing of non-ductile connectors.

3.6.3 Transverse reinforcement

The reinforcing bars shown in Fig. 3.20 are longitudinal reinforcement for the concrete slab, to enable it to span between the beam shown and those either side of it. They also enhance the resistance to longitudinal shear of vertical cross-sections such as B–B. Bars provided for that purpose are known as 'transverse reinforcement', as their direction is transverse to the axis of the composite beam. Like stirrups in the web of a reinforced concrete T-beam, they supplement the shear strength of the concrete, and their behaviour can be represented by a truss analogy.

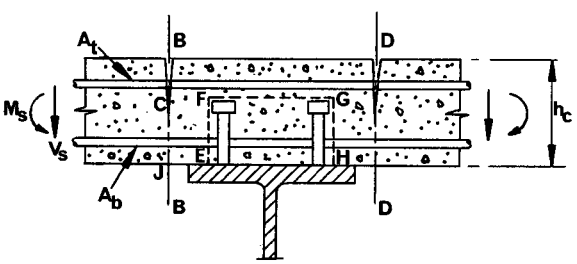

Fig. 3.20 Surfaces of potential failure in longitudinal shear.

The design rules for these bars are extensive, as account has to be taken of many types and arrangements of shear connectors, of haunches, of the use of precast or composite slabs, and of interaction between the longitudinal shear per unit length on the section considered, v_{Sd}, and the transverse bending moment, shown as M_s in Fig. 3.20. The loading on the slab also causes vertical shear stress on planes such as B–B; but this is usually so much less than the longitudinal shear stress v_{Sd}/A_{cv} on the plane, that it can be neglected.

The notation here is that of Eurocode 4: Part 1.1;[12] A_{cv} is the cross-sectional area per unit length of beam of the concrete shear surface being considered. The word 'surface' is used here because EFGH in Fig. 3.20, although not a plane, is another potential surface of shear failure. In practice, the rules for minimum height of shear connectors ensure that in slabs of uniform thickness, planes such as B–B are more critical; but this may not be so for haunched slabs, considered later.

The design longitudinal shear per unit length for surface EFGH is the same as that for the shear connection, and in a symmetrical T-beam half of that value is assumed to be transferred through each of planes B–B and D–D. For an L-beam or where the flange of the steel beam is wide (Fig. 3.21), the more accurate expressions should be used:

$$v_{BB} = \frac{vb_1}{b} \quad \text{and} \quad v_{DD} = \frac{vb_2}{b}$$

where v is the design shear for the shear connection and b is the effective width of the concrete flange.

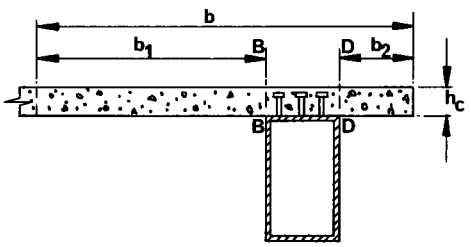

Fig. 3.21 T-beam with asymmetrical concrete flange.

Effective area of reinforcement

For planes such as B–B in Fig. 3.20, the effective area of transverse reinforcement per unit length of beam, A_e, is the whole of the reinforcement that is fully anchored on both sides of the plane (i.e. able to develop its yield strength in tension). This is so even where the top bars are fully stressed by the bending moment M_S, because this tension is balanced by

transverse compression, which enhances the shear resistance in the region CJ by an amount at least equivalent to the contribution the reinforcement would make, in absence of transverse bending.

Effective areas are treated in more detail in Volume 2.

3.6.3.1 Design rules for transverse reinforcement in solid slabs

Part of a composite beam is shown in plan in Fig. 3.22. The truss model for transverse reinforcement is illustrated by triangle ACE, in which CE represents the reinforcement for a unit length of the beam, A_e, and v is the design shear force per unit length. The force v, applied at some point A, is transferred by concrete struts AC and AE, at 45° to the axis of the beam. The strut force at C is balanced by compression in the slab and tension in the reinforcement. The model fails when the reinforcement yields. The tensile force in it is equal to the shear on a plane such as B–B caused by the force v, so the model gives a design equation of the form

$$\frac{v}{2} = v_{Rd} = A_{cv}\, f\left(\frac{f_{ck}}{\gamma_c}\right) + \frac{A_e f_{sk}}{\gamma_s} \tag{3.74}$$

where the first term is the contribution from the strength of the concrete in shear.

This result is assumed to be valid whatever the length of the notional struts in the slab (e.g. FG), and relies to some extent on the shear flow v being fairly uniform within the shear span, because the reinforcement associated with the force v at A is in practice provided at cross-section A, not at some point between A and midspan. The type of cracking observed in tests where shear failure occurs, shown in Fig. 3.22, is consistent with the model.

The design equation in Eurocode 4: Part 1.1 is

$$v_{Rd} = 2.5\, A_{cv} \eta \tau_{Rd} + A_e \frac{f_{sk}}{\gamma_s}, \tag{3.75}$$

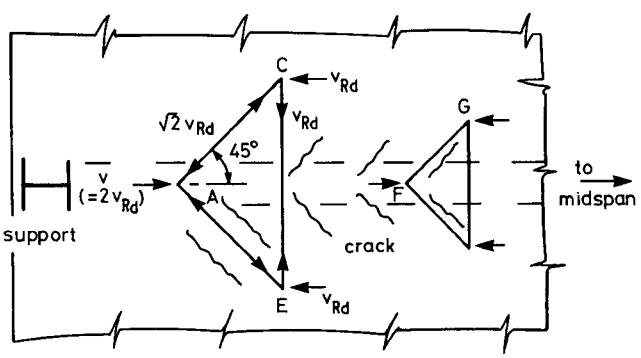

Fig. 3.22 Truss model for transverse reinforcement.

where

$$\tau_{Rd} = 0.25 \frac{f_{ctk0.05}}{\gamma_c} \tag{3.76}$$

and $f_{ctk0.05}$ is the characteristic tensile strength (lower 5% fractile) of the concrete. This strength, as given in Eurocodes 2 and 4, ranges from about $0.06\, f_{ck}$ for strong concrete to $0.07\, f_{ck}$ for weak concrete. The first term in equation (3.75) is thus approximately $0.04\, A_{cv}\eta f_{ck}/\gamma_c$.

The corresponding equation in the British code BS 5950[14] is (when $\gamma_c = 1.5$, $\gamma_s = 1.15$)

$$v_{Rd} = 0.045\, A_{cv}\eta \frac{f_{cu}}{\gamma_c} + 0.805 A_e \frac{f_{sk}}{\gamma_s}. \tag{3.77}$$

The cube strength f_{cu} is approximately $1.25\, f_{ck}$, so the British code assumes a higher contribution from the concrete and a lower one from the reinforcement, but is otherwise the same as that of Eurocode 4. The rules have been checked against test data, as far as possible, but these data cover only a few of the many situations that can occur.

The symbol η in equations (3.75) and (3.77) is a modification factor for lightweight-aggregate concrete. It allows for the reduction in the ratio E_c/f_{ck} as the unit weight of the concrete, ρ, is reduced below 24 kN/m^3, and is given in Eurocode 4 by

$$\eta = 0.3 + 0.7 \frac{\rho}{24}. \tag{3.78}$$

The British code[14] gives $\eta = 0.8$ for all lightweight-aggregate concretes with $\rho \geq 17.2$ kN/m^3. This agrees closely with Eurocode 4 when $\rho = 17.2$ kN/m^3.

Limits to the use of equation (3.75)

As with stirrups in reinforced concrete beams, an upper limit to the validity of the model of Fig. 3.22 is set, as the area A_e is increased, by the crushing strength of the concrete in the diagonal struts. The limit is given in Eurocode 4 as

$$v_{Rd} \leq 0.2\, A_{cv}\eta \frac{f_{ck}}{\gamma_c}. \tag{3.79}$$

The expression was copied from the rule in Eurocode 2: Part 1.1[10] for a similar situation, for consistency. It corresponds to $A_e \leq 0.85\%$ when $f_{ck} = 32$ N/mm^2, $f_{sk} = 460$ N/mm^2, and $\eta = 1$.

The compressive stress in the concrete struts when the limit of equation (3.79) is reached can be estimated as follows. For unit length of beam, the strut is $1/\sqrt{2}$ wide and A_{cv} deep. The force in it is $\sqrt{2}v_{Rd}$, so the compressive stress is limited by equation (3.79) to $0.4\, \eta f_{ck}/\gamma_c$, which appears to be rather conservative.

The corresponding limit in the British code[14] was deduced from a

study[39] of test data for composite beams, not on a method for reinforced concrete T-beams. It is:

$$v_{Rd} \leqslant 0.8\, A_{cv}\eta(f_{cu})^{1/2}. \tag{3.80}$$

This is over 30% higher than the Eurocode limit when $f_{ck} = 25$ N/mm^2, and about the same at $f_{ck} = 45$ N/mm^2.

A minimum area for transverse reinforcement, irrespective of the longitudinal shear, is specified in Eurocode 4, as 0.002 times the effective area of the concrete slab. This empirical rule provides some protection against fracture or excessive local strain of the reinforcement when cracks first occur. It is suggested that the area of slab assumed to be effective should be the area used for the calculation of A_{cv} in equation (3.75), which may include concrete within ribs where the sheeting spans transversely.

Haunched slabs

Further design rules are required for the transverse reinforcement in haunches of the type shown in Fig. 2.1(b). These are more common in bridges than in buildings, so the subject is covered in Volume 2. Haunches encased in thin steel sheeting are considered below.

3.6.3.2 Transverse reinforcement in composite slabs

Where profiled sheeting spans in the direction transverse to the span of the beam, as shown in Fig. 3.15(a), it can be assumed to be effective as bottom transverse reinforcement where the sheets are continuous over the beam. Where they are not, as in the figure, the effective area of sheeting depends on how the ends of the sheets are attached to the steel top flange.

Where studs are welded to the flange through the sheeting, resistance to transverse tension is governed by local yielding of the thin sheeting around the stud. The design bearing resistance of a stud with a weld collar of diameter d_{do} in sheeting of thickness t is given in Eurocode 4 as

$$P_{pb.Rd} = k_\phi d_{do} t \frac{f_{yp}}{\gamma_{ap}} \tag{3.81}$$

where

$$k_\phi = 1 + \frac{a}{d_{do}}, \leqslant 4.0,$$

f_{yp} is the yield strength of the sheeting, and dimension a is shown in Fig. 3.23. The formula corresponds to the assumption that yielding of the sheet occurs in direct tension along BC and in shear, at stress $f_{yp}/2$, along AB and CD. For studs at longitudinal spacing s, the contribution to v_{Rd} (equation (3.75)) is

$$v_{pd} = \frac{P_{pb.Rd}}{s}. \tag{3.82}$$

This contribution is significant in practice where conventional studs are

used: but small-diameter shot-fired pins are less effective, because of the limit $k\phi \leqslant 4$.

Where the span of the sheeting is parallel to that of the beam, transverse tension causes the corrugations to open out, so v_{pd} is taken as zero.

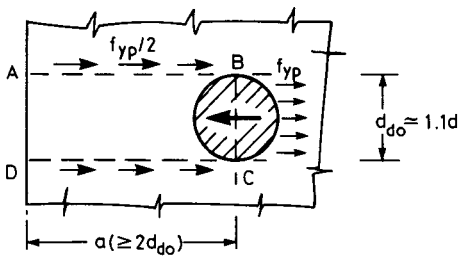

Fig. 3.23 Bearing resistance of profiled sheeting.

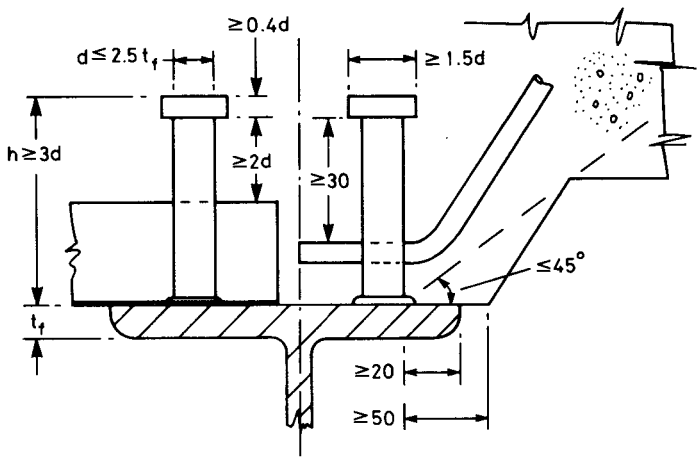

Fig. 3.24 Detailing rules for shear connection.

3.6.4 Detailing rules

Where shear connectors are attached to a steel flange, there will be transverse reinforcement, and there may be a haunch (local thickening of the slab, as in Fig. 2.1(b)) or profiled steel sheeting. No reliable models exist for the three-dimensional state of stress in such a region, even in the elastic range, so the details of the design are governed by arbitrary rules of proportion, based essentially on experience.

Several of the rules given in Eurocode 4: Part 1.1 are shown in Fig. 3.24. The left-hand half shows profiled sheeting that spans transversely, and the right-hand half shows a haunch.

The minimum dimensions for the head of a stud, the rule $h \geqslant 3d$, and the 30-mm projection above bottom reinforcement, are to ensure sufficient resistance to uplift.

The rule $d \leqslant 2.5t_f$ is to avoid local failure of the steel flange, caused by load from the connector. For repeated (fatigue) loading, a lower limit to d/t_f is specified (Volume 2).

The 50-mm side cover to a connector and the $\leqslant 45°$ rule are to prevent local bursting or crushing of the concrete at the base of the connector; and the 20-mm dimension to the flange tip is to avoid local overstress of the flange and to protect the connector from corrosion.

The minimum centre-to-centre spacing of stud connectors of diameter d is $5d$ in the longitudinal direction, $2.5d$ across the width of a steel flange in solid slabs, and $4d$ in composite slabs. These rules are to enable concrete to be properly compacted, and to avoid local overstress of the slab.

The maximum longitudinal spacing of connectors is normally limited to the lesser of 800 mm and six times the total slab thickness, because the transfer of shear is assumed in design to be continuous along the span, and also to avoid excessive uplift.

There are corresponding rules for connectors other than studs. All such rules relevant to stresses should in principle give ratios of dimensions; where actual dimensions are given, there may be an implied assumption (e.g. that studs are between 16 mm and 22 mm in diameter), or it may be that corrosion or crack widths are relevant.

3.7 Stresses and deflections in service

A composite beam is usually designed first for ultimate limit states. Its behaviour in service must then be checked. For a simply-supported beam, the most critical serviceability limit state is usually excessive deflection, which can govern the design where unpropped construction is used. Floor structures subjected to dynamic loading (e.g. as in a gymnasium) are also susceptible to excessive vibration (Section 3.11.3.2).

Cracking of concrete is a problem only in fully-encased beams, which are rarely used, and in hogging regions of continuous beams (Section 4.2.5).

Some codes of practice limit stresses in service; but excessive stress is not itself a limit state. It may however invalidate a method of analysis (e.g. linear-elastic theory) that would otherwise be suitable for checking compliance with a serviceability criterion. No stress limits are specified in Eurocode 4: Part 1.1. The policy is to use elastic analysis, allowing for shear lag and creep; and to modify the results, where necessary, to allow for yielding of steel and, where partial shear connection is used, for excessive slip.

If yielding of structural steel occurs in service, in a typical composite

beam for a building, it will be in the bottom flange, near midspan. The likelihood of this depends on the ratio between the characteristic variable and permanent loads, given by

$$r = \frac{q_k}{g_k},$$

on the partial safety factors used for both actions and materials, on the method of construction used, and on the shape factor for the composite section. This factor is given by

$$Z = \frac{M_{pl}}{M_y}$$

where M_y is the bending moment at which yield of steel first occurs. For sagging bending, it is typically between 1.25 and 1.35 for propped construction, but can rise to 1.45 or above, for unpropped construction.

Deflections are usually checked for the rare combination of actions, given in equation (1.8). So for a beam designed for distributed loads g_k and q_k only, the ratio of design bending moments (ultimate/serviceability) is

$$\mu = \frac{1.35g + 1.5q}{g + q} = \frac{1.35 + 1.5r}{1 + r}. \tag{3.83}$$

This ratio ranges from 1.42 at $r = 0.8$ to 1.44 at $r = 1.6$.

For this comparison, it can be assumed that

$$M_{pl.Rd} \simeq \frac{M_{pl}}{\gamma_a},$$

and from these expressions, the stress in steel in service will reach or exceed the yield stress if

$$Z > \gamma_a \mu.$$

The values given above show that this is unlikely for propped construction, but might occur for unpropped construction when γ_a for structural steel is assumed to be 1.05 or less, rather than 1.10 as recommended in Eurocode 4.

Where the bending resistance of a composite section is governed by local buckling, as in a Class 3 section, elastic section analysis is used for ultimate limit states, and then stresses and/or deflections in service are less likely to influence design.

As shown below, elastic analysis of a composite section is more complex than plastic analysis, because account has to be taken of the method of construction and of the effects of creep. The following three types of loading then have to be considered separately:

- load carried by the steel beam,
- short-term load carried by the composite beam,
- long-term load carried by the composite beam.

3.7.1 Elastic analysis of composite sections in sagging bending

It is assumed first that full shear connection is provided, so that the effect of slip can be neglected. All other assumptions are as for the elastic analysis of reinforced concrete sections by the method of transformed sections. The algebra is different because the flexural rigidity of the steel section alone is so much greater than that of reinforcing bars.

For generality, the steel section is assumed to be asymmetrical (Fig. 3.25) with cross-sectional area A_a, second moment of area I_a, and centre of area distance z_g below the top surface of the concrete slab, which is of uniform overall thickness h_t and effective width b_{eff}.

The modular ratio for short-term loading is

$$n = \frac{E_a}{E_c}$$

where the subscripts a and c refer to structural steel and concrete, respectively. For long-term loading, a value $n/3$ is a good approximation. For simplicity, a single value $n/2$ is sometimes used for both types of loading. From here onwards, the symbol n is used for whatever modular ratio is appropriate, so it is defined by

$$n = \frac{E_a}{E_c'} \tag{3.84}$$

where E_c' is the relevant effective modulus for the concrete.

It is usual to neglect reinforcement in compression, concrete in tension, and also concrete between the ribs of profiled sheeting, even when the sheeting spans longitudinally. The condition for the neutral-axis depth x to be less than h_c is

$$A_a(z_g - h_c) < \frac{1}{2} b_{eff} \frac{h_c^2}{n}. \tag{3.85}$$

The neutral-axis depth is then given by the usual 'first moments of area' equation,

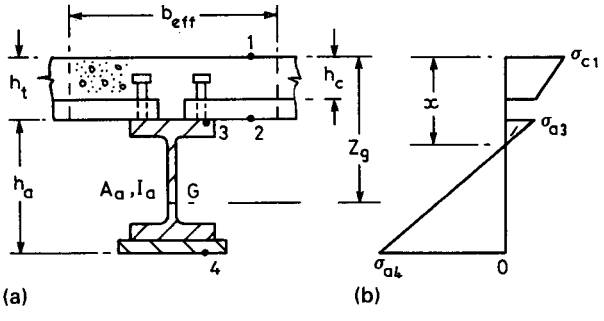

Fig. 3.25 Elastic analysis of composite beam section in sagging bending.

$$A_a(z_g - x) = \frac{1}{2} b_{eff} \frac{x^2}{n}, \tag{3.86}$$

and the second moment of area, in 'steel' units, by

$$I = I_a + A_a(z_g - x)^2 + b_{eff} \frac{x^3}{3n}. \tag{3.87}$$

If condition (3.85) is not satisfied, then the neutral-axis depth exceeds h_c, and is given by

$$A_a(z_g - x) = b_{eff} h_c \frac{x - h_c/2}{n}. \tag{3.88}$$

The second moment of area is

$$I = I_a + A_a(z_g - x)^2 + \frac{b_{eff} h_c}{n} \left[\frac{h_c^2}{12} + \left(x - \frac{h_c}{2} \right)^2 \right]. \tag{3.89}$$

In global analyses, it is sometimes convenient to use values of I based on the uncracked composite section. The values of x and I are then given by equations (3.88) and (3.89) above, whether x exceeds h_c or not. In sagging bending, the difference between the 'cracked' and 'uncracked' values of I is usually small.

Stresses due to a sagging bending moment M are normally calculated in concrete only at level 1 in Fig. 3.25, and in steel at levels 3 and 4. These stresses are, with tensile stress positive:

$$\sigma_{c1} = -\frac{Mx}{nI} \tag{3.90}$$

$$\sigma_{a3} = \frac{M(h_t - x)}{I} \tag{3.91}$$

$$\sigma_{a4} = \frac{M(h_a + h_t - x)}{I}. \tag{3.92}$$

Deflections

These are calculated by the well-known formulae from elastic theory, using Young's modulus for structural steel. For example, the deflection of a simply-supported composite beam of span L due to distributed load q per unit length is

$$\delta_c = \frac{5qL^4}{384E_aI}. \tag{3.93}$$

Where the shear connection is partial (i.e. $N/N_f < 1$), the increase in deflection due to longitudinal slip depends on the method of construction. The total deflection δ is given approximately in both Eurocode 4[12] and BS 5950[14] as

$$\delta = \delta_c \left[1 + k\left(1 - \frac{N}{N_f}\right)\left(\frac{\delta_a}{\delta_c} - 1\right)\right] \tag{3.94}$$

with $k = 0.5$ for propped construction
$k = 0.3$ for unpropped construction

where δ_a is the deflection for the steel beam acting alone. This expression is obviously correct when $N/N_f = 1$, and gives too low a result when $N/N_f = 0$. Its use is allowed where $N/N_f \geqslant 0.4$.

Eurocode 4, unlike BS 5950, allows this increase in deflection to be ignored in unpropped construction where:

- either $N/N_f \geqslant 0.5$ or the forces on the connectors do not exceed $0.7\,P_{Rk}$, where P_{Rk} is their characteristic resistance, and
- for slabs with transverse ribs, the height of the ribs does not exceed 80 mm.

The arbitrary nature of these rules underlines the difficulty of predicting deflections accurately.

3.7.2 The use of limiting span-to-depth ratios

Calculations using formulae like those derived above are not only long; they are also inaccurate. It is almost as much an art as a science to predict during design the long-term deflection of a beam in a building. It is possible to allow in calculations for some of the factors that influence deflection, such as creep and shrinkage of concrete; but there are others that cannot be quantified. In developing the limiting span/depth ratios for the British code CP 110, Beeby[40] identified nine reasons why deflections of reinforced concrete beams in service were usually less than those calculated by the designers, and increased his theoretical span/depth ratios by 36% to allow for them. Many of the reasons apply equally to composite beams, the most significant of them being the variations in the elasticity, shrinkage and creep properties of the concrete, the stiffening effect of finishes, and restraint and partial fixity at the supports.

The other problem is the difficulty of defining when a deflection becomes 'excessive'. In practice, complaints often arise from the cracking of plaster on partition walls, which can occur when the deflection of the supporting beam is as low as span/800.[40] For partitions and in-fill panels generally, the relevant deflection is that which takes place after their construction. This can exceed that due to the finishes and imposed load, for dead-load creep deflections continue to increase for several years after construction. It is good practice to provide partitions with appropriate joints and clearances. When this is not done the relevant deflection should not exceed span/350. Where appearance is the only criterion, it is recommended that the full-load deflection, including the effects of creep and shrinkage, of a

suspended span below the level of its supports should not exceed span/250; but for roof beams constructed to a fall, greater deflection may be acceptable. The difficulty of assessing the accuracy and significance of a calculated deflection is such that simplified methods of calculation are justified.

3.8 Effects of shrinkage of concrete and of temperature

In the fairly dry environment of a building, an unrestrained concrete slab could be expected to shrink by 0.03% of its length (3 mm in 10 m) or more. In a composite beam, the slab is restrained by the steel member, which exerts a tensile force on it, through the shear connectors near the free ends of the beam, so its apparent shrinkage is less than the 'free' shrinkage. The forces on the shear connectors act in the opposite direction to those due to the loads, and so can be neglected in design.

The stresses due to shrinkage develop slowly, and so are reduced by creep of the concrete, but the increase they cause in the deflection of a composite beam may be significant. An approximate and usually conservative rule of thumb for estimating this deflection in a simply supported beam is to take it as equal to the long-term deflection due to the weight of the concrete slab acting on the *composite* member.

In the beam studied in Section 3.11, this rule gives an additional deflection of 9 mm, whereas the calculated long-term deflection due to a shrinkage of 0.03% (with a modular ratio $n = 22$) is 10 mm.

In beams for buildings, it can usually be assumed that tabulated span/depth ratios are sufficiently conservative to allow for shrinkage deflections; but the designer should be alert for situations where the problem may be unusually severe (e.g. thick slabs on small steel beams, electrically heated floors, and concrete mixes with high 'free shrinkage').

It is recommended in Eurocode 4 that effects of shrinkage should be considered when the span/depth ratio of the beam exceeds 20 and the free shrinkage strain exceeds 0.04%. For dry environments, typical values of this strain are given as 0.0325% for normal-weight concrete and 0.05% for lightweight concrete.

Composite beams also deflect when the slab is colder than the steel member. Such differential temperatures rarely occur in buildings, but are important in beams for bridges. Methods of calculation for shrinkage and temperature effects are given in Volume 2.

3.9 Vibration of composite floor structures

In British Standard 6472, 'Evaluation of human exposure to vibration in buildings (1 Hz to 80 Hz)',[41] the performance of a floor structure is

considered to be satisfactory when the probability of annoyance to users of the floor, or of complaints from them about interference with activities, is low. There can be no simple specification of the dynamic properties that would make a floor structure 'serviceable' in this respect, because the local causes of vibration, the type of work done in the space concerned, and the psychology of its users are all relevant.

An excellent guide to this complex subject is available.[42] It and BS 6472 provided much of the basis for the following introduction to vibration design, which is limited to the situation in the design example – a typical floor of an office building, shown in Fig. 3.1.

Sources of vibration excitation

Vibration from external sources, such as highway or rail traffic, is rarely severe enough to influence design. If it is, the building should be isolated at foundation level.

Vibration from machinery in the building, such as lifts and travelling cranes, should be isolated at or near its source. In the design of a floor structure, it should be necessary to consider only sources of vibration on or near that floor. Near gymnasia or dance floors, the effects of rhythmic movement of groups of people can be troublesome; but in most buildings only two situations need be considered:

- people walking across a floor with a pace frequency between 1.4 Hz and 2.5 Hz; and
- an impulse, such as the effect of the fall of a heavy object.

Typical reactions on floors from people walking have been analysed by Fourier series. The basic fundamental component has an amplitude of about 240 N. The second and third harmonics are smaller, but are relevant to design. Fundamental natural frequencies of floor structures (f_0) often lie within the frequency range of third harmonics (4.2 Hz to 7.5 Hz). The number of cycles of this harmonic, as a person walks across the span of a floor, can be sufficient for the amplitude of forced vibration to approach its steady-state value. This situation will be considered in more detail later.

Pedestrian movement causes little vibration of floor structures with f_0 exceeding about 7 Hz, but these should be checked for the effect of an impulsive load. The consequences that most influence human reactions are the peak vertical velocity of the floor, which is proportional to the impulse, and the time for the vibration to decay, which increases with reduction in the damping ratio of the floor structure. Design guidance is available for this situation,[41,42] which is not further discussed here.

Human reaction to vibration

Models for human response to continuous vibration are given in BS 6472. For vibration of a floor that supports people who are standing or sitting,

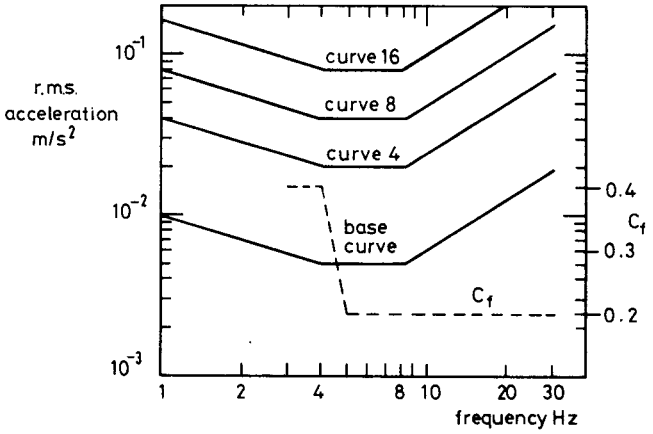

Fig. 3.26 Curves of constant human response to vibration, and Fourier component factor.

rather than lying down, the model consists of a base curve of root-mean-square (r.m.s.) acceleration against fundamental natural frequency of the floor, and higher curves of similar shape. These are shown in the double logarithmic plot of Fig. 3.26. Each curve represents an approximately uniform level of human response. The base curve, denoted by $R = 1$, where R is the response factor, corresponds to a 'minimal level of adverse comment from occupants' of sensitive locations such as hospital operating theatres and precision laboratories.

Curves for other values of R are obtained by multiplying the ordinates of the base curve of R. Those for $R = 4$, 8 and 16 are shown. The appropriate value of R for use in design depends on the environment. The British Standard gives:

$R = 4$ for offices,
$R = 8$ for workshops,

with the comment that use of double those values 'may result in adverse comment', which 'may increase significantly' if the magnitudes of vibration are quadrupled.

Some relaxation is possible if the vibration is not continuous. Wyatt[42] recommends that a floor subject to a person walking at resonant frequency once a minute could reasonably be permitted a response double the value acceptable for continuous oscillation.

3.9.1 Prediction of fundamental natural frequency

In composite floors that need checking for vibration, damping is sufficiently low for its influence on natural frequencies to be neglected. For free

elastic vibration of a beam or one-way slab of uniform section, the fundamental natural frequency is

$$f_0 = K\left(\frac{EI}{mL^4}\right)^{1/2} \tag{3.95}$$

where $K = \pi/2$ for simple supports, and
$K = 3.56$ for both ends fixed against rotation.

Values for other end conditions and multi-span members are given by Wyatt.[42] The relevant flexural rigidity is EI (per unit width, for slabs), L is the span, and m the vibrating mass per unit length (beams) or unit area (slabs). Concrete in slabs should normally be assumed to be uncracked, and the dynamic modulus of elasticity should be used for concrete, in both beams and slabs. This modulus, E_{cd}, is typically about 8 kN/mm^2 higher than the static modulus, for normal-density concrete, and 3 to 6 kN/mm^2 higher, for lightweight-aggregate concretes of density not less than 1800 kg/m^3. For composite beams in sagging bending, approximate allowance for these effects can be made by increasing the value of I for variable loading by 10%.

Unless a more accurate estimate can be made, the mass m is usually taken as the mass of the characteristic permanent load plus 10% of the characteristic variable load .

A convenient method of calculating f_0 is to find first the midspan deflection, δ_m say, caused by the weight of the mass m. For simply-supported members this is

$$\delta_m = \frac{5mgL^4}{384EI}.$$

Substitution for m in equation (3.95) gives

$$f_0 = \frac{17.8}{\sqrt{\delta_m}} \tag{3.96}$$

with δ_m in millimetres.

Equation (3.96) is useful for a beam or slab considered alone. But in a typical floor, with composite slabs continuous over a series of parallel composite beams, the total deflection (δ, say) is the sum of deflections δ_s, for the slab relative to the beams that support it, and δ_b, for the beams. A good estimate of the fundamental natural frequency is then given by

$$f_0 = \frac{17.8}{\sqrt{\delta}}. \tag{3.97}$$

It follows from equations (3.96) and (3.97) that

$$\frac{1}{f_0^2} = \frac{1}{f_{0s}^2} + \frac{1}{f_{0b}^2}, \tag{3.98}$$

where f_{0s} and f_{0b} are the frequencies for the slab and the beam, respectively, each considered alone. Equations (3.97) and (3.98) can be used also for members that are not simply-supported.

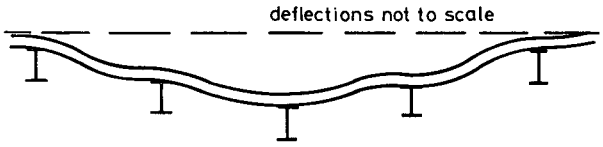

Fig. 3.27 Cross-section of vibrating floor structure showing typical fundamental mode.

For a single-span layout of the type shown in Fig. 3.1, each beam vibrates as if simply-supported, so the length L_{eff} of the vibrating area can be taken as the span, L. The width S of the vibrating area will be several times the beam spacing, s. A cross-section through this area is likely to be as shown in Fig. 3.27, with most spans of the composite slab vibrating as if fixed-ended. It follows from equation (3.95) that:

- for the beam, $$f_{0b} = \frac{\pi}{2}\left(\frac{EI_b}{msL^4}\right)^{1/2} \tag{3.99}$$
- for the slab, $$f_{0s} = 3.56\left(\frac{EI_s}{ms^4}\right)^{1/2} \tag{3.100}$$

where m is the vibrating mass per unit area, and s is the spacing of the beams, and subscripts b and s mean beam and slab, respectively.

3.9.2 Response of a composite floor to pedestrian traffic

It is assumed that the floor reaches its steady state of damped vibration under harmonic excitation from a person walking at between 1.4 Hz and 2 Hz, and that for the floor, $f_0 > 3$ Hz, to avoid resonance with the first harmonic, which has an amplitude of 240 N. The effective force amplitude is

$$\bar{F} = 240\,C_f \tag{3.101}$$

where C_f is the Fourier component factor. It takes account of the difference between the frequency of the pedestrian's paces and the natural frequency of the floor, and is given as a function of f_0 in Fig. 3.26.

The static deflection of the floor is $\bar{F}/k_e$, and the magnification factor at resonance is $1/(2\zeta)$, where ζ is the critical damping ratio. This should normally be taken as 0.03 for open-plan offices with composite floors, though Wyatt[42] reports values as low as 0.015 for unfurnished floors. The vertical displacement y for steady-state vibration thus has frequency f_0 and is given approximately by

$$y = \frac{\bar{F}}{2k_e\zeta}\sin 2\pi f_0 t.$$

The r.m.s. value of the acceleration is found by differentiating twice and dividing by $\sqrt{2}$:

$$a_{\text{rms}} = 4\pi^2 f_0^2 \frac{\overline{F}}{2\sqrt{2k_e\zeta}}. \tag{3.102}$$

The effective stiffness k_e depends on the vibrating area of floor, LS. The width S can be computed in terms of the relevant flexural rigidities per unit width of floor, which are I_s and I_b/s. It is given by Wyatt[42] as

$$S = 4.5 \left(\frac{EI_s}{mf_0^2}\right)^{1/4}. \tag{3.103}$$

This can be explained as follows. For a typical floor, f_{0b} is several times f_{0s}, so from equation (3.98), f_{0b} is a good estimate of f_0. Substituting mf_0^2 from equation (3.99) into equation (3.103) gives

$$\frac{S}{L} = 3.6 \left(\frac{I_s S}{I_b}\right)^{1/4}.$$

Thus, the higher the ratio between the stiffness of the slab and the beam, the greater is the ratio of the equivalent width of the slab to the span of the beams, as would be expected.

By analogy with a simple spring–mass system, the fundamental frequency can be defined by

$$f_0 = \frac{1}{2\pi}\left(\frac{k_e}{M_e}\right)^{1/2} \tag{3.104}$$

where k_e is the effective stiffness. The effective mass M_e is given approximately by

$$M_e = \frac{mSL}{4}.$$

From equation (3.104),

$$k_e = \pi^2 f_0^2 mSL.$$

With $\overline{F}$ from equation (3.101), equation (3.102) then gives

$$a_{\text{rms}} = 340 \frac{C_f}{mSL\zeta}, \tag{3.105}$$

with S given by equation (3.103).

From the definition of the response factor R,

$$a_{\text{rms}} = 5 \times 10^{-3} R \text{ m/s}^2$$

so from equation (3.105),

$$R = 68\,000 \frac{C_f}{mSL\zeta} \tag{3.106}$$

in kg, m units. This equation is given on p.28 of Reference 42.

For floors with layouts of the type shown in Fig. 3.1, and that satisfy the assumptions made above, checking for susceptibility to vibration caused by

pedestrian traffic consists of finding f_0 from equation (3.98), and a_{rms} or R, as given above, and comparing the result with the target response curve, as in Fig. 3.26.

Relevant calculations are given in Section 3.11.3.2.

The preceding summary is intended only to provide an introduction to a versatile design method, and to apply it to a single type of structure. For use in practice, reference should be made to more complete accounts of the method and its background.[41, 42]

3.10 Fire resistance of composite beams

Fire design, based on the 1993 draft Eurocode 4: Part 1.2, 'Structural fire design', is introducted in Section 3.3.7, the whole of which is applicable to composite beams, as well as to slabs, except Section 3.3.7.5.

Beams rarely have insulation or integrity functions, and have then to be designed only for the loadbearing function, R. The fire resistance class is normally the same as that of the slab that acts as the top flange of the beam, so only the structural steel section needs further protection. This may be provided by full encasement in concrete or a lightweight fire-resisting material. A more recent method is to encase only the web in concrete. This can be done before the beam is erected (except near end connections), and gives a cross-section of the type shown in Fig. 3.31.

In a fire, the exposed bottom flange loses its strength, but the protected web and top flange do not. For the higher load levels η^* (defined in Section 3.3.7.2) and longer periods of fire resistance, minimum areas of longitudinal reinforcement within the encasement, A'_s, are specified, in terms of the cross-sectional area A_f of the steel bottom flange. The minimum depth h_a and breadth b_f of the steel I-section are also specified, for each standard fire resistance period.

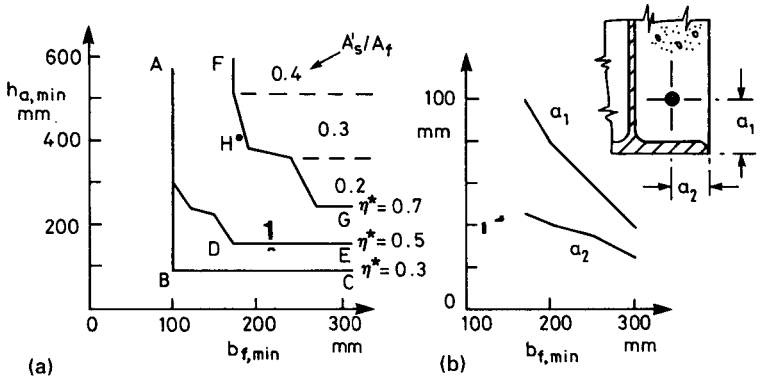

Fig. 3.28 Tabulated data for web-encased beams, class R60.

The requirements of draft Eurocode 4: Part 1.2 for 60 minutes' fire exposure (class R60) are shown in Fig. 3.28. The minimum dimensions h_a and b_f increase with η^*, as shown by the three lines in Fig. 3.28(a). For other values of η^*, interpolation may be used.

The minimum ratios A_s'/A_f are zero for $\eta^* = 0.3$ (ABC) and $\eta^* = 0.5$ (ADE). For $\eta^* = 0.7$ they are indicated within the regions where they apply. To ensure that the additional reinforcement maintains its strength for the period of fire exposure, minimum distances a_1 and a_2 are specified, in terms of $b_{f,min}$ and the fire class. Those for class R60 are shown in Fig. 3.28(b).

The validity of tabulated data of this type is inevitably limited. The principal conditions for its use, given in the Eurocode, are as follows. The notation is as in Fig. 3.15.

(a) The composite beam must be simply-supported with

$$t_w \leqslant b_f/18, \quad t_f \leqslant 2t_w, \quad h_t \geqslant 120\,\text{mm}, \quad f_y \leqslant 355\,\text{N/mm}^2, \quad b_{eff} \leqslant 5\,\text{m}.$$

(b) If the slab is composite, the voids formed above the steel beam by trapezoidal profiles must be filled with fire-resistant material.

(c) The web must be encased in normal-density concrete, held in place by stirrups, fabric, or stud connectors that pass through or are welded to the steel web.

The data given in Fig. 3.28 are used for the design example in Section 3.11.4. The Eurocode also gives both simple and advanced calculation models, which are often less conservative than the tabulated data, and have wider applicability. These are outside the scope of this volume.

3.11 Example: simply-supported composite beam

In this example, a typical composite T-beam is designed for the floor structure shown in Fig. 3.1, using the materials specified in Section 3.2, and the floor design given in Section 3.4. Ultimate limit states are considered first. An appropriate procedure that minimises trial and error is as follows:

(1) Choose the types and strengths of materials to be used.

(2) Ensure that the design brief is complete. For this example it is assumed that:
- no special provision of holes for services is required;
- the main source of vibration is pedestrian traffic on the floor, and occupants' sensitivity to vibration is typical of that found in office buildings;
- the specified fire resistance class is R60.

(3) Make policy decisions. For this design (for example):
- steel member to be rolled universal beam (UB) section;
- propped construction to be avoided, even if this involves pre-cambering the steel beam;
- fire resistance to be provided by encasing the web, but not the bottom flange, in concrete.

(4) With guidance from typical span-to-depth ratios for composite beams, guess the overall depth of the beam, and hence the depth h_a of the steel section.

(5) Guess the weight of the beam, and hence estimate the design mid-span bending moment, M_{Sd}.

(6) Assume the lever arm to be (in the notation of Fig. 3.2)

$$\frac{h_a}{2} + h_t - \frac{h_c}{2}$$

and find the required area of steel, A_a, if full shear connection is to be used, from

$$A_a \frac{f_y}{\gamma_a}\left(\frac{h_a}{2} + h_t - \frac{h_c}{2}\right) \geqslant M_{Sd}. \qquad (3.107)$$

For partial shear connection, A_a should be increased.

(7) If full shear connection is to be used, check that the yield force in the steel, $A_a(f_y/\gamma_a)$, is less than the compressive resistance of the concrete slab, $b_{eff}h_c(0.85f_{ck}/\gamma_c)$. If it is not, the plastic neutral axis will be in the steel – unusual in buildings – and A_a as found above will be too small.

(8) Knowing h_a and A_a, select a rolled steel section. Check that its web can resist the design vertical shear at an end of the beam.

(9) Design the shear connection to provide the required bending resistance at midspan.

(10) Check deflections and vibration in service.

(11) Design for fire resistance.

3.11.1 Composite beam – flexure and vertical shear

From Section 3.4, the uniform characteristic loads from a 4.0-m width of floor are:

permanent,	$g_{k1} = 2.4 \times 4 = 9.6$ kN/m	on steel alone
	$g_{k2} = 2.5 \times 4 = 10$ kN/m	on the composite beam
variable,	$q_k = 5 \times 4 = 20$ kN/m	on the composite beam.

The weight of the beam and its fire protection is estimated to be 2.2 kN/m, so the design ultimate loads are:

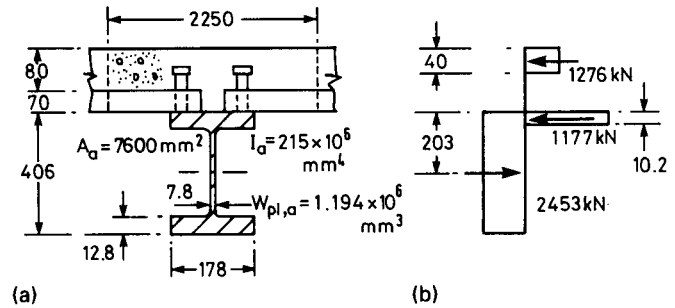

Fig. 3.29 Cross-section and stress blocks for composite beam in sagging bending.

$$g_d = 1.35(19.6 + 2.2) = 29.4 \text{ kN/m}$$

$$q_d = 1.5 \times 20 \qquad = 30 \text{ kN/m}.$$

The midspan bending moment for $L = 9.0$ m is:

$$M_{Sd} = 59.4 \times \frac{9^2}{8} = \mathbf{601\ kNm}, \tag{3.108}$$

and the design vertical shear is:

$$V_{Sd} = 59.4 \times 4.5 = \mathbf{267\ kN}. \tag{3.109}$$

It has been assumed that the composite section will be in Class 1, so that the effects of unpropped construction can be ignored at ultimate limit states.

Deflection of this beam is likely to influence its design, because of the use of steel with $f_y = 355$ N/mm^2 (grade 50), lightweight-aggregate concrete, and unpropped construction. The relatively low span-to-depth ratio of 16 is therefore chosen, giving an overall depth of 9000/16 = 562 mm. The slab is 150 mm thick (Fig. 3.9), so for the steel beam, $h_a \approx 412$ mm. From equation (3.107) the required area of steel is

$$A_a \approx \frac{601 \times 10^6}{(355/1.1)\,(206 + 150 - 40)} = 5890 \text{ mm}^2.$$

The most suitable rolled I-section appears to be 406 × 178 UB 54 ($A_a = 6840$ mm^2); but with profiled sheeting it is usually necessary to use partial shear connection, so the next size larger is chosen, 406 × 178 UB 60. Its relevant properties are shown in Fig. 3.29.

We guess that for full shear connection, the depth x of the plastic neutral axis is less than h_c (80 mm), so x is found from equation (3.56) with $b_{eff} = 2.25$ m from equation (3.55):

$$N_{cf} = 7600 \times \frac{0.355}{1.1} = 2.25x\left(0.85 \times \frac{25}{1.5}\right)$$

whence

$$x = 77 \text{ mm},$$

and $N_{cf} = 2453$ kN. From equation (3.57), the full-interaction moment of resistance is

$$M_{pl.Rd} = 2453\left(0.203 + 0.15 - \frac{0.077}{2}\right) = 771 \text{ kN m}. \qquad (3.110)$$

This is well above M_{Sd}, as expected.

From equation (3.69) the shear area of this rolled section is

$$A_v = 1.04 \times 406 \times 7.8 = 3293 \text{ mm}^2.$$

From equation (3.70) the resistance to vertical shear is

$$\boldsymbol{V_{pl,Rd}} = 3293\,\frac{0.355/\sqrt{3}}{1.1} = \mathbf{614\ kN}, \qquad (3.111)$$

which far exceeds V_{Sd}, as is usual in composite beams when rolled steel I-sections are used.

3.11.2 Composite beam – shear connection and transverse reinforcement

The required degree of shear connection is first found by the interpolation method, assuming that the connectors are ductile. The plastic resistance moment of the steel section is

$$M_{apl.Rd} = \frac{W_{apl} f_y}{\gamma_a} = \frac{1.194 \times 355}{1.1} = 386 \text{ kN m} \qquad (3.112)$$

(W is the Eurocode symbol for section modulus). The ratio N/N_f is given by equations (3.67) and (3.68):

$$\frac{N}{N_f} = \frac{F_c}{F_{cf}} = \frac{601 - 386}{771 - 386} = 0.56.$$

The condition for stud connectors to be treated as ductile when the span is 9.0 m is given by Fig. 3.19 as

$$\frac{N}{N_f} \geqslant 0.52.$$

To provide an example of the use of the equilibrium method, the bending resistance is now calculated using $N = 0.52\ N_f$. The notation of Fig. 3.15(d) will be used.

The force F_c is 0.52 times the full-interaction value:

$$F_c = 0.52 \times 2453 = 1276 \text{ kN} \tag{3.113}$$

and since for N_{cf}, $x = 77$ mm, $x_c = 0.52 \times 77 = 40$ mm.
Assuming that there is a neutral axis within the steel top flange, the depth of flange in compression is

$$\frac{2453 - 1276}{0.178 \times 2 \times 355/1.1} = 10.2 \text{ mm}.$$

This is less that t_f (12.8 mm) so the assumption is correct, and the stress blocks are as shown in Fig. 3.29(b). Taking moments about the top surface of the slab,

$$\begin{aligned} \boldsymbol{M_{pl,Rd}} &= 2453 \times 0.353 - 1276 \times 0.020 - 1177 \times 0.155 \\ &= \mathbf{658 \text{ kN m}} \end{aligned} \tag{3.114}$$

which exceeds M_{Sd} (601 kN m).

The interpolation method (above) gave $M_{pl,Rd} = 601$ kN m with $N/N_f = 0.56$, so the equilibrium method is significantly less conservative. It is possible that when Eurocode 4: Part 1.1 comes into regular use, some countries may allow for this by specifying a value of γ_a for use with the equilibrium method about 5% higher than the value used generally.

For this example, $N/N_f = 0.52$ will be used.

Number and spacing of shear connectors

It is assumed that 19-mm stud connectors will be used, 100 mm long. The length after welding is about 5 mm less, so the height of the studs is taken as 95 mm. P_{Rd} is given by equation (3.2) as 57.9 kN per stud.

For the sheeting used here, the width b_o (Fig. 2.14) is 162 mm, from Fig. 3.9, and the other dimensions that influence the reduction factor k_t for the resistance of studs in ribs are:

$$h_p = 70 - 15 = 55 \text{ mm}, \quad h = 95 \text{ mm}.$$

So from equation (2.17),

$$\begin{aligned} k_t = \frac{0.7}{\sqrt{N_r}} \frac{162}{55} \left[\frac{95}{55} - 1\right] &= 1.50 \quad (N_r = 1) \\ &= 1.06 \quad (N_r = 2), \end{aligned}$$

but k_t may not exceed 1.0. These values show that no reduction need be made, so that $P_{Rd} = 57.9$ kN per stud.

From equation (3.113) the number of studs needed in each half span is

$$N = \frac{F_c}{P_{Rd}} = \frac{1276}{57.9} = 22.04, \text{ say } 23.$$

There is one trough every 300 mm, or 15 in a half span. Two studs are provided in each of the eight troughs nearest to a support, and one in each of the other seven troughs, giving a total of 23.

Transverse reinforcement

The rules of Eurocode 4 for the use of profiled sheeting as transverse reinforcement are explained in Section 3.6.3.2. The cross-section in Fig. 3.30, which is drawn to scale, illustrates the difficulty of complying with the rule that the sheeting should extend at least $2d_{do}$ beyond the centre of a stud welded through it, where d_{do} is an estimate of the diameter of the stud weld, taken as $1.1d$, or 20.9 mm here. The 30-mm dimension just satisfies the relevant rule shown in Fig. 3.24. The clear gap of 34 mm between the ends of the sheeting will be reduced by tolerances, and could easily fall below the minimum needed for satisfactory placing of concrete (about 25 mm).

The longitudinal shear on a plane such as D–D in Fig. 3.30 is greatest where there are two studs per trough. The total longitudinal shear is

$$v = 2 \times \frac{57.9}{0.3} = 386 \text{ kN/m},$$

so the design shear for plane D–D is just under half this, so

$$v_{Sd} \approx 193 \text{ kN/m}.$$

The contribution from the sheeting is calculated next. In equation (3.81),

$$k_\phi = 1 + \frac{42}{21.9} = 2.9, \quad t = 0.9 \text{ mm}, \quad f_{yp} = 280 \text{ N/mm}^2, \quad \text{and} \quad \gamma_{ap} = 1.1,$$

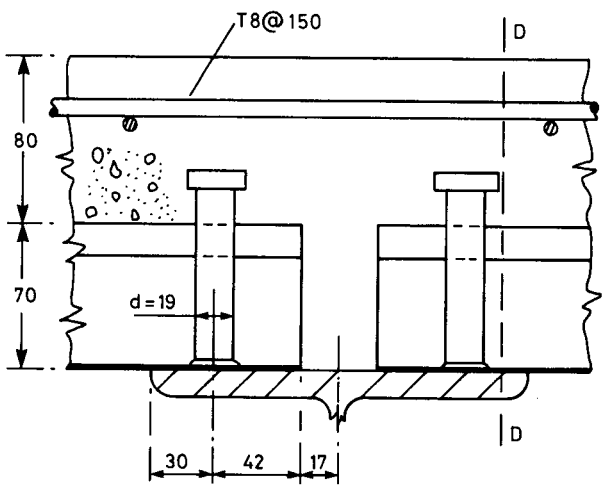

Fig. 3.30 Detail of shear connection.

so $P_{pb,Rd} = 13.9$ kN. From equation (3.82),

$$v_{pd} = \frac{13.9}{0.3} = 46.3 \text{ kN/m}. \tag{3.115}$$

Equation (3.75) is now used to find the required area of transverse reinforcement, putting $v_{Rd} = v_{Sd}$:

$$193 = 2.5A_{cv}\eta\tau_{Rd} + A_e\frac{f_{sk}}{\gamma_s} + 46.3. \tag{3.116}$$

From Fig. 3.9, the effective area of concrete in shear is approximately

$$A_{cv} = 162 \times \frac{55}{0.3} + 95 \times 1000 = 125 \times 10^3 \text{ mm}^2/\text{m}.$$

From equation (3.78),

$$\eta = 0.3 + 0.7\left(\frac{19}{24}\right) = 0.85.$$

From equation (3.76),

$$\tau_{Rd} = 0.25 \times \frac{1.8}{1.5} = 0.3 \text{ N/mm}^2.$$

Assuming that welded mesh reinforcement is used, with $f_{sk} = 500$ N/mm^2, equation (3.116) gives

$$193 = 79.7 + 0.435A_e + 46.3,$$

whence $A_e = 154$ mm^2/m. (3.117)

The minimum transverse reinforcement for longitudinal shear is given in Eurocode 4: Part 1.1 as $0.002\,A_{cv}$, or 250 mm^2/m here. This can include the effective area of sheeting, so there is no need to increase A_e for this reason. But for control of cracking of the slab above the beam, it was found (equation (3.47)) that 320 mm^2/m is required, and this governs. The detail proposed in Section 3.4.6 (8-mm bars at 150 mm spacing) gives 336 mm^2/m and is satisfactory.

3.11.3 Composite beam – deflection and vibration

3.11.3.1 Deflection

The rare combination of loading on the beam consists of the characteristic loads. From data given in Section 3.11.1 these are:

$$\left.\begin{array}{ll} \text{permanent (steel beam)} & g_1 = 9.6 + 2.2 = 11.8 \text{ kN/m} \\ \text{permanent (composite beam)} & g_2 = 10.0 \text{ kN/m} \\ \text{variable (composite beam)} & q = 20.0 \text{ kN/m}. \end{array}\right\} \tag{3.118}$$

For a simply-supported span of 9 m with distributed load w kN/m and second moment of area I mm^4, the midspan deflection is

$$\delta = \frac{5wL^4}{384\,EI} = \frac{5 \times 9^4 \times 10^9 w}{384 \times 210\,I} = 407 \times 10^6 \frac{w}{I} \text{ mm}. \qquad (3.119)$$

For the steel beam, $I = 215 \times 10^6$ mm^4, so its deflection during construction is

$$\delta_a = 407 \times \frac{11.8}{215} = 22.3 \text{ mm} \quad \text{(span/403)}.$$

From Section 3.2, the short-term elastic modulus for the concrete is 19.1 kN/mm^2, so for variable loading the modular ratio is

$$n_q = \frac{210}{191} = 11.0.$$

For permanent loading, $n_g = 3n_q = 33$.

The second moment of area of the composite section is calculated using equations (3.85) to (3.89). From Fig. 3.29, relevant values are:

$$A_a = 7600 \text{ mm}^2, \quad z_g = 353 \text{ mm}, \quad b_{eff} = 2250 \text{ mm}, \quad I_a = 215 \times 10^6 \text{ mm}^4.$$

The minimum thickness of the slab is 80 mm, but for over 90% of its area it is at least 95 mm thick (Fig. 3.9). For deflection and vibration, mean values of I are appropriate, so h_c is here taken as 95 mm.

For variable load, expression (3.85) gives

$$1.96 \times 10^6 < 0.923 \times 10^6.$$

This is not correct, so the neutral-axis depth exceeds h_c, and equation (3.88) gives

$$x = 133 \text{ mm}. \qquad (3.120)$$

From equation (3.89),

$$10^{-6}I = 215 + 7600(0.353 - 0.133)^2 + \frac{2250 \times 95}{11}\left(\frac{0.095^2}{12} + 0.085^2\right)$$
$$= 215 + 368 + 155 = 738 \text{ mm}^4. \qquad (3.121)$$

(Numerical values are always of more convenient size in this calculation if $10^{-6}I$ is calculated, rather than I.)

Similar calculations using $n = 33$ give:

$$x = 212 \text{ mm}, \quad 10^{-6}I = 547 \text{ mm}^4. \qquad (3.122)$$

The deflection of the composite beam due to permanent load is

$$\delta_g = 407 \times \frac{10}{547} = 7.4 \text{ mm},$$

and its deflection due to variable load is

$$\delta_q = 407 \times \frac{20}{738} = 11.0 \text{ mm} \quad \text{(span/816)}.$$

The total deflection is thus 22.3 + 7.4 + 11.0 = 40.7 mm (span/221).

This exceeds the limit recommended in Section 3.7.2 (span/250), so the steel beam should be cambered by an amount roughly equivalent to the short-term deflection due to permanent load. This amount is

$$\delta_{g,i} = 22.3 + 407 \times \frac{10}{738} = 28 \text{ mm}.$$

This reduces the subsequent deflection to about 13 mm, or span/692, which should be satisfactory in most circumstances.

No account was taken in these calculations of any increase in deflection due to slip, because the conditions under which Eurocode 4 allows use of equation (3.94) to be omitted are satisfied. In practice, deflections would be slightly reduced by the stiffness of the concrete in the bottom 55 mm of the slab, and by the stiffness of the beam-to-column connections.

The use of camber was included here to illustrate the method. In practice, the designer might prefer to use a slightly heavier steel section (e.g. 406 × 178 UB67).

Maximum bending stress in the steel section

It is clear from Section 3.7 that the steel member is unlikely to yield under service loading. The maximum bending stress occurs in the bottom fibre at midspan. This stress is now calculated, to illustrate the method.

Separate calculations are needed for the three loadings given in equations (3.118). For distributed load w per unit length, the stress is

$$\sigma = \frac{My}{I} = \frac{wL^2y}{8I} = 10.1\frac{wy}{I}$$

where y is the distance of the bottom fibre below the neutral axis. From values given above, the stresses are:

$$\text{for } g_1\text{:} \quad \sigma = 10.1 \times 11.8 \times \frac{203}{215} = 113 \text{ N/mm}^2$$

$$\text{for } g_2\text{:} \quad \sigma = 10.1 \times 10 \, \frac{556 - 212}{547} = 64 \text{ N/mm}^2$$

$$\text{for } q\text{:} \quad \sigma = 10.1 \times 20 \, \frac{556 - 133}{738} = 116 \text{ N/mm}^2.$$

The total stress is 293 N/mm^2, well below the yield stress of 355 N/mm^2.

Other bending stresses can be calculated in the same way.

3.11.3.2 Vibration

The method given in Section 3.9 is used. It is assumed that the source of vibration is intermittent pedestrian traffic. The target value for the response factor R is 4, if the traffic is continuous, increasing to 8, if there is about one disturbance per minute.

Fundamental natural frequency

From equations (3.118), the permanent load per beam is 21.8 kN/m. This includes an allowance of 4.8 kN/m for partitions, which will be treated here as imposed load. The total imposed (variable) load is then 24.8 kN/m, and only one-tenth of this will be included, because vibration is likely to be worse where there are few partitions and little imposed load. The design load is thus 19.2 kN/m for beams at 4 m centres, giving a vibrating mass:

$$m = \frac{19200}{4 \times 9.81} = 400 \text{ kg/m}^2.$$

For the beam, the second moment of area is taken as 10% above the value in equation (3.121):

$$10^{-6} I_b = 1.1 \times 738 = 812 \text{ mm}^4.$$

For the slab, the 'uncracked' value found in Section 3.4.5 is too low, because the dynamic modulus E_{cd} is taken as 22 kN/mm^2, so that the modular ratio is $n = 210/22 = 9.5$. This increases the second moment of area, in 'steel' units, from 12.1×10^6 mm^4/m to:

$$10^{-6} I_s = 25.1 \text{ mm}^4/\text{m}.$$

From equation (3.99) with $s = 4$ m, $L = 9$ m,

$$f_{0b} = \frac{\pi}{2}\left(\frac{210000 \times 812}{490 \times 4 \times 9^4}\right)^{1/2} = 5.72 \text{ Hz}.$$

From equation (3.100),

$$f_{0s} = 3.56\left(\frac{210000 \times 25.1}{490 \times 4^4}\right)^{1/2} = 23.1 \text{ Hz}.$$

From equation (3.98),

$$f_0 = 5.6 \text{ Hz}.$$

This is below 7 Hz, so no check need be made for impulsive loads.

Response of composite floor

Following Section 3.9.2, $C_f = 0.2$ from Fig.3.26. From equation (3.103), the vibrating width of slab is

$$S = 4.5\left(\frac{210000 \times 25.1}{490 \times 5.6^2}\right)^{1/4} = 19.3 \text{ m},$$

or the actual dimension of the floor normal to the span of the beams, if less. For a small value of S, the natural frequency would be higher than f_0 as calculated here, so it is assumed that the building considered is more than 19.3 m long, and this value is used.

With $\zeta = 0.03$, equation (3.106) gives the response factor:

$$R = \frac{68000 \times 0.2}{490 \times 19.3 \times 9 \times 0.03} = 5.3.$$

This value exceeds 4 but is well below 8. The conclusion is that continuous pedestrian traffic might result in adverse comment, but the level of movement typical of an open-plan office would not do so.

3.11.4 Composite beam – fire design

The method used below is explained in Sections 3.3.7 and 3.10.

From equations (3.118) the characteristic loads per unit length of beam are:

$$g_k = 21.8 \text{ kN/m}, \quad q_k = 20.0 \text{ kN/m}.$$

From equation (3.31),

$$\eta_f = \frac{1 + 0.7(20/21.8)}{1.35 + 1.5(20/21.8)} = 0.60.$$

The beam will be designed to have a bending resistance at midspan in fire resistance class R60. The design bending moment at midspan for cold design is 601 kN m, from equation (3.108) and the resistance is 658 kN m, from equation (3.114). The resistance ratio (equation (3.32)) is

$$\eta^* = 0.60 \times \frac{601}{658} = 0.55.$$

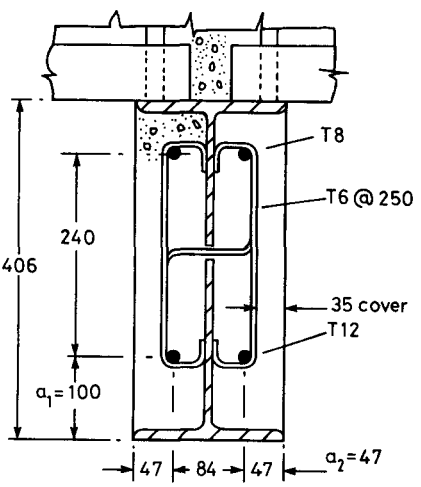

Fig. 3.31 Detail of concrete-encased web.

Fire protection is provided by encasing the web in normal-density concrete, as shown in Fig.3.31, and filling the voids above the steel top flange with fire-resistant material. This satisfies conditions (b) and (c) of Section 3.10, and all of conditions (a) are satisfied.

For the steel beam, $h_a = 406$ mm and $b_f = 178$ mm. This plots as point H in Fig. 3.28(a). By interpolation, these dimensions are sufficient, when $\eta^* = 0.55$.

No additional reinforcement A'_s would be required for $\eta^* = 0.5$, and for

$$\eta^* = 0.7, \quad A'_s \geqslant 0.3A_f.$$

So for $\eta^* = 0.55$,

$$A'_s = 0.25 \times 0.3A_f = 0.075 \times 178 \times 12.8 = 171 \text{ mm}^2.$$

Two T12 bars will be provided ($A'_s = 226$ mm^2).

The encasement does not increase the resistance of the composite section to sagging bending, because all of the concrete is in longitudinal tension. The width of cracks in the concrete should be controlled, and Eurocode 4 gives rules for this purpose. Where the design crack width is 0.5 mm, it requires that the spacing of longitudinal bars should not exceed 250 mm. For fire, the rules for the location of bars are, from Fig. 3.28(b) with $b_f = 178$ mm,

$$a_1 \geqslant 95 \text{ mm}, \quad a_2 \geqslant 44 \text{ mm}.$$

A possible detail for the web encasement, in accordance with these rules, is shown in Fig. 3.31. The 6-mm stirrups are either welded to the web or passed through holes in it.

The weight of the encased beam is just below the 2.2 kN/m assumed in Section 3.11.1.

In a fire, the web encasement preserves the resistance of the beam to vertical shear, and the slab is thick enough to protect the top transverse reinforcement and the shear connection.

Chapter 4

Continuous Beams and Slabs, and Beams in Frames

4.1 Introduction

The definition of 'continuous composite beam' given in Eurocode 4: Part 1.1[12] is:

> A beam with three or more supports, in which the steel section is either continuous over internal supports or is jointed by full-strength and rigid connections, with connections between the beam and each support such that it can be assumed that the support does not transfer significant bending moment to the beam. At the internal supports the beam may have either effective reinforcement or only nominal reinforcement.

Beam-to-column connections in steelwork are classified in Eurocode 3: Part 1.1[11] both by stiffness, as:

- nominally pinned,
- rigid, or
- semi-rigid,

and by strength, as:

- nominally pinned,
- full-strength, or
- partial-strength.

In Eurocode 4: Part 1.1[12], a 'composite connection' is defined as:

> A connection between a composite member and any other member in which reinforcement is intended to contribute to the resistance of the connection.

The system of classification is as for steel connections, except that semi-rigid connections are omitted, because design methods for them are not yet sufficiently developed.

A 'full-strength and rigid' connection has to be at least as stiff and strong as the beams connected, so a 'continuous composite beam' can be analysed for bending moments as one long member without internal connections, by methods to be explained in Section 4.3. Bridge girders (Volume 2) are

usually of this type. The example to be used here is a two-span beam continuous over a wall or supporting beam.

In multi-bay plane frames, commonly used in structures for buildings, the beam-to-column connections are often 'nominally pinned'. The beams are then designed as simply-supported. Where full-strength connections are used, the frame should be analysed as a whole, and the beams are not 'continuous' as defined above. These beams are referred to here as 'beams in frames', as are those with partial-strength connections. In comparison with simple spans, beams in frames have the same advantages and disadvantages as continuous beams. The global analysis is more complex than for continuous beams, because the properties of columns and connections are involved, but the design of hogging moment regions of the beams is the same. In Section 4.3 on global analysis, only continuous beams are considered.

For a given floor slab and design load per unit length of beam, the advantages of continuous beams over simple spans are:

- higher span/depth ratios can be used, for given limits to deflections;
- cracking of the top surface of a floor slab near internal columns can be controlled, so that the use of brittle finishes (e.g. terrazzo) is feasible;
- the floor structure has a higher fundamental frequency of vibration, and so is less susceptible to vibration caused by movements of people;
- the structure is more robust (e.g. in resisting the effects of fire or explosion).

The principal disadvantage is that design is more complex. Actions on one span cause action effects in adjacent spans, and the stiffness and bending resistance of a beam vary along its length.

It is not possible to predict accurately the stresses or deflections in a continuous beam for a given set of actions. Apart from the variation over time caused by the shrinkage and creep of concrete, there are the effects of cracking of concrete. In reinforced concrete beams, these occur at all cross-sections, and so have little influence on distributions of bending moment. In composite beams, significant tension in concrete occurs only in hogging regions. It is influenced by the sequence of construction of the slab, the method of propping used (if any), and by effects of temperature, shrinkage, and longitudinal slip.

The flexural rigidity of a fully cracked composite section can be as low as a quarter of the 'uncracked' value, so a wide variation in flexural rigidity can occur along a continuous beam of uniform section. This leads to uncertainty in the distribution of longitudinal moments, and hence in the amount of cracking to be expected. The response to a particular set of actions also depends on whether it precedes or follows another set of actions that causes cracking in a different part of the beam.

For these reasons, and also for economy, design is based as far as

possible on predictions of ultimate strength (which can be checked by testing) rather than on analyses based on elastic theory. Methods have to be developed from simplified models of behaviour. The limits set to the scope of some models seem arbitrary, as they correspond to the range of available research data, rather than to known limitations of the model.

Almost the whole of Chapter 3, on simply-supported beams and slabs, applies equally to the sagging moment regions of continuous members. The properties of hogging moment regions of beams are treated in Section 4.2, which applies also to cantilevers. Then follows the global analysis of continuous beams, and the calculations of stresses and deflections.

Both rolled steel I- or H-sections and small plate or box girders are considered, with or without web encasement and composite slabs. It is always assumed that the concrete slab is above the steel member, because the use of slabs below steel beams with which they are composite is almost unknown in buildings, though it occurs in bridges.

4.2 Hogging moment regions of continuous composite beams

4.2.1 Classification of sections, and resistance to bending

4.2.1.1 General

Section 3.5.1, on effective cross-sections of beams, is applicable, except that the effective width of the concrete flange is usually less at an internal support than at midspan. This width defines the region of the slab where longitudinal reinforcement may be assumed to contribute to the hogging moment of resistance of the beam. There is no contribution from concrete in compression, because the neutral axis invariably lies below the slab. The lower part of the encasement to a web is in compression, but its crushing could limit the rotation capacity of the region, so this compression is at present ignored in design.

In Eurocode 4, the effective width is given as $l_o/8$ on each side of the steel web, where l_o is the approximate length of the hogging moment region, which can be taken as one-quarter of each span. So at a support between spans of length L_1 and L_2, the effective width is:

$$b_{\text{eff}} = 2 \times \frac{0.25(L_1 + L_2)}{8} = \frac{L_1 + L_2}{16} \qquad (4.1)$$

provided that at least $b_{\text{eff}}/2$ is present on each side of the web.

The rules for the classification of steel elements in compression (Section 3.5.2) strongly influence the design of hogging moment regions. The proportions of rolled steel I-sections are so chosen that when they act in bending, most webs are in Class 1 or 2. But in a composite section,

addition of longitudinal reinforcement in the slab rapidly increases the depth of steel web in compression, αd in Fig. 3.14. This figure shows that when $d/t>60$, an increase in α of only 0.05 can move a web from Class 1 to Class 3, which can reduce the design moment of resistance of the section by up to 30%. This anomaly has led to a rule[12, 14] that allows a web in Class 3 to be replaced (in design) by an 'effective' web in Class 2. This 'hole-in-the-web' method is explained later. It does not apply to flanges, which can usually be designed to be in Class 1 or 2, even where plate girders are used.

Design of hogging moment regions is based on the use of full shear connection (Section 4.2.3).

4.2.1.2 Plastic moment of resistance

A cross-section of a composite beam in hogging bending is shown in Fig. 4.1(a). The numerical values are for a section that is used in the following worked example and the diagram is to scale for these values (except for b_{eff}). The steel bottom flange is in compression, and its class is easily found, as explained in Section 3.5.2. To classify the web, the distance x_c of the plastic neutral axis above G, the centre of the area of the steel section, must first be found.

Let A_s be the effective area of longitudinal reinforcement within the effective width b_{eff} of the slab. Welded mesh is normally excluded, because it may not be sufficiently ductile to ensure that it will not fracture before the design ultimate load for the beam is reached. The design tensile force in this reinforcement is

$$f_s = \frac{A_s f_{sk}}{\gamma_s} \tag{4.2}$$

where f_{sk} is its characteristic yield strength.

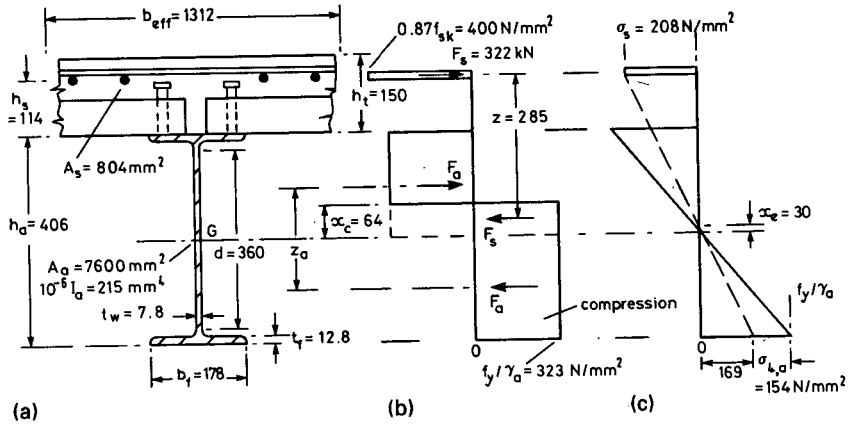

Fig. 4.1 Cross-section and stress distributions for composite beam in hogging bending.

If there were no tensile reinforcement, the bending resistance would be that of the steel section,

$$M_{\text{apl,Rd}} = \frac{W_a f_y}{\gamma_a} = F_a z_a \tag{4.3}$$

where W_a is the plastic section modulus and f_y is the yield strength. For rolled sections it is not necessary to calculate the forces F_a in the stress blocks of depth $h_a/2$, nor the lever arm z_a, because values of W_a are tabulated; but for plate girders F_a and z_a have to be calculated.

The simplest way of allowing for the reinforcement is to assume that the stress in a depth x_c of web changes from tension to compression, where x_c is given by

$$x_c t_w \frac{2f_y}{\gamma_a} = F_s, \tag{4.4}$$

provided that (as is usual)

$$x_c \leqslant \frac{h_a}{2} - t_f.$$

The depth of web in compression is given by

$$\alpha d = \frac{d}{2} + x_c, \tag{4.5}$$

and knowledge of α, d/t_w, and f_y enables the web to be classified, as shown in Fig. 3.14 for $f_y = 355$ N/mm^2. If, by this method, a web is found to be in Class 4, the calculation should be repeated using the elastic neutral axis, as the curve that separates Class 3 from Class 4 is based on the elastic behaviour of sections. This is why, in Fig. 3.14, the ratio ψ is used rather than α.

Concrete-encased webs in Class 3 are treated as if in Class 2, because the encasement helps to stabilise the web.

The lever arm z for the two forces F_s in Fig. 4.1(b) is given by

$$z = \frac{h_a}{2} + h_s - \frac{x_c}{2}$$

where h_s is the height of the reinforcement above the interface. If both the compression flange and the web are in Class 1 or 2, this is the appropriate model, and the moment of resistance is

$$M_{\text{h,Rd}} = M_{\text{apl,Rd}} + F_s z. \tag{4.6}$$

If the flange is in Class 1 or 2 and the (uncased) web is in Class 3, it is still possible to use plastic section analysis, by neglecting a region in the centre of the compressed part of the web, that is assumed to be ineffective because of buckling. The calculations are more complex, as explained elsewhere,[15] because this assumption changes the position of the plastic

neutral axis, and in plate girders may even move it into the steel top flange. This 'hole-in-the-web' method is analogous to the use of effective widths for the design of steel compression elements in Class 4, which is outside the scope of this volume. It is an alternative to the use of elastic analysis, as follows, which is the only method available where the compression flange is in Class 3.

Worked example

Figure 4.1(a) shows a cross-section in a region of hogging moment where the steel section is 406 × 178 UB 60 with $f_y = 355$ N/mm^2 and dimensions as shown. Its plastic section modulus, from tables, is $W_a = 1.194 \times 10^6$ mm^4. At an internal support between spans of 9.0 m and 12.0 m, the longitudinal reinforcement is T16 bars, with $f_{sk} = 460$ N/mm^2, at 330 mm spacing. The thickness of slab above the profiled sheeting is 80 mm, so the reinforcement ratio is $64\pi/(330 \times 80) = 0.76\%$.

What are the class of the section and its design resistance to hogging moments?

From equation (4.1),

$$b_{\text{eff}} = \frac{L_1 + L_2}{16} = \frac{21}{16} = 1.312 \text{ m},$$

so that four T16 bars are effective, and $A_s = 804$ mm^2. Assume initially that the web is in Class 1 or 2, so that the rectangular stress blocks shown in Fig. 4.1(b) are relevant. The bottom (compression) flange has $c/t < 7$ and so is in Class 1, from Table 3.1.

From equation (4.2) with $\gamma_s = 1.15$,

$$F_s = \frac{A_s f_{sk}}{\gamma_s} = \frac{804 \times 0.46}{1.15} = 322 \text{ kN}.$$

From equation (4.4), with $\gamma_a = 1.1$,

$$x_c = \frac{F_s \gamma_a}{2 t_w f_y} = \frac{322 \times 1.1}{15.6 \times 0.355} = 64 \text{ mm}.$$

From equation (4.5), the ratio α is

$$\alpha = 0.5 + \frac{x_c}{d} = 0.5 + \frac{64}{360} = 0.678.$$

The ratio d/t is 46.1. The maximum ratio for a Class 2 web is $456\epsilon/(13\alpha - 1)$ where $\epsilon = (235/355)^{1/2} = 0.814$, so the limit is

$$\frac{d}{t} \leqslant \frac{456 \times 0.814}{7.81} = 47.5$$

and the web is just within Class 2. This can also be seen from Fig. 3.14.

From Fig. 4.1(b), the lever arm for the forces F_s is

$$z = \frac{h_a}{2} + h_s - \frac{x_c}{2} = 203 + 114 - 32 = 285 \text{ mm}.$$

For the steel section,

$$M_{\text{apl.Rd}} = W_a \frac{f_y}{\gamma_a} = 1.194 \times \frac{355}{1.1} = 385 \text{ kN m},$$

so from equation (4.6)

$$\boldsymbol{M_{\text{h.Rd}}} = 385 + 322 \times 0.285 = \mathbf{477\ kN\ m}.$$

4.2.1.3 Elastic moment of resistance

In the preceding calculation, it was possible to neglect the influence of the method of construction of the beam, and the effects of creep, shrinkage, and temperature, because these become negligible before the plastic moment of resistance is reached.

Where elastic analysis is used, creep is allowed for in the choice of the modular ratio $n(= E_a/E_c')$, and so has no influence on the properties of all-steel cross-sections. In buildings the effects of shrinkage and temperature on moments of resistance can usually be neglected, but the method of construction has to be allowed for. Here, we assume that at the section considered, the loading causes hogging bending moments $M_{a.Sd}$ in the steel member alone, and $M_{c.Sd}$ in the composite member. The small difference ($\approx 3\%$) between the elastic moduli for reinforcement and structural steel is usually neglected.

The height x_e of the elastic neutral axis of the composite section (Fig. 4.1(c)) above that of the steel section is found by taking first moments of area about the latter axis:

$$x_e(A_a + A_s) = A_s\left(\frac{h_a}{2} + h_s\right), \tag{4.7}$$

and the second moment of area of the composite section is

$$I = I_a + A_a x_e^2 + A_s\left(\frac{h_a}{2} + h_s - x_e\right)^2. \tag{4.8}$$

The yield moment is almost always governed by the total stress in the steel bottom flange (at level 4 in Fig. 3.25(a)). The compressive stress due to the moment $M_{a.Sd}$ is:

$$\sigma_{a4} = M_{a.Sd}\frac{h_a/2}{I_a}. \tag{4.9}$$

The remaining stress available is $f_y/\gamma_a - \sigma_{a4}$, so the yield moment is:

$$M_{a.Sd} + M_{c.Rd} = M_{a.Sd} + \frac{(f_y/\gamma_a - \sigma_{a4})I}{(h_a/2 + x_e)}. \tag{4.10}$$

The design condition is:

$$M_{c.Sd} \leqslant M_{c.Rd}. \tag{4.11}$$

The bending moment $M_{a.Sd}$ causes no stress in the slab reinforcement. In propped construction, the tensile stress σ_{sl} in these bars may govern design. It is

$$\sigma_{sl} = M_{c.Rd} \frac{(h_a/2 + h_s - x_e)}{I} \tag{4.12}$$

and must not exceed f_{sk}/γ_s.

Worked example

Let us now assume that the composite section shown in Fig. 4.1(a) is in Class 3, and that at the ultimate limit state, a hogging moment of 163 kN m acts on the steel section alone, due to the use of unpropped construction.

What is the design resistance of the section to hogging moments?

From equation (4.7) the position of the elastic neutral axis of the composite section, neglecting concrete in tension, is given by

$$x = \frac{804(0.203 + 0.114)}{7600 + 804} = 0.030 \text{ m}.$$

From equation (4.8), the second moment of area is

$$10^{-6}I = 215 + 7600 \times 0.03^2 + 804(0.203 + 0.114 - 0.03)^2$$
$$= 288 \text{ mm}^4.$$

From tables, the elastic section modulus for the steel section is 1.058×10^6 mm^3, so the moment $M_{a.Sd}$ causes a compressive stress at level 4 (the bottom flange):

$$\sigma_{a4} = \frac{163}{1.058} = 154 \text{ N/mm}^2.$$

The design yield strength is 355/1.1 = 323 N/mm^2, so this leaves 169 N/mm^2 for resistance to the load applied to the composite member. The distance of the bottom fibre from the elastic neutral axis is $h_a/2 + x_e = 0.203 + 0.03 = 0.233$ m, so the remaining resistance is

$$M_{c.Rd} = \frac{\sigma I}{y} = 169 \times \frac{288}{233} = 208 \text{ kN m}.$$

It is evident from the stress distributions in Fig. 4.1(c) that yield occurs first in the bottom fibre. The design resistance is

$$\boldsymbol{M_{a.Sd} + M_{c.Rd} = 163 + 208 = 371 \text{ kN m}}.$$

From the preceding worked example, the shape factor is

$$S = \frac{M_{h.Rd}}{M_{el.Rd}} = \frac{477}{371} = 1.29.$$

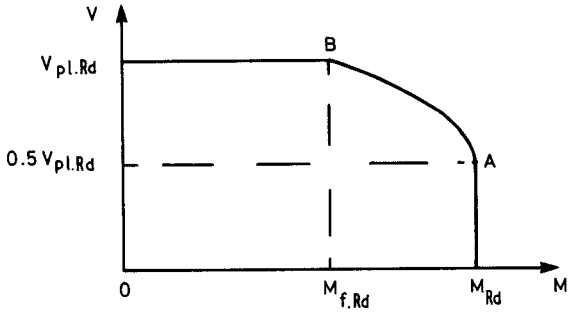

Fig. 4.2 Resistance to combined bending and vertical shear.

4.2.2 Vertical shear, and moment–shear interaction

As explained in Section 3.5.4, vertical shear is assumed to be resisted by the web of the steel section (equations (3.69) and (3.70)). The action effect V_{Sd} must not exceed the plastic shear resistance $V_{pl.Rd}$ (or some lower value if shear buckling, not considered here, can occur).

The design rule of Eurocode 4: Part 1.1[12] for resistance in combined bending (whether hogging or sagging) and shear is shown in Fig. 4.2. It is based on evidence from tests that there is no reduction in bending resistance until $V_{Sd} > 0.5V_{pl.Rd}$ (point A in the figure), and the assumption that the reduction at higher shears follows the parabolic curve AB. At point B the remaining bending resistance $M_{f.Rd}$ is that contributed by the flanges of the composite section, including the reinforcement in the slab. Along curve AB, the reduced bending resistance is given by

$$M_{v.Rd} = M_{f.Rd} + (M_{Rd} - M_{f.Rd})\left[1 - \left(\frac{2V_{Sd}}{V_{pl.Rd}} - 1\right)^2\right] \qquad (4.13)$$

where M_{Rd} is the resistance when $V_{Sd} = 0$.

When calculating $M_{f.Rd}$, it is usually accurate enough to ignore the reinforcement in the slab. When it is included, or where the steel flanges are of unequal size, only the weaker of the two flanges will be at its design yield stress.

4.2.3 Longitudinal shear

Section 3.6 on longitudinal shear is applicable to continuous beams and cantilevers, as well as to simply-supported spans. Some additional comments, relevant to continuous beams, are now given.

For a typical span with uniformly distributing loading, there are only three critical cross-sections: at the supports and at the section of maximum sagging moment. Points of contraflexure are not treated as critical sections

because their location is different for each load case; a complication best avoided. The number of shear connectors required for a typical critical length is

$$N = \frac{F_c + F_t}{P_{Rd}} \qquad (3.73)\text{bis}$$

where F_t is the design tensile force in the reinforcement that is assumed to contribute to the hogging moment of resistance, and F_c is the compressive force required in the slab at midspan, which may be less than the full-interaction value.

Full shear connection is assumed in regions of hogging moment, when N is calculated; but as the connectors may be spaced uniformly between a support and the critical section at midspan, the number provided in the hogging region may not correspond to the force F_t. It is required in Eurocode 4 that the shear connectors shall be spaced to suit the curtailment of tension reinforcement; but in practice it is more likely that the length of these reinforcing bars will be related to the spacing of the shear connectors, as the latter is constrained by the size and spacing of the troughs in profiled sheeting.

There are several reasons for the apparently conservative requirement of Eurocode 4 that full shear connection be provided in hogging regions:

(1) To compensate for some simplifications that may be unconservative:
- neglect of the tensile strength of concrete,
- neglect of strain-hardening of reinforcement,
- neglect of shear due to reinforcement (e.g. welded mesh) provided for crack-width control that is neglected at ultimate limit states.

(2) Because the design resistance of connectors, P_{Rd}, is assumed not to depend on whether the surrounding concrete is in compression or tension. There is evidence that this is slightly unconservative for hogging regions,[24] but slip capacity is probably greater, which is beneficial.

(3) For simplicity in design, including design for lateral buckling (Section 4.2.4) and for vertical shear with tension-field action.[43]

The worked example in Section 4.6 illustrates the situation where the design resistance to hogging bending is that of the steel section alone, so that $F_t = 0$ in equation (3.73), even though light reinforcement is present. It would be prudent then to provide shear connection for that reinforcement, as otherwise the uniform spacing of connectors could lead to under-provision in the sagging region.

Transverse reinforcement

As for sagging regions, this reinforcement should be related to the shear resistance of the connectors provided, even where, for detailing reasons, their resistance exceeds the design longitudinal shear.

4.2.4 Lateral buckling

Conventional 'non-distortional' lateral buckling occurs where the top flange of a simply-supported steel beam of I-section has insufficient lateral restraint in the midspan region. Both flanges are assumed to be restrained laterally at the supports, where the member may be free to rotate about a vertical axis. The top flange, in compression, is prevented by the web from buckling vertically, but if the ratio of its breadth b_f to the span L is low, it may buckle laterally as shown in Fig. 4.3(a). The cross-section rotates about a longitudinal axis, but maintains its shape.

It has to be checked that this 'lateral torsional' buckling does not occur during casting of the concrete for a composite beam; but once the concrete has hardened, the shear connection prevents buckling of this type. The relevant design methods, being for non-composite beams, are outside the scope of this book.

Near internal supports of continuous beams, the compressed bottom flange of the steel section receives lateral support only through a flexible web; but the slab does prevent twisting of the steel section as a whole. The flange can only buckle if the web bends, as shown in Fig. 4.3(b). This is known as 'distortional' lateral buckling, and is the subject of this section.

The buckle consists of a single half-wave each side of an internal support, where lateral restraint is invariably provided. The half-wave extends over most of the length of the hogging moment region. It is not sinusoidal, as the point of maximum lateral displacement is within two or three beam depths of the support, as shown in Fig. 4.4.

It is unlike local flange buckling, where the movement is essentially vertical, not lateral, and where the cross-section of maximum displacement is within one flange-width of the support. There is some evidence from tests[44,45] that local buckling can initiate lateral buckling, but in design they are considered separately, and in different ways. Local buckling is allowed for by the classification system for steel elements in compression

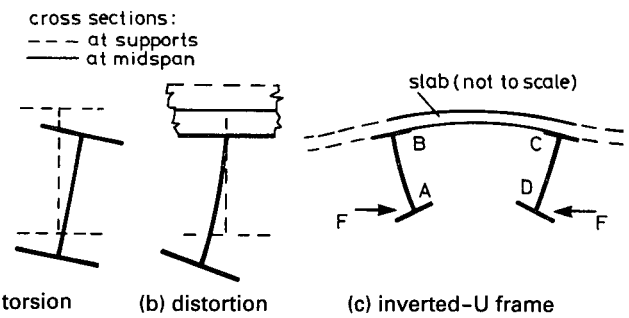

Fig. 4.3 Lateral buckling.

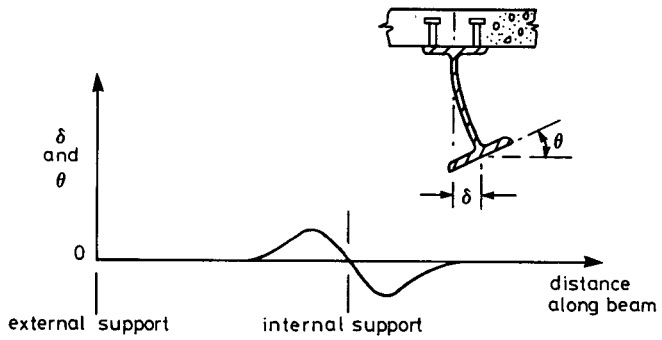

Fig. 4.4 Typical deformation of steel bottom flange in distortional lateral buckling.

(Section 3.5.2). Lateral buckling is avoided by reducing the design moment of resistance at the internal support, $M_{h.Rd}$, to a lower value, $M_{b.Rd}$. Local buckling occurs where the breadth-to-thickness ratio of the flange (b_f/t_f) is high; lateral buckling occurs where it is low.

Where, as is usual in buildings, the beam is one of several parallel members, all attached to the same concrete or composite slab, design is usually based on the 'continuous inverted-U frame' model. The tendency for the bottom flange to displace laterally causes bending of the steel web, and twisting at top-flange level, which is resisted by bending of the slab, as shown in Fig. 4.3(c).

Elastic critical moment

Design to Eurocode 4: Part 1.1 is based on the elastic critical moment M_{cr} at the internal support. The theory for M_{cr} considers the response of a single U-frame (ABCD in Fig. 4.3(c)) to equal and opposite horizontal forces F at bottom-flange level. It leads to the following rather complex expression for M_{cr}:

$$M_{cr} = \frac{k_c C_4}{L}\left[\left(GI_{at} + \frac{k_s L^2}{\pi^2}\right) E_a I_{afz}\right]^{1/2} \tag{4.14}$$

where: E_a and G are the elastic modulus and shear modulus of steel,
I_{at} is the St Venant torsion constant for the steel section,
I_{afz} is $b_f^3 t_f/12$ for the steel bottom flange, and
L is the span.

Where the steel section is symmetric about both axes, k_c is a property of the composite section (which properties A and I_y) given by

$$k_c = \frac{h_s I_y / I_{ay}}{\left[\dfrac{h_s^2/4 + (I_{ay} + I_{at})/A_a}{e}\right] + h_s} \tag{4.15}$$

where

$$e = \frac{AI_{ay}}{A_a z_c (A - A_a)} \tag{4.16}$$

and A_a, I_{ay} and I_{az} are properties of the structural steel section. (It should be noted that in Eurocodes, and here, subscripts y and z refer to the major and minor axes of a steel section, respectively. British practice has been to use x and y.) The dimensions h_s and z_c are shown in Fig. 4.5.

The term k_s is the stiffness of the U frame, per unit length along the span, given by

$$k_s = \frac{k_1 k_2}{k_1 + k_2}. \tag{4.17}$$

The stiffness of the slab is represented by k_1. Where the slab is in fact continuous over the beams, even when it is designed as simply-supported, the stiffness may be taken as

$$k_1 = \frac{4E_a I_2}{a} \tag{4.18}$$

where a is the spacing of the beams and I_2 is the 'cracked' flexural stiffness of the slab above the beams, when calculated using the area of top reinforcement per unit length of beam. This reinforcement should be sufficient to provide the slab with a resistance to hogging bending, M_{Rd}, that satisfies

$$M_{Rd} \geq \frac{t_w^2}{4} \frac{f_y}{\gamma_a}. \tag{4.19}$$

This is to ensure that the slab can resist the transverse bending moment applied to it by the steel web (Fig. 4.3(c)), even when the slab is designed as simply-supported on the beams. The reinforcement provided for control of

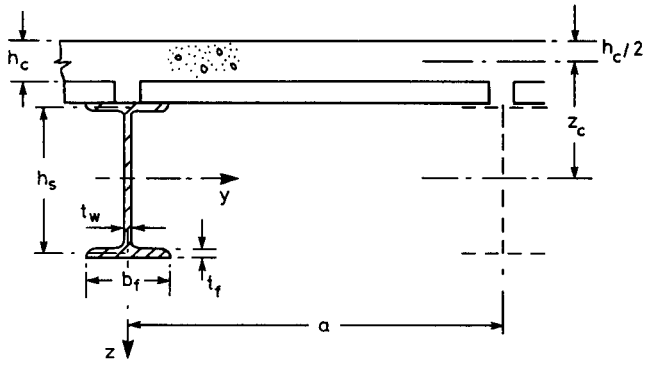

Fig. 4.5 Inverted-U frame.

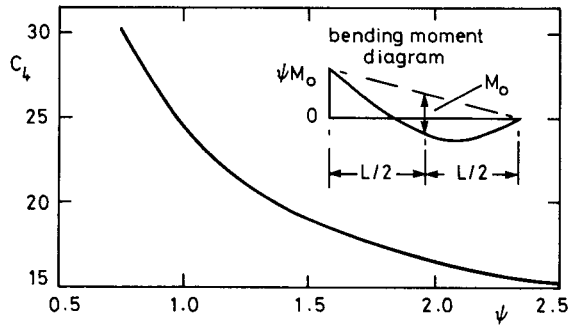

Fig. 4.6 Factor C_4 for an end span of a continuous beam.

cracking and for fire design of the slab will often be sufficient for this purpose.

The stiffness of the web is represented by k_2. For an uncased web,

$$k_2 = \frac{E_a t_w^3}{4(1 - \nu_a^2) h_s} \tag{4.20}$$

where ν_a is Poisson's ratio for steel. For an I-section with the web (only) encased in concrete, as used in the design example here,

$$k_2 = \frac{E_a t_w b_f^2}{16 h_s (1 + 4nt_w/b_f)} \tag{4.21}$$

where n is the modular ratio for long-term effects. Equation (4.21) was derived by elastic theory, treating the concrete on one side of the web (Fig. 3.31) as a strut that restrains upward movement of the steel bottom flange below it.

The buckling moment M_{cr} is strongly influenced by the shape of the bending-moment distribution for the span considered. This is allowed for by the factor C_4, values for which were obtained by finite-element analyses. They range from 6.2 for uniform hogging moment, to above 40 where the region of hogging moment is less than one-tenth of the span. Values relevant to the design example are given in Fig. 4.6.

In equation (4.14) the term GI_{at} gives the contribution from St Venant torsion of the section. It is usually small compared with $k_s L^2/\pi^2$ and then can be neglected with little loss of economy. The expression then becomes

$$M_{cr} \approx \frac{k_c C_4}{\pi} (k_s E_a I_{afz})^{1/2} \tag{4.22}$$

which is independent of the span L. This enables the values of C_4 to be used for all span lengths.

Equation (4.14) for M_{cr} is valid only where rules for minimum spacing of connectors, bending stiffness of the composite slab, and proportions of the

steel I-section, are satisfied. A more detailed explanation of this method and simplified versions of some of its rules are available elsewhere.[15]

Buckling moment

The value M_{cr} is relevant only to an initially perfect member that remains elastic. Evidence is limited on the influence of initial imperfections, residual stresses, and yielding of steel on this type of buckling; but the Perry–Robertson formulation and the strut curves developed for overall buckling of steel columns provide a suitable basis. The method of Eurocode 4: Part 1.1 is therefore as follows.

The slenderness $\bar{\lambda}_{LT}$ is given for a Class 1 or 2 section by

$$\bar{\lambda}_{LT} = \left(\frac{M_{pl}}{M_{cr}}\right)^{1/2} \tag{4.23}$$

where M_{pl} is the value that would be obtained for $M_{h.Rd}$ (equation (4.6)) if γ_a and γ_s were taken as 1.0. This is because these factors do not occur in the calculation of M_{cr}. For a Class 3 section, M_{pl} is replaced by the yield moment.

The buckling moment is given by

$$M_{b.Rd} = \chi_{LT} M_{h.Rd} \tag{4.24}$$

where χ_{LT} is a function of $\bar{\lambda}_{LT}$ that in practice is taken from the relevant strut curve in Eurocode 3: Part 1.1. For rolled steel sections this curve is given by

$$\chi_{LT} = \left[\phi_{LT} + (\phi_{LT}^2 - \bar{\lambda}_{LT}^2)^{1/2}\right]^{-1} \quad \text{but} \quad \chi_{LT} \geqslant 1 \tag{4.25}$$

where

$$\phi_{LT} = 0.5\left[1 + 0.21(\bar{\lambda}_{LT} - 0.2) + \bar{\lambda}_{LT}^2\right]. \tag{4.26}$$

From these equations $\chi_{LT} = 1$ when $\bar{\lambda}_{LT} \leqslant 0.2$.

However, evidence from tests and from experience shows that distortional lateral buckling does not reduce bending resistance to below $M_{h.Rd}$ until $\bar{\lambda}_{LT}$ exceeds about 0.4, so Eurocode 4 gives a rule that χ_{LT} may be taken as 1.0 where $\bar{\lambda}_{LT} \leqslant 0.4$. It then drops suddenly (e.g. to 0.95 where $\bar{\lambda}_{LT} = 0.41$), which is a minor defect of the code.

Simplified expression for $\bar{\lambda}_{LT}$

For cross-sections in Class 1 or 2, and with some loss of economy, equation (4.23) can be replaced by

$$\bar{\lambda}_{LT} = 5.0\left(1 + \frac{t_w h_s}{4 b_f t_f}\right)\left[\left(\frac{f_y}{E_a C_4}\right)^2 \left(\frac{h_s}{t_w}\right)^3 \left(\frac{t_f}{b_f}\right)\right]^{0.25} \tag{4.27}$$

provided that the steel section is symmetrical about both axes. This gives a much simpler calculation. An account of its derivation is available.[15]

Exemption from check on buckling
Extensive computations based on $\lambda_{LT} = 0.4$ enabled conditions to be given in Eurocode 4 under which no detailed check on resistance to lateral buckling need be made. The principal condition relates to the overall depth h_a of the steel I-section. For steel with $f_y = 355$ N/mm^2, this is that for IPE sections

$$\left.\begin{aligned} h_a &\leqslant 400 \text{ mm} \\ \text{or, if the web is encased,} \qquad & \\ h_a &\leqslant 600 \text{ mm.} \end{aligned}\right\} \tag{4.28}$$

The IPE sections generally have thicker webs than British UB sections. To qualify for this relaxation, UB sections must satisfy

$$\left(\frac{h_s}{t_w}\right)^3 \frac{t_f}{b_f} \leqslant \frac{5.52 \times 10^8}{f_y^2} \tag{4.29}$$

and

$$h_s t_w \leqslant 0.45 A_a \tag{4.30}$$

where f_y is in N/mm^2 units, and other symbols are as in Fig. 4.5. Many of them do not conform, so further work on simplification is needed.

Use of bracing
Where the buckling resistance of a beam has to be checked, and has been found using equation (4.24) to be less than the required resistance, the possibilities are as follows:

(1) Use the longer method of calculation for M_{cr}, equation (4.14), which is generally less conservative.
(2) Use a steel section with a less slender web or an encased web.
(3) Provide lateral bracing to compression flanges in the hogging moment region.

Lateral bracing is commonly used in bridges, but is less convenient in buildings, where the spacing between adjacent beams is usually wider, relative to their depth. Some examples of possible types of bracing are given in a book that covers lateral buckling of haunched composite beams.[46]

Little else has been published on the use of bracing for beams in buildings. It interferes with the provision of services, and is best avoided.

4.2.5 Cracking of concrete

'Cracking is almost inevitable where reinforced concrete elements of composite beams are subject to tension resulting from either direct loading or restraint of imposed deformations'. This clause from Eurocode 4: Part

1.1[12] distinguishes between two types of cracking. These are treated separately in Eurocode 4, which follows closely the rules for crack-width control given in Eurocode 2: Part 1.1.[10] In the design of reinforced concrete it is usually obvious whether reinforcement is required to resist 'direct loading', or whether cracking will result from tensile strains imposed on the element considered. The origin of these strains can be 'extrinsic' (external to the member), such as differential settlement of the supports of a continuous beam, or 'intrinsic' (inherent in the member), such as a temperature gradient or shrinkage of the concrete.

In reinforced concrete, cracking has little influence on tensile forces caused by direct loading, but it reduces the restraint of an imposed deformation, and so reduces the tensile force that caused the cracks. Calculations for load-induced cracking are therefore based on the tensile force in the reinforcement after cracking (i.e. on the analysis of cracked cross-sections), whereas calculations for restraint cracking are based on the tensile force in the concrete just before it cracks.

These concepts are more difficult to apply to composite members, where there is local restraint from the axial and flexural stiffnesses of the structural steel component, applied through the shear connectors or by bond. In a web-encased beam, for example, where the steel tension flange is stressed by direct loading, the result strains and curvature impose a deformation on the concrete that encases the web. Are the resulting cracks load-induced or restraint-induced?

Such dilemmas, and the differences between beam-to-column connections in composite and reinforced concrete frames, made it impossible to cover cracking in Eurocode 4 simply by cross-reference to Eurocode 2 for reinforced concrete; and led to a 'stand-alone' treatment of two situations: cracking in a slab that is part of the tension flange of a composite beam, and in the concrete encasement of a steel web.

'Cracking shall be limited to a level that will not be expected to impair the proper functioning of the structure or cause its appearance to be unacceptable'. This quotation, also from Eurocode 4: Part 1.1, refers to function and appearance. Within buildings, the concrete of composite beams is usually subjected to exposure, Class 1 of Eurocode 2: Part 1.1, 'dry environment', where crack width has no influence on corrosion of reinforcement or on durability. This would not be true, however, for the humid environment of a laundry or an open-air multi-storey car park.

The appearance of a concrete surface may be important where a web-encased beam is visible from below, but the top surface of a slab is usually concealed by the floor finish or roof covering. Where the finish is flexible (e.g. a fitted carpet) there may be no need to specify a limit to the width of cracks; but for brittle finishes or exposed slabs, crack-width control is essential.

Limiting crack widths are normally specified as a characteristic value w_k,

with a 20% probability of exceedence. Provision is made in Eurocode 4 for design to the following specifications:

(1) no control (for Class 1 exposure only);
(2) $w_k = 0.5$ mm;
(3) $w_k = 0.3$ mm (for exposure Classes 2 to 4, but not Class 5, 'aggressive chemical environment');
(4) $w_k < 0.3$ mm.

For cases (1) to (3), simplified rules are given that do not involve the calculation of crack widths. These are outlined below. For case (4), crack widths have to be calculated, in accordance with the Principles of Eurocode 2: Part 1.1. This case rarely arises in buildings and is not considered further.

4.2.5.1 No control of crack width

This statement is relevant to serviceability limit states. It is still necessary to ensure that the concrete retains sufficient integrity to resist shear at ultimate limit states, by acting as a continuum. It is therefore specified in Eurocode 4 that longitudinal reinforcement in a concrete flange in tension shall be not less than:

- 0.4% of the area of concrete, for propped construction, or
- 0.2% of the area of concrete, for unpropped construction.

At present, no account is taken of the presence of profiled steel sheeting, which may be conservative in some situations.

4.2.5.2 Control of restraint-induced cracking

Uncontrolled cracking between widely-spaced bars is avoided, and crack widths are limited, by:

- using small-diameter bars, which have better bond properties and have to be more closely spaced than larger bars;
- using 'high-bond' bars (ribbed bars or welded mesh);
- ensuring that the reinforcement remains elastic when cracking first occurs.

The last of these requirements is relevant to restraint cracking, and leads to a design rule for minimum reinforcement, irrespective of the loading, as follows.

Let us assume that an area of concrete in uniform tension, A_c, with an effective tensile strength, f_{cte}, has an area A_s of reinforcement with yield strength f_s. Just before the concrete cracks, the force in it is $A_c f_{cte}$ and the whole of the force is transferred to the reinforcement, which will not yield if

$$A_s f_s \geqslant A_c f_{cte}. \tag{4.31}$$

This condition is modified, in Eurocode 4, by a factor 0.8 that takes account of self-equilibrating stresses within the member (that disappear on cracking), and by a factor

$$k_c = \frac{1}{1 + (h_c/2z_o)} \geqslant 0.7 \tag{4.32}$$

that allows for the non-uniform tension in the concrete prior to cracking. In equation (4.32), h_c is the thickness of the concrete flange, excluding any ribs, and z_o is the distance of the centroid of the uncracked composite section (for short-term loading) below the centroid of the concrete flange. Thus, in a very deep beam, where the tension in the flange is almost uniform, $z_o \gg h_c$, and $k_c \approx 1$.

Finally, f_s in equation (4.31) is replaced by σ_{st}, the maximum stress permitted in the reinforcement immediately after cracking ($\leqslant f_{sk}$) which influences the crack width. This leads to the design rule

$$A_s \geqslant \frac{0.8\, k_c f_{cte} A_c}{\sigma_{st}}. \tag{4.33}$$

To use this rule, it is necessary to estimate the value of the tensile strength f_{cte} when the concrete first cracks. If the intrinsic deformation due to the heat of hydration or the shrinkage of the concrete is large, cracking could occur within a week of casting, when f_{cte} is still low. Where this is uncertain, it may be appropriate to use the mean value of the tensile strength corresponding to the specified 28-day strength of the concrete, f_{ctm}, which is approximately $0.1 f_{ck}$, or $0.08 f_{cu}$, where f_{cu} is the specified cube strength.

The stress σ_{st} depends on the design crack width, w_k, the diameter ϕ of the reinforcing bars, and the value of f_{cte}. For $f_{cte} = 2.5$ mm^2, σ_{st} is as given in Fig. 4.7, but not exceeding f_{sk} for the bars to be used.

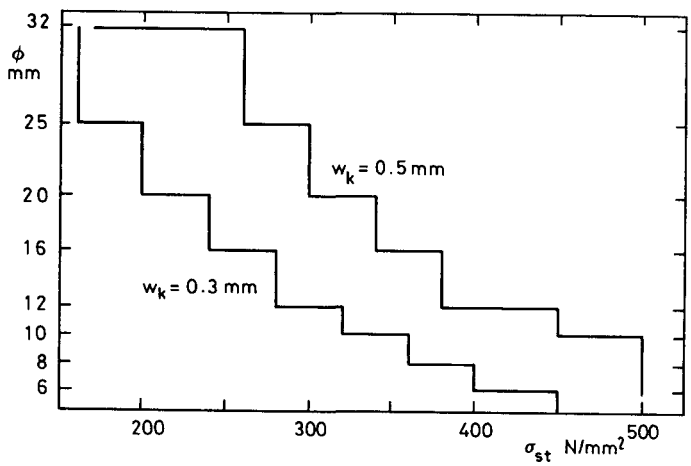

Fig. 4.7 Maximum steel stress for minimum reinforcement, high bond bars.

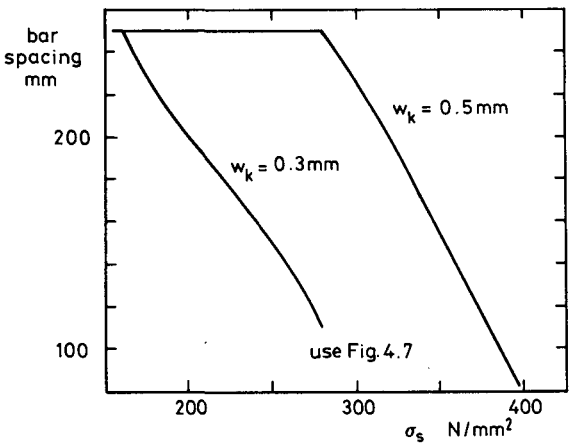

Fig. 4.8 Maximum bar spacing for high bond bars.

4.2.5.3 Control of load-induced cracking

A global analysis is required, to determine the bending moment at the cross-section considered. This is usually a cross-section at an internal support, where the hogging bending moment is a maximum.

The crack-width limit of 0.3 mm for exposure Classes 2 to 4 is associated in Eurocode 2: Part 1.1 with the quasi-permanent combination of actions (Section 1.3.2.4). It is thus assumed that there are no adverse effects if the cracks are wider for short periods when heavier variable loads are present. Where unpropped construction is used, load resisted by the steel member alone is excluded. The global analysis is elastic (Section 4.3.2). If relative stiffnesses are based on uncracked concrete in regions where the slab is in tension, the hogging moments will be overestimated, so limited redistribution of moments is allowed in Eurocode 4: up to 15% for hogging regions in Class 1 or 2, and up to 10% for Class 3 or 4.

The tensile stress in the reinforcement nearest to the relevant concrete surface is calculated by elastic section analysis, neglecting concrete in tension. This stress, σ_{se}, is then increased to a value σ_s by a correction for tension stiffening, given by

$$\sigma_s = \sigma_{se} + 0.4\frac{f_{ctm}A_c}{\alpha A_s} \tag{4.34}$$

where $\alpha = AI/A_aI_a$, and A and I are area of section and second moment of area, respectively, of the cracked composite section. The subscripts a, c, and s refer respectively to the structural steel section, the concrete flange, and the longitudinal reinforcement. The correction is largest for lightly reinforced slabs (high A_c/A_s) of strong concrete (high tensile strength f_{ctm}).

Crack control is achieved by limiting the spacing of the longitudinal reinforcing bars to the values shown in Fig. 4.8, which depend on σ_s and w_k. Where σ_s is outside the range of Fig. 4.8, bar diameter is limited instead, using Fig. 4.7.

A fuller explanation and discussion of the treatment of crack-width control in Eurocode 4: Part 1.1 is available.[15] These methods are not fully satisfactory or comprehensive, being based on a model originally developed for reinforced concrete beams. Research on crack control in composite members is limited (e.g. References 47 and 48). Further work will be needed for the Eurocode on composite bridges, where reliable control of cracking is more important than it is in buildings.

4.3 Global analysis of continuous beams

4.3.1 General

The subject of Section 4.3 is the determination of design values of bending moment and vertical shear for 'continuous beams' as defined in Section 4.1, caused by the actions specified for both serviceability and ultimate limit states.

Methods based on linear-elastic theory, treated in Section 4.3.2, are applicable for all limit states and all four classes of cross-section. The use of rigid-plastic analysis, also known as plastic hinge analysis, is applicable only for ultimate limit states, and is subject to the restrictions explained in Section 4.3.3; the resulting members may be lighter and/or shallower, and the analyses are simpler. This is because the design moments for one span are in practice independent of the actions on adjacent spans, of variation along the span of the stiffness of the member, of the sequence and method of construction, and of the effects of temperature and of creep and shrinkage of concrete. Accurate elastic analysis has none of these advantages, so simplifications have to be made.

Section 3.5.1, on effective cross-sections, applies also to midspan regions of continuous beams. For analysis of cross-sections, effective widths of hogging moment regions are generally narrower than those of midspan regions (Section 4.2.1), but for simplicity, effective widths for global analysis are assumed to be constant over the whole of each span, and are taken as the value at midspan. This does not apply to cantilevers, where the value at the support is used.

It is assumed in global analysis that the effects of longitudinal slip are negligible. This is reasonable, because partial shear connection is not used in regions of hogging moment. Its use slightly reduces the flexural stiffness of a midspan region, but for current levels of minimum shear connection, the uncertainty is probably less than that which results from cracking of concrete in hogging regions.

4.3.2 Elastic analysis

Elastic global analysis requires knowledge of relative (but not absolute) values of flexural rigidity (EI) over the whole length of the member analysed. At least three different values of EI are required at each cross-section, as follows:

(a) for the steel member alone (E_aI_a), for actions applied before the member becomes composite, where unpropped construction is used;
(b) for permanent loading on the composite member (E_aI), where I is determined, in 'steel' units, by the method of transformed sections using a modular ratio E_a/E'_c, where E'_c is an effective modulus that allows for creep of concrete;
(c) for variable loading on the composite member, as above, except that the modular ratio is E_a/E_{cm}, and E_{cm} is the mean secant modulus for short-term loading.

The values (b) and (c) also depend on the sign of the bending moment. In principle, separate analyses are needed for the actions in (a), and (b), and for each relevant arrangement of variable loading in (c).

In practice, the following simplifications are made wherever possible.

(1) A value I calculated for the uncracked composite section (denoted I_1 in Eurocode 4) is used throughout the span. This is referred to as 'uncracked' analysis.
(2) A single value of I, based on a modular ratio $\frac{1}{2}[(E_a/E'_c) + (E_a/E_{cm})]$, is used for analyses of both types (b) and (c).
(3) Where all spans of the beams have cross-sections in Class 1 or 2 only, the influence of method of construction is neglected in analyses for ultimate limit states only, and actions applied to the steel member alone are included in analyses of type (b).

Separate analyses of type (c) are always needed for different arrangements of variable loading. It is often convenient to analyse the member for unit distributed loading on each span in turn, and then obtain the moments and shears for each load arrangement by scaling and combining the results.

The alternative to 'uncracked' analysis is to use in regions where the slab is cracked a reduced value of I (denoted I_2 in Eurocode 4), calculated neglecting concrete in tension but including its reinforcement. This is known as 'cracked' analysis. Its weakness is that there is no simple or reliable method for deciding which parts of each span are 'cracked'. They are different for each load arrangement, and are modified by the effects of tension stiffening, previous loadings, temperature, creep, shrinkage, and longitudinal slip. A common assumption is that 15% of each span, adjacent to each internal support, is 'cracked'. (Relevant evidence is given in Volume 2.)

In practice, 'uncracked' analysis is usually preferred for ultimate limit states, with allowance for cracking by redistribution of moments. 'Cracked' analysis is used for deflections, as explained in Section 4.3.2.3.

4.3.2.1 Redistribution of moments in continuous beams

Redistribution is an approximate but simple method of modifying the results of an elastic global analysis to allow for the inelastic behaviour that occurs in all materials in a composite beam before maximum load is reached, and also to allow for the effects of cracking of concrete at serviceability limit states. It is also used in the analysis of beams and frames of structural steel and of reinforced concrete, with limitations appropriate to the material and type of member.

It consists of modifying the bending-moment distribution found for a particular loading while maintaining equilibrium between the actions (loads) and the bending moments. Moments are reduced at cross-sections where the ratio of action effect to resistance is highest (usually, at the internal supports). The effect is to increase the moments of opposite sign (usually, in the midspan region).

For continuous composite beams, the ratio of action effect to resistance is higher at internal supports, and lower at midspan, than for most beams of a single material, and the use of redistribution is essential for economy in design. It is limited by the onset of local buckling of steel elements in compression, as shown in Table 4.1, which is taken from Eurocode 4: Part 1.1.

Table 4.1 Limits to redistribution of hogging moments, per cent of the initial value of the bending moment to be reduced.

Class of cross-section in hogging moment region	*1*	*2*	*3*	*4*
For 'uncracked' elastic analysis	40	30	20	10
For 'cracked' elastic analysis	25	15	10	0

The differences between the two sets of figures show that 'uncracked' analyses have been assumed to give hogging moments that are higher than those from 'cracked' analyses by amounts that are respectively 12%, 13%, 9% and 10% for Classes 1 to 4 (e.g. 140/125 = 1.12).

The hogging moments referred to are the peak values at internal supports, which do not include supports of cantilevers (at which the moment is determined by equilibrium and cannot be changed). Where the composite section is in Class 3 or 4, moments due to loads on the steel member alone are excluded. The values in Table 4.1 are based on research (e.g. Reference 49).

The use of Table 4.1, and the need for redistribution, is illustrated in the following example. The Eurocode also allows limited redistribution from midspan regions to supports, but this is rare in practice.

4.3.2.2 Example: redistribution of moments

A composite beam of uniform section (apart from reinforcement) is continuous over three equal spans L. The cross-sections are in Class 1. For the ultimate limit state, the design permanent load is g per unit length, and the variable load is q per unit length, with $q = 2_g$. The sagging moment of resistance, M_{Rd}, is twice the hogging moment of resistance, M'_{Rd}. Find the minimum required value for M_{Rd}:

(a) by elastic analysis without redistribution,
(b) by elastic analysis with redistribution to Table 4.1,
(c) by rigid-plastic analysis.

For simplicity, consider only the middle span ABC, and only symmetrical arrangements of variable load.

Bending moment distributions for the middle span given by 'uncracked' elastic analysis are shown in Fig. 4.9 for permanent load plus the following arrangements of variable load:

(1) q on all spans,
(2) q on the centre span only,
(3) q on the end spans only.

The moments are given as multiples of $gL^2/8$. Questions (a) to (c) are now answered.

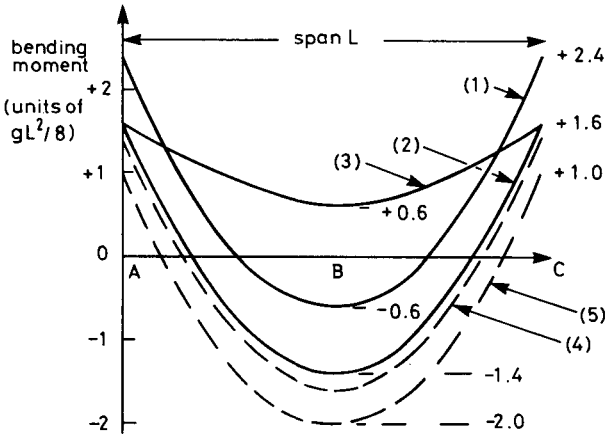

Fig. 4.9 Bending moment diagrams with redistribution.

(a) The peak hogging moment, 2.4 $gL^2/8$, governs the design, and since $M_{Rd} = 2M'_{Rd}$,

$$M_{Rd} \geq 4.8 \frac{gL^2}{8}.$$

(b) The peak hogging moment at each support is reduced by 40% to 1.44 $gL^2/8$. The corresponding sagging moment is $(0.6 + 0.96)gL^2/8 = 1.56$ $gL^2/8$ (curve (4)). For loadings (2) and (3), 10% redistribution is used, so that their peak hogging moments are also 1.44 $gL^2/8$. This value governs the design, so that

$$M_{Rd} \geq 2.88 \frac{gL^2}{8}.$$

(c) The method used is explained in Section 4.3.3. Redistribution is unlimited, so that support moments for loading (1) are reduced by 58%, to 1.0 $gL^2/8$.

The corresponding sagging moment is $(0.6 + 1.4)gL^2/8$ (curve (5)).Smaller redistributions are required for the other loadings.The available resistances at the supports and at midspan are fully used, when

$$M_{Rd} = 2.0 \frac{gL^2}{8}.$$

The preceding three results for M_{Rd} show that the resistance required is significantly reduced when the degree of redistribution is increased.

For composite beams, use of rigid-plastic analysis can imply even larger redistribution than the 58% found here.

4.3.2.3 Analysis for deflections

Cracking of concrete and yielding of steel have less influence on deflections in service than they do on analyses for ultimate limit states, because the design loads are lower. In short cantilevers and at some internal supports there may be very little cracking, so deflections may be overestimated by an analysis where redistribution is used as explained above. Where a low degree of shear connection is used, deflections may be increased by longitudinal slip between the slab and the steel beam.

For these reasons, both Eurocode 4: Part 1.1[12] and BS 5950[14] give modified methods of elastic analysis for the prediction of bending moments at internal supports of continuous beams. Let these hogging moments be M_1 and M_2, for a loading that would give a maximum sagging moment M_o and a maximum deflection δ_o, if the span were simply-supported. It can be shown by elastic analysis of a member of uniform section with uniformly-distributed load, that the moments M_1 and M_2 reduce the midspan deflection from δ_o to δ_c, where

$$\delta_c = \delta_o \left[1 - 0.6 \frac{M_1 + M_2}{M_o}\right]. \qquad (4.35)$$

This equation is quite accurate for other realistic loadings, and is given in BS 5950 for general use. It shows the significance of end moments. For example, if $M_1 = M_2 = 0.42M_o$, the deflection δ_o is halved. It is not strictly correct to assume that the maximum deflection occurs at midspan but the error is negligible.

The method of Eurocode 4 is now described, followed by that of BS 5950. Shear lag has little effect on deflections, but section properties based on the effective flange width are often used, as they are needed for other calculations.

The general method given for allowing for the effects of cracking at internal supports involves two stages of calculation. The 'uncracked' flexural stiffness E_aI_1 is needed for each span, and also the 'cracked' flexural stiffness E_aI_2 at each internal support.

For the load arrangements considered, the bending moments due to the load applied to the composite member are first calculated using stiffnesses E_aI_1. At each internal support, the maximum tensile stress in the concrete due to the relevant moment is calculated. This is repeated for other relevant load arrangements. Let the highest tensile stress thus found, at a particular support, be σ_{ct}. If this stress exceeds $0.15f_{ck}$ (where f_{ck} is the characteristic cylinder strength), the stiffness E_aI_1 is replaced by E_aI_2 over 15% of the length of the span on each side of that support.

The analyses for bending moments are then repeated using the modified stiffnesses, and the results are used whether the new values σ_{ct} exceed $0.15f_{ck}$, or not. This method is based on one that has been used for composite bridge beams since 1967.[50]

Eurocode 4 gives an alternative to re-analysis of the structure, applicable for beams with critical sections in Class 1, 2 or 3. It is that at every support where $\sigma_{ct} > 0.15f_{ck}$, the bending moment is multiplied by f_1, where

$$f_1 = \left(\frac{E_aI_1}{E_aI_2}\right)^{-0.35} \geqslant 0.6, \tag{4.36}$$

and corresponding increases are made in the sagging moments in adjacent spans. This method is available only for spans with equal loadings and approximately equal length.

Where unpropped construction is used and redistribution exceeding 40% is made in global analyses for ultimate limit states, it is likely that serviceability loads will cause local yielding of the steel beam at internal supports. In design to Eurocode 4, allowance may be made for this by multiplying the moments at relevant supports by a further factor f_2,

where $f_2 = 0.5$ if f_y is reached before the slab has hardened,
$f_2 = 0.7$ if f_y is reached due to extra loading applied after the slab has hardened.

These methods are used in the worked example in Section 4.6.5.

In BS 5950, the simplified methods given are based on global analyses

where the 'uncracked' stiffnesses E_aI_1 are used, and variable load is present on all spans. The hogging moments so found are reduced by empirical factors that take account of other arrangements of variable load.

Local yielding of the steel beam, if it occurs, causes an additional permanent deflection. This is referred to as 'shakedown' in BS 5950, and is allowed for by further reducing the hogging moments at the supports.

The calculation of deflections, with allowance for the effects of slip, is treated in Section 4.4.

4.3.3 Rigid-plastic analysis

For composite beams, use of rigid-plastic analysis can imply even larger redistributions of elastic moments than the 58% found in the preceding example, particularly where spans are of unequal length, or support concentrated loads.

Redistribution results from inelastic rotations of short lengths of beam in regions where 'plastic hinges' are assumed in the theory. Rotation may be limited either by crushing of concrete or buckling of steel, and so depends on the proportions of the relevant cross-sections, as well as on the shape of the stress–strain curves for the materials.

Research has led to limitations to the use of rigid-plastic global analysis for continuous composite beams. Those given in Eurocode 4: Part 1.1 include the following.

(1) At each plastic hinge location:
- lateral restraint shall be provided,
- the effective cross-section shall be in Class 1,
- the cross-section of the steel component shall be symmetrical about the plane of its web.

(2) All effective cross-sections in the member should be in Class 1 or 2.

(3) Adjacent spans should not differ in length by more than 50% of the shorter span.

(4) End spans should not exceed 115% of the length of the adjacent span.

(5) The member shall not be susceptible to lateral-torsional buckling (i.e. $\bar{\lambda}_{LT} \leqslant 0.4$).

(6) In any span L where more than half of the design load is concentrated within a length of $L/5$, then at any sagging hinge, not more than 15% of the overall depth of the member should be in compression, unless it can be shown that the hinge will be the last to form in that span.

The method of analysis is well known, being widely used for steel-framed structures, so only an outline is given here. The principal assumptions are as follows.

(1) Collapse (failure) of the structure occurs by rotation of plastic hinges at constant bending moment, all other deformations being neglected.

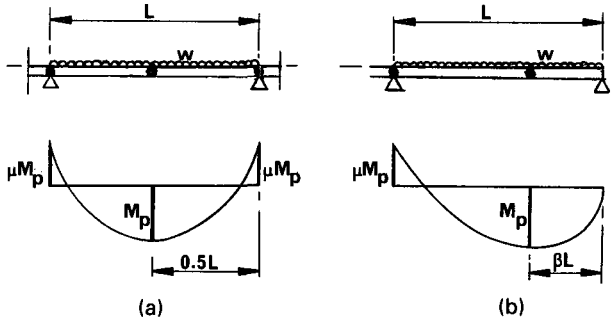

Fig. 4.10 Rigid-plastic global analysis.

(2) A plastic hinge forms where the bending moment due to the actions reaches the bending resistance of the member.
(3) All loads on a span increase in proportion until failure occurs, so the loading has to be represented by a single parameter.

The value of this parameter at collapse is normally found by assuming a collapse mechanism, and equating the loss of potential energy of the loads, due to a small movement of the mechanism, with the energy dissipated in the plastic hinges.

For a beam of uniform section, the only properties required are the moments of resistance at midspan, M_p, and at the internal support or supports, M'_p. Let

$$\frac{M'_p}{M_p} = \mu. \tag{4.37}$$

If the beam is continuous at both ends, Fig. 4.10(a), hinges occur at the ends and at midspan, and

$$(1 + \mu)M_p = \frac{wL^2}{8}. \tag{4.38}$$

If the beam is continuous at one end only, the bending moment diagram at collapse is as shown in Fig. 4.10(b). It can easily be shown that

$$\beta = \left(\frac{1}{\mu}\right)\left[(1 + \mu)^{1/2} - 1\right] \tag{4.39}$$

and

$$M_p = \frac{1}{2} w\beta^2 L^2. \tag{4.40}$$

4.4 Stresses and deflections in continuous beams

Values of bending stresses at serviceability limit states may be needed in calculations for control of load-induced cracking of concrete (Section

4.2.5.3). For prediction of deflections, stresses in the structural steel member should be calculated at internal supports where unpropped construction is used (Section 4.3.2.3), to establish whether a correction is needed for the effects of yielding.

Bending moments are determined by elastic global analysis (Section 4.3.2) and then stresses are found as in Section 3.5.3 for sagging moments, or Section 4.2.1 for hogging moments.

Deflections are much less likely to be excessive in continuous beams than in simply-supported spans, but they should always be checked where design for ultimate limit states is based on rigid-plastic global analysis. Once the bending moments at the ends of a span have been determined, the maximum deflection for a beam with full shear connection is given with sufficient accuracy by equation (4.35).

For simply-supported beams, the increase in deflection due to the use of partial shear connection can be neglected in certain circumstances (Section 3.7.1) and is otherwise given by equation (3.94). These same rules can be used for continuous beams, where they are a little conservative because partial shear connection is used only in regions of sagging bending moment.

The influence of shrinkage of concrete on deflections is treated in Section 3.8. For continuous beams, the effect is rarely significant. The method of calculation is rather complex, because shrinkage causes bending moments as well as sagging curvature. Details are given in Volume 2.

4.5 Design strategies for continuous beams

Until experience has been gained, the design of a continuous beam may involve much trial and error. There is no ideal sequence in which decisions should be made, but the following comments on this subject may be useful.

It is assumed that the span and spacing of the beams is known, that the floor or roof slab spanning between them has been designed, and that most or all of the loading on the beams is uniformly-distributed, being either permanent (g) or variable (q). The beams add little to the total load, so g and q are known.

One would not be designing a continuous beam if simply-supported spans were satisfactory, so it can be assumed that simple spans of the maximum available depth are too weak, or deflect or vibrate too much; or that continuity is needed for seismic design, or to avoid wide cracks in the slab, or for some other specific reason.

The provision for services must be considered early. Will the pipes and ducts run under the beams, through holes in the webs, or above the slab? Heavily-serviced buildings needing special solutions (castella beams, stub girders, haunched beams, etc.) are not considered here. The provision

of holes in webs of continuous beams is easiest where the ratio q/g is low, and a low q/g is also the situation where the advantages of continuity over simple spans are greatest.

Continuity is more advantageous in beams with three or more spans than where there are only two; and end spans should ideally be shorter than interior spans. The least benefit is probably obtained where there are two equal spans. Careful study of the worked example in this volume will show why. Using a steel section that could span 9.0 m simply-supported, it was quite difficult to design two continuous spans of only 9.5 m.

A decision with many consequences is the class of the composite section at internal supports. Two distinct strategies are now compared.

(1) Only crack-control reinforcement is provided in the slab, and is ignored in the ultimate-strength design. The composite section will probably be Class 1, and rigid-plastic global analysis can be used, unless $\bar{\lambda}_{LT} > 0.4$ (Section 4.2.4). Good use is made of the available bending resistance at midspan.

(2) The reinforcement in the slab at internal supports is used in ultimate-strength design, and has an effective area at least 1% of that of the slab. The composite section will certainly be in Class 2, perhaps Class 3. Restrictions on redistribution of moments will probably cause the design hogging moments, M'_{Sd} to increase (cf. strategy (1)) faster than the increase in resistance, M'_{Rd}, provided by the reinforcement, and further increase in the latter may put the section into Class 4. So the steel section may have to be heavier than for strategy (1), and there will be more unused bending resistance at midspan. However, that will allow a lower degree of shear connection to be used. With higher M'_{Sd} the bending-moment diagram for lateral–torsional buckling is more adverse. Deflections are less likely to be troublesome, but the increase in the diameter of the reinforcing bars makes crack-width control more difficult.

The method of fire protection to be used may have consequences for the structural design. For example, web encasement improves the class of the steel web and the resistance to lateral buckling.

Finally, it has to be decided whether construction will be propped or unpropped. Propped construction allows a shallower steel beam to be used – but it will be less stiff, so the dynamic behaviour may be less satisfactory. Propped construction costs more, and crack-width control is more difficult; but design is much less likely to be governed by excessive deflection.

The design presented in Section 4.6 is based on strategy (1) above, using a lightweight-concrete slab and an encased web. This is done to illustrate methods. It may not be an optimum solution.

4.6 Example: continuous composite beam

4.6.1 Data

So that use can be made of previous work, the design problem is identical with that of Chapter 3, except that the building (Fig. 3.1) now consists of two bays each of span 9.5 m. The transverse beams at 4 m centres are assumed to be continuous over a central longitudinal wall, and are simply supported on columns in the outer wall. Thus each beam is as shown in Fig. 4.11. The use of continuity should offset the increase in span from 9 m to 9.5 m, so it is assumed initially that the design of the slab and the midspan region of the beam are as before (Figs 3.12, 3.29 and 3.31), with the same materials, loads, and partial safety factors. The design loads per unit length of beam, represented by the general symbol w, and the corresponding values of the bending moment $wL^2/8$ for a span of 9.5 m are as given in Table 4.2.

Other design data from Chapter 3 are as follows.

Structural steel:	f_y	=	355 N/mm^2,	f_y/γ_a	=	323 N/mm^2.
Concrete:	f_{ck}	=	25 N/mm^2,	f_{ck}/γ_c	=	16.7 N/mm^2.
Bar reinforcement:	f_{sk}	=	460 N/mm^2,	f_{sk}/γ_s	=	400 N/mm^2.
Welded fabric:	f_{sk}	=	500 N/mm^2,	f_{sk}/γ_s	=	435 N/mm^2.
Shear connectors:	P_R	=	72.4 kN,	P_R/γ_v	=	57.9 kN.

Profiled steel sheeting: type CF 70/0.9, shown in Fig. 3.9.

Composite slab: 150 mm thick, with T8 bars at 150 mm (top) and at 300 mm (bottom), shown in Fig. 3.12, and concrete with $\rho = 1900$ kg/m^3.

Composite beam: steel section 406 × 178 UB 60, shown in Fig. 3.29, with shear connection as in Fig. 3.30 and encased web as in Fig. 3.31.

For the steel section:

$A_a = 7600$ mm^3, $10^{-6}W_{a.pl} = 0.208$ mm^3,
$10^{-6}I_{ay} = 215.1$ mm^4, $10^{-6}I_{az} = 12.0$ mm^4,
$M_{apl.Rd} = 386$ kN m, $V_{pl.Rd} = 614$ kN.

For the composite section at midspan:

$N_f = 42.4$ studs, $M_{pl.Rd} = 771$ kN m when $N = N_f$.

(The effect of the small increase in b_{eff}, for the longer span, is negligible.)

$10^{-6}I_1 = 738$ mm^4 for $n = 11$, with $x = 133$ mm,
$10^{-6}I_1 = 616$ mm^4 for $n = 22$, with $x = 185$ mm,
$10^{-6}I_1 = 547$ mm^4 for $n = 33$, with $x = 212$ mm,

where x is the depth of the neutral axis below the top of the slab.

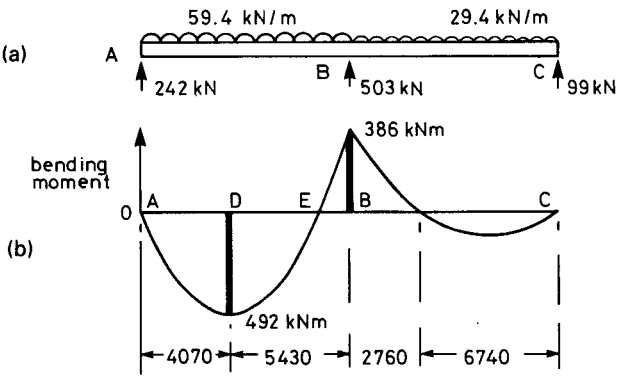

Fig. 4.11 Continuous beam, with collapse mechanism for span AB.

4.6.2 Flexure and vertical shear

If rigid-plastic global analysis can be used, the value of $wL^2/8$ that can be resisted by each span is a little less than

$$M_{\text{pl.Rd}} + 0.5M_{\text{apl.Rd}} = 964 \text{ kN m}$$

if no account is taken of reinforcement in the slab at the internal support, B, in Fig. 4.11. This is well above $wL^2/8$ for the loading (669 kN m, from Table 4.2), so this approach to design for the ultimate limit state will be tried.

It is easily shown by the methods of Section 4.2.1 that both the steel web and the compression flange are in Class 1 at support B, and that the composite section at midspan is also in Class 1.

It is assumed now, and checked in Section 4.6.3, that for lateral buckling of the bottom flange near support B, $\bar{\lambda}_{LT} \leqslant 0.4$. The other conditions for the use of plastic analysis (Section 4.3.3) are satisfied, provided that there is lateral restraint to the steel flange in compression, at each location of a plastic hinge. For sagging bending, the concrete slab restrains the flange. For hogging bending, the attachment to the supporting wall must provide restraint. The resistance required is not specified, but it can be inferred from codes for structural steelwork that the lateral force at bottom-flange level will not exceed 2% of the compressive force in the bottom flange.

In conventional plastic analysis of a beam with two equal spans, the mechanism of Fig. 4.10(b) is assumed for one of the spans, and the method of Section 4.3.3 is used to find the required sagging resistance M_p, for an assumed ratio μ of hogging to sagging resistance. Here, the hogging resistance is known, but the sagging resistance is not, because partial shear

Table 4.2 Loads and bending moments for a span of 9.5 m.

	Serviceability limit states		*Ultimate limit states*	
	Load kN/m	$wL^2/8$ kN m	*Load* kN/m	$wL^2/8$ kN m
Permanent, on steel beam	11.8	133	15.9	179
Permanent, composite	10.0	113	13.5	152
Variable, composite	20.0	226	30.0	338
Total	41.8	472	59.4	669

connection will be used to provide the resistance required, which will be less than the 771 kN m given in Section 4.6.1.

Span AB is therefore analysed for a loading of 59.4 kN/m, assuming that the hogging moment at B is 386 kN m, as shown in Fig. 4.11(a). The reaction at A is

$$R_A = \frac{1}{2} \times 59.4 \times 9.5 - \frac{386}{9.5} = 242 \text{ kN}.$$

The vertical shear is zero at point D, so the length AD is 242/59.4 = 4.07 m, and the sagging moment at D is given by

$$M_{D.Sd} = \frac{1}{2} \times 4.07 \times 242 = \mathbf{492\ kN\ m}.$$

Shear connection will be provided along AD sufficient to give a resistance of at least 492 kN m at D, so the rigid-plastic analysis gives collapse of span AB with hinges at D and B.

The minimum design loading for span BC is 29.4 kN/m. Elastic global analysis of ABC for the loads shown in Fig. 4.11(a) gives a hogging moment at B well above 386 kN m, so the actual value can be assumed to be 386 kN m, and the bending-moment diagram is as shown in Fig. 4.11(b). This is the most critical load arrangement for lateral buckling, because the length of span BC in compression, 2.76 m, is longer than it would be (1.36 m) if span BC were fully loaded.

The maximum vertical shear in span AB, at B, is

$$V_{Sd} = 59.4 \times 9.5 - 242 = \mathbf{322\ kN}.$$

This is 0.53 $V_{pl.Rd}$, so in principle the bending resistance should be reduced, using equation (4.13). The term in square brackets is 0.996 when $V_{Sd}/V_{pl.Rd} = 0.53$, so the reduction is obviously negligible.

4.6.3 Lateral buckling

The lateral stability of the steel bottom flange adjacent to support B is checked using the 'continuous U-frame' model explained in Section 4.2.4 and the bending-moment distribution shown for span BC in Fig. 4.11(b).

The UB section used here is not exempt from a check on buckling, according to Eurocode 4: Part 1.1, because its web is too slender to satisfy the condition of equation (4.29):

$$\left(\frac{h_s}{t_w}\right)^3 \frac{t_f}{b_f} f_y^2 = \left(\frac{393}{7.8}\right)^3 \frac{12.8}{178} 355^2 = 1.16 \times 10^9,$$

which exceeds the limit of 5.52×10^8.

Use of the simplified expression for the slenderness $\bar{\lambda}_{LT}$, equation (4.27), gives a value exceeding 0.4, for which rigid-plastic global analysis is not valid. The less conservative method that leads to equation (4.22) will therefore be used. This gives the elastic critical moment at the internal support:

$$M_{cr} \approx \frac{k_c C_4}{\pi} (k_s E_a I_{afz})^{1/2}. \qquad (4.22)\text{bis}$$

For this beam, $A = A_a$ and $I_y = I_{ay}$,so from equations (4.15) and (4.16), $k_c = 1.0$. For span BC in Fig. 4.11, $wL^2/8 = 29.4 \times 9.5^2/8 = 332$ kN m, so from Fig. 4.6, $\psi = 1.17$ and $C_4 = 22.2$.

The term k_s represents the stiffness of the U-frame:

$$k_s = \frac{k_1 k_2}{k_1 + k_2}. \qquad (4.17)\text{bis}$$

Equation (4.21) gives k_2 for a concrete-encased web. It is assumed that the normal-density encasement has a modular ratio of 22 for long-term effects, so that

$$k_2 = \frac{E_a t_w b_f^2}{16 h_s (1 + 4nt_w/b_f)} = \frac{210000 \times 7.8 \times 178^2}{16 \times 393(1 + 88 \times 7.8/178)}$$

$$= 1.70 \times 10^6 \text{ N}.$$

From equation (4.18), $k_1 = 4E_a I_2/a$, where $E_a I_2$ is the 'cracked' stiffness of the composite slab in hogging bending. To calculate I_2 the trapezoidal rib shown in Fig. 3.9 is replaced by a rectangular rib of breadth 162−13 = 149 mm. Using a modular ratio $n = 22$, the breadth of 'steel' rib is $149/(0.3 \times 22) = 22.6$ mm per metre width of slab, since the ribs are at 0.3 m spacing. The transformed section is thus as shown in Fig. 4.12. Reinforcement within the rib (Fig. 3.12) is neglected.

The position of the neutral axis is given by

$$\frac{1}{2} \times 22.6x^2 = 336(126 - x), \text{ whence } x = 48 \text{ mm},$$

then

$$10^{-6} I_2 = 336 \times 0.078^2 + 22.6 \times 48^3/3 = 2.88 \text{ mm}^4/\text{mm}.$$

From equation (4.18), with the beam spacing $a = 4.0$ m,

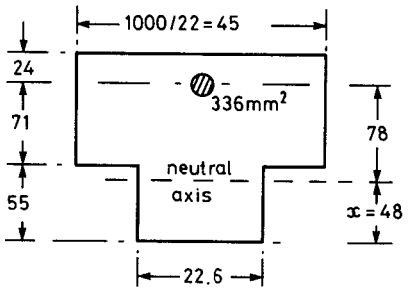

Fig. 4.12 Cracked section of composite slab for hogging bending.

$$k_1 = 4 \times 210000 \times \frac{2.88}{4} = 0.605 \times 10^6 \text{ N}.$$

From equation (4.17),

$$k_s = 0.605 \times 1.7 \times \frac{10^6}{2.305} = 0.446 \times 10^6 \text{ N}.$$

For the steel bottom flange,

$$I_{afz} = \frac{b_f^3 t_f}{12} = 178^3 \times \frac{12.8}{12} = 6.02 \times 10^6 \text{ mm}^4.$$

From equation (4.22),

$$M_{cr} = \frac{22.2}{\pi} (0.446 \times 210000 \times 6.02)^{\frac{1}{2}} = 5306 \text{ kN m}.$$

The slenderness $\bar{\lambda}_{LT}$ is given by equation (4.23), which is

$$\bar{\lambda}_{LT} = \left(M_{apl.Rd} \frac{\gamma_a}{M_{cr}}\right)^{1/2} = \left(386 \times \frac{1.1}{5306}\right)^{1/2} = \mathbf{0.283}.$$

This is less than 0.4, so the member is not weakened by lateral buckling, which is a condition for the use of rigid-plastic global analysis.

4.6.4 Shear connection and transverse reinforcement

For sagging bending, the resistance required, 492 kN m, is well below the resistance with full shear connection, 771 kN m, so the minimum degree of shear connection may be sufficient. For spans of 9.5 m, this is given by Fig. 3.19 as

$$\frac{N}{N_f} \geqslant 0.54.$$

In equation (3.67), F_c/F_{cf} may be replaced by N/N_f. This equation for the interpolation method (Fig. 3.16) then gives

$$\begin{aligned} \boldsymbol{M_{Rd}} &= M_{apl.Rd} + \frac{N}{N_f}(M_{pl.Rd} - M_{apl.Rd}) \\ &= 386 + 0.54(771 - 386) \\ &= \mathbf{594\ kN\ m}, \end{aligned}$$

which is sufficient.

From Section 4.6.1, $N_f = 42.4$, so the number of studs required in lengths of 4.07 m each side of point D in Fig. 4.11(b) is

$$N = 0.54 \times 42.4 = 22.9, \text{ say } 23.$$

The number of troughs in 4.07 m is 4.07/0.3 = 13.6, so:

- use 2 studs per trough in the ten troughs nearest to point A,
- use 1 stud per trough in the midspan region.

The longitudinal reinforcement at the internal support is determined by the rules for control of cracking, and the amount provided (Section 4.6.6) is 8-mm bars at 150-mm spacing. If shear connectors are provided only in the region of sagging moment, and these bars overlap the connectors near point E in Fig. 4.11(b), those connectors will be overloaded. If there is no overlap, wide cracks will occur near point E. Shear connection should therefore be provided along EB for the crack-control reinforcement.

From equation (4.1) the effective width at E is

$$b_{eff} = 2 \times \frac{9.5}{16} = 1.188 \text{ m}$$

and the number of bars within this width is 8. Their area is 402 mm^2, so the design tensile force at yield is

$$\frac{A_s f_{sk}}{\gamma_s} = 402 \times \frac{0.46}{1.15} = 161 \text{ kN}.$$

With $P_{Rd} = 57.9$ kN/stud, this requires 3 studs, so the total needed along DB in Fig. 4.11(b) is 26. There are 18 troughs in this length, so:

- use 2 studs per trough in the ten troughs nearest to point E,
- use 1 stud per trough in the midspan region.

The same number of troughs with two studs is used at each end of the span for simplicity of detailing and construction, even though this appears to provide two extra studs. The calculations that led to Fig. 4.11 are only for a simplified model. The real situations are more complex.

The transverse reinforcement should be exactly as determined for the sagging region in Chapter 3.

4.6.5 Check on deflections

The limits to deflections discussed in Section 3.7.2 correspond to the rare combination of loading (equation (1.8)). Where there is only one type of variable load, as here, this is simply $g_k + q_k$, but three sets of calculations are required, because part of the permanent load g acts on the steel section and part on the composite section.

In practice, it is usually accurate enough to combine the two calculations for the composite member, using a mean value of the modular ratio (e.g. $n = 22$ here).

For design purposes, maximum deflection occurs when the variable load is present on the whole of one span, but not on the other span. The three loadings are shown in Fig. 4.13, with the bending-moment distributions given by 'uncracked' elastic analyses, in which the beam is assumed to be of uniform section. The data and results are summarised in Table 4.3, where M_B is the hogging moment at support B at this stage of the analysis.

Table 4.3 Calculation of maximum deflection.

	w kN/m	M_o kN m	M_B kN m	f_1	f_2	M_1 kN m	$10^{-6}I_1$ mm^4	δ_c mm
g on steel	11.8	133	133	–	–	133	215	11.1
g on composite	10	113	113	0.765	0.7	60	547	6.3
q on composite	20	226	113	0.688	0.7	54	738	11.7

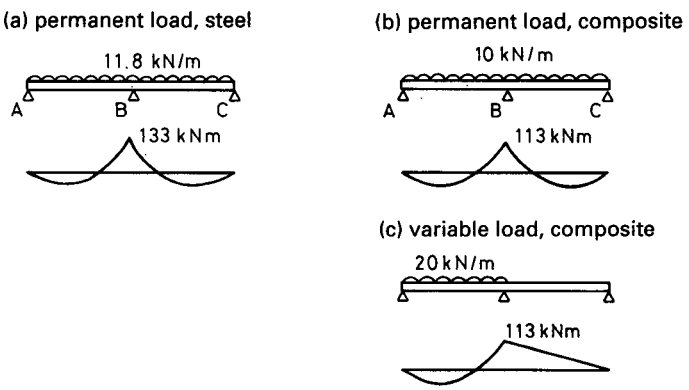

Fig. 4.13 Loading for deflection of span AB.

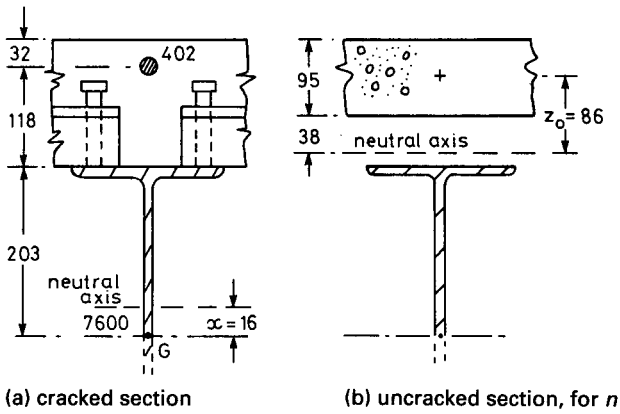

Fig. 4.14 Elastic properties of composite section.

Following the method of Section 4.3.2.3, the maximum tensile stress in the uncracked composite section at B, σ_{ct}, is now found. This will occur when variable load acts on both spans, and is calculated using $n = 11$ for variable load and $n = 33$ for permanent load. Using data from Section 4.6.1,

$$\sigma_{ct} = \sum\left(\frac{Mx}{nI_1}\right) = \frac{113 \times 212}{33 \times 547} + \frac{226 \times 133}{11 \times 738}$$

$$= 1.33 + 3.70 = 5.03 \text{ N/mm}^2,$$

where nI_1 is the 'uncracked' second moment of area in 'concrete' units.

This stress exceeds $0.15f_{ck}$ (3.75 N/mm^2). To avoid re-analysis with spans of non-uniform section, the correction factor f_1 given by equation (4.36) will be used. First, a value is needed for the 'cracked' second moment of area I_2 at the internal support, taking account of the longitudinal reinforcement. The area of this, A_s, is given in Section 4.6.4 as 402 mm^2. From Fig. 3.12, these 8-mm bars are located 24 + 8 = 32 mm below the top of the slab (Fig. 4.14). The elastic neutral axis is distance x above G. Equating first moments of area about G:

$$402 \times 321 = 8002x, \quad \text{whence } x = 16 \text{ mm}.$$

Hence,

$$10^{-6}I_2 = 215 + 7600 \times 0.016^2 + 402 \times 0.305^2 = 254 \text{ mm}^4.$$

The value of f_1 for $n = 33$ is:

$$f_1 = \left(\frac{I_1}{I_2}\right)^{-0.35} = \left(\frac{547}{254}\right)^{-0.35} = 0.765.$$

This and the value for $n = 11$ are given in Table 4.3.

The maximum compressive stress in the steel bottom fibre is now calculated, to determine whether the correction factor f_2 for yielding is required. As for σ_{ct}, variable load should be assumed to act on both spans. Using data from Section 4.6.1,

$$\sigma_{a4} = \sum\left(\frac{Mx_4}{I_2}\right) = \frac{133 \times 203}{215} + \frac{113 \times 219}{254} + \frac{226 \times 219}{254}$$

$$= 126 + 97 + 195 = 418 \text{ N/mm}^2,$$

where x_4 is the distance of the relevant neutral axis above the bottom fibre. The result shows that yielding occurs ($418 > 355$), but not until after the slab has hardened ($126 < 355$), so from Section 4.3.2.3, $f_2 = 0.7$. The hogging moments M_1 for use in equation (4.35) are

$$M_1 = f_1 f_2 M_B$$

and are given in Table 4.3.

Deflections δ_o for each loading acting on a simply-supported span are now required. These are, in general:

$$\delta_o = \frac{5wL^4}{384\,EI} = \frac{5 \times 9.5^4 \times 10^9}{384 \times 210}\left(\frac{w}{I_1}\right) = 505 \times 10^6\left(\frac{w}{I_1}\right) \text{mm}$$

with w in kN/m and I_1 in mm^4. Using values from Table 4.3 in equation (4.35) gives the total deflection:

$$\delta_c = 505 \times 10^6 \sum\left[\left(\frac{w}{I_1}\right)\left(1 - 0.6\frac{M_1}{M_0}\right)\right]$$

$$= 505\left[\left(\frac{11.8}{215}\right) \times 0.4 + \frac{10}{547}\left(1 - 0.6 \times \frac{60}{113}\right) + \left(\frac{20}{738}\right)\left(1 - 0.6 \times \frac{54}{226}\right)\right]$$

$$= 11.1 + 6.3 + 11.7 = \mathbf{29\ mm}.$$

This total deflection is span/327, less than the recommended limit of $L/250$ given in Eurocode 4 (by cross-reference to Eurocode 3). The change in deflection after construction (11.7 mm plus the creep-related part of 6.3 mm) is well below the limit of $L/350$, which is 27 mm.

Even so, these deflections are fairly large for a continuous beam with a ratio of span to overall depth of only 9500/556 = 17.1. This results from the use of unpropped construction, high-yield steel, and lightweight concrete. Deflections of a similar propped structure in mild steel and normal-density concrete would be much lower.

4.6.6 Control of cracking

The widest cracks will occur at the top surface of the slab, above an internal support. The reinforcement needed to control the crack width to 0.5 mm, and also to 0.3 mm, is now determined, as explained in Section 4.2.5.

No longitudinal reinforcement has been provided for resistance to loading, as design for the ultimate limit state was based on the resistance of the steel beam alone. The model is therefore that the hogging flexure of the steel beam under load imposes deformation on the slab above it, so that the reinforcement should be designed for restraint-induced cracking by the method of Section 4.2.5.2.

The minimum reinforcement required is given by equation (4.33). It depends on h_c, the 'thickness of the concrete flange'. This varies (Fig. 3.9) from 80 mm to 150 mm, and is taken for this purpose as 95 mm, as in Section 3.11.3.

The elastic neutral axis for the uncracked composite section for short-term loading (i.e. for $n = 11$) is 133 mm below the top of the slab. The distance z_o defined in Section 4.2.5.2 is therefore 86 mm, as shown in Fig. 4.14(b). From equation (4.32),

$$k_c = \left(1 + \frac{h_c}{2z_o}\right)^{-1} = \left(1 + \frac{90}{172}\right)^{-1} = 0.66, \text{ but } \geqslant 0.7,$$

so $k_c = 0.7$.

The tensile strength of the concrete when cracks may be expected to occur, f_{cte}, is taken as the mean 28-day tensile strength, f_{ctm}. For concrete with $f_{ck} = 25$ N/mm^2, this is given in Eurocode 4 as 2.6 N/mm^2.

For a one-metre width of slab, equation (4.33) gives

$$A_s \geqslant 0.8 k_c f_{cte} \frac{A_c}{\sigma_{st}} = 0.8 \times 0.7 \times 2.6 \times \frac{90000}{\sigma_{st}}$$
$$= 0.131 \times \frac{10^{-6}}{\sigma_{st}}.$$

The maximum stress permitted in the reinforcement immediately after cracking, σ_{st}, depends on the crack width w_k and the bar size ϕ, as given in Fig. 4.7. For $w_k = 0.5$ mm and $\phi \leqslant 10$ mm, $\sigma_{st} \leqslant 500$ N/mm^2. This gives $A_s \geqslant 262$ mm^2/m, which could be provided by 8-mm bars at 180 mm spacing (279 mm^2/m).

For $w_k = 0.3$ mm and $\phi \leqslant 8$ mm, Fig. 4.7 gives $\sigma_{st} \leqslant 400$ N/mm^2, whence $A_s \geqslant 327$ mm^2/m. This can be provided by **8-mm bars at 150 mm spacing** (336 mm^2/m) and will be used. This is the same as the top transverse reinforcement, and so may be available as a welded fabric.

4.7 Continuous composite slabs

The concrete of a composite slab floor is almost always continuous over the supporting beams, but the individual spans are often designed as simply-supported (Section 3.3), for simplicity. Where deflections are found to be excessive, continuous design may be used, as follows.

Elastic theory is used for the global analysis of continuous sheets acting as shuttering. Variations of stiffness due to local buckling of compressed parts can be neglected. Resistance moments of cross-sections are based on tests (Section 3.3).

Completed composite slabs are generally analysed for ultimate bending moments in the same way as continuous beams with Class 2 sections. 'Uncracked' elastic analysis is used, with up to 30% redistribution of hogging moments, assuming that the whole load acts on the composite member. Rigid-plastic global analysis is allowed by Eurocode 4 where cross-sections at plastic hinges have been shown to have sufficient rotation capacity, and this check is waived where the spans are less than 3.0 m and the reinforcement has 'high ductility' as defined in Eurocode 2.

At internal supports where the sheeting is continuous, resistance to hogging bending is calculated by rectangular-stress-block theory, as for composite beams, except that local buckling is allowed for by using an effective width for each flat panel of sheeting in compression. This width is given in Eurocode 4 as twice the value specified for a Class 1 steel web, thus allowing for the partial restraint from the concrete on one side of the sheet. Where the sheeting is not continuous at a support, the section is treated as reinforced concrete.

For the control of cracking at internal supports, Eurocode 4 refers to Eurocode 2, for reinforced concrete. In practice, the reinforcement to be provided may be governed by design for resistance to fire, as in Section 3.3.7, or by the transverse reinforcement required for the composite beam that supports the slab.

Chapter 5

Composite Columns and Frames

5.1 Introduction

A composite frame is defined in Eurocode 4: Part 1.1 as a 'framed structure for a building or similar construction works, in which some or all of the beams and columns are composite members and most of the remaining members are structural steel members. The use of reinforced or prestressed concrete or masonry members in bracing systems (as defined in Eurocode 3) is not excluded'.

It is implied by this definition that a composite frame is more similar to a structural steel frame than to one in reinforced or prestressed concrete. It is likely to be built by first erecting a frame of steel beams and columns, then fixing profiled sheeting to the steelwork to provide working platforms, and finally constructing the reinforced concrete. It follows that the beam-to-column connections are primarily of structural steel. The resistance of a connection to bending may exceed that of the beam connected, but in practice it is more likely to be much lower, even negligible. The behaviour of the composite frame is then fundamentally different from that of a reinforced concrete frame, where the connections between beams and columns are usually monolithic.

The treatment of composite frames in Eurocode 4: Part 1.1 is therefore related closely to the treatment of steel frames in Eurocode 3, and does not refer to Eurocode 2, for concrete structures. It provides the basis for this chapter, because in the UK there is no code of practice for composite frames or connections, and none that gives a modern method for composite columns in buildings.

Only one of the many types of framed structure is considered in this chapter. It is often used for multi-storey buildings, and consists of a three-dimensional assemblage of horizontal beams and vertical columns on a rectangular grid. The beams support floor slabs. In the frame now dis-

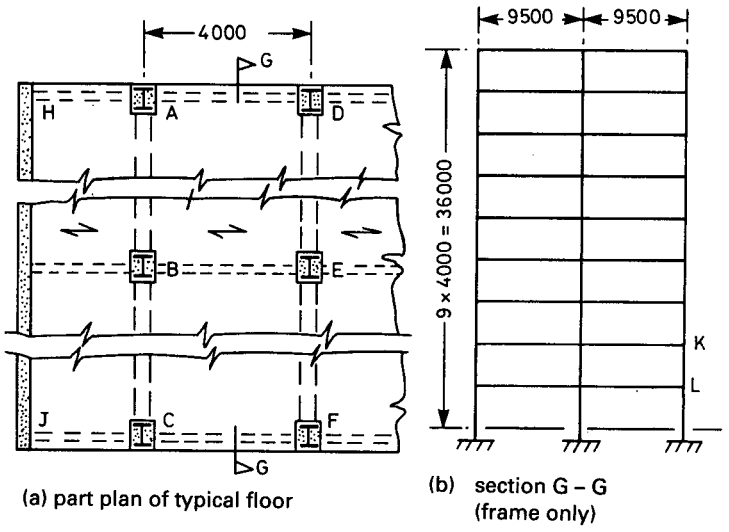

Fig. 5.1 A composite frame (simplified).

cussed, Fig. 5.1, the slabs, beams, and columns are all composite. The slabs span in one direction only, from beam to beam.

At each intersection between beams and columns, the columns are usually continuous, and the beams are attached to their external faces by connections. These are usually assumed in design to act as pin joints, but they may be 'semi-rigid' or 'rigid'.

The bending stiffness of steel columns of H- or I-section is much greater in the plane of the web ('major-axis bending') than in a plane parallel to the flanges ('minor-axis bending'). The columns are usually designed with their webs co-planar with those of the main beams, as shown in Fig. 5.1(a), so that beam-column interaction causes major-axis bending in both members.

The beams of type ABC at each floor level and their supporting columns form a *plane frame*, as shown in Fig. 5.1(b). The frames also support *minor-axis beams* such as AD and CF in Fig. 5.1(a). These are required to stabilise the columns during erection, and they support the external walls at each floor level. With the columns, they form a second set of plane frames, orthogonal to the major-axis frames.

For global analysis for gravity loads, each plane frame is assumed to be independent of the others. For each storey-height column length, an axial load N_y and end moments M_{1y} and M_{2y} are found for the major-axis frame, and corresponding values N_z, M_{1z}, and M_{2z} for the minor-axis frame. The column length is then designed (or an assumed design is checked) for axial load $N_y + N_z$ and for the biaxial bending caused by the four end moments.

Multi-storey plane frames of this type have little resistance to horizontal

loads, especially where the connections are designed as pin joints. However, each concrete floor slab acts as a deep beam of great stiffness, when subjected to horizontal forces in its plane. It can therefore transfer wind loads to a small number of vertical cantilevers, placed where convenient in the building. These are designed to resist horizontal loads, and have lateral stiffness so much greater than that of the plane frames, that the latter can be designed for gravity loads only.

The vertical cantilevers usually consist of end walls, known as *shear walls*, as shown at HJ in Fig. 5.1(a), or enclosures to lift shafts, staircases, and vertical ducts, referred to as 'services cores'. These may be diagonally-braced steel frames, but are often built in reinforced concrete, even where the plane frames are steel or composite. Their design is outside the scope of this volume.

Columns and connections are discussed separately in Sections 5.2 and 5.3. The Eurocode methods for analysis of frames are then explained, with a worked example. Details of the design method of Eurocode 4 for columns are then given, followed by calculations for one of the columns in the frame.

5.2 Composite columns

Steel columns in multi-storey buildings need protection from fire. This is often provided by encasement in concrete. Until the 1950s, it was normal practice to use a wet mix of low strength, and to neglect the contribution of the concrete to the strength and stability of the column. Tests by Faber[51] and others then showed that savings could be made by using better-quality concrete and designing the column as a composite member. This led to the 'cased strut' method of design. This was originally (in BS 449) a permissible-stress method for the steel member, which had to be of H- or I-section. It is now available in limit-state form.[52] The presence of the concrete is allowed for in two ways. It is assumed to resist a small axial load, and to reduce the effective slenderness of the steel member, which increases its resistance to axial load. Resistance to bending moment is assumed to be provided entirely by the steel. No account is taken of the resistance of the longitudinal reinforcement in the concrete.

Tests on cased struts under axial and eccentric load show that the BS 449 method gives a very uneven and usually excessive margin of safety. For example, Jones and Rizk[53] quote load factors ranging from 4.7 to 6.7, and work by Faber[51] supports this conclusion. The method has been improved in BS 5950, but is still generally very conservative. Its main advantage is that it is simpler than the more rational and economical methods now available.

One of the earliest methods to take proper account of the interaction

between steel and concrete in a concrete-encased H-section column is due to Basu and Sommerville.[54] It has been extended to include biaxial bending, and agrees quite well with the results of tests and numerical simulations.[55,56] It was thought to be too complex for routine use for columns in buildings, but is included in the British code for composite bridges.[22] Its scope includes concrete-filled steel tubes[57] which are used as bridge piers, for example in multi-level motorway interchanges. The method is fully described in Volume 2, with worked examples.

The Basu and Sommerville method is based on the use of algebraic approximations to curves obtained by numerical analyses. For Eurocode 4: Part 1.1, preference was given to a method developed by Roik, Bergmann, and others at the University of Bochum. It has wider scope, is based on a clearer conceptual model, and is slightly simpler. It is described in Section 5.6, with a worked example.

5.3 Beam-to-column connections

5.3.1 Properties of connections

Three types of connection between a steel beam and the flange of an H-section steel column are shown in Fig. 5.2, and a short end-plate connection is shown in Fig. 5.17. They are all bolted, because they are made on site, where welding is expensive and difficult to inspect. The column shown in Fig. 5.2(a) is in an external wall. At an internal column, another beam would be connected to the other flange. There may also be minor-axis beams, connected to the column web as shown in Fig. 5.2(c).

Where the beams are composite and the column is internal, longitudinal reinforcement in the slab will be continuous past the column, as shown in Fig. 5.2(c). It may be provided only for the control of cracking; but if it consists of individual bars, rather than welded fabric, the tension in the bars may be assumed to contribute to the bending resistance of the connection, as shown in Fig. 5.2(d). Where rigid-plastic global analysis is used, small-diameter bars may fracture before the rotation of the hogging region of the beam becomes large enough for the collapse mechanism to develop, so these bars should probably be at least 12 mm in diameter. This limit is the subject of current research.

In the fin-plate connection of Fig. 5.2(a), the bolts are designed mainly for vertical shear, and the flexural stiffness is low. The end-plate connection of Fig. 5.2(c) is likely to be 'semi-rigid' (defined later). The bolts at A resist a combination of tension and shear, and bolts in the compression zone (B and C) are designed for vertical shear only. The web of the column has to be checked for yielding in tension, in region D, for yielding or buckling in compression, in region E, and (if an external column) for shear.

To achieve a 'rigid' connection it may be necessary to use an extended end plate and to stiffen the column web in regions D and E, as shown in Fig. 5.2(b).

Assuming that no failure occurs in the column web, the resistance of the composite connection of Fig. 5.2(c) to hogging bending may be calculated by simple plastic theory, as shown in Fig. 5.2(d).

Design yield forces are calculated for the reinforcement, F_{sd}, and for the bolts at A, F_{bd}, taking account in the latter of any vertical shear in excess of the shear resistance of the bolts at B and C. (It is here assumed that the end plate and column flange are thick enough to develop the force F_{bd} in the bolts.) If the design yield force for the bottom flange, F_{afd}, exceeds $F_{sd} + F_{bd}$, the bending resistance is found by taking moments about mid-depth of the bottom flange:

$$M_{Rd} = F_{sd}\left(h_s + h_a - \frac{t_f}{2}\right) + F_{bd}\left(h_b - \frac{t_f}{2}\right). \tag{5.1}$$

If $F_{afd} < F_{sd} + F_{bd}$, a depth of web x_c is assumed to be at yield in compression (or, if necessary, in combined shear and compression), such that

$$F_{awd} = F_{sd} + F_{bd} - F_{afd},$$

and the moment $F_{awd}(x_c + t_f)/2$ is deducted from M_{Rd} as calculated above.

The other information needed for design is a curve of hogging bending moment against rotation of the connection, ϕ. This is defined as the

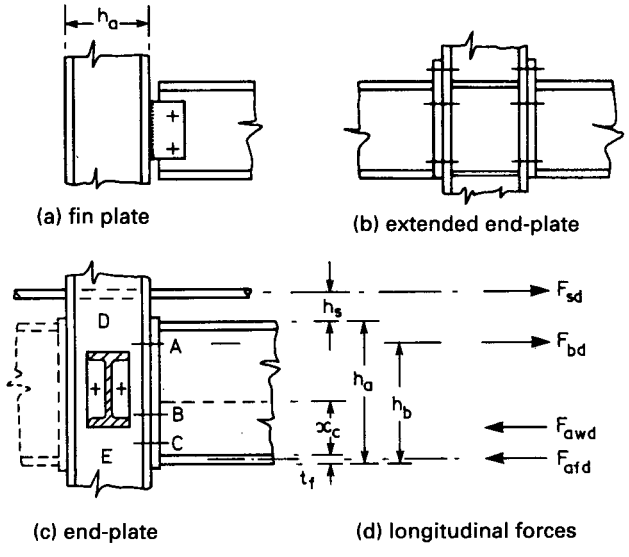

Fig. 5.2 Elevations of beam-to-column connections.

rotation additional to that which would occur if the beam continued to its intersection with the centre-line of the column, as shown in Fig. 5.3. For steel connections, methods are given in Eurocode 3: Part 1.1[11] for the prediction of this curve. Research on the extension of these methods to composite connections is in progress.[58]

It is now assumed that some M–ϕ curves are available from tests, for a particular composite connection. The characteristic curve should be estimated (e.g. by using the lowest of the experiment curves), and its ordinates should be divided by γ_a (presumably take as 1.1, though Eurocode 3 is not clear on this) to obtain a design curve, such as OABCD in Fig. 5.4. For design purposes, this is conveniently replaced by the tri-linear diagram OBEF. The three properties needed for design are:

- the resistance M_{Rd};
- the maximum rotation at M_{Rd}, shown as ϕ_d;
- the secant stiffness C.

If for a particular load case the design moment M_{Sd} is lower than M_{Rd}, the corresponding stiffness (C_S in Fig. 5.4) may be used.

The analysis and design of beam-to-column connections of the types shown in Fig. 5.2 is covered in Eurocode 3 and also in textbooks on

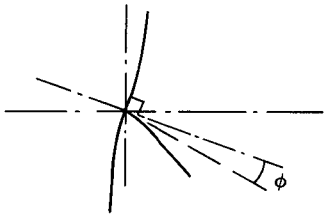

Fig. 5.3 Rotation of a connection.

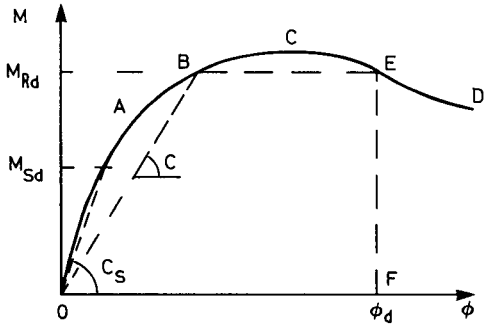

Fig. 5.4 Moment–rotation curve for a connection.

structural steelwork. The addition of reinforcing bars in the slab is assumed to have no effect on the resistance to vertical shear, and the effect on the resistance to bending is given by the term in F_{sd} in equation (5.1). Care must be taken to avoid connections that are strong but brittle. The plastic deformation of end plates enhances rotation capacity, so they should not be too thick; 8 mm or 10 mm is usually sufficient, if a connection is to be treated as pinned.

5.3.2 Classification of connections

Beam-to-column connections are classified in Eurocode 4, as in Eurocode 3, by rotational stiffness, which is relevant to elastic global analysis, and by resistance to bending moment, which is relevant to the resistance of a frame to ultimate loads. For stiffness, the three classes are as follows.

(1) A *nominally pinned connection* is so designed that it cannot develop significant moments which might adversely affect members of the structure.

A connection may be classified as nominally pinned if

$$C \leqslant 0.5\, E_a \frac{I_b}{L_b} \tag{5.2}$$

where C is the rotational stiffness of the connection, and E_aI_b is the rotational stiffness of the connected beam, of length L_b. The value of E_aI_b should be consistent with that taken for a section adjacent to the connection in global analysis of the frame. The significance of this limit to C can be illustrated by considering a beam of span L_b and uniform section that is connected at each end to rigid columns, by connections with $C = 0.5\, E_aI_b/L_b$. It can be shown by elastic analysis that for a uniformly-distributed load w per unit length, the restraining (hogging) moments at each end of the beam are

$$M_e = \frac{wL_b^2/8}{7.5}.$$

These end moments act also on the columns, the flexibility of which would in practice reduce the moments below M_e.It is thus assumed that columns designed for $M_e = 0$ would not be 'adversely affected' by bending moment from the connection.

(2) A *rigid connection* is so designed that its deformation has no significant influence on the distribution of internal forces and moments in the structure, nor on its overall deformation.

The condition for a connection in a braced frame to be 'rigid' is that the rising portion of its moment-rotation curve should lie above line 0AB in

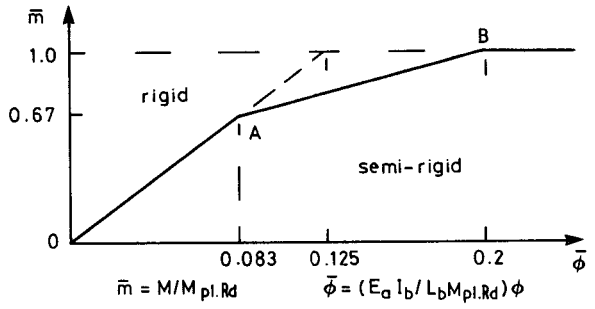

Fig. 5.5 Classification of connections.

Fig. 5.5. In this figure, E_aI_b and L_b are as defined above, and $M_{pl.Rd}$ is that for the cross-section of the beam adjacent to the connection, so it will normally be the resistance to hogging moment.

The amount of redistribution of elastic moment caused by the flexibility of a connection that is just 'rigid' can be quite significant. As an example, we consider the same beam as before, with properties E_aI_b and L_b, supported at each end by rigid columns, through connections represented by point A on Fig. 5.5. The beam is so loaded that both end moments are $0.67\ M_{pl.Rd}$. The end slopes are therefore given by $\bar{\phi} = 0.083$. The additional end moments that would be needed to reduce the end slopes to zero (as they would be for truly 'rigid' connections) are $0.167\ M_{pl.Rd}$, so the flexibility of the connections causes a redistribution of end moments $0.167/(0.67 + 0.167)$, or 20%. The situation for a composite beam in practice is more complex because E_aI_b is not uniform along the span, and the columns are not rigid.

(3) A *semi-rigid connection* is one that provides a predictable degree of interaction between members, but is neither rigid nor nominally pinned. No application rules are given in Eurocode 4 for the use of semi-rigid connections, which are the subject of much current research.

The classification of connections by resistance is as follows.

(1) A *nominally pinned connection* is one that is capable of transmitting the forces calculated in design, without developing significant moments which might adversely affect members of the structure. The principal 'force' (action effect) for such a connection is vertical shear.

A connection with design resistance M_{Rd} may be classified as nominally pinned if M_{Rd} is less than 25% of $M_{pl.Rd}$ for the connected beam, and if it has sufficient rotation capacity. It is not difficult to design connections that satisfy these conditions. An example is given in Section 5.7.5.

(2) A *full-strength connection* has a design resistance (to bending, taking account of co-existing shear) at least equal to that of the member connected (e.g. $M_{Rd} \geqslant M_{pl.Rd}$). There is a separate requirement to check that the rotation capacity of the connection is sufficient. This can be difficult. It is waived if

$$M_{Rd} \geqslant 1.2\, M_{pl.Rd}, \tag{5.3}$$

so in practice a 'full-strength' connection is usually designed to satisfy condition (5.3). It can then be assumed that inelastic rotation occurs in the beam adjacent to the connection. The rotation capacity is then assured by the classification system for steel elements in compression.

(3) A *partial-strength connection* may have a resistance less than that of the member connected; but must have sufficient rotation capacity, if at the location of a plastic hinge, to enable all the necessary plastic hinges to develop under the design loads. These connections are at present rarely used, pending further information on rotation capacity.

5.4 Design of non-sway composite frames

5.4.1 Imperfections

The scope of this section is limited to multi-storey structures of the type shown in Fig. 5.1, modelled as two sets of plane frames as explained in Section 5.1. It is assumed that the layout of the beams and columns and the design ultimate gravity loads on the beams are known.

The first step is to define the imperfections of the frame. These arise mainly from lack of verticality of columns, but also have to take account of lack of fit between members, effects of residual stresses in steelwork, and other minor influences, such as non-uniform temperature of the structure. The term 'column' is used here to mean a member that may extend over the whole height of the building. A part of it with a length equal to a storey height is referred to as a 'column length', where this is necessary to avoid ambiguity.

The imperfections within a column length are allowed for by the curves that give the reduction factor for slenderness, χ (Section 5.6.3), not in the frame imperfections.

Imperfections in beams are allowed for in the classification system for steel elements in compression, and in design for lateral buckling.

Frame imperfections are represented by an initial sidesway, ϕ, as shown in Fig. 5.6(a) for a single column length of height h, subjected to an axial load N. The action effects in the column are the same as if it were vertical and subjected to horizontal forces, $N\phi$, as shown.

It is assumed that the angle ϕ for a composite frame is the same as for the

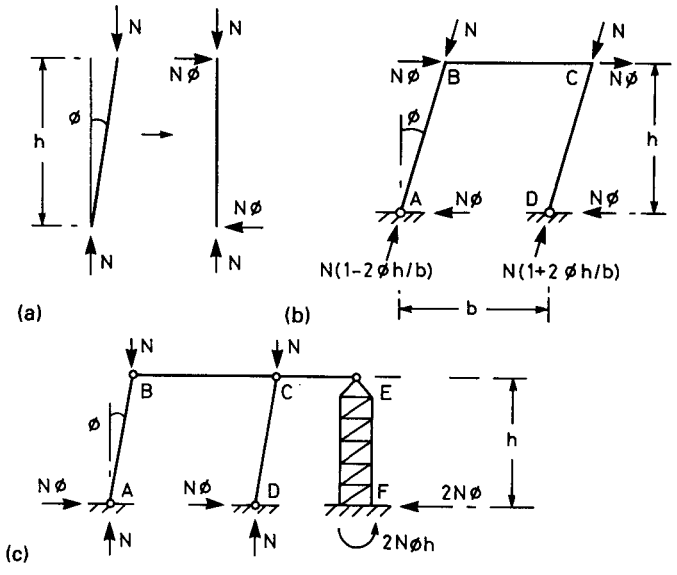

Fig. 5.6 Unbraced and braced frames.

corresponding steel frame. This is given in Eurocode 3: Part 1.1 as a function of the number of storeys n_s and the number of columns in the plane frame considered, n_c, as follows:

$$\phi = \frac{k_c k_s}{200}, \geqslant \frac{1}{400} \tag{5.4}$$

where

$$k_c = \left(0.5 + \frac{1}{n_c}\right)^{1/2}, \leqslant 1.0 \tag{5.5}$$

and

$$k_s = \left(0.2 + \frac{1}{n_s}\right)^{1/2}, \leqslant 1.0. \tag{5.6}$$

Thus, a five-storey structure with two-bay plane frames (three columns) has $k_c = 0.913$, $k_s = 0.632$, and $\phi = 1/347 = 2.89 \times 10^{-3}$. This initial sway applies in all horizontal directions, and is uniform over the height of the frame. If, in this example, the storey height were 3.8 m, the overall out-of-plumb of each column would be assumed to be $3.8 \times 5/347 = 0.055$ m.

Let the total design ultimate gravity load on the frame, for a particular combination of actions, be $G + Q$ per storey. The imperfections can then be represented by a notional horizontal force ϕ $(G + Q)$ at each floor level – but there may or may not be an equal and opposite reaction at foundation level.

To illustrate this, we consider the single-bay single-storey unbraced

frame ABCD shown in Fig. 5.6(b), with pin joints at A and D, and we assume $\sin\phi = \phi$, $\cos\phi = 1$. The use of additional forces $N\phi$ at B and C is associated with the assumption that the loads N still act along the columns, as shown. There are obviously horizontal reactions $N\phi$ at A and D; but the vertical reactions N are replaced by reactions $N(1 \pm 2\phi h/b)$ at angle ϕ to the vertical. The total horizontal reaction at A is therefore

$$N_\phi - N_\phi\left(1 - 2\phi\frac{h}{b}\right) = 2\,N\phi^2\,\frac{h}{b} \approx 0.$$

The maximum first-order bending moment in the perfect frame is zero. The imperfection ϕ increases it to $N\phi h$, at corners B and C, which may not be negligible.

If there are pin joints at these corners, the frame has to be braced against sidesway by connection to the top of a stiff vertical cantilever EF (Fig. 5.6(c)). The external reactions now do include horizontal forces $N\phi$ at A and D, with an opposite reaction $2N\phi$ at F; and the vertical reactions at A and D are independent of ϕ.

These simple analyses are *first order*. That is, they neglect any increase in the assumed sway ϕ caused by the deformations of the structure under load. Analyses that take account of this effect are referred to as *second order*. A simple example is the elastic theory for the lateral deformation of an initially crooked pin-ended strut.

5.4.2 Resistance to horizontal forces

In Eurocodes 3 and 4, frames are classified as *braced* or *unbraced*, depending on the layout of the complete structure. They are also classified as *sway* or *non-sway*, depending on the stiffness of the frame for in-plane horizontal forces.

A *braced frame* is one where resistance to sway is provided by a separate *bracing system*, which is sufficiently stiff to reduce its response to horizontal loads by at least 80%. It is then also a non-sway frame. An example is ABCD in Fig. 5.6(c).

An *unbraced frame* (Fig. 5.6(b)) has to resist the horizontal forces that represent its imperfections, and also horizontal actions such as wind or earthquake loading. For a particular load case, let the design value of the total vertical load on the frame be V_{Sd}. It is possible to calculate the multiple of this loading, λV_{Sd} ($= V_{cr}$, say), that would cause elastic critical buckling of the initially perfect frame in a sway mode. There is a well-known hand method of calculation for simple frames involving s and c functions, which have been tabulated.[59] Computer programs are available for more complex frames.

An unbraced frame is classified as a *non-sway frame* if $\lambda \geqslant 10$. Its design may then be based on first-order global analysis. If $\lambda < 10$, it is a *sway frame*, and second-order analysis must be used. Sway frames are outside

the scope of Eurocode 4: Part 1.1, and are not further considered here. In multi-storey construction, use of braced frames is almost always cheaper.

Where elastic global analysis is used for beam-and-column plane frames in building structures, Eurocode 3 gives a simpler alternative to the calculation of λ, for classifying a frame as sway or non-sway. It is applied to each storey separately, using first-order global analysis. The frame may be treated as non-sway if, for every storey,

$$\frac{\delta}{h} \leqslant 0.1 \frac{H}{V}, \tag{5.7}$$

where δ is the relative horizontal displacement over the storey height h, and H and V are the total horizontal and vertical reactions at the bottom of the storey.

In large buildings, the bracing system for one wing will usually be another part of the building, to which this wing is attached at each floor level. An end of a long thin building is often braced by a shear wall, and most tower blocks have a central services cores, as explained in Section 5.1. Sometimes, the bracing system may also be a plane frame, as shown by EF in Fig. 5.6(c). It too is classified as sway or non-sway, as explained above (but with V_{Sd} taken as the total vertical load on all the frames braced), and has to be designed to resist the horizontal forces (real and notional) acting on all the frames that it braces, as well as the effects of its own imperfections. For a steel or composite frame, diagonal bracing will often be required, to form a triangulated structure.

5.4.3 Global analysis of braced frames

5.4.3.1 Actions

This section should be read with reference to Section 4.3, on global analysis of continuous beams, much of which is applicable. Braced frames do not have to be designed for horizontal actions, so the load cases are similar to those for beams. No serviceability checks are normally required for braced frames, or for composite columns. The columns are designed using elastic global analysis and plastic section analysis; that is, as if their cross-sections were in Class 2. The method of construction, propped or unpropped, is therefore not relevant.

For certain types of imposed load, such as furniture or people, but not for storage loads, the probability of the occurrence of the factored design load becomes less as the loaded area increases. The characteristic imposed load on a column that carries load from n storeys is therefore reduced (in draft Eurocode 1[9]) by applying the factor

$$\alpha = \frac{0.6 + 0.7n}{n} \tag{5.8}$$

for $n > 2$ for areas of categories A and B (essentially, areas for dwelling, and public premises where crowds rarely congregate); but not for areas susceptible to overcrowding or used for storage. This reduction does not apply for load combinations where the imposed load is reduced by a ψ factor (Section 1.3.2.1).

Maximum bending moments in columns in rigid-jointed frames occur when not all of the nearby floors carry imposed load. For a column length AB in a frame with many similar storeys, the most adverse combination of axial load and bending moment is likely to occur when the imposed load is applied as in Fig. 5.7(a), for an external column, or Fig. 5.7(b), for an internal column. The bending-moment distributions for the column are likely to be as shown.

5.4.3.2 Eccentricity of loading, for columns

The use of 'nominally pinned' beam-to-column connections reduces bending moments in the columns, with corresponding increases in the sagging moments in the beams. For the beams, it is on the safe side to assume that the moments in the connections are zero. If this were true, the load from each beam would be applied to the column at an eccentricity slightly greater than half the depth h_a of the steel column section (Fig. 5.2(a)) for major-axis connections.

An elastic analysis that modelled the real (non-zero) stiffness of the connection would give an equivalent eccentricity greater than this. The real behaviour is more complex. Initially, the end moments increase the tendency of each column length to buckle; but as the load increases, and it begins to do so, the end moments change sign, and the greater the stiffness of the connections, the more beneficial is their effect on the column.

Typically, British codes of practice for steel columns have allowed for

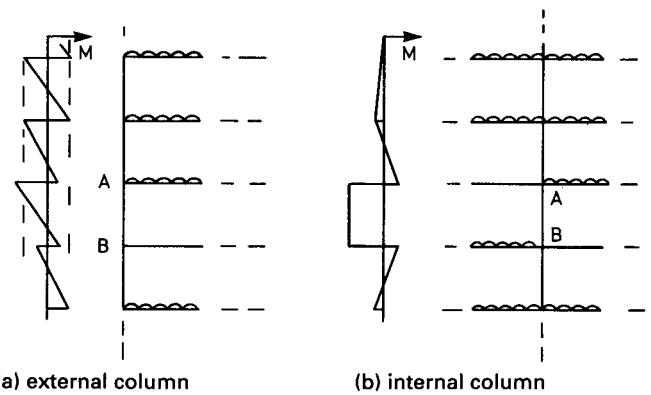

Fig. 5.7 Arrangements of imposed load, for column design.

this stabilising effect by modelling each storey-height column with an 'effective length' about 70% of its actual length (i.e. $L_e/L \approx 0.7$), but have specified an 'equivalent eccentricity of loading', $e \approx 0.5h_a + 100$ mm, for the calculation of end moments.

In some other European countries, the practice has been to assume $L_e \approx L$, which makes buckling more critical, and $e = 0$, which eliminates bending moments from columns. One justification for using $e = 0$ is that the bending moments in the beams are calculated using the span between column centres, rather than the smaller span between the centres of the 'pin' connections. This subject is not yet covered in Eurocodes 3 and 4, and may be treated in a future annex to Eurocode 3 on the modelling of structures for buildings. In the following worked example, it is assumed that $L_e = L$ and that the load from a nominally pinned connection acts at 100 mm from the face of the composite column section. For a typical encased H-section this gives $e \approx 0.5h_a + 160$ mm.

5.4.3.3 Elastic global analysis

This method of analysis is generally applicable to braced composite frames with rigid or nominally pinned connections. The flexural stiffness of hogging moment regions of beams is treated as in Section 4.3.2. For columns, concrete is assumed to be uncracked, and the stiffness of the longitudinal reinforcement may be included, as it may not be negligible.

Bending moments in beams may be redistributed as in Section 4.3.2, but end moments found for composite columns may not be reduced, because there is insufficient knowledge of the rotation capacity of columns.

Where the beam-to-column connections are nominally pinned, as in the external columns in the worked example in Section 5.5, the bending moments in a column are easily found by moment distribution for that member alone.

5.4.3.4 Rigid-plastic global analysis

The use of this method for a braced frame is not excluded by Eurocode 4: Part 1.1, but there are several conditions that make it unattractive in practice. In addition to the conditions that apply to beams (Section 4.3.3), these include the following.

(1) All connections must be shown to have sufficient rotation capacity, or must be full-strength connections with $M_{Rd} \geqslant 1.2M_{pl.Rd.}$, as explained in Section 5.3.2.
(2) Design must ensure that plastic hinges do not occur in composite columns.

5.5 Example: composite frame

5.5.1 Data

To enable previous calculations to be used, the structure to be designed has a composite slab floor that spans 4.0 m between two-span continuous composite beams with spans of 9.5 m. There are nine storeys, each with floor-to-floor height of 4.0 m, as shown in Fig. 5.1. For simplicity, it is assumed that the roof has the same loading and structure as the floors, though this would not be so in practice. The building stands alone, and is 60 m long.

The materials and loadings are as used previously, and the composite floor is as designed in Section 3.4. The two-span composite beams are as designed in Section 4.6, with nominally pinned connections to the external columns (Section 5.7.5), except that they are not continuous over a central point support, provided by a wall. There is instead a composite column at mid-length of each beam, to which each span is connected by a 'rigid' and 'full-strength' connection. These terms are defined in Section 5.3.2.

The only gravity loads additional to those carried by the beams are the weight of the columns and the external walls. The characteristic values are assumed to be as follows:

- for each column $g_k = 3.0$ kN/m, $= 12.0$ kN per storey,
- for each external wall $g_k = 60$ kN per bay per storey.

The 60-kN load is for $4 \times 4 = 16\,m^2$ of wall, which is assumed to be supported at each floor level by a beam spanning 4.0 m between adjacent columns.

The design ultimate gravity load per storey for each column is therefore the load from one main beam plus:

- for the internal column, $12 \times 1.35 = 16.2$ kN
- for an external column, $72 \times 1.35 = 97.2$ kN. (5.9)

The characteristic wind load is based on wind in a direction parallel to the longitudinal axes of the main beams. It causes pressure on the windward wall and suction (i.e. pressure below atmospheric) on the leeward wall. The sum of these two effects is assumed to be:

$$q_{k,wind} = 1.5 \text{ kN/m}^2 \text{ of windward wall.} \tag{5.10}$$

The effects of wind blowing along the building are not considered.

The properties of materials are as summarised in Section 4.6.1, except that the concrete in the composite columns is of normal density, with properties

$$f_{ck} = 25 \text{ N/mm}^2, \quad E_{cm} = 30.5 \text{ kN/mm}^2. \tag{5.11}$$

The design initial sidesway of a frame such as DEF in Fig. 5.1 is calculated following Section 5.4.1. The number of storeys, n_s, is nine, and

the number of columns in a plane frame, n_c, is three. From equations (5.4) to (5.6),

$$k_c = 0.913, \quad k_s = 0.558, \quad \phi = \frac{1}{393} = 2.55 \times 10^{-3}. \tag{5.12}$$

This exceeds 1/400, as required.

5.5.2 Design for horizontal forces

It is assumed initially that the bracing system for horizontal load consists of a reinforced concrete wall at each end of the building, one of which appears as HJ in Fig. 5.1(a), and a concrete or steel tower enclosing services, halfway along.

Wind loads are transferred by the external walls to each floor slab which, for simplicity, is assumed to span 30 m as a simply-supported horizontal beam 19 m deep, between one wall and the services core. The end walls will be shown to be feasible, but are not designed. In practice, some of the horizontal load would probably be resisted by other walls, provided for fire protection of lift shafts and staircases.

The horizontal load for a typical floor slab (Fig. 5.8) thus consists of a horizontal load w per unit length, applied along one edge. A typical frame, such as DEF, can be treated as 'braced' and 'non-sway', and designed for gravity loads only.

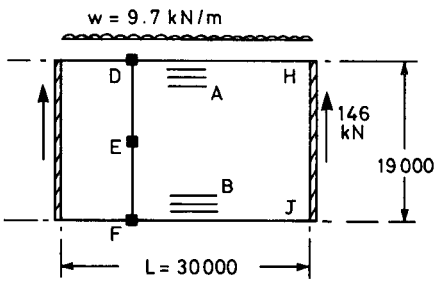

Fig. 5.8 Plan of typical floor slab.

Frame imperfections are allowed for, as in Fig. 5.6, by applying to each floor slab a notional force that is ϕ times the total permanent and variable gravity load for that floor. The characteristic values for an area of floor 19 m by 1 m are:

$$\left.\begin{aligned} Q_k &= 5 \times \frac{19}{393} = 0.242 \text{ kN/m} \\ G_k &= \frac{5.45 \times 19 + (2 \times 72 + 12)/4}{393} = 0.363 \text{ kN/m}. \end{aligned}\right\} \tag{5.13}$$

The value 5.45 is the mean permanent load per square metre, including the weight of the beams.

The characteristic value for wind loading, from equation (5.10), is

$$W_k = 1.5 \times 4 = 6.0 \text{ kN/m}.$$

This far exceeds the values Q_k and G_k, so the maximum design load will be found by taking wind, rather than imposed load, as the leading variable in the combination expression (1.6), explained in Section 1.3.2.4.

From Table 1.3, ψ_o for imposed floor loading is 0.7, so the design load is

$$\begin{aligned} w &= \gamma_G G_k + \gamma_Q W_k + \gamma_Q \psi_o Q_k \\ &= 1.35 \times 0.363 + 1.5(6.0 + 0.7 \times 0.242) = 9.7 \text{ kN/m}. \end{aligned} \tag{5.14}$$

For a span of 30 m, the maximum bending moment and shear force are:

$$M = \frac{wL^2}{8} = 1091 \text{ kN m}, \quad V = \frac{wL}{2} = 146 \text{ kN}. \tag{5.15}$$

To estimate the response of the concrete floor slab, it is assumed initially to be a beam of depth 19 m and breadth 80 mm. The maximum bending stress, by simple elastic theory, is

$$\sigma_{max} = \frac{6M}{bh^2} = 6 \times \frac{1091}{80 \times 19^2} = 0.23 \text{ N/mm}^2.$$

The mean shear stress is

$$\tau_m = \frac{146}{80 \times 19} = 0.10 \text{ N/mm}^2.$$

These stresses are obviously acceptable, but a more detailed check should be made on the reinforcement in regions A and B on Fig. 5.8. The horizontal deflection of each floor, relative to its supports, is less than 1 mm.

An end wall such as HJ in Fig. 5.8 is assumed, for simplicity, to be 36.0 m high (Fig. 5.1(b)). From equation (5.15), its design horizontal load at each floor level is 146 kN. The bending moment at the base is

$$M = \frac{146}{4} \times \frac{36^2}{2} = 23700 \text{ kN m}.$$

To check the feasibility of designing the wall, it is assumed to be 19 m wide and 300 mm thick. The maximum bending stress at the base, calculated as above, is

$$\sigma_{max} = \frac{6 \times 23700}{300 \times 19^2} = 1.31 \text{ N/mm}^2,$$

which is less than one-tenth of the design compressive stress for concrete with $f_{ck} = 25$ N/mm^2. The deflection at the top is about 7 mm.

It is recommended in Eurocode 3 that for serviceability loads, the maximum horizontal deflection of the structure for a multi-storey building of height h should not exceed $h/500$, which is 72 mm for this building.

These calculations show only that a bracing system of the type proposed is feasible. It can easily be shown that it would be at least five times as stiff as a typical plane frame (DEF in Fig. 5.1(a)) for horizontal loading. Each frame can therefore be treated as 'braced' and 'non-sway'.

5.5.3 Design action effects for columns

The whole of the design variable load for a typical frame is transferred to its three columns by the major-axis beams. Permanent loading is symmetrical about the plane of the frame, so the minor-axis bending moments applied to the columns are negligible. The additional gravity loads (expressions (5.9)) are assumed to cause no major-axis bending moments. These are caused in the external columns only by the end reactions of the major-axis beams, which have maximum and minimum values of 242 kN and 99 kN (Fig. 4.11). The most adverse bending moment distribution in a column length is when the beam reaction at one end is a minimum (Fig. 5.7), so the model for analysis is as shown in Fig. 5.9(a). Following Section 5.4.3.2, the eccentricity is taken as 0.26 m, as it is assumed that the column cross-section will be 320 mm square.

For an internal column, rigidly connected to the beams, the model for elastic analysis is that of Fig. 5.9(c), with fully-loaded beams as in Fig. 5.7(b). Where both spans are fully loaded, each has a bending-moment

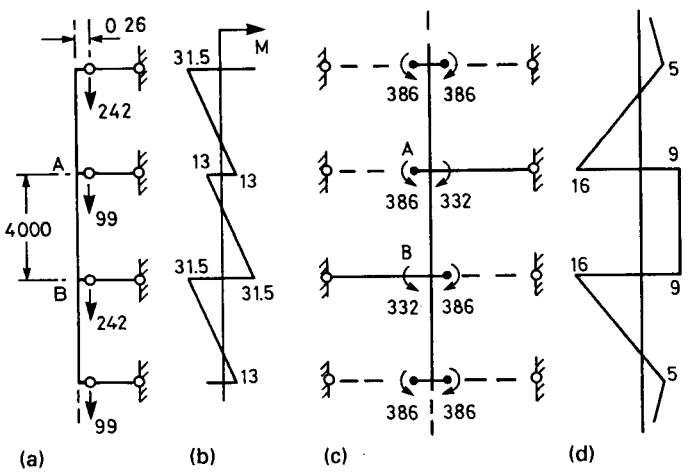

Fig. 5.9 Analytical models and bending moments for columns (units: kN and m).

diagram as for span AB in Fig.4.11. There are plastic hinges each side of the column, so the net moment applied to it is zero.

A span with permanent load only is first assumed to be elastic (an assumption discussed later). Its fixed-end moment is $wL^2/8$:

$$M_f = 29.4 \times \frac{9.5^2}{8} = 332 \text{ kN m}. \tag{5.16}$$

For moment distribution, the stiffness EI/L of the fully-loaded spans is zero, because the plastic hinges can rotate at constant bending moment. The bending stiffnesses of both the beam and the column can be based on uncracked concrete, and the modular ratios are taken as twice the short-term values, to allow for creep. For the column, $E_a I_1$ is taken as 25.5×10^{12} N mm^2(from Section 5.7.2) giving

$$\left(\frac{EI}{L}\right)_{col} = 25.5 \times \frac{10^9}{4} = 6.38 \times 10^9 \text{ N mm}.$$

For the beam, $I_1 = 616 \times 10^6$ mm^4 (Section 4.6.1), and the far end is simply-supported, so the stiffness is

$$0.75\frac{EI}{L} = 0.75 \times 210 \times 616 \times \frac{10^6}{9.5} = 10.2 \times 10^9 \text{ N mm}.$$

Moment distribution for the models of Fig. 5.9(a) and (c) gives bending-moment distributions as in Fig. 5.9(b) and (d). The out-of-balance moment at end B of the internal column is 386 − 332 = 54 kNm, of which the column resists 16 + 9 = 25 kN m, so the end moment for the lightly loaded span increases by 29 kN m to 361 kN m. This is 94% of $M_{pl.Rd}$ for the section in hogging bending, so the stiffness assumed above for this span is certainly too high. The design bending moments shown in Fig. 5.9(d) should therefore be increased.

A conservative assumption would be that the beam has no stiffness. The effect would be to share the out-of-balance bending moment, 54 kN m, equally between the upper and lower column lengths at each floor level. A column length such as AB should then be designed for $M_1 = M_2 = 27$ kN m. This is still quite low for a column of the size assumed, for which the loading is mainly axial.

Each connection between a beam and the column should be designed with

$$M_{Rd} \geqslant 1.2 \times 386 = 463 \text{ kN m},$$

as an alternative to checking its rotation capacity.

Design calculations for an external column are given in Section 5.7. The connections to the internal column are not designed.

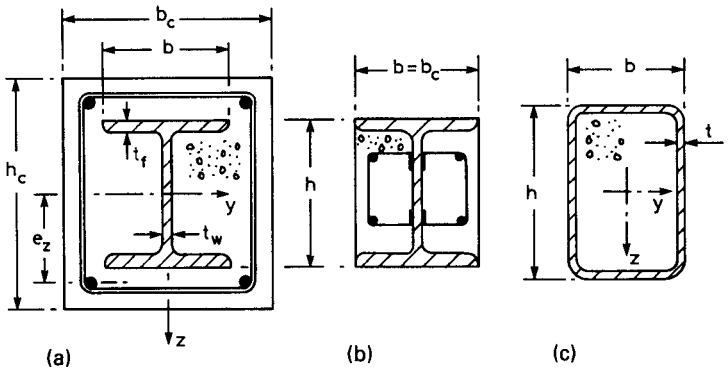

Fig. 5.10 Typical cross-sections of composite columns.

5.6 Simplified design method of Eurocode 4, for columns

5.6.1 Introduction

Background information for Section 5.6 is provided in Section 5.2, 'Composite columns', and in Section 5.5.3, on the global analysis of braced plane frames. Global analysis provides for each column length a design axial force, N_{Sd}, and applied end moments $M_{1.Sd}$ and $M_{2.Sd}$. By convention, M_1 is the greater of the two end moments, and they are both of the same sign where they cause single-curvature bending.

Initially, concrete-encased H- or I-sections are considered (Fig. 5.10(a) and (b)). Where methods for concrete-filled steel tubes (Fig. 5.10(c)) are different, this is explained in Section 5.6.7. The encased sections are assumed to have biaxial symmetry, and to be uniform along each column length. Applied moments are resolved into the planes of major-axis and minor-axis bending of the column, and their symbols have additional subscripts (y and z, respectively) where necessary.

Each end of a column length is assumed to be connected to one or more beams and to be braced laterally at these points, distance L apart. The effective length of each column length is here assumed to be L, as explained in Section 5.4.3.2. Lateral loads on columns are assumed here to be applied only at the ends of each column length.

The methods explained below are applied separately for each plane of bending. It often happens that all significant bending occurs in one plane only. If this is minor-axis bending, no major-axis verification is needed. If it is major-axis bending, minor-axis buckling must be checked, as explained in Section 5.6.5.2, because of interaction between the axial load and the minor-axis imperfections.

5.6.2 Fire resistance, and detailing rules

Before doing any calculations based on an assumed cross-section for a composite column, it is wise to check that the section satisfies relevant limitations on its dimensions.

The resistance to fire of a concrete-encased I-section column is determined by the thickness of the concrete cover to the steel section and the reinforcement. For a 90-minute period of resistance, for example, the limits given by Eurocode 4: Part 1.2 are 40 mm and 20 mm, respectively.

The rules of Eurocode 2: Part 1.1 for minimum cover and reinforcement, and for maximum and minimum spacing of bars, should be followed. These ensure resistance to corrosion, safe transmission of bond forces, and avoidance of spalling of concrete and buckling of longitudinal bars. The ratio of area of reinforcement to area of concrete allowed for in calculating resistances should satisfy

$$0.003 \leqslant \frac{A_s}{A_c} \leqslant 0.04 \,. \tag{5.17}$$

The upper limit is to ensure that the bars are not too congested at overlaps.

The thickness of concrete cover to the steel section that may be used in calculations has a minimum of 40 mm. A maximum of about one-third of the depth of the steel member is also specified. This relates to the proportions of columns for which this design method has been validated. The *steel contribution ratio* δ and the *slenderness* $\bar{\lambda}$ (Section 5.6.3) are limited for the same reason.

The steel contribution ratio is defined by

$$\delta = \frac{A_a f_y / \gamma_a}{N_{pl.Rd}} \tag{5.18}$$

and must satisfy the condition

$$0.2 \leqslant \delta \leqslant 0.9 \,.$$

If $\delta < 0.2$, the column should be treated as reinforced concrete; and if $\delta > 0.9$, as structural steel. The term $A_a f_y/\gamma_a$ is the contribution of the structural steel section to the plastic resistance $N_{pl.Rd}$, given by equation (5.27).

5.6.3 Second-order effects

The interaction of the axial load with the initial imperfection of the column length in the plane of bending considered is allowed for by reducing the axial resistance of the short column, $N_{pl.Rd}$, by a factor χ that is a function of the slenderness of the column length, $\bar{\lambda}$. The 'buckling curves' that relate χ to $\bar{\lambda}$ are the same for composite columns as for steel columns. There are

four of them, labelled a to d, given in Eurocode 3: Part 1.1. They differ only in the allowance made for imperfections within the column length, curve a being the most favourable. It is used for concrete-filled tubes. For encased sections, curves b and c (Fig. 5.11) are used, for major-axis and minor-axis bending, respectively.

The buckling curves do not allow for the second-order effects of bending moments applied to the column length. This is done by increasing the greatest first-order bending moment, using a factor k given by

$$k = \frac{\beta}{1 - (N_{sd}/N_{cr})} \geqslant 1.0 \tag{5.19}$$

where

$$\beta = 0.66 + 0.44\left(\frac{M_2}{M_1}\right) \geqslant 0.44, \tag{5.20}$$

and N_{cr} is the elastic critical load for the column length. The coefficient β allows for the more adverse effect of single-curvature bending, shown in Fig. 5.12(a), than of double-curvature bending, Fig. 5.12(b).

The non-dimensional slenderness $\bar{\lambda}$ is given by

$$\bar{\lambda} = \left(\frac{N_{pl.R}}{N_{cr}}\right)^{0.5}, \tag{5.21}$$

which is similar to equation (4.23) for $\bar{\lambda}_{LT}$, and to the definition used for steel columns. The elastic critical load is

$$N_{cr} = \pi^2 \frac{(EI)_e}{l^2} \tag{5.22}$$

where l is the buckling length of the column, which is here taken as equal to its actual length L between centres of restraining beams (known as the *system length*).

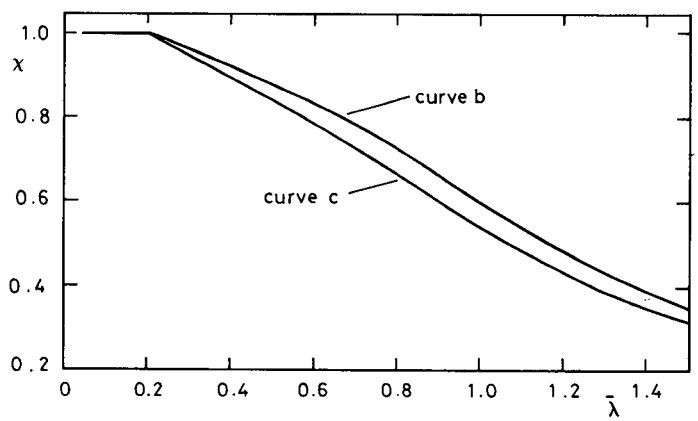

Fig. 5.11 Buckling curves for χ, as a function of slenderness $\bar{\lambda}$.

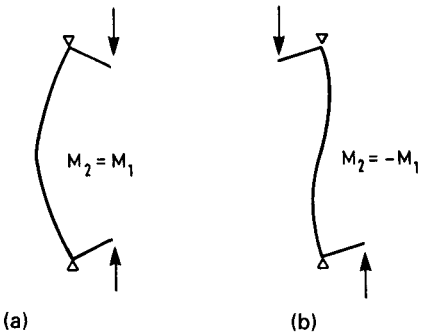

Fig. 5.12 Single-curvature and double-curvature bending.

The 'effective elastic flexural stiffness' $(EI)_e$ is given by

$$(EI)_e = E_a I_a + 0.8 E_{cd} I_c + E_s I_s \tag{5.23}$$

where

$$E_{cd} = \frac{E_{cm}}{\gamma_c}$$

and the (boxed) value of γ_c is given as 1.35. This is a rare example of the use of a γ factor for an elastic property of a material. In the term $0.8\,E_{cd}I_c$, I_c is the second moment of area of the concrete about the centroid of the uncracked column section. The term is the effective stiffness of the concrete part of the section. It is based partly on test data, and takes some account of creep; but not sufficient for design of columns with an adverse combination of slenderness and low bending moments, for which a further reduction in the effective modulus is specified.

No partial safety factors are applied to the terms for structural steel and reinforcement in equation (5.23). Despite the use of γ_c above, N_{cr} is considered to be a 'characteristic' (i.e. unfactored) value. Hence, the axial resistance $N_{pl.R}$ in equation (5.21) is also calculated with all $\gamma_M = 1$, from

$$N_{pl.R} = A_a f_y + A_c(0.85\, f_{ck}) + A_s f_{sk}. \tag{5.24}$$

This is the resistance to axial load of a perfect column too short to buckle, and is known as the 'squash load'. The area A_c is conveniently calculated from

$$A_c = b_c h_c - A_a - A_s, \tag{5.25}$$

in the notation of Fig. 5.10(a). It should not be taken as $b_c h_c$.

It is explained in Section 1.3.2.2 that provision is made in Eurocodes 3 and 4 for the value of γ_a to be increased where resistance is influenced by buckling, though this is not reflected in the boxed values given in the current (ENV) versions of the codes. For columns, the increase occurs where both

$$\bar{\lambda} > 0.2 \quad \text{and} \quad \frac{N_{Sd}}{N_{cr}} > 0.1. \tag{5.26}$$

This increase in γ_a, if made, influences many subsequent calculations. This is why $\bar{\lambda}$ and N_{cr} should be calculated first.

The design resistance of the column length to axial load, allowing for second-order effects within the column, is given by

$$N_{Rd} = \chi N_{pl.Rd}$$

where χ is given in terms of $\bar{\lambda}$ by the relevant buckling curve in Eurocode 3: Part 1.1 (Fig. 5.11). The equations for χ are as equations (4.25) and (4.26) without the subscripts LT, and with the imperfection factor 0.21 in equation (4.26) replaced by 0.34, for curve b, or 0.49, for curve c.

5.6.4 Properties of cross-sections of columns

Design for a combination of axial load and bending about a particular axis is based on the interaction curve between axial resistance N_{Rd} and resistance to bending about that axis, M_{Rd}. The method is best explained using the non-dimensional curve shown in Fig. 5.13.

The plastic resistance $N_{pl.Rd}$ is easily found from the design version of equation (5.24):

$$N_{pl.Rd} = A_a \frac{f_y}{\gamma_a} + A_c \frac{0.85 f_{ck}}{\gamma_c} + A_s \frac{f_{sk}}{\gamma_s}. \tag{5.27}$$

The complexity of hand methods of calculation for $M_{pl.Rd}$ and other points on the curve has been a major disincentive to the use of composite columns. The assumptions are as for calculating $M_{pl.Rd}$ for beams: rectangular stress blocks with structural steel at a stress $\pm f_y/\gamma_a$, reinforcement at $\pm f_{sk}/\gamma_s$, and concrete at $0.85 f_{ck}/\gamma_c$ in compression or cracked in tension. Full shear connection is assumed.

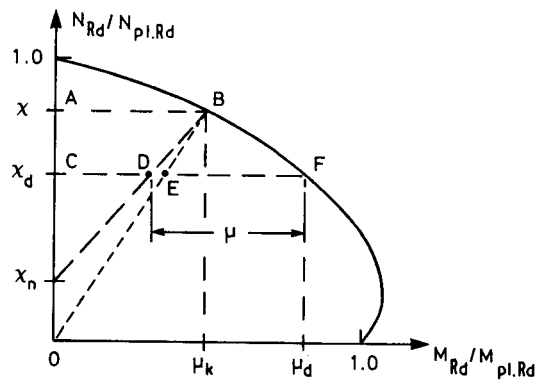

Fig. 5.13 Interaction curve for compression and uniaxial bending.

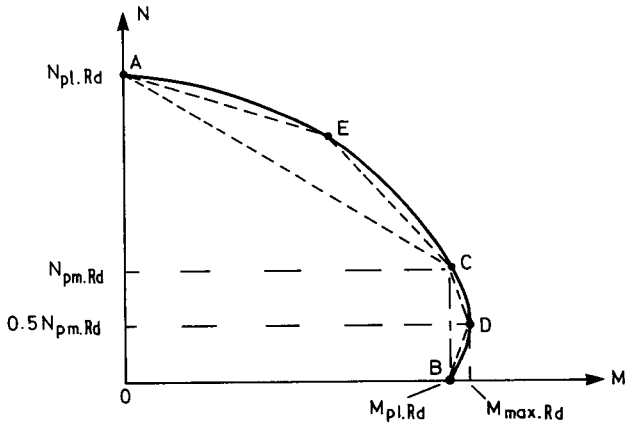

Fig. 5.14 Polygonal approximations to interaction curve.

The problem lies in the algebra. For major-axis bending of the section shown in Fig. 5.10(a), there are at least five possible locations of the plastic neutral axis, each leading to rather complex expressions for N_{Rd} and M_{Rd}. With this approach, the most practicable hand method is to guess a position for the neutral axis, and calculate N_{Rd} by summing the forces in the stress blocks, and M_{Rd} by taking moments of these forces about the centroid of the uncracked section. This gives one point on Fig. 5.13. Other points, and hence the curve, are found by repeating the process.

The simplification made in Eurocode 4: Part 1.1 is to replace the curve by a polygonal diagram, AECDB in Fig. 5.14. An ingenious and fairly simple method of calculating the coordinates of points B, C, and D is given in Annex C of the code, and is explained in Appendix B of this volume. For major-axis bending of encased I-sections, AC may be taken as a straight line, but for other situations, point E has to be found by the method outlined above. Its location is not specified, and the first guessed neutral-axis position is usually good enough.

Transverse shear force may be assumed to be resisted by the steel section alone. The design method for moment–shear interaction in beams (Section 4.2.2) may be used. In columns, V_{Sd} is usually less than $0.5V_{pl.Rd}$, so no reduction in bending resistance need be made.

5.6.5 Resistance of a column length

5.6.5.1 Uniaxial bending

It is assumed that the interaction curve, Fig. 5.13, has been determined, that the design axial force N_{Sd} and maximum bending moment are known, and that the slenderness factor χ has been calculated. Let

$$\chi_d = \frac{N_{Sd}}{N_{pl.Rd}} \tag{5.28}$$

so that χ_d on Fig. 5.13 represents the design axial load.

Point B on the interaction curve represents failure of the column under axial load $\chi N_{pl.Rd}$, in absence of any applied bending moment. The bending resistance AB is thus assumed to be equal to the maximum bending moment caused by the axial load, just before the column fails. When $M_2 = M_1$, this secondary bending moment is assumed to be proportional to the axial load; so at some lower load $\chi_d N_{pl.Rd}$, its value is given by length CE. The bending resistance is now CF, so that resistance EF is available for the applied bending moment.

The secondary bending moment for a given axial load diminishes as M_2/M_1 falls below 1.0, as illustrated in Fig. 5.12. This is allowed for by replacing line BEO by BDG, where the ordinate of G is given by

$$\chi_n = \chi \frac{1 - M_2/M_1}{4} \quad \text{but} \quad \chi \leqslant \chi_d. \tag{5.29}$$

The bending resistance is thus increased from EF to DF.

A further correction is required for the unconservative assumption that the rectangular stress block for concrete extends to the plastic neutral axis (Section 3.5.3.1). It is made by reducing the bending resistance by 10%, so that the verification condition is

$$M_{Sd} \leqslant M_{Rd} = 0.9\, \mu M_{pl.Rd} \tag{5.30}$$

where

$$\mu = \mu_d - \mu_k \frac{\chi_d - \chi_n}{\chi - \chi_n}, \tag{5.31}$$

and μ_d and μ_k are given by the interaction curve, for χ_d and χ_k respectively. Use of a polygonal diagram that lies within the interaction curve appears to be conservative, but in fact is not. This is because it increases μ, for given χ, χ_d and χ_n. The error can be excessive, particularly for minor-axis bending and for filled tubes. This is why the use of an additional point E is then required.

5.6.5.2 Biaxial bending

It is now assumed that the maximum design bending moments about both axes, $M_{y.Sd}$ and $M_{z.Sd}$, are known, and also N_{Sd} and χ. It has to be decided in which plane failure is expected to occur. This is usually obvious; but if not, two verifications are required, one for each plane.

For failure in the z-plane, μ ($= \mu_z$) is determined as in Section 5.6.5.1, allowing for imperfections. For the y-plane, imperfections are neglected, so that μ_y is given by the length CF in Fig. 5.13. The verification conditions are:

$$M_{y.Sd} \leqslant 0.9\mu_y M_{pl.y.Rd} \tag{5.32}$$

$$M_{z.Sd} \leqslant 0.9\mu_z M_{pl.z.Rd} \tag{5.33}$$

$$\frac{M_{y.Sd}}{\mu_y M_{pl.y.Rd}} + \frac{M_{z.Sd}}{\mu_z M_{pl.z.Rd}} \leqslant 1.0. \tag{5.34}$$

5.6.6 Longitudinal shear

For end moments M_1 and M_2 as defined in Section 5.6.1, the transverse shear in a column length is $(M_1 - M_2)/L$. An estimate can be made of the longitudinal shear stress at the interface between steel and concrete, by elastic analysis of the uncracked composite section. This is rarely necessary in multi-storey structures, where these stresses are usually very low.

Higher stresses may occur near connections at a floor level where the axial load added to the column is a high proportion of the total axial load. Load added after the column has become composite, N_{Sd} say, may be assumed to be shared between the steel section, of area A_a, and its encasement on a transformed area basis:

$$N_{S.c} = N_{Sd}\left(1 - \frac{A_a}{A}\right) \tag{5.35}$$

where $N_{S.c}$ is the force that causes shear at the surface of the steel section and A is the transformed area of the column in 'steel' units.

There is no well-established method for calculating longitudinal shear stress at the surface of the steel section. Design is usually based on mean values, found by dividing the force by the perimeter of the section, u_a, and an assumed transmission lenght, l_v:

$$\tau_{Sd} = \frac{N_{S.c}}{u_a l_v}. \tag{5.36}$$

Design shear strengths τ_{Rd} due to bond and friction are given in Eurocode 4: Part 1.1 for several situations. For completely encased sections,

$$\tau_{Rd} = 0.6 \text{ N/mm}^2. \tag{5.37}$$

This is a low value, to take account of the approximate nature of τ_{Sd}. The length l_v should not exceed twice the 'relevant transverse dimension' which for an encased H-section is probably the breadth of the steel flange.

No account need be taken of the further transfers of force by shear between steel and concrete as failure is approached. The best protection against local failure is provided by the transverse reinforcement (links) which are required by Eurocode 2 to be more closely spaced near beam-column intersections than elsewhere.

If local shear stresses are excessive, columns should be provided with

ultimate loads for this external column, calculated in Sections 5.5.1 and 5.5.3, are as follows:

- axial load per storey, $N_{Sd} = 242 + 97.2 = 339$ kN
- bending moments (Fig. 5.9(b)): $M_{1y} = +$ **31.5 kN m**
  $M_{2y} = -$ **13 kN m**. (5.40)

Minor-axis bending is caused only by permanent loads that are equal on the two sides of the column, so it is assumed that

$$M_{1z} = M_{2z} \approx 0. \tag{5.41}$$

The factor α_n for number of storeys carried (equation (5.8)) does not apply because the imposed loading is in Category C; so the design axial load is

$$N_{Sd} = 339 \times 8 = \mathbf{2712\ kN}. \tag{5.42}$$

Design consists of verifying a column of assumed cross-section (Fig. 5.15) using the methods explained in Section 5.6.

The assumed concrete cover to the reinforcement, 30 mm and to the structural steel, 57 mm, satisfy the requirements for 90 minutes' fire resistance; and also for exposure class 2(b), humid environment, with frost, which may be appropriate for the external face of the column.

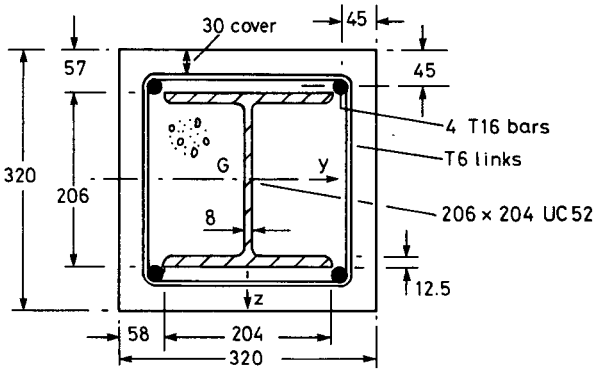

Fig. 5.15 Cross-section of external column.

5.7.2 Slenderness, and properties of the cross-section

The cross-sectional areas of the three materials are:

$$A_a = 6640\ \text{mm}^2, \quad A_s = 804\ \text{mm}^2, \quad A_c = 94950\ \text{mm}^2.$$

The ratio A_s/A_c is 0.0085, which satisfies expression (5.17).

From equation (5.27) the design plastic resistance to axial load is

$$N_{pl.Rd} = \frac{2357}{\gamma_a} + \frac{2017}{\gamma_c} + \frac{370}{\gamma_s} = 2143 + 1345 + 322 = 3810\ \text{kN} \tag{5.43}$$

shear connectors. These are best attached to the web of a steel H- or I-section, because their resistance is enhanced by the confinement provided by the steel flanges. Design rules are given in Eurocode 4: Part 1.1.

5.6.7 Concrete-filled steel tubes

A typical cross-section of a column of this type is shown in Fig. 5.10(c). To avoid local buckling of the steel, slendernesses of the walls must satisfy

$$\frac{h}{t} \leqslant 52\epsilon \tag{5.38}$$

where

$$\epsilon = \left(\frac{235}{f_y}\right)^{0.5}$$

and f_y is the yield strength in N/mm^2 units. For concrete-filled circular hollow sections of diameter d the limit is more generous:

$$\frac{d}{t} \leqslant 90\epsilon^2. \tag{5.39}$$

Design is essentially as for encased H-sections, except that in calculating the squash load $N_{pl.Rd}$, account is taken of the higher resistance of the concrete, caused by lateral restraint from the steel tube, as follows.

The term $0.85f_{ck}$ in equations (5.24) and (5.27) is replaced by f_{ck}. Also, for circular sections only, f_{ck} is increased to an extent that depends on the ratios t/d and $M_{Sd}/N_{Sd}d$, and provided that $\bar{\lambda} \leqslant 0.5$. For a circular section, there is also a reduction in the effective yield strength of the steel wall used in calculating $N_{pl.Rd}$, to take account of the circumferential tensile stress in the wall. This stress provides restraint to lateral expansion of the concrete caused by the axial load on the column.

A further advantage of filled tubes is that buckling curve a is used, rather than curve b or c.

5.7 Example: composite column

5.7.1 Data

A design is required for length KL of an external column of the frame DEF shown in Fig. 5.1. The materials are as used previously (Section 5.5.1). Values needed here are:

$f_y = 355$ N/mm^2, $f_{sk} = 460$ N/mm^2, $f_{ck} = 25$ N/mm^2, $E_{cm} = 30.5$ kN/mm^2.

The frame has been designed as braced (Section 5.5.2). The design

when $\gamma_a = 1.10$, $\gamma_c = 1.5$, and $\gamma_s = 1.15$. With these factors taken as 1.0:

$$N_{pl.R} = 2357 + 2017 + 370 = 4744 \text{ kN}. \tag{5.44}$$

From equation (5.18),

$$\delta = \frac{2143}{3810} = 0.562, \tag{5.45}$$

which is within the permitted range.

Second moments of area of the uncracked section are needed for the calculation of the elastic critical load, N_{cr}.

For the steel section,
from tables, $10^{-6} I_a = 52.6 \text{ mm}^4$.

For the reinforcement, $10^{-6} I_s = 804 \times 0.115^2 = 10.6 \text{ mm}^4$.

For the concrete, $10^{-6} I_c = 320^2 \times 0.32^2/12 - 52.6 - 10.6 = 811 \text{ mm}^4$

and $E_{cd} = 30.5/1.35 = 22.6 \text{ kN/mm}^2$.

From equation (5.23)

$$10^{-12}(EI)_e = 0.21 \times 52.6 + 0.8 \times 0.0226 \times 811 + 0.20 \times 10.6$$
$$= 27.8 \text{ N mm}^2. \tag{5.46}$$

For global analysis of the frame, account is taken of creep by using an effective modulus $E_c' = E_{cm}/2 = 15.25 \text{ kN/mm}^2$. By this method,

$$10^{-12} E_a I_1 = 25.5 \text{ N mm}^2 . \tag{5.47}$$

This value is used in Section 5.5.3.

The effective length of the column is taken as equal to the actual length, so from equation (5.22)

$$N_{cr} = \pi^2 \times 27.8 \times \frac{1000}{16} = 17150 \text{ kN}. \tag{5.48}$$

From equations (5.21) and (5.44)

$$\bar{\lambda} = \left(\frac{N_{pl.R}}{N_{cr}}\right)^{0.5} = \left(\frac{4744}{17150}\right)^{0.5} = 0.526 . \tag{5.49}$$

From column curve b in Fig. 5.11, the slenderness reduction factor is

$$\chi = 0.872 . \tag{5.50}$$

From equations (5.26) and (5.43), the resistance to axial load is

$$N_{Rd} = \chi N_{pl.Rd} = 0.872 \times 3810 = \mathbf{3322 \text{ kN}}. \tag{5.51}$$

The design bending moment is now calculated. From equation (5.20),

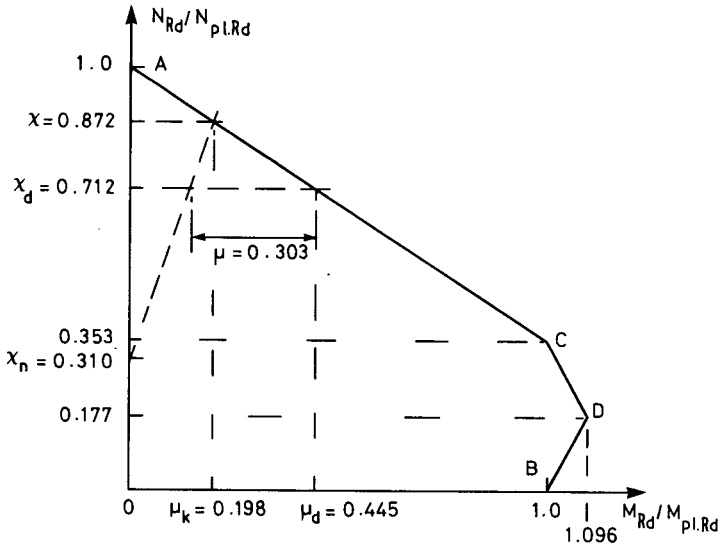

Fig. 5.16 Interaction diagram for major-axis bending.

$$\beta = 0.66 + 0.44\,\frac{M_2}{M_1} = 0.66 - 0.44 \times \frac{13}{31.5} = 0.48.$$

From equations (5.19), (5.42), and (5.48)

$$k = \frac{\beta}{1 - (N_{sd}/N_{cr})} = \frac{0.48}{1 - 2712/17150} = 0.57, \text{ but } \geqslant 1.0,$$

whence

$$\boldsymbol{M_{Sd}} = kM_1 = 1.0 \times 31.5 = \mathbf{31.5\ kN\ m}. \tag{5.52}$$

Coordinates of the polygonal interaction diagram for major-axis bending, Fig. 5.16, are now calculated by the method of Appendix B. From equations (B.1),

$$f_{yd} = \frac{355}{1.1} = 323\ \text{N/mm}^2, \quad f_{sd} = \frac{460}{1.15} = 400\ \text{N/mm}^2,$$

$$f_{cd} = 0.85 \times \frac{25}{1.5} = 14.2\ \text{N/mm}^2.$$

The plastic section moduli are given by equations (B.2) to (B.4):

$$10^{-6}W_{pa} = 0.568\ \text{mm}^3 \text{ (from tables)}$$

$$10^{-6}W_{ps} = 0.804 \times 0.115 = 0.0925\ \text{mm}^3$$

$$10^{-6}W_{pc} = 3.2^3/4 - 0.568 - 0.0925 = 7.53\ \text{mm}^3.$$

From equation (B.8)

$$N_{\text{pm.Rd}} = 94.95 \times 14.2 = 1345 \text{ kN}. \tag{5.53}$$

From equation (B.9)

$$h_{\text{n}} = \frac{1345}{0.64 \times 14.2 + 0.016(646 - 14.2)} = 70.0 \text{ mm}\,. \tag{5.54}$$

The dimension $h/2 - t_{\text{f}}$ is 91 mm, so h_{n} satisfies expression (B.11).

The bending resistance at point D is given by equation (B.7):

$$M_{\text{max.Rd}} = 0.568 \times 323 + 0.0925 \times 400 + 7.53 \times \frac{14.2}{2}$$

$$= 184 + 37 + 53 = 274 \text{ kN m}. \tag{5.55}$$

The bending resistance at points B and C is found using equations (B.5), (B.6), and (B.10):

$$10^{-6} W_{\text{pan}} = 8 \times 0.07^2 = 0.0392 \text{ mm}^3$$

$$10^{-6} W_{\text{pcn}} = (320 - 8) \times 0.07^2 = 1.529 \text{ mm}^3$$

$$M_{\text{pl.Rd}} = 274 - 0.0392 \times 323 - 1.529 \times \frac{14.2}{2} = 250 \text{ kN m}. \tag{5.56}$$

The ratios plotted in Fig. 5.16 are:

$$\frac{N_{\text{pm.Rd}}}{N_{\text{pl.Rd}}} = \frac{1345}{3810} = 0.353$$

$$\frac{M_{\text{max.Rd}}}{M_{\text{pl.Rd}}} = \frac{274}{250} = 1.096$$

and polygon ACDB can be drawn.

5.7.3 Resistance of the column length, for major-axis bending

The ratios χ_{d} and χ_{n} in Fig. 5.16 depend on the design action effects. From equations (5.28), (5.42), and (5.43),

$$\chi_{\text{d}} = \frac{N_{\text{Sd}}}{N_{\text{pl.Rd}}} = \frac{2712}{3810} = 0.712\,. \tag{5.57}$$

From equations (5.29), (5.40), and (5.50),

$$\chi_{\text{n}} = \chi \frac{1 - M_2/M_1}{4} = 0.872 \frac{1 + 13/31.5}{4} = 0.310.$$

From Fig. 5.16 or by calculation:

$$\mu_{\text{k}} = 0.198, \quad \mu_{\text{d}} = 0.445.$$

From equation (5.31) or from Fig. 5.16,

$$\mu = \mu_d - \frac{\mu_k(\chi_d - \chi_n)}{\chi - \chi_n}$$

$$= 0.445 - \frac{0.198 \times 0.402}{0.872 - 0.310} = 0.303.$$

The design bending resistance is given by equation (5.30):

$$M_{\mathbf{Rd}} = 0.9\,\mu M_{\text{pl.Rd}} = 0.9 \times 0.303 \times 250 = \mathbf{68\ kN\ m}.$$

From equation (5.52), $M_{\text{Sd}} = 31.5$ kN m, so the column length has sufficient resistance, subject to checks on biaxial bending and longitudinal shear.

5.7.4 Checks on biaxial bending and longitudinal shear

The possibility of buckling about the minor axis is now examined. The column section is square, but for the steel section, $I_{\text{az}} < I_{\text{ay}}$, so N_{cr} will be lower, $\bar{\lambda}$ higher, and χ lower than for major-axis buckling. The design minor-axis bending moment is zero (equation (5.41)),so the design is safe if $\mu_z \geqslant 0$.

For the cross-section, $M_{\text{pl.Rd.z}} < M_{\text{pl.Rd.y}}$, so the polygonal interaction diagram is different; but there is no need to use it. It is evident from Fig. 5.16 that $\mu_z \geqslant 0$ when

$$\chi_d \leqslant \chi_z. \tag{5.58}$$

It is found by calculations similar to those in Section 5.7.3 that:

$$10^{-12}(EI)_{\text{e.z}} = 21.1\ \text{N mm}^2; \quad N_{\text{cr.z}} = 13020\ \text{kN}; \bar{\lambda} = 0.604.$$

Curve c in Fig. 5.11 then gives $\chi_z = 0.783$. The ratio χ_d ($= N_{\text{Sd}}/N_{\text{pl.Rd}}$) is the same for both axes, 0.712, so condition (5.58) is satisfied.

Checks on longitudinal shear are described in Section 5.6.6. The design transverse shear for this column length is

$$V_{\text{Sd}} = \frac{M_1 - M_2}{L} = \frac{31.5 + 13}{4} = 11\ \text{kN}.$$

This is obviously negligible; $V_{\text{pl.Rd}}$ for the web of the steel section is 320 kN.

The total vertical load applied to the column at one floor level is 339 kN, equation (5.40), and 46 kN of this is load applied to the steel beam alone. It is assumed that the encasement to the column is cast before the floor slab, so that local longitudinal shear stress at a beam–column intersection should be calculated for $N_{\text{Sd}} = 339$ kN.

The ratio A_a/A in equation (5.35) is evaluated using $E'_c = 15.25\ \text{kN/mm}^2$,

as in Section 5.7.2. From cross-sectional areas given there, the transformed area is

$$10^{-3}A = 6.64 + 0.804 + 94.95 \times \frac{15.25}{210} = 14.3 \text{ mm}^2.$$

From equation (5.35),

$$N_{S.c} = 339\left(1 - \frac{6.64}{14.3}\right) = 182 \text{ kN}.$$

The perimeter of the steel section is $u_a = 1140$ mm. From equations (5.36) and (5.37), the transmission length l_v is

$$l_v = \frac{N_{S.c}}{u_a \tau_{Sd}} = \frac{182}{1.14 \times 0.6} = 266 \text{ mm}.$$

This is less than twice the relevant transverse dimension, 203 mm, so local bond stress is not excessive.

This calculation neglects any load transferred to the concrete encasement by direct bearing of the three steel beams that are connected to each floor level, and so is conservative.

This completes the validation of the design assumed for this column length.

5.7.5 Beam-to-column connection

The connections used for this structure do not make use of composite action, and so should be designed using a code of practice for structural steelwork, such as Eurocode 3. As an example, a possible connection between a main beam and an external column is shown in Fig. 5.17.

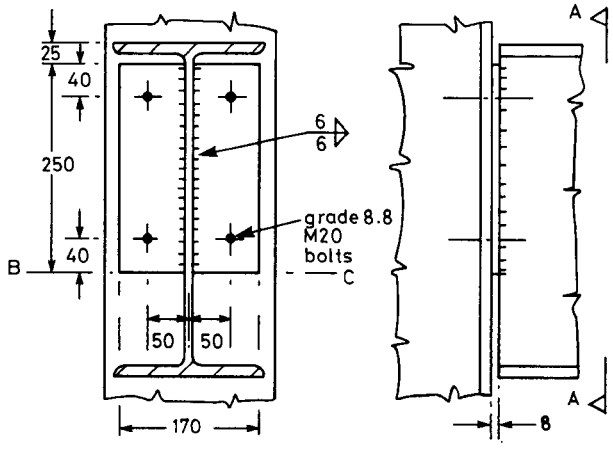

Fig. 5.17 Beam-to-column connection.

The connection is 'nominally pinned'; as defined in Section 5.3.2. Flexibility in bending is achieved by using a thin end plate (8 mm), and a wide spacing (100 mm) of the pairs of M20 bolts, so that plastic deformation of the end plate allows the end of the beam to rotate about line BC in Fig. 5.17(a), as it deflects under load, without applying much bending moment to the column.

Both Eurocodes 3 and 4 state a principle of structural integrity, relevant to the consequences of events like explosions or impacts, but give no application rules. The British National Application Document for Eurocode 3: Part 1.1 requires a connection of the type shown in Fig. 5.17 to resist a design tensile force of at least 75 kN, acting along the axis of the beam.

The only other design action effect is a vertical shear of 242 kN, from Fig. 4.11, because the shear is assumed to be transferred in the plane of the connection to the column, so that the bending moment is negligible.

The connection shown in Fig. 5.17 is designed for these two forces, following rules given in Eurocode 3 for bearing and shear strength of bolts, shear strength of welds, vertical shear in the end plate, and edge and end distances for bolt holes, which in this case are 22 mm in diameter.

It will be noted that the bending moment at the face of the steel column has been assumed to be sagging, in design of the beam (since its span is taken to the centre-line of the column), hogging (Section 5.5.3) in design of the column, and zero in design of the connection. These are all simplifications that are known to be satisfactory in practice.

Appendix A
Partial-interaction Theory

A.1 Theory for simply-supported beam

This subject is introduced in Section 2.6, which gives the assumptions and notation used in the theory that follows. On first reading, it may be found helpful to rewrite the algebraic work in a form applicable to a beam with the very simple cross-section shown in Fig. 2.2. This can be done by making these substitutions.

Replace A_c and A_a by bh, and d_c by h.
Replace I_c and I_a by $bh^3/12$.
Put $k_c = n = 1$, so that E'_c, E_c, and E_s are replaced by E.

The beam to be analysed is shown in Fig. 2.15, and Fig. A.1 shows in elevation a short element of the beam, of length dx, distant x from the midspan cross-section. For clarity, the two components are shown separated, and displacements are much exaggerated. The slip is s at cross-section x, and increases over the length of the element to $s + (ds/dx)\,dx$, which is written as s^+. This notation is used in Fig. A.1 for increments in the other variables, M_c, M_a, F, V_c, and V_a, which are respectively the bending moments, axial force, and vertical shears acting on the two components of the beam, the suffixes c and a indicating concrete and steel. It follows from longitudinal equilibrium that the forces F in steel and concrete are equal. The interface vertical force r per unit length is unknown, so it cannot be assumed that V_c equals V_a.

If the interface longitudinal shear is v per unit length, the force on each component is $V\,dx$. It must be in the direction shown, to be consistent with the sign of the slip, s. The load–slip relationship is

$$pv = ks \tag{A.1}$$

since the load per connector is pv.

We first obtain equations deduced from equilibrium, elasticity, and compatibility, then eliminate M, F, V, and v from them to obtain a differential equation relating s to x, and finally solve this equation and insert the boundary conditions. These are as follows.

(1) Zero slip at midspan, from symmetry, so

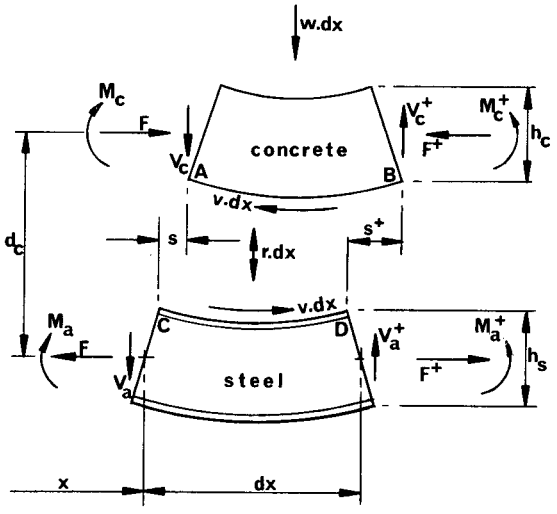

Fig. A.1 Elevation of element of composite beam.

$$s = 0 \quad \text{when} \quad x = 0. \tag{A.2}$$

(2) At the supports, M and F are zero, so the difference between the longitudinal strains at the interface is the differential strain, ϵ_c, and therefore

$$\frac{ds}{dx} = -\epsilon_c \quad \text{when} \quad x = \pm\frac{L}{2}. \tag{A.3}$$

Equilibrium

Resolve longitudinally for one component:

$$\frac{dF}{dx} = -v. \tag{A.4}$$

Take moments:

$$\frac{dM_c}{dx} + V_c = \frac{1}{2}vh_c, \quad \frac{dM_a}{dx} + V_a = \frac{1}{2}vh_s. \tag{A.5}$$

The vertical shear at section x is wx, so

$$V_c + V_a = wx. \tag{A.6}$$

Now $\frac{1}{2}(h_c + h_s) = d_c$, so from (A.5) and (A.6),

$$\frac{dM_c}{dx} + \frac{dM_a}{dx} + wx = vd_c. \tag{A.7}$$

Elasticity

In beams with adequate shear connection, the effects of uplift are negligible in the elastic range. If there is no gap between the two components, they must have the same curvature, ϕ, and simple beam theory gives the moment–curvature relations. Using (2.19) for E_c', then

$$\phi = \frac{M_a}{E_s I_a} = \frac{nM_c}{k_c E_a I_c}. \tag{A.8}$$

The longitudinal strains in concrete along AB (Fig. A.1) and in steel along CD are:

$$\epsilon_{AB} = \frac{1}{2} h_c \phi - \frac{nF}{k_c E_a A_c} - \epsilon_c \tag{A.9}$$

$$\epsilon_{CD} = -\frac{1}{2} h_s \phi + \frac{F}{E_a A_a}. \tag{A.10}$$

Compatibility

The difference between ϵ_{AB} and ϵ_{CD} is the slip strain, so from (A.9) and (A.10), and putting $\frac{1}{2}(h_c + h_s) = d_c$,

$$\frac{ds}{dx} = \phi d_c - \frac{F}{E_a}\left(\frac{n}{k_c A_c} + \frac{1}{A_a}\right) - \epsilon_c. \tag{A.11}$$

It is now possible to derive the differential equation for s. Eliminating M_c and M_a from (A.7) and (A.8),

$$E_a\left(\frac{k_c I_c}{n} + I_a\right)\frac{d\phi}{dx} + wx = vd_c. \tag{A.12}$$

From (A.1) and (2.22),

$$\frac{d\phi}{dx} = \frac{kd_c s/p - wx}{E_a I_0}. \tag{A.13}$$

Differentiating (A.11) and eliminating ϕ from (A.13), F from (A.4), and v from (A.1):

$$\frac{d^2 s}{dx^2} = \frac{kd_c^2 s/p - wd_c x}{E_a I_0} + \frac{ks}{E_a A_0 p} = \frac{ks}{pE_a I_0}\left(d_c^2 + \frac{I_0}{A_0}\right) - \frac{wd_c x}{E_a I_0}.$$

Introducing A' from (2.21), α^2 from (2.23) and β from (2.24) gives result (2.25), which is in a standard form:

$$\frac{d^2 s}{dx^2} - \alpha^2 s = -\alpha^2 \beta wx\,. \tag{2.25}$$

Solving for s,

$$s = K_1 \sinh \alpha x + K_2 \cosh \alpha c + \beta wx. \tag{A.14}$$

The boundary conditions (A.2) and (A.3) give

$$K_2 = 0, \quad \epsilon_c = -K_1\alpha \cosh(\alpha L/2) - \beta w$$

and substitution in (A.14) gives s in terms of x:

$$s = \beta w x - \left(\frac{\beta w + \epsilon_c}{\alpha}\right) \operatorname{sech}\left(\frac{\alpha L}{2}\right) \sinh \alpha x. \qquad (2.27)\text{ bis}$$

Other results can now be found as required. For example, the slip strain at midspan is

$$\left(\frac{ds}{dx}\right)_{x=0} = \beta w - (\beta w + \epsilon_c) \operatorname{sech}(\alpha L/2) \qquad (A.15)$$

and the slip at $x = L/2$ due to ϵ_c alone (i.e. with $w = 0$), is

$$(s)_{x=L/2} = -\frac{\epsilon_c}{\alpha} \tanh\left(\frac{\alpha L}{2}\right). \qquad (A.16)$$

A.2 Example: partial interaction

These calculations are introduced in Section 2.7. They relate to a beam shown in section in Fig. 2.16, which carries a distributed load w per unit length over a simply supported span L. The materials are assumed to be concrete with a characteristic cube strength of 30 N/mm^2 and mild steel, with a characteristic yield strength of 250 N/mm^2. Creep is neglected ($k_c = 1$) and we assume $n = 10$, so for the concrete $E_c = E'_c = 20$ kN/mm^2, from (2.19).

The dimensions of the beam (Fig. 2.16) are so chosen that the transformed cross-section is square: $L = 10$ m, $b = 0.6$ m, $h_c = h_s = 0.3$ m. The steel member is thus a rectangle of breadth 0.06 m, so that $A_a = 0.018$ m^2, $I_a = 1.35 \times 10^{-4}$ m^4.

The design of such a beam on an ultimate-strength basis is likely to lead to a working or 'service' load of about 35 kN/m. If stud connectors 19 mm in diameter and 100 mm long are used in a single row, an appropriate spacing would be 0.18 m. Push-out tests give the ultimate shear strength of such a connector as about 100 kN, and the slip at half this load is usually between 0.2 and 0.4 mm. Connectors are found to be stiffer in beams than in push-out tests, so a connector modulus $k = 150$ kN/mm will be assumed here, corresponding to a slip of 0.33 mm at a load of 50 kN per connector.

The distribution of slip along the beam and the stresses and curvature at midspan are now found by partial-interaction theory, using the results obtained in Section A.1, and also by full-interaction theory. The results are discussed in Section 2.7.

First α and β are calculated. From (2.22) with $I_c = nI_a$ (from the shape of the transformed section) and $k_c = 1$, $I_0 = 2.7 \times 10^{-4}$ m^4.

From (2.20) with $A_c = nA_a$ and $k_c = 1$, $A_0 = 0.009$ m^2.
From (2.21), $1/A' = 0.3^2 + (2.7 \times 10^{-4})/0.009 = 0.12$ m^2.
From (2.23), with $k = 150$ kN/mm and $p = 0.18$ m,

$$\alpha^2 = \frac{150 \times 0.12}{0.18 \times 200 \times 0.27} = 1.85 \text{ m}^{-2}$$

whence $\alpha = 1.36$ m^{-1}. Now $L = 10$ m, so $\alpha L/2 = 6.8$, and sech $(\alpha L/2) = 0.00223$. From (2.24),

$$\beta = \frac{0.18 \times 0.3}{0.12 \times 150 \times 1000} = 3.0 \times 10^{-6} \text{ m/kN}.$$

We assumed $w = 35$ kN/m, so $\beta w = 1.05 \times 10^{-4}$ and $\beta w/\alpha = 0.772 \times 10^{-4}$ m. An expression for the slip in terms of x is now given by (2.27) with $\epsilon_c = 0$:

$$10^4 s = 1.05x - 0.0017 \sinh (1.36x). \tag{2.28}$$

This gives the maximum slip (when $x = \pm 5$ m) as ± 0.45 mm.

This may be compared with the maximum slip if there were no shear connection, which is given by (2.6) as

$$\frac{wL^3}{4Ebh^2} = \frac{35 \times 10^3}{4 \times 20 \times 0.6 \times 0.3^2 \times 1000} = 8.1 \text{ mm}.$$

The stresses at midspan can be deduced from the slip strain and the curvature. Differentiating (2.28) and putting $x = 0$,

$$10^4 \left(\frac{ds}{dx}\right)_{x=0} = 1.05 - 0.0017 \times 1.36 = 1.05$$

so the slip strain at midspan is 105×10^{-6}. From (A.13),

$$\frac{d\phi}{dx} = 4.64s - 6.5 \times 10^{-4}x.$$

Using (2.28) for s and integrating,

$$10^6 \phi = -81.5x^2 - 0.585 \cosh (1.36x) + K.$$

The constant K is found by putting $\phi = 0$ when $x = L/2$, whence at $x = 0$,

$$\phi = 0.0023 \text{ m}^{-1}.$$

The corresponding change of strain between the top and bottom faces of a member 0.3 m deep is 0.3×0.0023, or 690×10^{-6}. The transformed cross-section is symmetrical about the interface, so the strain in each material at this level is half the slip strain, say 52×10^{-6}, and the strain

distribution is as shown in Fig. 2.17. The stresses in the concrete, found by multiplying the strains by E_c (20 kN/mm^2), are 1.04 N/mm^2 tension and 12.8 N/mm^2 compression. The tensile stress is below the cracking stress, as assumed in the analysis.

The maximum compressive stress in the concrete is given by full-interaction theory (equation (2.7)) as

$$\sigma_{cf} = \frac{3wL^2}{16bh^2} = \frac{3 \times 35 \times 100}{16 \times 0.6 \times 0.09 \times 10^3} = 12.2 \text{ N/mm}^2.$$

Appendix B

Interaction Curve for Major-axis Bending of Encased I-section Column

Reference is made in Section 5.6.4 to the simplified calculation method given in Annex C of Eurocode 4: Part 1.1.[12] This method is now used to determine the coordinates of points B, C, and D of the polygonal interaction curve shown in Fig. 5.14, for major-axis bending of the encased I-section column shown in Fig. B.1. The notation is as used in Eurocode 4, and in Chapter 5 of this volume.

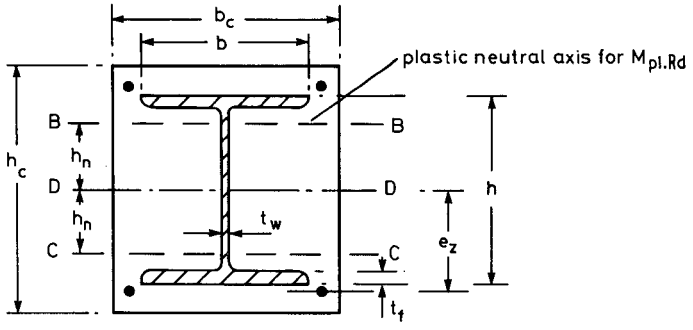

Fig. B.1 Plastic neutral axes for encased I-section.

It is assumed that for pure bending, the plastic neutral axis lies between the steel flanges, at distance h_n from the centre of area, G. It is shown in Eurocode 4 that for points B, C, and D the plastic neutral axes are BB, CC, and DD in Fig. B.1, respectively.

Design strengths of materials are defined as follows:

$$f_{yd} = \frac{f_y}{\gamma_a}, \quad f_{sd} = \frac{f_{sk}}{\gamma_s}, \quad f_{cd} = 0.85\frac{f_{ck}}{\gamma_c}. \tag{B.1}$$

Plastic section moduli for the three materials, assuming concrete to be uncracked, are as follows:

$$W_{pa} = \frac{(h - 2t_f)t_w^2}{4} + bt_f(h - t_f) \quad \text{(or from tables)} \tag{B.2}$$

$$W_{ps} = A_s e_z \tag{B.3}$$

$$W_{pc} = \frac{b_c h_c^2}{4} - W_{pa} - W_{ps}. \tag{B.4}$$

Plastic section moduli for the region of depth $2h_n$ between axes BB and CC are:

$$W_{pan} = t_w h_n^2 \tag{B.5}$$

$$W_{pcn} = (b_c - t_w)h_n^2, \tag{B.6}$$

where h_n is given by equation (B.9).

For bending about axis DD, only half of the concrete is effective, so that the bending resistance at point D is

$$M_{max.Rd} = W_{pa} f_{yd} + W_{ps} f_{sd} + \frac{W_{pc} f_{cd}}{2}. \tag{B.7}$$

The longitudinal forces in the steel section and the reinforcement sum to zero, from symmetry, so the axial compression is $N_{pm.Rd}/2$, where

$$N_{pm.Rd} = A_c f_{cd}. \tag{B.8}$$

The depth h_n is found from the condition that when the plastic neutral axis moves from DD to BB, the axial compression changes from $N_{pm.Rd}/2$ to zero. The stress in area $h_n t_w$ of steel web changes by $2f_{yd}$ (from compression to tension), and the stress in an area $h_n(b_c - t_w)$ of concrete changes from f_{cd} to zero, whence

$$\frac{A_c f_{cd}}{2} = 2h_n t_w f_{yd} + h_n(b_c - t_w) f_{cd}).$$

Rearranging

$$h_n = \frac{A_c f_{cf}}{2b_c f_{cd} + 2t_w(2f_{yd} - f_{cd})}. \tag{B.9}$$

When the plastic neutral axis moves from DD to CC, the axial compression changes from $N_{pm.Rd}/2$ to $N_{pm.Rd}$, because the changes in axial force are of the same size (but of opposite sign) as when it moves from DD to BB.

When the plastic neutral axis moves from BB to CC, the resultant of all the changes in axial force passes through G (from symmetry), so that the bending resistances at B and C are the same, and are

$$M_{pl.Rd} = M_{max.Rd} - W_{pan} f_{yd} - W_{pcn} \frac{f_{cd}}{2}. \tag{B.10}$$

The coordinates of points B, C, and D are thus as shown in Fig. 5.14, where $N_{pm.Rd}$, $M_{max.Rd}$ and $M_{pl.Rd}$ are given by equations (B.8), (B.7), and (B.10) respectively, provided that

$$h_n \leqslant \frac{h}{2} - t_f. \tag{B.11}$$

Equations for sections where this condition is not satisfied, and for minor-axis bending and for concrete-filled tubes are obtained by similar reasoning, and are given in Annex C of Eurocode 4: Part 1.1.

The preceding results are used in an example in Section 5.7.2.

References

1. Fisher J.W. Design of composite beams with formed metal deck. *Eng. J., Amer. Inst. Steel Constr.*, 7, 88–96, July 1970.
2. Lawson R.M. and Newman G.M. Fire resistant design of steel structures; a Handbook to BS 5950: Part 8. *Publication 080*, Steel Construction Institute, Ascot, 1990.
3. Lawson R.M. Fire resistance and protection of structural steelwork. In *Constructional Steel Design*, (Ed. by P.J. Dowling, J.E. Harding, and R. Bjorhovde), pp. 871–885. Elsevier Applied Science, London, 1992.
4. Kerensky O.A. and Dallard N.J. The four-level interchange between M4 and M5 motorways at Almondsbury, *Proc. Instn Civil Engrs*, **40**, 295–322, July 1968.
5. Johnson R.P., Finlinson J.C.H. and Heyman J. A plastic composite design, *Proc. Instn Civil Engrs*, **32**, 198–209, Oct. 1965.
6. Cassell A.C., Chapman J.C. and Sparkes S.R. Observed behaviour of a building of composite steel and concrete construction, *Proc. Instn Civil Engrs*, **33**, 637–658, April 1966.
7. European Convention for Constructional Steelwork. *Composite Structures*, The Construction Press, London, 1981.
8. ENV 1991–1. Eurocode 1: Part 1, *Basis of design*. In preparation, 1994.
9. ENV 1991–2. Eurocode 1, *Basis of design, and actions on structures*. Part 2, *General rules and gravity and impressed loads, snow, wind, and fire*. In preparation, 1994.
10. DD ENV 1992–1–1. Eurocode 2, *Design of concrete structures*. Part 1.1, *General rules and rules for buildings (with U.K. National Application Document)*. British Standards Institution, London, 1992.
11. DD ENV 1993–1–1. Eurocode 3, *Design of steel structures*. Part 1.1, *General rules and rules for buildings (with U.K. National Application Document)*. British Standards Institution, London, 1992.
12. DD ENV 1994–1–1. Eurocode 4, *Design of composite steel and concrete structures*. Part 1.1, *General rules and rules for buildings (with U.K. National Application Document)*. British Standards Institution, London, 1994.
13. DD ENV 1994–1–2. Eurocode 4, *Design of composite steel and con-*

crete structures. Part 1.2, *Structural fire design (with U.K. National Application Document)*. British Standards Institution, London, to be published, 1994.

14. BS 5950: Part 3: Section 3.1. *Code of practice for design of simple and continuous composite beams*. British Standards Institution, London, 1990.
15. Johnson R.P. and Anderson D. *Designers' Handbook to Eurocode 4: Part 1.1, Design of steel and composite structures*. Thomas Telford, London, 1993.
16. EN 10080. Standard for reinforcing steel. In preparation, 1993.
17. BS EN 10025. *Hot rolled products of non-alloy structural steels and their technical delivery conditions*. British Standards Institution, London, 1993.
18. BS 8110: Parts 1 and 2. *Structural use of concrete*. British Standards Institution, London, 1985.
19. Johnson R.P. Design of encased composite beams, *Consulting Engr*, **32**, No. 11, 40–45, Nov. 1968.
20. Goble G.G. Shear strength of thin-flange composite specimens, *Eng. J. Amer. Inst. Steel Constr.*, **5**, 62–65, April 1968.
21. Chapman J.C. and Teraskiewicz J.S. Research on composite construction at Imperial College, *Proc. Conf. Steel Bridges*, 49–58, British Constructional Steelwork Association, 1969.
22. BS 5400: Part 5, *Design of composite bridges*. British Standards Institution, London, 1979.
23. Mottram J.T. and Johnson R.P. Push tests on studs welded through profiled steel sheeting, *The Structural Engineer*, **68**, 187–193, 15 May 1990.
24. Johnson R.P., Greenwood R.D. and van Dalen K. Stud shear-connectors in hogging moment regions of composite beams, *The Structural Engineer*, **47**, 345–350, Sept. 1969.
25. Grant J.A., Fisher J.W. and Slutter R.G. Composite beams with formed metal deck, *Eng. J. Amer. Inst. Steel Constr.*, No. 1, 24–42, 1977.
26. CP 117, *Composite construction in structural steel and concrete*. Part 2, *Beams for bridges*. British Standards Institution, London, 1967.
27. BS 5950: Part 4, *Code of practice for design of composite slabs with profiled steel sheeting*. British Standards Institution, London, 1994.
28. Patrick M. and Bridge R.Q. Design of composite slabs for vertical shear. In *Composite construction in steel and concrete II*, (Ed. by Easterling W.S. and Roddis W.M.K.), pp. 304–322, Proc. of an Engineering Foundation Conference, Amer. Soc. Civil Engrs. New York, 1993.
29. *Specifications for the design and construction of composite slabs, and Commentary*. Amer. Soc. Civil Engrs, New York, Oct. 1984.

30. Patrick M. and Poh K.W. Controlled tests for composite slab design parameters. Symposium, Mixed structures, including new materials, Brussels. *Reports, Int. Assoc. for Bridge and Struct. Engrg*, **60**, 227–231, 1990.
31. Patrick M. A new partial shear connection strength model for composite slabs. *Steel Constr. J., Austr. Inst. of Steel Constr.*, **24**, August, 2–17, 1990.
32. DD ENV 1993–1–3. Eurocode 3, *Design of steel structures*. Part 1.3, *Cold formed thin gauge members and sheeting*. British Standards Institution, London, 1994.
33. Bode H. and Sauerborn I. Modern design concept for composite slabs with ductile behaviour. In *Composite construction in steel and concrete II*, (Ed. by Easterling W.S. and Roddis W.M.K.), pp. 125–141, Proc. of an Engineering Foundation Conference, Amer. Soc. Civil Engrs, New York, 1993.
34. Patrick M. and Bridge R.Q. Parameters affecting the design and behaviour of composite slabs. Symposium, Mixed structures, including new materials, Brussels. *Reports, Int. Assoc. for Bridge and Struct. Engrg*, **60,** 221–225, 1990.
35. Lawson R.M. Commentary on BS 5950: Part 3: Section 3.1, Composite beams. *Publication 078*, Steel Construction Institute, Ascot, 1990.
36. DD ENV 1991–2–2. Eurocode 1, *Basis of design, and actions on structures*. Part 2.2, *Actions on structures exposed to fire*. British Standards Institution, London, 1994.
37. Johnson R.P. and Willmington R.T. Vertical shear in continuous composite beams. *Proc. Instn Civil Engrs*, **53**, 189–205, Sept. 1972.
38. Johnson R.P. and Molenstra N. Partial shear connection in composite beams for buildings. *Proc. Instn Civil Engrs, Part 2*, **91**, 679–704, Dec. 1991.
39. Johnson R.P. Design of composite bridge beams for longitudinal shear. In *Developments in Bridge Design and Construction*, (Ed. by K.C. Rockey, J.L. Bannister and H.R. Evans), pp. 387–99. Crosby Lockwood Staples, London, 1971.
40. Beeby A.W. *The prediction and control of flexural cracking in reinforced concrete members*, 55–75, Publication SP 30, American Concrete Institute, Detroit, March 1971.
41. BS 6472. *Evaluation of human exposure to vibration in buildings (1 Hz to 80 Hz)*. British Standards Institution, London, 1984.
42. Wyatt T.A. Design guide on the vibration of floors. *Publication 076*, Steel Construction Institute, Ascot, 1989.
43. Allison R.W., Johnson R.P. and May I.M. Tension field action in composite plate girders. *Proc. Instn Civil Engrs, Part 2*, **73**, 255–276, June 1982.

44. Johnson R.P. and Fan C.K.R. Distortional lateral buckling of continuous composite beams. *Proc. Instn Civil Engrs, Part 2*, **91**, 131–161, March 1991.
45. Johnson R.P. and Chen S. Stability of continuous composite plate girders with U-frame action. *Proc. Instn Civil Engrs, Struct. and Bldgs*, **99**, 187–197, May 1993.
46. Lawson R.M. and Rackham J.W. Design of haunched composite beams in buildings. *Publication 060*, Steel Construction Institute, Ascot, 1989.
47. Randl E. and Johnson R.P. Widths of initial cracks in concrete tension flanges of composite beams. *Proc. Int. Assoc. for Bridge and Struct. Engrg*, P-54/82, 69–80, Nov. 1982.
48. Roik K., Hanswille G. and Cunze-O. Lanna A. Report on Eurocode 4, clause 5.3, cracking of concrete. *Report EC4/4/88*, University of Bochum, March 1989.
49. Johnson R.P. and Chen S. Local buckling and moment redistribution in Class 2 composite beams. *Struct. Engrg International*, **1**, 27–34, Nov. 1991.
50. CP 117, *Composite construction in structural steel and concrete*. Part 2,*Beams for bridges*. British Standards Institution, London, 1967.
51. Faber O. More rational design of cased stanchions. *The Structural Engineer*, **34**, 88–109, March 1956.
52. BS 5950, *Structural use of steelwork in building*. Part 1, *Code of practice for design in simple and continuous construction: hot rolled sections*. British Standards Institution, London, 1990.
53. Jones R. and Rizk A.A. An investigation on the behaviour of encased steel columns under load. *The Structural Engineer*, **41**, 21–33, Jan. 1963.
54. Basu A.K. and Sommerville W. Derivation of formulae for the design of rectangular composite columns. *Proc. Instn Civil Engrs, Supp. vol.*, 233–280, 1969.
55. Virdi K.S. and Dowling P.J. The ultimate strength of composite columns in biaxial bending. *Proc. Instn Civil Engrs, Part 2*, **55**, 251–272, March 1973.
56. Johnson R.P. and May I.M. Tests on restrained composite columns. *The Structural Engineer*, **56B**, 21–28, June 1978.
57. Neogi P.K., Sen H.K. and Chapman J.C. Concrete-filled tubular steel columns under eccentric loading. *The Structural Engineer*, **47**, 187–195, May 1969.
58. Leon R.T. and Zandonini R. Composite connections. In *Constructional Steel Design* (Ed. by P.J. Dowling, J.E. Harding and R. Bjorhovde), pp. 501–522. Elsevier Applied Science, London, 1992.
59. Coates R.C., Coutie M.G. and Kong F.K. *Structural Analysis*, 3rd edn., Van Nostrand Reinhold (UK), Wokingham, 1988.

Index

This book provides an introduction to the theory and design of composite structures of steel and concrete. All material of a fundamental nature that is applicable to both buildings and bridges is included, plus more detailed information relating to buildings.

All the design methods explained in this volume are those of the draft Eurocodes. The book has been substantially rewritten to take account of these (Parts 1.1 of Eurocodes 2, 3 and 4 for the design of concrete, steel and composite structures, and Eurocode 4: Part 1.2 for resistance to fire). A completely new set of worked examples relating to buildings is presented, in a way that does not require reference to the codes of practice.

The book will be of interest to undergraduate and graduate students, university teachers and practising engineers seeking familiarity with composite structures and the new Eurocodes.

THE AUTHOR

R. P. Johnson MA, FEng, FICE, FIStructE, Professor of Civil Engineering at the University of Warwick, has worked for many years on the theory and applications of composite structures. He is Chairman of the Drafting Committee for Eurocode 4 on composite steel and concrete structures.

ALSO OF INTEREST

Steel Designers' Manual
Fifth Edition
The Steel Construction Institute
0-632-03877-2 (paperback)
0-632-02488-7 (hardback)

Composite Structures of Steel and Concrete
Volume 2: Bridges
Second Edition
R. P. Johnson and R. J. Buckby
0-00-383153-1

ISBN 0-632-02507-7

BLACKWELL SCIENTIFIC PUBLICATIONS
OXFORD LONDON EDINBURGH BOSTON
MELBOURNE PARIS BERLIN VIENNA